

## Aerobic Granular Sludge in Continuous-Flow Reactors

Haaksman, V.A.

**DOI**

[10.4233/uuid:83e160a1-ec44-4d2a-b2d4-a3609be7517b](https://doi.org/10.4233/uuid:83e160a1-ec44-4d2a-b2d4-a3609be7517b)

**Publication date**

2024

**Document Version**

Final published version

**Citation (APA)**

Haaksman, V. A. (2024). *Aerobic Granular Sludge in Continuous-Flow Reactors*. [Dissertation (TU Delft), Delft University of Technology]. <https://doi.org/10.4233/uuid:83e160a1-ec44-4d2a-b2d4-a3609be7517b>

**Important note**

To cite this publication, please use the final published version (if applicable). Please check the document version above.

**Copyright**

Other than for strictly personal use, it is not permitted to download, forward or distribute the text or part of it, without the consent of the author(s) and/or copyright holder(s), unless the work is under an open content license such as Creative Commons.

**Takedown policy**

Please contact us and provide details if you believe this document breaches copyrights. We will remove access to the work immediately and investigate your claim.

**Aerobic Granular Sludge  
in  
Continuous-Flow Reactors**



# **Aerobic Granular Sludge in Continuous-Flow Reactors**

## **Proefschrift**

ter verkrijging van de graad van doctor  
aan de Technische Universiteit Delft,  
op gezag van de Rector Magnificus prof. dr. ir. T.H.J.J. van der Hagen,  
voorzitter van het College voor Promoties,  
in het openbaar te verdedigen op  
donderdag 16 mei 2024 om 15:00 uur

door

**Viktor Albert HAAKSMAN**

Master of Science in Life Science and Technology,  
Technische Universiteit Delft, Nederland,  
geboren te Leiden, Nederland.

Dit proefschrift is goedgekeurd door de promotor.

Samenstelling promotiecommissie bestaat uit:

Rector Magnificus,	voorzitter
Prof. dr. ir. M.C.M. van Loosdrecht	Technische Universiteit Delft, promotor
Dr. M. Pronk	Technische Universiteit Delft, copromotor

*Onafhankelijke leden:*

Prof. dr. ir. C. Picioreanu	KAUST, Saoedi-Arabië
Prof. dr. ir. E.I.P. Volcke	Universiteit Gent, België
Prof. dr. ir. M.K. de Kreuk	Technische Universiteit Delft
Prof. dr. D. Brdjanovic	UNESCO-IHE / Technische Universiteit Delft
Dr. Y. Lin	Technische Universiteit Delft (reservelid)

*Overige leden:*

Dr. ir. E.J.H. van Dijk	Royal HaskoningDHV
-------------------------	--------------------

Dr. ir. E.J.H. van Dijk has, as supervisor and co-author of chapters 4 and 5, contributed significantly to this thesis.

The research was carried out within the Environmental Biotechnology section of the Department of Biotechnology as part of the HarnAschpoldeR KORrelSlib (HARKOS) project, a collaboration of the Delfland Water Authority, Defluent Services, Evides Industriewater, the Rijnland District Water Control Board and Royal HaskoningDHV. The pilot-scale research was conducted in the DBI facility at the Harnaschpolder WWTP.



*Printed by:* Drukkerij Mostert & Van Onderen, Leiden (The Netherlands)  
*Cover:* M.C. Escher's "Waterfall" ©2024 The M.C. Escher Company, The Netherlands. All rights reserved. [www.mcescher.com](http://www.mcescher.com)

Copyright © 2024 by V.A. Haaksman

ISBN 978-94-90858-86-5

An electronic version of this dissertation is available at  
<http://repository.tudelft.nl/>.

# Contents

<b>Summary</b>	<b>ix</b>
<b>Samenvatting</b>	<b>xiii</b>
<b>Preface</b>	<b>xvii</b>
<b>1 General introduction</b>	<b>1</b>
1.1 Municipal wastewater treatment . . . . .	2
1.1.1 ‘Conventional’ activated sludge . . . . .	2
1.2 Process intensification in activated sludge systems . . . . .	7
1.3 Concepts for process intensification . . . . .	7
1.4 Additional biomass on carrier media . . . . .	8
1.5 Increasing overall sludge settleability. . . . .	9
1.5.1 Addition of carriers . . . . .	9
1.5.2 Self-aggregation . . . . .	10
1.6 Aerobic granulation in CFAS systems . . . . .	15
1.7 Scope and outline of the thesis . . . . .	18
<b>2 Impact of aerobic availability of readily biodegradable organic substrate</b>	<b>21</b>
2.1 Introduction . . . . .	22
2.2 Methodology. . . . .	24
2.2.1 Experimental set-up and operation. . . . .	24
2.2.2 Stepwise increase of the aerobically dosed acetate fraction . . . . .	25
2.2.3 Analysis of reactor performance . . . . .	25
2.2.4 Imaging of sludge morphology . . . . .	26
2.2.5 Maximum specific acetate up take rate under aerobic conditions . . . . .	26
2.2.6 Fluorescent in-situ hybridization (FISH) . . . . .	26
2.3 Results . . . . .	27
2.3.1 Reference reactor operation . . . . .	27
2.3.2 Effect of aerobic transport-limited acetate uptake rate on sludge morphology and settleability . . . . .	28
2.3.3 Biological phosphorus removal during the stepwise increase of the aerobic acetate load . . . . .	31
2.4 Discussion . . . . .	35
2.4.1 Theoretical aspects of sludge morphology . . . . .	35
2.4.2 Reactor operation and the morphological effect of rbCOD . . . . .	36

---

2.4.3	Limits of morphological stabilization by anaerobic storage . . . . .	37
2.5	Conclusions . . . . .	40
<b>3</b>	<b>Distribution of rbCOD via the anaerobic feeding mode</b>	<b>43</b>
3.1	Introduction . . . . .	44
3.2	Methodology. . . . .	45
3.2.1	Reactor set-up and operation . . . . .	45
3.2.2	Composition of synthetic wastewater . . . . .	46
3.2.3	Anaerobic kinetics and storage capacity for uptake of acetate . . . . .	47
3.2.4	Analytical procedures . . . . .	47
3.2.5	Calculation procedures. . . . .	49
3.3	Results . . . . .	50
3.3.1	Start-up . . . . .	50
3.3.2	Steady-state operation . . . . .	51
3.4	Discussion . . . . .	56
3.4.1	Acetate distribution over granule size fractions. . . . .	56
3.4.2	COD loading rate versus SRT. . . . .	59
3.4.3	Residual levels of PHA after aeration. . . . .	59
3.4.4	Impact of the feeding mode on anaerobic storage metabolism . . . . .	61
3.4.5	Practical implications . . . . .	62
3.5	Conclusions . . . . .	63
<b>4</b>	<b>On the mechanisms for aerobic granulation - model based evaluation</b>	<b>67</b>
4.1	Introduction . . . . .	68
4.2	Methodology. . . . .	71
4.2.1	Theoretical background . . . . .	71
4.2.2	Model overview . . . . .	73
4.2.3	Mathematical model description . . . . .	76
4.2.4	Metrics for the inequality of substrate distribution . . . . .	80
4.2.5	Size distribution . . . . .	80
4.3	Results and discussion . . . . .	82
4.3.1	Reference case . . . . .	82
4.3.2	Microbial selection . . . . .	84
4.3.3	Selective wasting. . . . .	85
4.3.4	Concentration gradients . . . . .	85
4.3.5	Selective feeding . . . . .	86
4.3.6	Granule forming substrate . . . . .	86
4.3.7	Breakage. . . . .	87
4.3.8	Model validity . . . . .	88
4.3.9	Further analysis . . . . .	88
4.3.10	Practical implications . . . . .	89
4.4	Conclusions . . . . .	90

---

<b>5</b>	<b>Implementation of selective pressures in a continuous-flow reactor</b>	<b>91</b>
5.1	Introduction . . . . .	92
5.2	Methodology . . . . .	94
5.2.1	Description of the Harnaschpolder WWTP . . . . .	94
5.2.2	Description of the pilot-scale CFR . . . . .	94
5.2.3	Anaerobic stage configurations . . . . .	95
5.2.4	Analytical procedures . . . . .	97
5.2.5	Specific activities of sludge size classes . . . . .	97
5.2.6	Calculation procedures . . . . .	99
5.3	Results . . . . .	102
5.3.1	Seed sludge characteristics . . . . .	102
5.3.2	Period I: two alternating anaerobic upflow selectors . . . . .	104
5.3.3	Period II: mixed anaerobic selector and anaerobic tank . . . . .	108
5.3.4	Biological treatment performance . . . . .	110
5.4	Discussion . . . . .	113
5.4.1	From mechanisms for growth of AGS in a SBR to a CFR . . . . .	113
5.4.2	Differences between selective pressures in SBRs and CFRs . . . . .	115
5.4.3	Distribution of microbial growth and activity . . . . .	116
5.4.4	Treatment capacity in a AGS-CFR versus a CFAS system . . . . .	117
5.5	Conclusions . . . . .	118
<b>6</b>	<b>Outlook</b>	<b>119</b>
6.1	Anaerobic distribution of substrate . . . . .	120
6.1.1	Experimental measurement . . . . .	120
6.1.2	Mathematical modeling . . . . .	121
6.2	Biomass redistribution within the sludge . . . . .	122
6.3	Stability of the granular matrix . . . . .	123
6.4	Development of continuous-flow AGS processes . . . . .	124
6.5	Application niche of AGS in CFRs . . . . .	126
6.6	Thoughts on research at pilot-scale . . . . .	127
	<b>References</b>	<b>128</b>
	<b>Acronyms</b>	<b>142</b>
	<b>Nomenclature</b>	<b>144</b>
	<b>Dankwoord</b>	<b>145</b>
	<b>Curriculum Vitæ</b>	<b>150</b>
	<b>List of publications</b>	<b>151</b>





# Summary

The development of the aerobic granular sludge (AGS) technology for the retrofit of existing continuous-flow reactors (CFRs) of wastewater treatment plants (WWTPs) using conventional activated sludge (CAS) has garnered increasing interest over the past decade, following the worldwide adoption of AGS technology in sequencing batch reactors (SBRs). The better settleability of AGS compared to flocculent AS would allow for process intensification of existing WWTPs, without the difficult conversion of often relatively shallow CFRs to deeper AGS-SBRs. The desire to extend the lifespan of the relatively new assets at the Harnaschpolder WWTP (Den Hoorn, The Netherlands) led to the initiation of the HARKOS research project. The primary goals were to determine the conditions for AGS formation in continuous-flow activated sludge (CFAS) systems, and to optimize process configurations for increased biological and hydraulic treatment capacity using AGS. Spontaneous aerobic granulation in CAS systems designed with an anaerobic stage for enhanced biological phosphorus removal (EBPR) has been reported for several WWTPs. Efforts have been made to identify the common denominators between these installations, mostly regarding the anaerobic selector stage. The principles behind the design of anaerobic selectors to select for well-settling flocculent sludge are shared to some extent with the process conditions that select for AGS in SBRs. Significant correlations between the design of the anaerobic selector stage, the wastewater composition and the observed degree of spontaneous granulation have not yet been found. As outlined in **Chapter 1**, this thesis project aimed to further clarify the role of the anaerobic phase in SBRs in the formation of AGS. In turn, this would facilitate the translation of the required process conditions to CFAS systems for process intensification.

In **Chapter 2**, first the role of anaerobic bottom-feeding of AGS-SBRs was investigated in light of the function of anaerobic selectors of continuous-flow CAS systems to ensure complete removal of readily biodegradable chemical oxygen demand (rbCOD) prior to the aeration stage. This prevents so-called 'overshoot' of rbCOD and subsequent transport-limited substrate uptake under aerobic conditions, which in turn prevents filamentous bulking of the AS and ensures good settleability. Although anaerobic selectors are designed with a certain degree of plug-flow, substantial dispersion can occur in practice leading to incomplete anaerobic removal of rbCOD and the aforementioned adverse effects on the settleability of flocculent sludge. The anaerobic bottom-feeding in AGS-SBRs shares this purpose to ensure a well-settling sludge morphology. However, the effect of a partial overshoot the rbCOD in the wastewater to the aeration stage on the morphology and settleability of AGS has not been studied, specifically considering the stability of the

microbial selection for anaerobic storage and the selective wasting of excess sludge based on settleability. This was experimentally investigated using a lab-scale SBR in which a fraction of the total acetate load was dosed aerobically. This aerobically dosed fraction was increased stepwise while monitoring granular morphology. A good granular morphology and a sludge volume index after settling (SVI) of  $40 \text{ mL g}_{\text{TSS}}^{-1}$  were obtained during initial enrichment and maintained for  $\leq 20\%$  aerobic acetate load dosed at  $4 \text{ mg}_{\text{COD}} \text{ g}_{\text{VSS}}^{-1} \text{ h}^{-1}$ . Biological phosphorus removal efficiency was initially unaffected, but the aerobic acetate dosage rate did decrease the specific phosphate uptake rate (SPUR). This led to loss of phosphorus removal for  $>20\%$  aerobic acetate load dosed at  $8 \text{ mg}_{\text{COD}} \text{ g}_{\text{VSS}}^{-1} \text{ h}^{-1}$  over the course of 12 days. Subsequently, significant outgrowth formed on the granular surfaces and developed over time into finger-like structures. Under these high aerobic acetate loads the SVI increased to  $80 \text{ mL g}_{\text{TSS}}^{-1}$  and resulted in significant biomass washout due to deteriorating settling properties. The sludge settleability and biological phosphorus removal recovered 10 days after the aerobic feeding of acetate was stopped. Aerobic presence of rbCOD can be tolerated if mostly anaerobic acetate uptake is maintained, thereby ensuring stable granular morphology and good settleability. The high enrichment of polyphosphate-accumulating organisms (PAOs) in the granular sludge resulting from bottom-feeding and selective wasting of flocs makes AGS resilient to morphological deterioration in aerobic presence of rbCOD.

The attention then turned to the role of the anaerobic stage in the distribution of substrate over the sludge particle population in **Chapter 3**. The concept of substrate distribution is unique for biofilm systems since the granule size distribution gives the opportunity to impose a different loading based on differences in settleability, while this is not the case for flocculent AS with a more uniform size distribution. AGS has been formed in lab-scale reactors fed with synthetic wastewater containing only rbCOD with both anaerobic bottom-feeding through a settled bed (i.e. resembling the operation of full-scale AGS-SBRs) and pulse-feeding with all sludge in suspension (i.e. a proxy for an anaerobic selector of a CFAS system with a perfect plug-flow) combined with selective wasting of excess sludge. How both modes of anaerobic contact affect the distribution of substrate, the resulting granule size distribution and biological nutrient removal (BNR) was unknown. Therefore, two lab-scale SBRs were operated: one using bottom-feeding through a settled sludge bed, and another in which synthetic wastewater was fed as a pulse at the start of the anaerobic phase while the reactor was mixed through sparging of nitrogen gas. The distribution of substrate over the sludge population as storage polymers was quantified and combined with the obtained granule size distribution. Bottom-feeding was found to primarily direct substrate towards the large granular size classes (i.e. large volume and close to the bottom), while completely mixed pulse-feeding gives a more equal distribution of substrate over all granule sizes (i.e. surface area dependent). The anaerobic feeding mode directly controls the substrate distribution over the different granule sizes, irrespective of the solids retention time (SRT) of a granule as an entity. Preferential feeding of the larger granules will enhance and stabilize the granulation compared to

pulse-feeding, certainly under less advantageous conditions imposed by real sewage that only partially consists of rbCOD.

Both anaerobic feeding modes were again compared in **Chapter 4**, where the process conditions in the anaerobic feeding phase that affect the distribution of substrate were combined with other factors in a framework of six mechanisms hypothesized to govern aerobic granulation. The distribution of the limited amount of rbCOD in domestic wastewater over the sludge particle population in the anaerobic phase was again of interest. The role of the anaerobic stage to ensure microbial selection for anaerobic storage of rbCOD and the maximization of the penetration depth of rbCOD into sludge particles were the first two mechanisms. Both are also functions of the anaerobic selector in CFAS systems. In addition, selective feeding of the best settling sludge fraction with the available rbCOD through bottom-feeding in the anaerobic phase was investigated as a driver of aerobic granulation in full-scale AGS-SBRs. All three were combined with three other mechanisms (selective wasting, the type of substrate and breakage of granules) in a numerical model that was developed using four main components: a 1D convection-dispersion model to describe the flow dynamics in a reactor, a reaction-diffusion model describing the essential conversions for growth inside a granule, a setting model to track granules during settling and feeding, and a population model containing up to 100,000 clusters of granules to capture the stochastic behavior of the granulation process. The model could explain the dynamics of the granulation process observed in practice, including the presence of a lag phase and a granulation phase. Selective feeding was identified as an important mechanism that was not yet reported in literature. The ratio of granule forming substrates (GFS) to non-GFS together with the feast/famine ratio determine if the transition from the lag phase to the granulation phase can be successful. The efficiency of selective wasting and selective feeding both determine the rate of this transition. Breakage of large granules into smaller well settling particles was shown to be an important source for new granules. The granulation process was found to be the combined result from all six mechanisms and if conditions for either one are not optimal, other mechanisms can, to some extent, compensate. This model provides a theoretical framework to analyze the different relevant mechanisms for AGS formation and can form the basis for a model that includes detailed nutrient removal conversions.

In **Chapter 5**, the insights from the previous chapters were used to develop a CFR concept that best mimics the selective pressures for aerobic granulation from full-scale AGS-SBRs. The concept was implemented in a pilot-scale CFR, fed with pre-settled wastewater from the Harnaschpolder WWTP. The growth of AGS was investigated, with again a focus on the effect of the design of the anaerobic stage on the distribution of rbCOD. Metrics were established to assess the degree to which the mechanisms proposed in chapter 4 were implemented in the pilot-scale CFR. The selective pressures for granular sludge formation were implemented using anaerobic upflow selectors with a water depth of 2.5 meters, which yielded a sludge with properties similar to AGS from full-scale SBRs. In comparison to the CFAS system at Harnaschpolder WWTP treating the same

pre-settled wastewater, a more than two-fold increase in volumetric removal capacity for both phosphorus and nitrogen was achieved. The use of a completely mixed anaerobic selector, as opposed to an anaerobic upflow selector, caused a shift in EBPR activity from the largest towards the smallest size class, while nitrification was largely unaffected. Using an anaerobic upflow selector with bottom-feeding is, therefore, favorable for the long-term stability of AGS, especially for less fermented wastewater. The research underlines the potential of AGS for enhancing the hydraulic and biological treatment capacity of existing continuous-flow CAS systems.

**Chapter 6** discusses research topics to further develop the understanding of the formation of AGS and to expedite the application of AGS in existing CFAS systems.

# Samenvatting

De ontwikkeling van de aerob korrelslib-technologie (AGS) voor het vergroten van de capaciteit van bestaande continu doorstroomde reactoren (CFR's) binnen afvalwaterzuiveringsinstallaties (AWZI's) met conventioneel actiefslib (CAS) heeft het afgelopen decennium steeds meer aandacht gekregen, volgend op de wereldwijde uitrol van de AGS-technologie in batchgewijs bedreven reactoren (SBR's). De betere bezinkbaarheid van AGS in vergelijking met vlokkig actiefslib (AS) maakt procesintensivering van bestaande AWZI's mogelijk binnen de bestaande ruimte, zonder de ombouw van continue actiefslibprocessen (CFAS) met vaak relatief ondiepe bassins naar diepere AGS-SBR's. De wens om de levensduur van de relatief nieuwe installaties van AWZI Harnaschpolder (Den Hoorn, Nederland) te verlengen, was de aanleiding voor het HARKOS onderzoeksproject. De belangrijkste doelen waren om de voorwaarden voor de vorming van AGS in CFAS-processen te bepalen, en te onderzoeken hoe CFAS-configuraties te optimaliseren voor een verhoogde biologische en hydraulische zuiveringscapaciteit met behulp van AGS. Spontane groei van AGS in CFAS-systemen ontworpen met een anaerobe fase voor biologische fosfaatverwijdering (bio-P) werd reeds geobserveerd in verschillende AWZI's. Er zijn pogingen gedaan om de gemeenschappelijke kenmerken tussen deze installaties te identificeren, vooral met betrekking tot het ontwerp van de anaerobe selector. De principes achter het ontwerp van anaerobe selectoren met als doel om goed bezinkend vlokslib te vormen, komen overeen met de procesomstandigheden die in SBR's leiden tot de vorming van AGS. Significante correlaties tussen het ontwerp van anaerobe selectoren, de samenstelling van het afvalwater en de mate van spontane korrelvorming waren echter nog niet gevonden. Zoals uiteengezet in **Hoofdstuk 1** beoogde dit proefschrift het begrip van de rol van de anaerobe fase in SBR's bij de vorming van AGS verder te verduidelijken, om vervolgens de hiervoor benodigde procesomstandigheden te vertalen naar CFAS-systemen voor procesintensivering.

In **Hoofdstuk 2** is eerst de rol van anaerobe bodemvoeding van AGS-SBR's onderzocht in het licht van de functie van anaerobe selectoren van CFAS-systemen om volledige verwijdering van direct biodegradeerbaar organisch substraat (dbCZV) vóór de aeratiezone te waarborgen. Dit voorkomt doorslag van dbCZV en daaropvolgende transportgelimiteerde opname van substraat onder aerobe omstandigheden, wat vervolgens de groei van draadvormende bacteriën in het actiefslib voorkomt en een goede bezinkbaarheid waarborgt. Hoewel anaerobe selectoren worden ontworpen met een bepaalde mate van propstroming, kan in de praktijk aanzienlijke dispersie optreden,

wat leidt tot onvolledige anaerobe verwijdering van dbCZV en de eerder genoemde nadelige effecten op de bezinkbaarheid van het vlokslib. anaerobe bodemvoeding in AGS-SBR's heeft dezelfde functie. Het effect van gedeeltelijke doorslag van het dbCZV in het afvalwater naar het beluchtungsstadium op de morfologie en bezinkbaarheid van AGS is echter nog onvoldoende bestudeerd, waarbij met name de stabiliteit van de microbiële selectie voor anaerobe opslag in combinatie met het selectief onttrekken van surplusslib op basis van bezinkbaarheid aandacht verdient. Dit werd experimenteel onderzocht met behulp van een SBR op laboratoriumschaal waarin een fractie van de totale acetaatbelasting in de aerobe fase werd gedoseerd. Deze fractie werd stapsgewijs verhoogd terwijl de morfologie van het korrelslib werd gevolgd. Een goede korrelmorfologie en een slibvolume-index van  $40 \text{ mL g}_{\text{DS}}^{-1}$  werden verkregen tijdens de opstart met enkel anaerobe belasting en bleven behouden tot een aerobe acetaatbelasting van  $\leq 20\%$ , gedoseerd bij  $4 \text{ mg}_{\text{CZV}} \text{ g}_{\text{VS}}^{-1} \text{ uur}^{-1}$ . De efficiëntie van biologische fosfaatverwijdering werd aanvankelijk niet beïnvloed, maar de snelheid van aerobe fosfaatopname nam wel af met toenemende doseersnelheid. Dit leidde tot verlies van biologische fosfaatverwijdering bij  $>20\%$  aerobe acetaatbelasting, gedoseerd bij  $8 \text{ mg}_{\text{CZV}} \text{ g}_{\text{VS}}^{-1} \text{ uur}^{-1}$  gedurende 12 dagen. Vervolgens vormde zich significante uitgroei op het oppervlak van de korrels die zich in de loop van de tijd tot vingerachtige structuren ontwikkelden. Onder deze hoge aerobe acetaatbelastingen nam de SVI toe tot  $80 \text{ mL g}_{\text{DS}}^{-1}$ , wat aanzienlijke uitspoeling van biomassa tot gevolg had door verslechterde bezinkeigenschappen. De bezinkbaarheid van het slib en de biologische fosfaatverwijdering herstelden zich 10 dagen nadat de aerobe acetaatvoeding was gestopt. aerobe aanwezigheid van dbCZV kan dus worden getolereerd als voornamelijk anaerobe acetaatopname wordt gehandhaafd, wat zorgt voor een stabiele korrelmorfologie en goede bezinkbaarheid. De hoge verrijking van fosfaataccumulerende organismen in het korrelslib door anaerobe bodemvoeding en het selectief afvoeren van vlokslib als surplusslib maakt AGS bestand tegen morfologische achteruitgang in de aanwezigheid van dbCZV onder aerobe condities.

Voor **Hoofdstuk 3** verschoof de aandacht naar de rol van de anaerobe fase in de verdeling van substraat over de slibdeeltjespopulatie. Het concept van substraatverdeling is uniek voor biofilmsystemen, aangezien de korrelgrootteverdeling de mogelijkheid biedt om een verschillende belasting op te leggen op basis van verschillen in bezinkbaarheid, terwijl dit niet het geval is voor vlokkig actiefslib met een meer uniforme grootteverdeling. AGS is in eerder onderzoek gevormd in SBR's gevoed met synthetisch afvalwater dat alleen dbCZV bevatte via zowel anaerobe bodemvoeding door een bezonken slibbed (vergelijkbaar met de werking van volleschaal AGS-SBR's), als via pulsdosering met al het slib in suspensie (een proxy voor de anaerobe selector van een CFAS-systeem met een perfecte propstrooming) in combinatie met selectieve afvoer van surplusslib. Hoe beide modi van anaerobe voeding de verdeling van substraat, de resulterende korrelgrootteverdeling en biologische nutriëntenverwijdering beïnvloeden, is onbekend. Daarom werd onderzoek gedaan met twee SBR's op laboratoriumschaal: één met bodemvoeding door een bezonken slibbed, en een andere waarbij synthetisch afvalwater

als puls aan het begin van de anaerobe fase werd gevoed terwijl de reactor werd opgemengd door met stikstofgas. De verdeling van het substraat over de slibpopulatie in de vorm van opslagpolymeren werd gekwantificeerd en per reactor gecombineerd met de korrelgrootteverdeling. Bodemvoeding blijkt het substraat voornamelijk richting de grote korrels te leiden (met een groot volume en dicht bij de bodem), terwijl volledig gemengde pulsdosering zorgt voor een meer gelijke verdeling van substraat over alle korrelgroottes (afhankelijk van het oppervlak van een korrel). De anaerobe voedingsmodus bepaalt daarmee rechtstreeks de verdeling van het substraat over de verschillende korrelgroottes, ongeacht de slibleeftijd van een korrel in de reactor. Selectieve voeding van de grootste korrels zal de korrelvorming verbeteren en stabiliseren in vergelijking met pulsdosering, zeker onder minder gunstige omstandigheden bij de behandeling van echt afvalwater dat slechts gedeeltelijk bestaat uit dbCZV.

In **Hoofdstuk 4** werden beide anaerobe voedingsmodi opnieuw vergeleken. De procesomstandigheden in de anaerobe voedingsfase die de verdeling van substraat beïnvloeden, werden gecombineerd met andere factoren. Samen vormden ze zes mechanismen waarvan werd verondersteld dat deze gezamenlijk de vorming van aerob korrelslib kunnen beschrijven. De verdeling van de beperkte hoeveelheid dbCZV in huishoudelijk afvalwater over de slibdeeltjespopulatie in de anaerobe fase is opnieuw een belangrijk aspect. De eerste twee mechanismen in de anaerobe fase zijn het waarborgen van de selectie voor anaerobe opslag van al het beschikbare dbCZV en het maximaliseren van de penetratiediepte van dbCZV in slibdeeltjes door het stromingsprofiel. Beide principes worden ook toegepast in anaerobe selectoren van CFAS-systemen om de bezinkbaarheid van vlokkelig actiefslib te maximaliseren. Daarnaast werd selectieve voeding van de best bezinkende slibfractie met het beschikbare dbCZV via bodemvoeding in de anaerobe fase toegevoegd om de rol in groei van korrelslib in full-scale SBR's te onderzoeken. Deze drie werden gecombineerd met drie andere mechanismen (selectieve afvoer van surplusslib, het type substraat en het opbreken of eroderen van korrels) in een numeriek model dat bestond uit vier hoofdcomponenten: een 1D-convectie-dispersiemodel om de stromingsdynamiek in een reactor te beschrijven, een reactie-diffusiemodel dat de indringing en opname van substraat in korrels beschrijft, een model om de positie van korrels tijdens de bezinkfase en de voedingsfase bij te houden, en een populatiemodel met maximaal 100.000 clusters van korrels om het stochastische gedrag van het proces van korreling te vangen. Het model kon de dynamiek van de korrelvorming beschrijven zoals dat in de praktijk wordt waargenomen, inclusief de aanwezigheid van een opstartfase en korrelfase. Selectieve voeding is geïdentificeerd als een belangrijk mechanisme dat nog niet eerder in de literatuur is beschreven. De verhouding van korrelvormend en niet-korrelvormend substraat bepaalt samen met de feast/famine-verhouding of de overgang van de opstartfase naar de korrelfase kan plaatsvinden. De efficiëntie van het selectief spuien van slib en het selectief voeding bepalen de snelheid van deze overgang. Het opbreken van grote korrels in kleinere goed bezinkbare deeltjes bleek een belangrijke bron voor nieuwe korrels. Korrelvorming blijkt



het gecombineerde resultaat te zijn van alle zes mechanismen. Als de omstandigheden voor één mechanisme niet optimaal zijn, kunnen andere mechanismen dit tot op zekere hoogte compenseren. Dit model biedt een theoretisch kader om de verschillende relevante mechanismen voor de vorming van AGS te analyseren en kan de basis vormen voor een meeromvattend model dat eveneens nutriëntenverwijdering kan beschrijven.

In **Hoofdstuk 5** werden de inzichten uit de voorgaande hoofdstukken gebruikt om een continue reactorconfiguratie CFR te ontwikkelen waarin de selectiedruk voor aerobe korrelvorming het beste wordt nagebootst, zoals toegepast in AGS-SBR's op volleschaal. Het concept werd geïmplementeerd in een reactor op pilotschaal, gevoed met voorbezonden afvalwater van de AWZI Harnaschpolder. De groei van AGS werd onderzocht, met opnieuw de nadruk op het effect van het ontwerp van de anaerobe zone op de verdeling van dbCZV. Eveneens werden maatstaven voorgesteld om te beoordelen in welke mate de mechanismen, zoals voorgesteld in hoofdstuk 4, zijn toegepast in de CFR. De anaerobe selectiedruk voor de vorming van AGS werd geïmplementeerd door gebruik te maken van selectoren met een waterdiepte van 2,5 meter en een opwaartse stroming van influent door een gestapeld slibbed, wat resulteerde in een slib met eigenschappen vergelijkbaar met AGS uit volleschaal SBR's. In vergelijking met het CFAS-systeem van Harnaschpolder WWTP dat hetzelfde verbezonden afvalwater behandelt, werd meer dan een verdubbelde volumetrische verwijderingscapaciteit bereikt voor zowel fosfaat als stikstof. Het gebruik van een volledig gemengde anaerobe selector, in plaats van een selector met opwaartse stroming, veroorzaakte een verschuiving in bio-P activiteit van de grootste naar de kleinste korrelfracties, terwijl de verdeling van nitrificerende activiteit grotendeels onaangetast bleef. anaerobe selectieve voeding via bodemvoeding is daarom gunstig voor de stabiliteit van AGS op lange termijn, vooral bij behandeling van minder voorverzuurd afvalwater. Deze uitkomst benadrukt het potentieel van AGS om de hydraulische en biologische zuiveringscapaciteit van bestaande CFAS-systemen te verbeteren.

**Hoofdstuk 6** bespreekt onderzoeksonderwerpen om het begrip van de vorming van AGS verder te verbeteren en de toepassing van AGS in bestaande CFAS-systemen naderbij te brengen.

# Preface

This thesis is an outcome of the HARKOS project, centered around the Harnaschpolder WWTP. The research project was initiated by the public-private partnership (PPP) between the Deland Water Authority (DWA) and the Delfluent consortium, which was founded specifically to register for the tender of the project Afvalwater Haagse Regio (AHR). The AHR project was initiated in 1999 by the DWA due a demand for increased sewage treatment capacity in the The Hague area (The Netherlands) and the more stringent effluent requirements from the first European Union (EU) Council Directive (91/271/EEC) [28] concerning urban wastewater treatment. The main pillar of the project was the construction of the Harnaschpolder WWTP, which has to this day the largest design capacity of the The Netherlands, able to treat 1.3 million population equivalents. The PPP with a design, build, finance and operate (DBFO) contract until 2033 was the first of its kind in The Netherlands due to the unprecedented scale of the project, which also included the upgrade of the existing Houtrust WWTP (400,000 population equivalents) and more than 100 km of sewer works.

In 2015, almost a decade after the commissioning of the Harnaschpolder WWTP in 2006, discussions began on how to make sure that the assets of DWA in the The Hague region would be ready for the future needs at the end of the PPP with the Delfluent consortium. These discussion took into account the continuing increase in population density of the catchment area, more stringent future effluent requirements, and ambitions towards more sustainable and climate neutral sewage treatment. At the time of writing, the agreements from the Paris Climate Accords of 2016 had been implemented in the Dutch national law as the 'Klimaatwet' in 2019, which were subsequently adopted by the DWA to achieve energy neutral operation by 2025 and climate neutrality by 2035 [155]. Furthermore, the revision of the EU Council Directive concerning urban wastewater treatment towards more stringent effluent requirements is currently underway [125]. Expanding the capacity of the Harnaschpolder WWTP by increasing the volume of the biological treatment stage was not considered feasible. The remaining area on site will be likely needed for the mandatory quaternary treatment (i.e. removal of organic micro-pollutants) and the capture of renewable energy, while off-site expansion was becoming increasingly difficult. Urbanization had, quite literally, arrived on the doorstep (figure 1).

Several concept were considered at the time, including the AGS technology that in the previous decade had been scaled-up from lab-scale to pilot-scale [39], and subsequently to full-scale [168, 57, 122]. The technology was developed at the Delft University of

Technology and commercialized by Royal HaskoningDHV under the trade name Nereda®. However, the conversion of a relatively new continuous-flow WWTP of this magnitude to the SBR concept was deemed not economical, and technically impractical. The desire to extend the lifespan of the existing assets, combined with the shared foundation between the CAS process used at the Harnaschpolder WWTP and the recently developed AGS process (see section 1.6), led to the initiation of the HARKOS research project. Two utilities (the Delfland Water Authority and the Rijnland Water District Control Board), members of the Delfluent consortium (Evides Industriewater and Delfluent Services), the Delft University of Technology and Royal HaskoningDHV formed a partnership to investigate the feasibility of a retrofit process based on AGS to increase the treatment capacity of CFAS systems. The project had two main goals, namely to

- determine which process conditions have to be implemented in an existing CFAS process for the formation of AGS, and
- investigate how to adjust the configuration of a CFAS system to make optimal use of the properties of the AGS for increased biological and hydraulic treatment capacity.

Lab-scale research and mathematical modeling were conducted within the Environmental Biotechnology research group of the Delft University of Technology (chapters 2 to 4). In parallel, a continuous-flow pilot-scale reactor was operated in the Delft Blue Innovations (DBI) [45] research facility located on-site the Harnaschpolder WWTP, using the pre-settled domestic wastewater as influent (chapter 5). Insights obtained from the experimental and numerical work were used to improve the pilot-scale reactor, and vice-versa. The outcomes of the research efforts are described in this thesis.



Figure 1: Aerial photographs of the Harnaschpolder WWTP in 2016 (left) and 2021 (right). The greenhouse horticulture has made room for a suburban neighborhood. On the other side, the foundations of a hotel are visible that is under construction. Courtesy of Delfluent Services.

# 1

## General introduction

## 1.1. Municipal wastewater treatment

The history of treatment of domestic wastewater has been covered extensively by others, also for the developments in The Netherlands [90], and here only the essentials will be covered. The development of sewer systems to discharge domestic wastewater further away from cities has been linked to urbanization of societies. As cities grew larger and the population density increased, disposal of solid and liquid organic waste became more and more important to prevent to spread of disease through contamination of sources used for drinking water. The societal impact of epidemics due to the lack of sanitation peaked during the industrial revolution at the end of the 19<sup>th</sup> century. The extent of the urbanization caused deterioration of the ecological quality of the surface waters receiving the domestic wastewater in increasingly larger areas around the cities. Not only were more sources of drinking water becoming contaminated, but eutrophication of surface waters caused problems for the production of food for human consumption as well. On the other hand, urine and feces from cattle and human origin were extensively used as a source of fertilizer for the same purpose well into the 20<sup>th</sup> century.

Technologies for the actual treatment of domestic wastewater were limited at the beginning of the 20<sup>th</sup> century (rather than only discharging it elsewhere through sewer systems and rivers, ultimately to the sea). Flow fields were the most used technique that removed biodegradable organic matter through aerobic microorganisms as the wastewater infiltrated into the soil, while at the same time the area could be used for cultivation of crops using the remaining nutrients as fertilizer (nitrogen and phosphorus). The wastewater was ultimately infiltrated into the soil. However, the required surface area was quite large: one hectare per 100-200 inhabitants [90]. In comparison: the Harnaspolder WWTP (Den Hoorn, The Netherlands) at present treats the wastewater of more than 1 million inhabitants at a surface area of only 25 ha, with a superior effluent quality. Septic tanks could provide a form of pre-treatment in which the solids in the wastewater were settled and retained, through which the organic matter in the solids was converted into (odorous) gases. This was a process known as (anaerobic) stabilization, meaning that remaining waste stream was less susceptible to rotting. Flow fields and septic tanks can be considered the first forms of biological treatment of wastewater by design. These techniques were successful in removing organic matter and phosphate, but removal of nitrogen was very limited.

### 1.1.1. 'Conventional' activated sludge

Several attempts were made to investigate the effect of blowing air through wastewater as a form of treatment in the USA and in Europe during the last two decades of the 19<sup>th</sup> century. Partial oxidation of organic matter and the oxidation of nitrogen was achieved in several occasions and it was shown that the removal was coupled to the presence of oxygen in the air. Whether this was due to physical or biological processes remained disputed until the 1930s [136], but was decided in favor of the latter. The breakthrough in terms of process development was achieved in 1914, when Ardern and Lockett [6] included a clarification

step in the sequential fill-and-draw process to retain the solids that had been produced during the aeration step. The solids, which accumulated after each batch of wastewater that was treated, showed an increasing oxidation rate of nitrogen over the course of several weeks, which shortened the required residence time from multiple days to several hours for the same treatment result. The solids were named 'activated sludge' (AS), later shown to be consortia of microorganisms. In the absence of mixing, the sludge flocculated to larger aggregates of several millimeters that settled sufficiently fast to separate it from the treated wastewater in a full-scale process.

The early history and the subsequent improvement of the AS process during the 20th century has been covered in detail elsewhere [71]. As the first full-scale treatment facilities were constructed in rapid succession, the batchwise fill-and-draw configuration was abandoned in favor of continuous-flow reactors in which the process steps were separated in space (i.e. aeration tanks and sedimentation tanks) to the lower operational complexity [185]. After the AS was separated from the effluent (i.e. treated wastewater), it was returned to the aeration stage to be combined with 'fresh' wastewater to be treated. The improvements up to the second world war were mostly made in the efficiency of the aeration system and configuration of the aeration stage. For example, compact AS systems used aerobic contact stabilization with a high loading rate ( $\text{kg}_{\text{BOD}_5} \text{kg}_{\text{TSS}}^{-1} \text{d}^{-1}$ ) or food-to-microbe (F/M) ratio, and short solids retention times (i.e. the average time AS was retained in the system prior to discharge as excess sludge) to remove most organic material from wastewater through biosorption with minimum oxidation. Anaerobic digestion was subsequently used for further stabilization. AS systems were also designed with extended aeration using long SRTs and low loading rates to perform aerobic stabilization and minimize sludge production. The conversion processes remained mainly the oxidation of organic matter to carbon dioxide and ammonia to nitrate (process of nitrification).

Major advances were made in the second half of the century with respect to the conditions to select for the desired microorganisms and biological conversion of nitrogen and phosphorus. The continuous-flow configuration remained the basis for most developments. An exception was the oxidation ditch developed by A. Pasveer in The Netherlands (figure 1.1) for low-cost wastewater treatment of small communities [111], which is a fill-and-draw process (later also developed into a continuous-flow concept under the tradename Carrousel®). Progress was made in two main areas [71]:

- development of the selector concept to improve sludge settleability and prevent filamentous bulking, deteriorating the settleability of the flocculent sludge and hampering final clarification (see section 1.6), and
- extension of the process configuration to include anaerobic and anoxic stages, leading to contemporary AS processes performing complete BNR of biochemical oxygen demand over 5 days ( $\text{BOD}_5$ ), ( ) and phosphorus (P) through enrichment for denitrification (i.e. reduction of nitrate to dinitrogen gas using organic carbon) and EBPR [142],

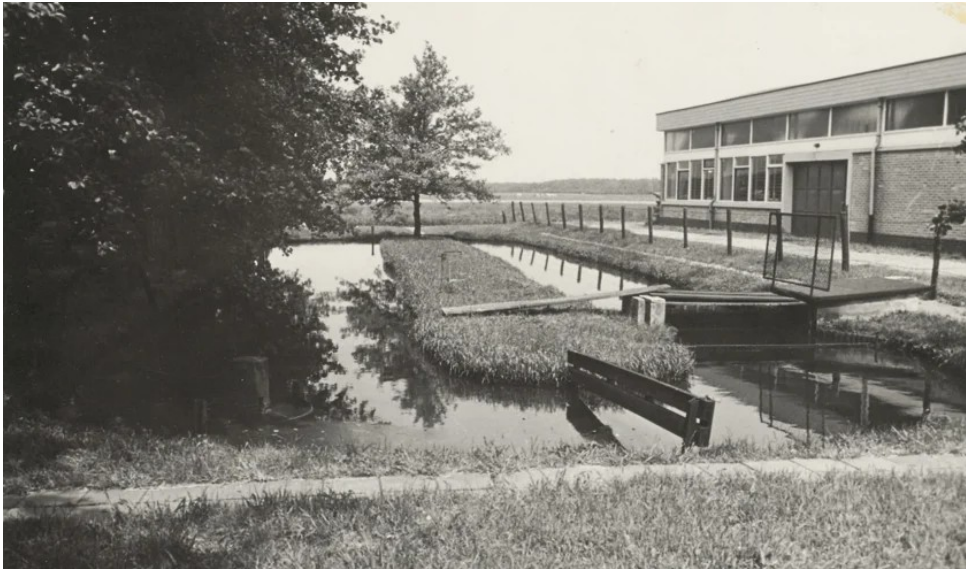


Figure 1.1: First oxidation ditch ('oxydatiesloot' in Dutch) in the Netherlands by the design of A. Pasveer in the town of Voorschoten, commissioned in 1954. It was decommissioned when the neighborhood 'Dobbewijk' (400 population equivalents) was connected to the main sewer networks and the centralized wastewater treatment system in 1996(!). Courtesy of the Rijnland District Water Control Board.

respectively.

The terminology to distinguish the various concepts also changed as altered process configurations were being developed. The adjective 'conventional' was already used shortly after the first conception to distinguish the initial system with uniform aeration from the concept of tapered aeration, for example [136]. At present, the term CAS is used to distinguish the state-of-the-art process configuration for BNR with complete nitrogen removal and EBPR with loading rates of  $<0.05 \text{ kg}_{\text{BOD}}, \text{ kg}_{\text{VSS}}^{-1} \text{ d}^{-1}$  from other technologies that allow for more compact treatment systems (section 1.3). Many variants exist, with a common strategy to maximize the use the available organic matter for anaerobic conversion to storage polymers for EBPR and the subsequent utilization of this stored carbon for denitrification [164]. Which configuration is most suited depends on the composition of the wastewater to be treated, the local effluent requirements and possibly the layout of existing infrastructure.

An overview of the Harnaschpolder WWTP is shown in figure 1.2 as an example of a contemporary WWTP. The hydraulic design capacity of the WWTP is a daily dry weather flow (DDWF) of  $215\,000 \text{ m}^3 \text{ d}^{-1}$ . Raw municipal wastewater, supplied via pressure mains, first passes step screens with a mesh size of 6 mm. It then passes through the primary clarifiers, from which the primary sludge is thickened and subsequently treated by the anaerobic digesters. The primary effluent flows to the BNR-stage with a water depth of

8 m. Primary effluent is first directed to the anaerobic selector and combined 45 % of the return sludge flow from the secondary clarifiers with a mean hydraulic residence time (HRT) of 24 min to select for EBPR. The mixed liquor is then combined with remaining 55 % of the return sludge in the pre-denitrification (pre-DN) zone with a mean HRT of 16 min, followed by a completely mixed anaerobic compartment with a mean HRT of 1.7 h. The mixed liquor then passes to the outer ring in which it is recirculated on average 27 times through an aerated zone using tube aeration and an anoxic zone of which the volumes can be adjusted through the aeration strategy. The outer ring has an average liquid velocity of  $25 \text{ cm s}^{-1}$  to ensure the suspension of the flocculent sludge. Mixed liquor finally overflows to the secondary clarifiers for solid-liquid separation, after which the effluent is discharged and the sludge returned to the anaerobic selector. Part of return sludge is directed as excess secondary sludge to the anaerobic digesters.

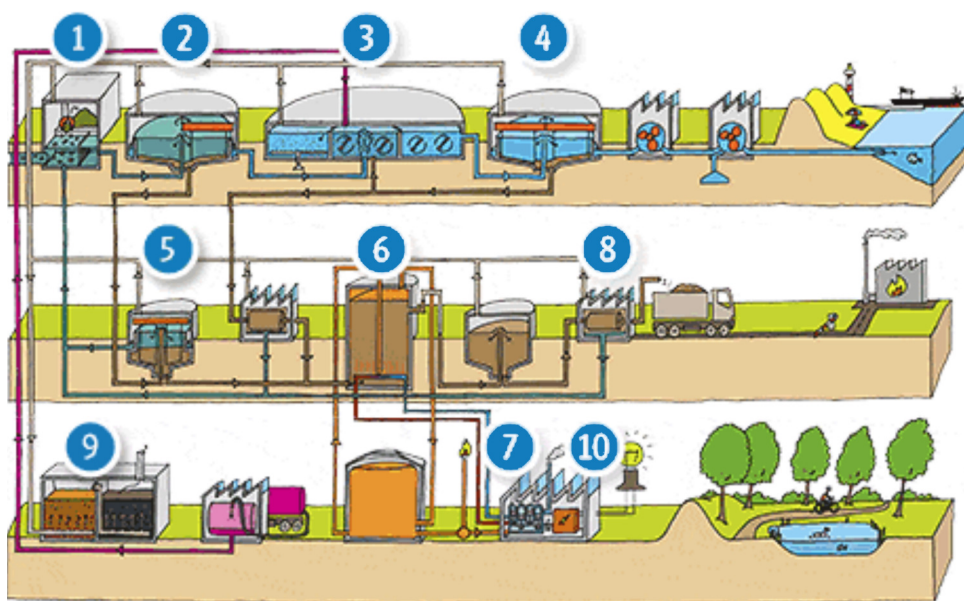
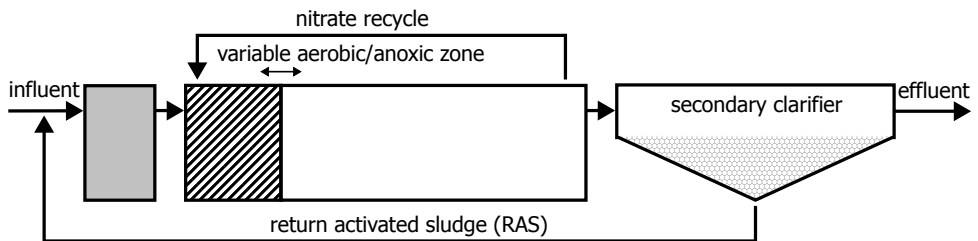


Figure 1.2: Stages of the water line, sludge line and utility line of the Harnaspolder WWTP: (1) step screens (6 mm), (2) primary clarification, (3) BNR, (4) secondary clarification, (5) primary sludge thickening and grit removal, (6) anaerobic digestion of primary sludge and excess AS, (7) cogeneration of heat and energy from biogas, (8) thickening of digested sludge and transport for incineration, (9) biological odor treatment and (10) emergency generators. Courtesy of Delfluent Services.

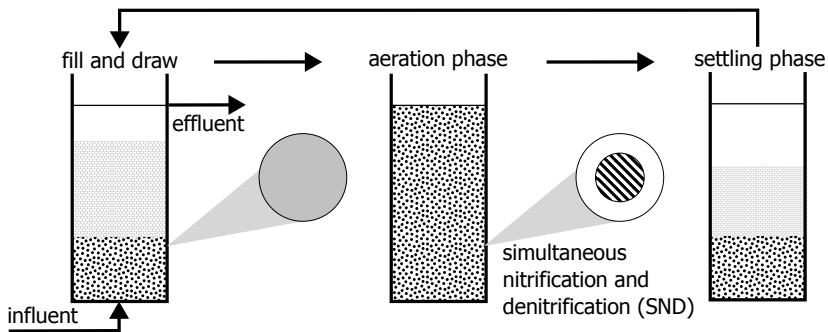
A more detailed schematic of the BNR-stage with a fixed recirculation of nitrate and aerobic/anoxic zones with variable volumes (PhoSim concept [164]) is depicted in figure 1.3a, as well as the biological conversions taking place. Strategies to increase the treatment capacity of similar existing WWTPs with CAS within the existing process volume will be discussed next.



## CONVENTIONAL ACTIVATED SLUDGE (CONTINUOUS-FLOW REACTOR)



## AEROBIC GRANULAR SLUDGE (SEQUENCING BATCH REACTOR)



- 
- anaerobic zone (EBPR: phosphate release)
  - anoxic zone (denitrification, EBPR: phosphate uptake)
  - aerobic zone (nitrification, oxidation of organics, EBPR: phosphate uptake)
  - flocculent sludge
  - granular sludge

Figure 1.3: (a, top) Schematic representation of the zones in of the BNR stage according to the PhoSim configuration and the biological conversions performed by the AS in the respective zones. (b, bottom) Schematic representation of the phases in a cycle of a typical AGS-SBR process and the biological conversions taking place in the respective phases and in the redox layers of the AGS.

## 1.2. Process intensification in activated sludge systems

Choosing the most suitable technology to obtain improved performance of an existing municipal WWTP is not a straightforward task. In most cases, an increase in treatment capacity within the existing infrastructure is the primary objective, either hydraulic, biological, or both. Although the technology chosen to achieve this has implications for the overall sustainability and climate neutrality, these aspects will be treated as secondary objectives. Further discussion will focus on technologies to increase the treatment capacity within existing continuous-flow CAS systems by means of increasing the kinetics of the removal of pollutants from the wastewater. It is assumed that the desired effluent quality lies below the achievable limits for BNR using AS [164].

An increase in treatment capacity of the BNR stage specifically entails an increase in the peak dry weather flow (PDWF) loading rate while achieving the same effluent quality, vice-versa or both. The common denominator is that higher volumetric removal rates are required (e.g.  $\text{kg}_{\text{pollutant}} \text{m}_{\text{reactor}}^{-3} \text{d}^{-1}$ ) for the nutrient with the limiting removal rate, which is often nitrogen removal. The microorganisms employed to perform nitrification are autotrophs that exhibit the lowest growth rate in the microbial community due to the need to fix and reduce  $\text{CO}_2$  as the carbon source. Therefore, they are prone to washout when operated at too low SRTs. The aerobic reactor volumes of AS systems are therefore sized for sufficient oxidation of ammonium at the lowest seasonal temperatures. More advanced BNR-systems designed for complete nitrogen removal employ additional anoxic volume for the process of denitrification. Also in this case, the nitrification capacity determines the required aerobic reactor volume. An increase in the volumetric loading rate would require a larger aeration zone which would come at the expense of the anoxic volume, limiting the total nitrogen removal and resulting in a loss of effluent quality. The decrease in effluent quality will be less in systems designed for (partial) simultaneous nitrification and denitrification (SND) [164], but the general principle holds: an increase in biological treatment capacity requires higher nutrient removal rates, of which the nitrification capacity is often the limiting factor.

## 1.3. Concepts for process intensification

One way to achieve increased removal rates is to increase the biomass specific conversion rates (e.g.  $\text{kg}_{\text{pollutant}} \text{kg}_{\text{biomass}}^{-1} \text{d}^{-1}$ ). The dependence of biomass specific conversion rates on residual concentrations can often be described by Monod-type kinetics [68]. Since CAS systems are often operated at residual nutrient concentrations in the first-order region, an increase these concentrations will lead to increased biological conversion rates and microbial growth rates. A concentration gradient in the mixed liquor can be achieved by compartmentalizing the reactor volume to increase the degree of plug-flow, since the design of AS systems has generally transitioned to completely mixed aerobic and anoxic zones with large recirculation factors for complete nitrogen removal. On the other hand, reducing the recirculation of mixed liquor between redox zones often inadvertently decreases the total nitrogen removal efficiency for which the system had been originally

designed (figure 1.3a). This approach is therefore not commonly applied for CAS systems.

The more common approach to obtain higher volumetric removal rates is to increase the amount of active biomass in the biological treatment stage. This ensures that the average SRT stays the same and therefore, the required minimum microbial growth rate stays the same. Several methods have been developed over the past two decades [33, 15] to increase volumetric removal rates in this way to varying extents. The concepts can be separated in two groups, depending on whether the additional biomass

- is retained in the biological treatment stage (section 1.4), or
- passes through the final clarification stage as well and is returned combined with the existing AS (section 1.5).

The distinction is relevant since the final clarification stage is sized at a certain hydraulic surface loading rate (SLR,  $m_{ML}^3 m_{area}^{-2} h^{-1}$ ) during peak rain weather flow (PRWF) in case of combined sewer systems for discharging sewage and storm water. The SLR is coupled to a certain the sludge volume after settling (SV,  $m_{SV} L_{ML}^{-1}$ ) through design guidelines to ensure that no sludge is lost via the effluent [110]. Concepts in which additional biomass passes through the clarifier would thus increase the sludge volume loading rate, which must be accompanied by an increase in overall sludge settleability to prevent washout of sludge during PRWF. For clarifier design, the sludge settleability is characterized by the SVI after 30 minutes (SVI<sub>30</sub>).

The characteristics of the technologies in both categories will be discussed next in more detail, mainly with respect to the means by which the increase in biomass is achieved.

## 1.4. Additional biomass on carrier media

The concept of these technologies is to increase the amount of biomass in the biological stage and retain it there, while (part) the existing AS in the mixed liquor is still transported to the final clarifier to be separated from the effluent. In this way the nutrient removal capacity is increased, while the sludge volume loading of the final clarifiers is not. The integrated fixed-film activated sludge (IFAS) or moving bed biofilm reactor (MBBR, higher media content than IFAS) technologies achieve this via addition of inert media that act as carriers for additional biomass to grow on in biofilms. Sieves retain the media in the aeration zone, while the suspended flocculent AS overflows with the mixed liquor to the final clarifier as before at the same or decreased sludge volume loading rate. IFAS was developed to increase the nitrification capacity in systems where the growth rate of autotrophic nitrifying bacteria would be too low compared the SRT of the system, for example in colder climates [128]. Ordinary heterotrophic organism (OHO)s grow more in flocs in suspension at relatively short SRT in an IFAS system, while more nitrifying bacteria grow at a lower rate in more dense biofilms on the carrier media and experience a longer SRT. Besides the addition of the carrier media and installation of the screens, the capacity increase requires additional energy for suspension and recirculation of the carrier

media. Furthermore, the aeration capacity is increased to maintain the higher dissolved oxygen (DO) concentration and make full use of the biofilm [67].

The membrane bioreactor (MBR) technology is a similar concept to increase the nitrification capacity by separating part of the effluent from the AS via ultrafiltration membranes. The membranes are submerged in the existing aeration stage or placed in a separate compartment [194]. Part of the AS is therefore recirculated within the biological stage, without having to be separated in the final clarifier. This reduces the hydraulic loading rate of the final clarification stage, which in turn allows for an increased biomass concentration in the biological stage and a longer average SRT. The filtration also substantially increases the effluent quality compared to final clarification, with respect to suspended solids and bound nutrients. The membranes do require regular (chemical) cleaning through back-washing and air scouring to remove fouling, and reduce the pressure drop over the membranes.

## 1.5. Increasing overall sludge settleability

Another strategy is to increase the settleability of the sludge mixture allow for an increased amount of biomass in the biological stage, without overloading of the final clarification stage during PRWF. This category is more actively researched for the case of upgrading existing CFAS systems since the clarifiers are already present and less adaptations to the biological stage might be required [33]. Furthermore, a more urgent application is not necessarily to expand the treatment capacity, but to allow existing CFAS systems to reach the original design capacity by mitigating the issue of bulking sludge, a common operational problem for CFAS systems (see section 1.6). This removes the need to dose chemicals to enhance the settleability of flocculent sludge, thereby leading to more sustainable operation [97]. All techniques in this category exploit differences in physical properties of the aggregates within the sludge to selectively enrich the population for well-settling sludge using either differences buoyant density, particle size, or, combined with the viscous drag coefficient, the actual settling velocity.

### 1.5.1. Addition of carriers

One set of methods employs the addition of carrier media which are larger and more dense than flocs in CAS, either of biological origin (e.g. mobile organic biofilms (MOBs) [20, 179], using kenaf carriers retained via drum sieves based on particle size) or plastic carriers (e.g. MIMICS<sup>®</sup> [33], retained using hydrocyclones based on density). The flocculent sludge is selectively discharged as excess sludge using the physical selector. Because the carrier media are selectively retained, this results in a so-called two-SRT or bimodal system. An above average SRT is imposed on the denser aggregates, while the flocculent sludge has an SRT lower than the average, similar to the IFAS concept. The settleability of the sludge as a whole is improved by lowering or maintaining the flocculent sludge fraction [172], while the carriers allow for a higher biomass concentrations in the biological treatment stage for the desired increase in capacity.

### 1.5.2. Self-aggregation

The last set of concepts is related to the topic of this thesis, namely the AGS technology in the form commercialized as Nereda<sup>®</sup> a the SBR configuration. The scale-up from lab-scale to pilot-scale [38, 36] has led to the successful full-scale application [122] at green field WWTPs or the retrofit of existing SBRs [124]. The potential for process intensification have spurred on world-wide research efforts to increase treatment capacity of existing WWTPs with a CFAS system through aerobic granulation [188]. The possible integration of recovery of phosphorus and extracellular polymeric substances (EPS) [73] and absence of a carrier material are additional appealing aspects. Before discussing the different avenues that are being pursued, a side-step into the definition and historical development of AGS is made to provide some context.

#### Historical development of aerobic granulation

The definition of AGS adopted by the scientific community in the early stages of the development was based on mostly physical characteristics of the granules themselves [41]. The predicate ‘aerobic’ was added to distinguish it clearly from already existing anaerobic granular sludge [81]. The threshold of 200  $\mu\text{m}$  for the size of an aggregate to qualify as a granule clearly separates it from flocculent AS, as well as property of the biomass in an aerobic granule to remain aggregated, even at higher hydrodynamic shear rates where flocculent sludge would de-coagulate. The settling properties of the biomass are also part of the definition, characterizing AGS by a ratio of the  $\text{SVI}_{10}$  to the  $\text{SVI}_{30}$  close to unity [139]. This distinguishes it further from flocculent AS, of which the sludge volume depends strongly on hindered settling and compression of the sludge blanket. This is not the case for discrete settling AGS with terminal settling velocities up to 100  $\text{m h}^{-1}$  [157] and a very limited compression phase. Nowadays, the ratio of the  $\text{SVI}_5$  over  $\text{SVI}_{30}$  is more commonly used [104]. The difference in settling behavior is illustrated by figure 1.4a. The property of self-aggregation through embedding in extracellular polymeric substances (EPS) sets it apart from aforementioned technologies that rely on addition of carrier media. The final consideration was that the microbial communities are expected to be similar to those observed in AS and aerobic biofilms, and therefore there was no need for any restriction in that respect.

The latter reflects the scientific history of the development of AGS up to that time. The growth of smooth biofilms had been achieved under aerobic conditions on slowly biodegradable substrates like, for example, ammonium (autotrophic) and methanol (heterotrophic). Smooth aerobic biofilms had been grown on rbCOD from high strength industrial wastewater in airlift reactors with basalt carriers [150] with biomass concentrations up to 30  $\text{g}_{\text{TSS}} \text{L}^{-1}$ . The growth rate of the biomass could not be matched with sufficiently high transport rate of oxygen to the biofilm surface, which led to a substrate gradient at the surface of biofilm favoring heterogenous outgrowth. This in turn resulted in the need to erode the protuberances using through particle-particle collisions [59]. Based on this, a general theory for biofilm morphology was developed [159, 161], stating that biofilm growth is by default heterogeneous under transport-limiting

conditions and is balanced by erosion to maintain a smooth surface morphology. Not transport-limited uptake of substrate was found to be the key for smooth biofilms without the need of strong shear forces [113]. The high biomass concentrations compared to flocculent AS systems (i.e. 3-6 g<sub>TSS</sub> L<sup>-1</sup>) made application in municipal wastewater treatment desirable. However, it is very difficult to design for the transport of oxygen to the biofilm surface at a sufficient rate to match the aerobic growth rate on rbCOD of OHOs. This hampered the application of aerobic biofilms for municipal wastewater treatment that were usually operated at much lower hydrodynamic shear rates than airlift reactors, but did require a smooth biofilm morphology for sufficient sludge settleability for final clarification.

Parallel to this development, the importance of storage polymers in wastewater treatment systems had become more apparent [162]. The design considerations for highly loaded aerobic selectors leading to well-settling flocculent and prevent proliferation of filamentous bacteria also selected for aerobic storage of rbCOD. It was realized that the lower growth rates on the storage polymers would allow for the formation of smooth biofilms with better settleability than flocculent sludge [102, 16], potentially not requiring secondary sedimentation tanks. AGS was developed, in which 40 % was used for direct growth, but 60 % stored as poly-β-hydroxybutyrate (PHB) in a short feast phase, after which a longer famine phase selected for growth on these storage polymers. However, operating a DO concentration below 2 mg<sub>O<sub>2</sub></sub> L<sup>-1</sup> (typical for AS systems) led to oxygen transport limitation, filamentous outgrowth and ultimately granular instability. A solution was found in selecting for storage of the rbCOD into PHB under anaerobic conditions without requiring oxygen as an internal electron acceptor. This led to the enrichment of PAOs [142] or GAOs [196] and alleviated the transport limitation of oxygen during an aerobic feast phase at a low DO concentration. Anaerobic bottom-feeding through a settled sludge bed was employed to limit the dilution of influent concentrations and ensure a strong concentration gradient for sufficient penetration of the rbCOD into the granular sludge [43]. The morphology of this granular sludge is smooth without applying the hydrodynamic shear rates required to maintain granular sludge grown under completely aerobic conditions. The following general drivers for aerobic granulation were identified at the time (adapted from [43]):

- The conversion of rapidly biodegradable substrates into slowly biodegradable stored substrate by applying a feast/famine regime [173, 17];
- The selection of rapid settling granules by applying short settling times [18];
- Sufficient high shear stress within the reactor during aeration [18, 87].

While the same set of process conditions drive the aerobic granulation, individual contributions and interactions are fundamentally different in reactors selecting for either anaerobic or aerobic storage of COD, for example. Only the selection for smooth biofilms without the need for excessive shear and stable at DO concentration below

$2 \text{ mgO}_2 \text{ L}^{-1}$  were deemed suitable for treating of domestic sewage due to the economics compared existing WWTPs using CAS [43]. Therefore, the good long-term stability of AGS that relied on the selection for anaerobic storage of rbCOD as storage polymers (i.e. polyhydroxyalkanoates (PHA)) by PAOs and GAOs and selective wasting based on settling speed, led to world-wide full-scale application in SBRs for treatment of domestic wastewater [124, 57, 168, 122].

The definition of AGS based on the physical characteristics and the general set of driving mechanisms led to the development of systems with different emphases, depending on whether anaerobic or aerobic feast conditions were applied. Since all research efforts are lumped under the common denominator of AGS in the scientific literature, it can be difficult to compare studies. Furthermore, these macroscale process conditions are not always clearly separated from the mechanisms that lead to granule formation on the cellular scale [135, 148]. These research efforts have provided valuable mechanistic insights through which granules are formed on a cellular level, but their combined discussion can somewhat distract from the more general understanding that has already been obtained on how process conditions steer biofilm morphology on the aggregate level [161]. Since the only AGS technology applied at full-scale relies on anaerobic storage of rbCOD for a stable morphology, the name AGS is used to indicate this type of process in this thesis.

### **Aerobic granular sludge in full-scale sequencing batch reactors**

The hallmark of AGS in full-scale SBRs is the combination of a smaller area footprint through the increased sludge settleability, and higher volumetric nutrient removal rates compared to CAS systems [122]. Increased removal rates are achieved through higher mixed liquor suspended solids (MLSS) concentrations and strong concentration gradients of nutrients during the aerated phase of a SBR. This yields sufficient penetration depth to utilize the granular biomass and maximizes the potential for SND (figure 1.3b) [122, 39]. Full-scale AGS-SBRs achieve higher MLSS concentrations of granular sludge compared to AS, while controlling the concentration of flocculent sludge, and limit the sludge volume as a whole [157]. AGS with undiluted  $\text{SVI}_{30}$  values between 35-60  $\text{ml g}^{-1}$  are readily achieved at MLSS concentrations between 6-12  $\text{ml g}_{\text{TSS}}^{-1}$  [157, 122, 168]. Since the flocculent fraction is actively limited, the settling occurs mostly by in the zone settling regime and little compression occurs [157], resulting in  $\text{SVI}_5/\text{SVI}_{30}$  ratios for fully granulated AGS-SBRs  $< 1.3$ . The fact that it is further from unity than typically observed in lab-scale systems reflects the presence of flocculent sludge fraction ( $< 200 \mu\text{m}$ ) when treating real wastewater with readily and slowly biodegradable COD. This is different from synthetic wastewater with only rbCOD often used in lab-scale reactors [41]. Furthermore, this is beneficial from the treatment perspective to prevent increased effluent suspended solids due to the more discrete settling behavior of the granular sludge fraction [158]. The limited compression phase for the settling of the granular sludge fraction, settling in the particulate regime, leads to substantially lower  $\text{SVI}_5$  and  $\text{SVI}_{30}$  values for AGS compared to AS. Granular

sludge fractions reported for full-scale AGS-SBRs are generally >80 % (see figure 1.4d), with a mean granule size >1 mm [169, 157].

The success of full-scale Nereda<sup>®</sup>-SBRs with an anaerobic feeding phase has made it the reference technology for research into achieving higher treatment capacity and better sludge settling properties in existing CFAS systems. Although spontaneous aerobic granulation has been observed in existing WWTPs [180], no continuous variant of the full-scale AGS-SBR technology using similar selective pressures has yet been developed that, by design, yields a stable AGS with similar MLSS concentrations, settleability and granule size. The aforementioned broadness of the definition of AGS, and the multitude of process conditions and mechanisms reported to affect aerobic granulation have also led to different emphases in prioritizing selective pressures that should ensure a stable granular morphology in continuous WWTPs, mainly in the USA and China [33, 74]. The competition over shares of the retrofit market for upgrading existing WWTPs between engineering consultants might also have contributed to the development of different technological concepts [188]. How to design for the formation of AGS in existing CFAS is the main topic of this thesis.

### Densified activated sludge

A technology that has already been applied in existing CFAS systems to increase settleability, is so-called densified activated sludge (dAS) [131]. The concept originated from studies that employed external selectors for the discharge as WAS to implement only the selective pressure on settling speed to drive aerobic granulation. Most research has focused on the use of hydrocyclones as external selectors. Hydrocyclones classify suspended solids in a liquid stream based on either differences in density or particle size into an underflow and an overflow. The hydrocyclones are supplied with mixed liquor or return activated sludge (RAS) and the overflow is discharged as the waste activated sludge (WAS). The use of hydrocyclones in a main-stream AS processes was first developed to retain more dense anammox granules seeded from side-stream DEMON<sup>®</sup> SBRs and waste the flocculent AS [184, 186, 134]. Due an improvement of the year-round dSVI<sub>30</sub> below 100 ml g<sup>-1</sup> of the AS and the prevention of episodes of bulking sludge [183], the possibility for aerobic granulation was further investigated. Clusters of PAOs have a higher buoyant density than ordinary heterotrophic organism (OHO) due to the intracellular polyphosphate molecules [138]. The aim is therefore to improve the overall settleability by enriching the sludge for these denser clusters, although the application has not been limited to WWTPs with an anaerobic stage to select for EBPR [54]. Hydrocyclones thus selectively waste or retain sludge based on properties affecting the settleability, but not the overall settleability itself like in AGS-SBRs. Microbial selection for the anaerobic storage of rbCOD as PHA is furthermore not selectively enhanced in the best settling sludge fraction. The underflow of the hydrocyclones is returned to the return sludge line and the existing anaerobic stage is unaltered.

The application of hydrocyclones as external selectors is commercially available as



InDENSE<sup>®</sup> or S::Select<sup>®</sup> [33]. Selective wasting using hydrocyclones has been applied at full-scale in several studies [131, 56, 10] and has yielded dAS with dSVI<sub>30</sub> values similar to the undiluted SVI<sub>30</sub> of AGS from full-scale SBRs [122] (see figure 1.4b), and substantially better than the AS from lanes without hydrocyclones [131]. The reported dSVI<sub>5</sub>/dSVI<sub>30</sub> ratios are between 1.2-1.8. The degree of granulation is more variable between studies than for full-scale AGS-SBRs, and the mean granule sizes were <1 mm in all cases reported (figure 1.4d). The improved sludge settleability was clearly visible in the decrease in sludge blanket height compared to reference lanes with the same MLSS concentration [56, 131]. Hydrocyclones are also able to condition part of the remaining flocculent sludge retained in the underflow via suspected erosion of filamentous organisms. Episodes of filamentous bulking have been successfully prevented using hydrocyclones [131], while another study showed that bulking could not be prevented during periods at lower process temperatures [56]. This exemplifies that the root cause of bulking is not eliminated when using hydrocyclones alone, which might indicate a malfunctioning of existing anaerobic selectors [92].

### Comparison of AGS and dAS

It is clear that similar settling properties can be achieved for dAS compared to AGS from full-scale SBRs (figure 1.4b). The fact that mostly dSVI values have been reported for dAS, as is customary for AS, complicates the comparison to studies into AGS in SBRs or CFRs that used undiluted SVI values as the main metric for settleability. However, the relation between the hindered settling speed and solids concentration differs for flocculent sludge (exponential decrease [172]) and granular sludge (quadratic decrease [157]). Comparison of settling behavior these sludges should therefore be made based on undiluted from the reactors under study. The data compiled from full-scale AGS-SBRs, dAS and spontaneous granulation in CFAS systems (see section 1.6) in figure 1.4 allow for some useful observations:

- For SVI<sub>30</sub> values >60 ml g<sup>-1</sup>, the settleability is not correlated to the granular sludge fraction and the coherence of the flocculent sludge fraction (i.e. compression versus zone settling) dominates the SVI<sub>30</sub> (figure 1.4b);
- SVI<sub>30</sub> values <60 ml g<sup>-1</sup> require a limited degree of compression settling that is only achieved with degrees of granulation (i.e. >200 μm) >20%. The actual degree of granulation hardly predicts the SVI<sub>30</sub>, since settling is always sufficiently fast to obtain a settled bed within 30 min (figure 1.4b);
- The limited granule size in dAS (i.e. <1 mm) causes the sludge to settle with a degree of coherence similar to CAS without stratification in the sludge bed [131]. In case of AGS from full-scale SBRs, the granules mainly >1 mm settle as discrete particles and more independent from the flocculent sludge fraction. dAS will therefore rely more on compression settling in case of increased MLSS concentrations, which is not the case for AGS from full-scale SBRs (figure 1.4c).

Diluted  $SVI_{30}$  values can therefore be similar for AGS and dAS, but they don't share the same relation between settling properties and the MLSS concentration. Hydrocyclones have until now only been successfully applied to ensure that the year-round  $SVI_{30}$  is at or below the design value and prevent failure of final clarifiers at the design MLSS concentrations during PRWF. The absence of selection for anaerobic storage of rbCOD in the best-settling sludge fraction through bottom-feeding, like in AGS-SBRs, and the suspected partial disintegration of the granular sludge in the hydrocyclones [131] will likely limit the extent of granule growth that can be obtained using external selectors alone. Considering process intensification of existing WWTPs requires considerably higher MLSS concentrations combined with increased settling properties at these higher MLSS concentrations, the development of a CFR configuration that selects for granulation using the same principles as full-scale AGS-SBRs seems the most promising avenue to pursue. The requirements for aerobic granulation in CFRs based on full-scale AGS-SBRs is discussed next (section 1.6).

## 1.6. Aerobic granulation in CFAS systems

Spontaneous aerobic granulation in continuous-flow activated sludge (CFAS) systems designed with an anaerobic stage for EBPR has been reported for several WWTPs [180, 129]. Efforts have been made to identify the common denominators between these installations. Due to the absence of a unit operation to selectively discharge excess sludge based on differences in sludge settleability, the organic loading rate (i.e. F/M ratio) of the sludge in the first anaerobic compartment of the selector zone has received the most attention. The principles behind the design of anaerobic selectors to select for well-settling flocculent sludge and prevent filamentous bulking [97] are shared with the process conditions that select for AGS in SBRs [43, 121]:

- a high floc loading by only directing part of the return sludge to the first anaerobic compartment to be contacted with the fresh wastewater [65], combined with
- the maximization of the penetration depth of substrate into flocs, achieved through a decreasing concentration gradient of substrate along the length of the anaerobic stage. This can be achieved with limited dispersion, or through a compartmentalized anaerobic stage of several tanks in series [23].

Converting a tanks-in-series configuration to an anaerobic step-feed did indeed increase the  $SVI_5/SVI_{30}$  ratio of the sludge, highlighting the importance of the concentration gradient in the bulk liquid and a high initial organic loading rate [129]. Unfortunately, no significant correlation between the  $BOD_5$  loading rate of the first anaerobic compartment and the degree of granulation was found. Since the  $BOD_5$  metric lumps readily and slowly biodegradable COD together in one metric, future research with a more detailed characterization of COD in wastewater could lead to different results. The importance of the selection for anaerobic storage of rbCOD for the formation of granular sludge was shown by the significant relation between the degree of granulation (i.e. the mass fraction

## 1

>200  $\mu\text{m}$ ) and the ratio of the relative abundance of PAOs and GAOs in the granular sludge compared to the flocculent sludge fraction.

On the other hand, proposals for novel continuous-flow reactor configurations that attempt to select for aerobic granulation by design have been reported in rapid succession over the past decade [74, 193]. Although they all implement some form of selective wasting of excess sludge based on differences in sludge settleability, nearly all have employed the selection for storage of rbCOD through aerobic feast/famine conditions, which has been shown to lead to instable morphology at lower DO concentrations [104]. Furthermore, this excludes the use of EBPR. A continuous reactor concept with both an anaerobic stage and selective wasting based on settleability has been applied, but at average SRTs that are too low to be applied as a retrofit technology for CFAS systems with BNR [47]. The translation of all the process conditions from full-scale AGS-SBRs to a continuous-flow concept has thus not yet been reported, and specifically the design requirements for the anaerobic stage are unclear.

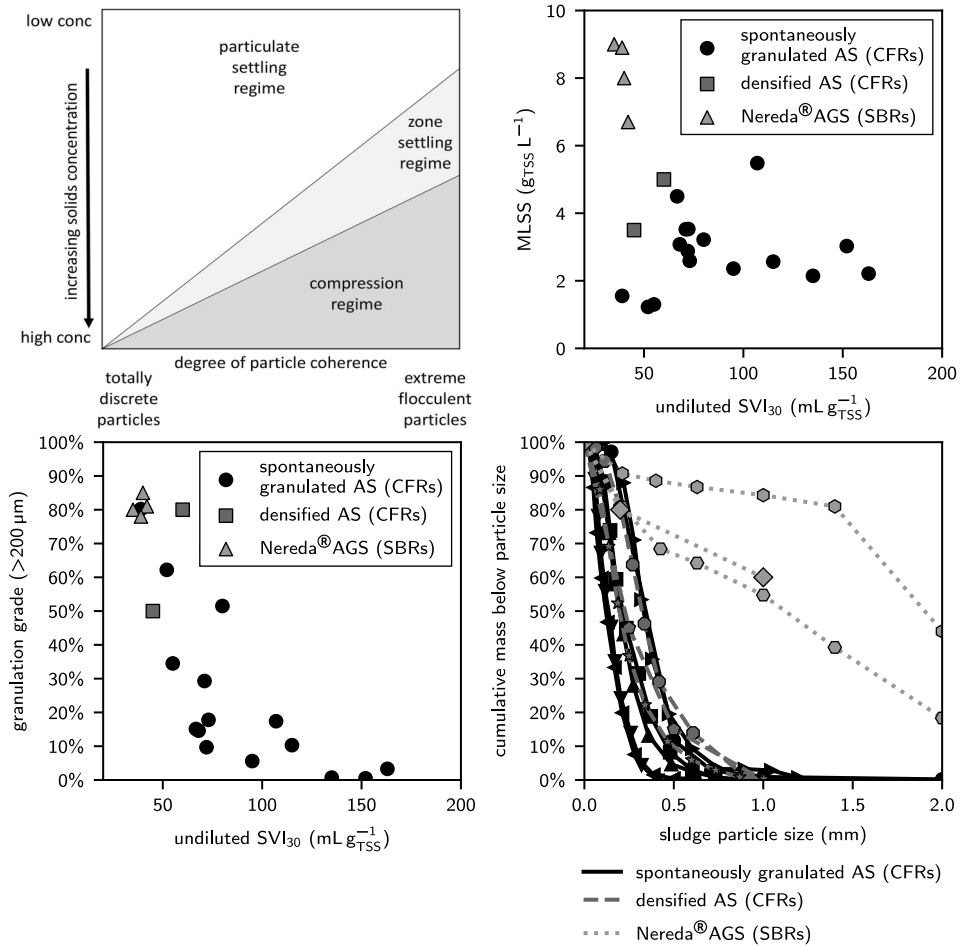


Figure 1.4: (a, top left) Difference between settling characteristics of flocculent sludge and discrete granular sludge. Taken from [157]. (b, bottom left) Granulation grade (i.e. >200 μm) versus undiluted sludge volume indices after 30 min (SVI<sub>30</sub>), (c, top right) undiluted SVI<sub>30</sub> versus reactor MLSS concentrations, and (d, bottom right) cumulative particle size distributions reported for full-scale AGS in SBRs [122, 157, 168], dAS in CFRs [131, 56] and spontaneous aerobic granulation observed in CFAS systems [129, 180].

## 1.7. Scope and outline of the thesis

Based on the aforementioned analyses, two main research topics were identified:

- how to translate the process conditions of full-scale AGS-SBRs to existing continuous-flow CAS systems to obtain the same, stable AGS, and
- how to make optimal use of the additional biomass for higher volumetric conversion rates for the removal of nutrients (i.e. nitrogen and phosphorus).

Although there is considerable overlap between these topics, the work in this thesis was limited to the translation of the conditions driving the formation and affect the stability of AGS. The interaction between the selective wasting of excess sludge based on settleability and the selective pressures applied using anaerobic bottom-feeding of full-scale AGS-SBRs were investigated, with a special focus on the latter with respect to the differences and similarities compared to anaerobic selectors of CFAS systems.

In **Chapter 2**, first the role of anaerobic bottom-feeding of AGS-SBRs was investigated in light of the function of anaerobic selectors of CFAS systems to ensure complete removal of rbCOD prior to the aeration stage. This prevents so-called 'overshoot' of rbCOD and subsequent transport-limited substrate uptake under aerobic conditions, which in turn prevents filamentous bulking of the AS and ensures good settleability. Although anaerobic selectors are designed with a certain degree of plug-flow, substantial dispersion can occur in practice, leading to incomplete anaerobic removal of rbCOD and the aforementioned adverse effects on the settleability of flocculent sludge. The anaerobic bottom-feeding used in AGS-SBRs shares this purpose to ensure a well-settling sludge morphology. However, the effect of partial overshoot the rbCOD in the wastewater to the aeration stage on the morphology and settleability of AGS has not been studied, specifically considering the stability of the microbial selection for anaerobic storage. The observed degree of stability will provide insight into the importance of the flow pattern in anaerobic selectors of existing CFAS systems eligible for a retrofit to AGS.

The attention then turned to the role of the anaerobic stage in the distribution of substrate over the sludge particle population in **Chapter 3**. The concept of substrate distribution is unique for biofilm systems since the granule size distribution gives the opportunity to impose a different loading based on differences in settleability. This is not the case for flocculent AS with a more uniform size distribution. AGS has been formed in lab-scale reactors fed with synthetic wastewater containing only rbCOD with both anaerobic bottom-feeding through a settled bed (i.e. resembling the operation of full-scale AGS-SBRs) and pulse-feeding with all sludge in suspension (i.e. a proxy for an anaerobic selector of a CAS system with a perfect plug-flow), combined with selective wasting of excess sludge. How both modes of anaerobic contact affect the distribution of substrate, the resulting granule size distribution and BNR is unknown. This is especially relevant considering the increased complexity of treating real domestic wastewater containing both readily biodegradable (mainly soluble) and slowly biodegradable (mainly particulate)

COD fractions, of which the former is most suited to select for anaerobic storage and drive granular growth.

Both extremes in anaerobic feeding modes were again compared in **Chapter 4**, where the process conditions in the anaerobic feeding phase that affect the distribution of substrate were combined with other factors in a framework of six mechanisms hypothesized to govern aerobic granulation. A sensitivity analysis was performed on the formation of AGS in full-scale AGS-SBRs using a numerical model, starting from a seed of uniformly sized flocculent AS. The distribution of limited amount of rbCOD in domestic wastewater over the sludge particle population in the anaerobic phase was again the main interest. The role of the anaerobic stage to ensure microbial selection for anaerobic storage of rbCOD and the maximization of the penetration depth of rbCOD into sludge particles were implemented as mechanisms. Both are also functions of the anaerobic selector in CFAS systems. In addition, selective feeding of the best settling sludge fraction with the available rbCOD through bottom-feeding in the anaerobic phase was investigated as a driver of aerobic granulation in full-scale AGS-SBRs.

In **Chapter 5**, the insights from the previous chapters were used to develop a CFR concept that best mimics the selective pressures for aerobic granulation from full-scale AGS-SBRs. The concept was implemented in a pilot-scale reactor, fed with pre-settled wastewater from the Harnaschpolder WWTP. The growth of AGS was investigated, with again a focus on the effect of the design of the anaerobic stage on the distribution of rbCOD. The obtained volumetric removal rates for nutrients were compared to the AS from Harnaschpolder WWTP treating the same pre-settled wastewater to assess the potential for process intensification.

Finally, **Chapter 6** discusses the how the understanding of the relation between process conditions and the formation of AGS has been improved, and the potential of continuous AGS as a retrofit technology for existing CAS systems, including topics for further research.



# 2

## **Impact of aerobic availability of readily biodegradable organic substrate**



## 2.1. Introduction

AGS is becoming a well-established technology for wastewater treatment due to the compactness, energy savings and good effluent quality [14, 46, 124]. The current commercial technology (Nereda<sup>®</sup>, a tradename owned by Royal HaskoningDHV) is based on sequentially operated batch reactors (SBRs) [57]. The influent is fed from the bottom of the reactor resulting in uptake of rbCOD and conversion to storage polymers in the microbial cells under anaerobic conditions. The storage polymers are oxidized in the subsequent aeration phase where they are used for microbial growth and nutrient removal. This process design selects for well-settling, granular sludge, which is further enhanced by subsequent selective discharge of the worst-settling, flocculent sludge fraction [19, 43, 88].

There has been a significant amount of research oriented towards the long-term morphological stability of AGS in SBRs. An increasing body of literature has been developed on AGS formed on various organic substrates and a variety of operational conditions. The results obtained on granular stability have led to the general view that long-term stability of AGS is very variable, and dependent on the applied process conditions [27, 43, 55, 74, 85]. A limitation of many studies is their empirical nature; different process conditions are evaluated but the underlying mechanisms explaining the observations are often not provided or even studied. Specific conclusions can therefore be difficult to extrapolate to a more general context. It is the authors' opinion that this clouds the current understanding of the principles governing the formation and stability of AGS in general. Moreover, this potentially hampers implementation and development of alternative technologies for acquiring granular sludge in full-scale municipal wastewater treatment.

The effect of the presence of both rbCOD and oxygen as electron acceptor is a prime example of such confusion. Strategies to prevent and mitigate bulking sludge in CAS processes have primarily focussed on the impact of substrate concentrations or floc loading rates (F/M ratio) on floc morphology [97]. The obtained insights initially led to the first investigations into AGS under full aerobic conditions [16, 66, 102]. In general, a dense and smooth biofilm requires substrate uptake limited by the maximum biomass specific uptake rate, while a transport-limited substrate uptake yields less dense and irregular biofilms [115, 161]. In the case of BNR using AS, design has focussed traditionally on maximizing rbCOD gradients in the AS reactors [24, 23]. This is implemented by designing plug-flow reactors or adding so-called aerobic selector tanks [25]. In these configurations, rbCOD is first converted into storage polymers such as PHA [162]. There are two important conditions to minimize the SVI. Firstly, a sufficiently high DO concentration ( $>2 \text{ mg}_{\text{O}_2} \text{ L}^{-1}$ ) is required, in case of aerobic conversion of rbCOD, to prevent transport-limitation for oxygen during formation of PHA [93]. Second, the ratio of the rbCOD sludge loading rate in the selector over the maximum biomass specific uptake rate should be close to unity for a good  $\text{SVI}_{30}$  ( $<100 \text{ ml g}_{\text{TSS}}^{-1}$ ) [95].

AGS can be cultivated with an aerobic feeding strategy (i.e., employing the same completely oxidative storage of rbCOD to PHA), but this requires a relatively high shear rate, a high selective pressure on settling speed, and a sufficiently high DO concentration to obtain a granular morphology [8, 18, 102, 104, 139, 149]. With the increase of granule size over time, the interior of these aerobically fed granules gets deprived of substrates and decays, resulting in granular instability. Long-term stability is in general not achieved in aerobically fed granular sludge processes [18, 102].

Design of anaerobic and anoxic selectors, to obtain well-settling sludge, has proven less problematic than for aerobic selectors. The general observation for anaerobic selectors is that complete uptake of rbCOD in the anaerobic contact zone yields a well-settling, dense flocculent sludge morphology, independent of the hydrodynamic conditions in the anaerobic selector [94, 177]. The removal of all rbCOD during the anaerobic stage of the process into PHA was shown to be a critical design criterion to form granular sludge in aerobic processes for nutrient removal as well [43]. Different from aerobic feeding, long-term stability of granular sludge morphology was obtained using a process with anaerobic feeding/aerobic growth [39, 42].

The sensitivity of anaerobically fed AGS reactors to the presence of rbCOD in the aeration phase has not been studied. This is an important aspect for design and operation, and knowledge on this sensitivity aids in the further development of AGS processes. Not only rbCOD bypassing the anaerobic stage, but also aerobic hydrolysis of slowly biodegradable COD makes rbCOD available in the aerated phase [121]. Both can result in transport-limited substrate uptake rates of either oxygen or rbCOD, and potentially lead to deterioration of sludge morphology and settleability. If there is some tolerance for the aerobic presence of rbCOD, it would ease the control and design of AGS processes.

The effect of aerobic presence of rbCOD on the morphology of AS and granular sludge, respectively, could vary due to the intrinsic differences in process configurations. In both cases, PAOs compete for substrate uptake with other OHOs under aerobic conditions due to the ability to sequester substrates under aerobic conditions [117]. For a completely mixed AS, a fraction of 20% of the rbCOD-load dosed aerobically was reported to have no negative effect on the SVI of a lab-scale system enriched for EBPR [94]. AGS processes might react differently than flocculent sludge systems due to the difference in feeding and the need to selectively waste flocculent sludge.

In this work, the effect of aerobic presence of rbCOD on the morphological stability of AGS was investigated. The first aim was to determine the fraction of rbCOD that can be consumed aerobically while maintaining well-settling AGS. In case of deterioration, the second aim was to clarify via which mechanism(s) it would occur. A lab-scale AGS system with acetate as carbon source was used to investigate the impact on granular morphology and overall sludge settling when a fraction of acetate is dosed under aerobic conditions. Acetate was aerobically dosed at a rate that ensured a negligible residual concentration (i.e., to force transport-limited substrate uptake rates). Changes in sludge morphology

and nutrient removal were monitored over time.

## 2.2. Methodology

### 2.2.1. Experimental set-up and operation

A lab-scale reactor with a working volume of 2.7 L and aspect ratio of 18 was operated as a sequential batch reactor with a volume exchange ratio of 0.55. The bioreactor was operated continuously in 3-hour cycles for 192 days. The cycle first consisted of an anaerobic phase where synthetic wastewater was fed through the bottom of a settled sludge bed (AN feeding, maximum duration of 60 min). A short mixing phase was then applied prior to enabling DO control to homogenize the bulk-liquid (AE mix, 4 min). Next, a mixed aerobic phase with dosage of acetate to mimic the continued availability of rbCOD was followed by a mixed aeration phase without additional dosage (AE feeding and AE reaction, combined minimum duration of both phases was 106 min). A settling period (settling, 5 min) was then followed by the discharge of effluent and unsettled sludge (discharge, 5 min). The duration of the respective anaerobic and aerobic (carbon source only) feeding phases were set according to the anaerobic/aerobic acetate distribution of the current stage (table 2.1), while maintaining a constant total cycle duration. The total organic loading rate ( $1.63 \text{ g}_{\text{COD}} \text{ L}^{-1} \text{ d}^{-1}$ ) was kept constant over the course of the study. AGS previously enriched at the same conditions as described in this section was used as inoculum (conditions listed in table 2.1, 0% aerobic rbCOD load).

A synthetic wastewater of 1.5 L per cycle was used as anaerobic feed and consisted of 1.2 L of deionized water together with 150 ml carbon source (medium A) and 150 ml nitrogen and phosphorous source (medium B). Medium A contained 63 mM  $\text{NaCH}_3\text{COO} \cdot 3\text{H}_2\text{O}$ , 3.6 mM  $\text{MgSO}_4 \cdot 7\text{H}_2\text{O}$ , and 4.7 mM KCl. Medium B contained 42.8 mM  $\text{NH}_4\text{Cl}$ , 4.2 mM  $\text{K}_2\text{HPO}_4$ , 2.1 mM  $\text{KH}_2\text{PO}_4$ , and 10 ml  $\text{L}^{-1}$  trace elements solution [174], but using  $2.2 \text{ mg L}^{-1}$   $\text{ZnSO}_4 \cdot 7\text{H}_2\text{O}$  instead of  $22 \text{ mg L}^{-1}$  [123, 121]. The combination of medium A, medium B, and tap water led to a synthetic wastewater composition of  $366 \text{ mg}_{\text{COD}} \text{ L}^{-1}$ ,  $60 \text{ mg}_{\text{NH}_4^+ \text{-N}} \text{ L}^{-1}$ , and  $9.3 \text{ mg}_{\text{PO}_4^{3-} \text{-P}} \text{ L}^{-1}$ . The synthetic wastewater was fed at a superficial liquid velocity of  $0.6 \text{ m h}^{-1}$ . The aerobic acetate load was dosed using a 10x more diluted solution of medium A (medium C). Medium C contained 6.3 mM  $\text{NaCH}_3\text{COO} \cdot 3\text{H}_2\text{O}$ , 0.36 mM  $\text{MgSO}_4 \cdot 7\text{H}_2\text{O}$ , and 0.47 mM KCl, resulting in a concentration  $366 \text{ mg}_{\text{COD}} \text{ L}^{-1}$ . All media were dosed using peristaltic pumps and only flow rate and feeding duration were changed according to experimental stage (see table 2.1). Media compositions remained the same throughout the study. The temperature was controlled at  $20 \pm 1 \text{ }^\circ\text{C}$  through the double-jacketed reactor wall using a water bath with thermostat. The pH was controlled during aeration at  $7.0 \pm 0.1$  by dosage of either a 1M solution of hydrochloric acid or a 1M sodium hydroxide solution. During aeration, a recirculation gas flow was maintained at  $6 \text{ L min}^{-1}$  (superficial gas velocity of  $4.2 \text{ cm s}^{-1}$ ). A DO concentration of  $2 \text{ mg}_\text{O}_2 \text{ L}^{-1}$  was maintained during the aeration phase via addition of compressed air or dinitrogen gas using mass flow controllers. The average SRT was controlled at 10 days by manual

removal of biomass at the end of the aeration phase on a two day basis (once per 16 cycles).

Table 2.1: Operational parameters of reactor operation during stepwise increase of aerobically dosed acetate load fraction. For each condition, the total cycle time was kept constant at 3h.

Aerobic acetate load (%)	SAADR ( $\text{mg}_{\text{COD}} \text{g}_{\text{VSS}}^{-1} \text{h}^{-1}$ )	Duration (d)	Operating phase duration (min)					
			AN feeding	AE mix	AE feeding	AE reaction	Settling	Discharge
0 <sup>a</sup>	0	27	60	4	-	106	5	5
2	4.6	15	58.8	4	12	95.2	5	5
5	3.6	9	57	4	30	79	5	5
10	3.5	33	54	4	60	52	5	5
15	4.0	5	51	4	90	25	5	5
20	4.4	23	48	4	118	-	5	5
25	7.8-13.2 <sup>b</sup>	24	45	4	75	46	5	5
35	11.1	29	39	4	106	21	5	5
0 <sup>c</sup>	0	27	60	4	-	106	5	5

<sup>a</sup> Reference period.

<sup>b</sup> The MLVSS concentration in the reactor remained stable for two weeks after increasing the aerobic acetate load to 25%, but then decreased due to an increase in washout of biomass from deteriorating settling properties. The SAADR therefore increased as the MLVSS concentration in the reactor decreased.

<sup>c</sup> Recovery period.

### 2.2.2. Stepwise increase of the aerobically dosed acetate fraction

To force transport-limited uptake of acetate during the stepwise increase of the aerobically dosed acetate load, the acetate sludge loading rate should be significantly lower than the maximum aerobic biomass specific uptake rate. By applying these conditions, the risk of obtaining bulking sludge and open porous biofilms [95, 115] is maximized. The maximum specific aerobic acetate uptake rate was determined during the reference period as  $49 \text{ mg}_{\text{COD}} \text{ g}_{\text{VSS}}^{-1} \text{ h}^{-1}$ . The aerobic acetate loading rate was initially set to 1/10 of this maximum rate (i.e.  $58 \text{ mg}_{\text{COD}} \text{ h}^{-1}$ ), thereby ensuring a transport-limited substrate uptake rate through a limiting specific aerobic acetate dosage rate (SAADR). The aerobic acetate loading rate was increased to 1/5 of the maximum substrate uptake rate (i.e.  $116 \text{ mg}_{\text{COD}} \text{ h}^{-1}$ ) as the aerobic acetate load was increased from 20% to 25% of the total load to maintain a constant cycle time. The load distribution was achieved by altering the duration of acetate dosage in the anaerobic phase and aerated phase (table 2.1). The reactor was operated at each aerobic acetate load fraction for at least one SRT prior to transitioning to the next step (table 2.1). A longer time period was applied when a clear morphological change was detected within one SRT.

### 2.2.3. Analysis of reactor performance

Samples were taken during aeration and filtered through a  $0.45 \mu\text{m}$  PVDF filter (Millipore).  $\text{NH}_4^+\text{-N}$ ,  $\text{NO}_x\text{-N}$ , and  $\text{PO}_4^{3-}\text{-P}$  concentrations were measured by using a Thermo Fisher

Gallery Discrete Analyzer (Thermo Fisher Scientific, Waltham, USA). The concentration of acetate was determined by high-performance liquid chromatography (HPLC) with an Aminex HPX-87H column from Biorad, coupled to an UV detector, using 0.01 M phosphoric acid as eluent. MLSS and mixed liquor volatile suspended solids (MLVSS) concentrations in the reactor were determined according to the standard methods [5]. The sludge volume after 10 minutes of settling and effluent discharge ( $SV_{10}$ ) was determined in between cycles in-situ. The SRT was calculated by dividing the average amount of VSS in the reactor over the sample period by the sum of the VSS in the effluent from selective wasting and manual, mixed wasting of sludge (averaged per week). The amount sludge wasted manually was adjusted to maintain the desired average SRT.

#### 2.2.4. Imaging of sludge morphology

The morphological features of the sludge were assessed from both the reactor and effluent prior to changing fraction of acetate dosed aerobically at each experimental stage or when a clear morphological change was observed. Sludge was collected from the reactor at the end of the aeration phase and from the effluent directly after discharge. A mixed sample from either source was transferred to a glass petri dish and examined by the means of an Olympus reverse microscope coupled with a Leica Digital Camera, together with its software QWin Pro (version 3.1.)

#### 2.2.5. Maximum specific acetate up take rate under aerobic conditions

During a cycle in the reference period, the DO controller was turned off 10 minutes after the aeration phase had started at the DO concentration set point of  $2 \text{ mgO}_2 \text{ L}^{-1}$ . The outputs of the mass flow controllers for both compressed air and nitrogen gas were fixed to their last setting. The reactor was then pulsed with a sodium acetate solution to obtain a bulk concentration of  $20 \text{ mgCOD L}^{-1}$ . The volumetric uptake rate was then determined by measuring the duration of the temporary drop in DO concentration due to the increased oxygen consumption rate. The reactor MLVSS concentration was used to calculate the biomass specific uptake rate ( $\text{mgCOD gVSS}^{-1} \text{ h}^{-1}$ ).

#### 2.2.6. Fluorescent in-situ hybridization (FISH)

The handling, fixation and staining of FISH samples was performed as described in [12]. A mixture of PAO462, PAO651, and PAO846 probes (PAOm<sub>ix</sub>) was used for visualizing PAOs [30]. A mixture of GAOQ431 and GAOQ989 probes (GAOm<sub>ix</sub>) was used for visualizing GAOs [31]. A mixture of EUB338, EUB338-II and EUB338-III probes was used for staining all bacteria [3, 35]. Images were taken with a Zeiss Axioplan 2 epifluorescence microscope equipped with filter set 26 (bp 575e625/FT645/bp 660e710), 20 (bp 546/12/FT560/bp 575e640), 17 (bp 485/20/FT 510/bp 5515e565) for Cy5, Cy3 and fluos respectively.

## 2.3. Results

### 2.3.1. Reference reactor operation

The reactor was seeded with AGS formed at lab-scale in an earlier cultivation using the same synthetic wastewater composition and initial operational conditions (table 2.1). Granulation and conversions were allowed to stabilize over the course of one month. Complete anaerobic acetate uptake and complete phosphorus removal were achieved during this period. The focus in this research was on stable granulation and conversions rather than the optimization of effluent concentrations (i.e., total nitrogen concentration). Figure 2.1 depicts the concentration profiles during one cycle prior to initiating the stepwise increase of the fraction of acetate dosed in the aerobic period. This period was used as a reference throughout the study.

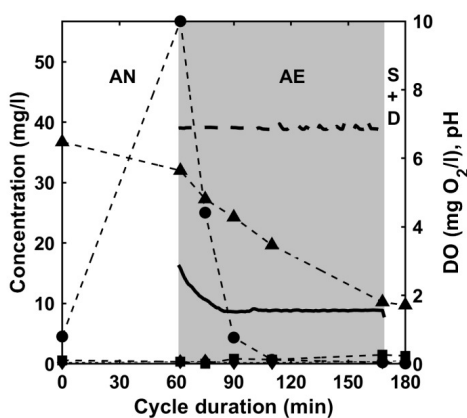


Figure 2.1: Concentration profiles for a typical cycle (27 days after the start of the experiments) during the reference period with complete anaerobic acetate uptake for  $\text{PO}_4^{3-}\text{-P}$  (circles),  $\text{NH}_4^+\text{-N}$  (triangles),  $\text{NO}_2^-\text{-N}$  (diamonds) and  $\text{NO}_3^-\text{-N}$  (squares) (left axis). pH (dashed line, controlled at 7) and DO (solid line) (right axis). Measurements were only meaningful in the mixed aeration phase. Alternating shading denotes phase changes within the cycle (AN: anaerobic phase; AE: aerobic phase; S+D: settling and discharge).

The effluent concentration of phosphate during the steady-state operation was always very low (i.e.  $<0.1 \text{ mg}_{\text{PO}_4^{3-}\text{-P}} \text{ L}^{-1}$ ). The maximum SPUR was  $20 \text{ mg}_{\text{P}} \text{ g}_{\text{VSS}}^{-1} \text{ d}^{-1}$ . The presence of a strong PAO-community was also indicated using FISH-microscopy (see figure 2.7). All the acetate was taken-up during the anaerobic feeding period. Nitrification was present, albeit not yet complete. The reactor fully granulated and sludge settleability was stable with low SVIs throughout the reference period ( $\text{SVI}_{10} = 3\text{-}40 \text{ ml g}_{\text{TSS}}^{-1}$ , figure 2.2a). Granules in the reactor had a smooth surface and were heterogeneous in size and shape, with an average diameter  $>1 \text{ mm}$  (figure 2.3a, stage I). Sludge wasted through selective discharge mainly consisted of the smallest granule size fraction (figure 2.3b, stage I). The MLVSS concentration was  $5.2 \pm 0.6 \text{ g}_{\text{VSS}} \text{ L}^{-1}$  (figure 2.2b). The SRT after start-up was controlled at 10 days.

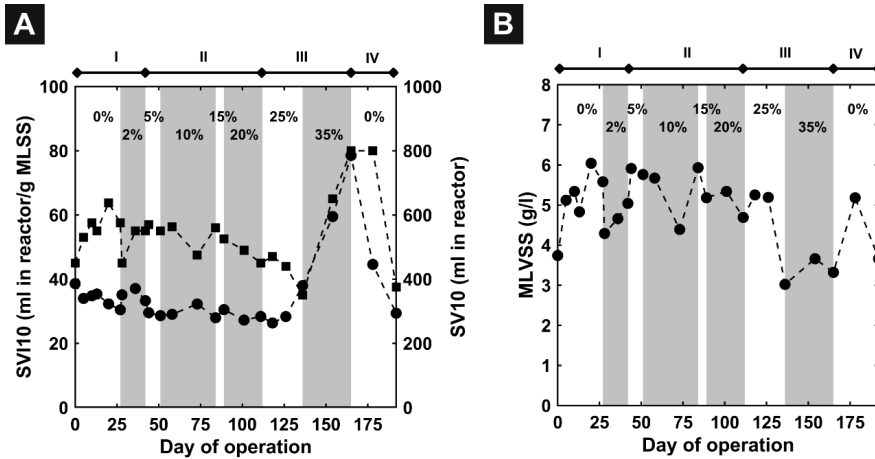


Figure 2.2: (a)  $SV_{10}$  (squares, dashed line) and  $SVI_{10}$  (circles, dashed line) as measured in the reactor at the end of a cycle. (b) MLVSS concentration in reactor (circles, dashed line). Alternating shading indicates the different aerobic acetate loads. Percentage annotations in graphs indicate the aerobically dosed acetate as fraction of the total acetate load. Roman numerals indicate stage in morphological transition described in the text.

### 2.3.2. Effect of aerobic transport-limited acetate uptake rate on sludge morphology and settleability

#### Stage II ( $\leq 20\%$ aerobic acetate load)

The effect of an increasing fraction of the aerobic acetate load on the SV and SVI after ten minutes of settling ( $SV_{10}$  and  $SVI_{10}$ , respectively) is shown in figure 2.2a. The applied aerobic acetate loading rate had no noticeable effect on settleability, nor on the MLVSS concentration up to dosing 20% of the acetate load in the aerobic period (figure 2.2b). The sudden decrease in MLVSS on days 28 and 73 of operation were caused by too much mixed sludge withdrawal for manual SRT control. The sludge morphology in the reactor remained smooth as well, with a small amount of filamentous bacteria extending from the surface of some granules. Suspended growth was not observed in the reactor (figure 2.3a, stage II). The settling speed (indicated by the  $SV_{10}$ ) and the packing density (indicated by the  $SVI_{10}$ ) were unaffected by the filamentous bacteria attached to the granules. The  $SV_{10}$  and  $SVI_{10}$  remained similar to the reference period with complete anaerobic acetate feeding (i.e.,  $SV_{10} = 400\text{--}500$  ml,  $SVI_{10} = 30\text{--}40$  ml  $g_{TSS}^{-1}$ ). As the aerobic acetate load increased to 20%, an increasing amount of suspended filamentous bacteria entangled with flocs and small granules were found in the effluent in addition to granules from the smallest size fraction (figure 2.3b, stage II). The selective wasting based on settling speed was sufficient to prevent accumulation of the filamentous bacteria in the reactor and a potential negative impact on the SVI.

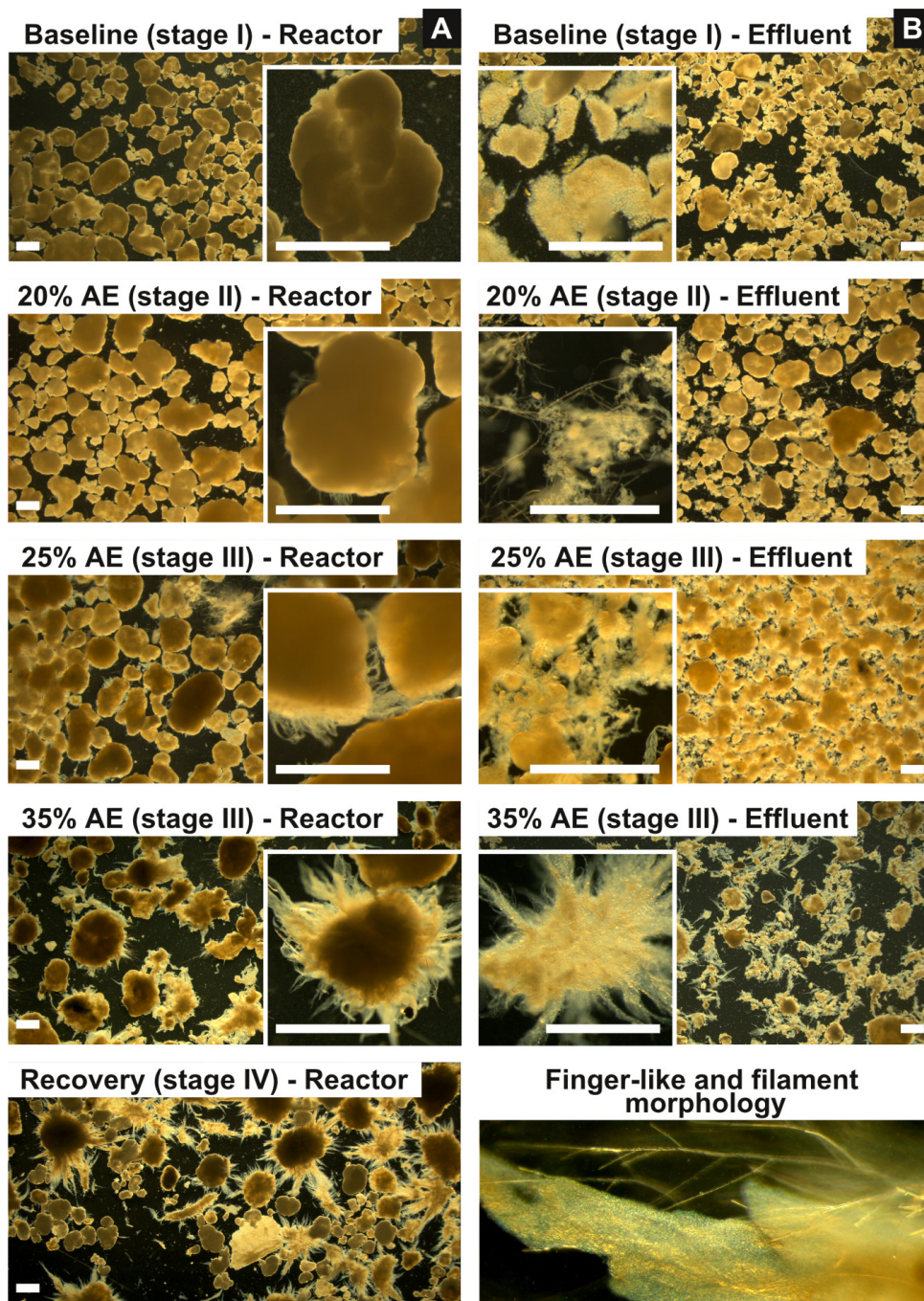


Figure 2.3: Granular morphology at various stages in the experiment as recorded using stereo-zoom microscopy. Label denotes percentage aerobic acetate load of total acetate load. (a) Overview of morphology in reactor and inset of best settling fraction. (b) Overview of morphology in effluent and inset with worst-settling sludge fraction. Effluent images taken from effluent collected from several cycles and concentrated via decanting. Bottom-right images depict difference between filamentous bacteria and finger-like growth films. Roman numerals indicate stage in morphological transition mentioned in the text. Length represented by the white scale bars is 1 mm.



### Stage III (>20% aerobic acetate load)

Sludge morphology in the reactor changed after the increase to 25% aerobic acetate load combined with an increase in aerobic acetate feeding rate (table 2.1), although it did not immediately lead to an increase in SV<sub>10</sub> or SVI<sub>10</sub> in the reactor during the two weeks. The surface coverage as well as the length of the outgrowth on granules increased and affected the majority of the granules (figure 2.3a, stage III). The outgrowth's shape changed from individual filaments to intertwined, finger-like structures that formed a shell around existing granules (figure 2.3b, morphological comparison). A small fraction of suspended filamentous bacteria was also observed in the reactor, but insufficient to affect overall sludge settleability. Suspended, tape-like films were the dominant morphology besides granules in sludge sampled from the effluent discharged after the settling period. Furthermore, small granules embedded in larger films were observed (figure 2.3b, stage III). Despite the change in sludge morphology, it had not altered the settling speed of the sludge fraction growing in suspension, and thus the sludge load discharged through the effluent. Therefore, the MLVSS in the reactor did not decrease compared to the reference period.

After two weeks (stage III), short circuit flows during anaerobic feeding were becoming more frequent and the anaerobic storage capacity of acetate was diminished (section 2.3.3, figure 2.5c). The increased aerobic conversion of acetate resulted in more poor-settling suspended growth and a subsequent decrease in MLVSS through an increased sludge load discharged through selective wasting. No manual SRT control was applied to prevent the average SRT from decreasing below 10 days. Although selective wasting stabilized the SV<sub>10</sub> and SVI<sub>10</sub> initially, the sludge volume started to increase noticeably after one month. The SVI kept deteriorating after the subsequent step to 35% aerobic acetate load, ultimately leading to a twofold increase to 80 ml g<sub>TSS</sub><sup>-1</sup> (stage III, figure 2.2a). The thin films now were the main suspended sludge morphology in the reactor and covered remaining granules in finger-like structures to a varying degree (figure 2.3a, stage III). Although not smooth surfaced, granular morphology remained the dominant morphology in terms of mass.

### Stage IV (recovery with complete anaerobic acetate dosage)

Within one SRT after switching back to the reference conditions the MLVSS concentration went back to the reference stage level by the formation of new smooth granules (figure 2.3a, stage IV). This improved the SVI<sub>10</sub> to 40 ml g<sub>TSS</sub><sup>-1</sup> as well, but the sludge volume took between 2-3 SRTs to completely recover to 400 ml. Short circuit flows during the anaerobic contact phase kept occurring on an irregular basis up to one SRT after the switch. This likely resulted in transport-limited acetate uptake during the aeration phase and delayed the recovery. Gradually granules covered in finger-like outgrowth decreased in number over time, either through wasting or disintegration. Newly formed smooth granules increased in number (figure 2.3a, stage IV), reminiscent of the original morphology at the start of the experiment. An overview of identified stages in morphological development is presented in table 2.2.

Table 2.2: Stages in morphological development of AGS as a result of an increase in aerobic acetate load dosed at a rate forcing transport-limited substrate uptake, linked to the observed overall settleability and effect on biological phosphorus removal performance.

Stage	Aerobic acetate load	Settleability	Sludge morphology		Biological phosphorus removal
			Suspended	Granular	
I	0%, 2%	$SVI_{10} = 30\text{-}40 \text{ ml g}_{TSS}^{-1}$	Not present	Smooth surface	No effect on the SPUR. Full P-removal.
II	5%, 10%, 15%, 20%	$SVI_{10} = 30\text{-}40 \text{ ml g}_{TSS}^{-1}$	Flocs with filaments in the effluent, not in the reactor.	Mainly smooth, with some filamentous bacteria attached to the surface.	Sharp decrease, then slight recovery of SPUR. Full P-removal.
III	25%, 35%	Increase of $SVI_{10}$ to $80 \text{ ml g}_{TSS}^{-1}$ in one month	Finger-like flocs made of tape-like films.	Surface covered with finger-like outgrowth.	Complete loss of anaerobic phosphate release and negligible SPUR.
IV	0%	Recovery of $SVI_{10}$ to $40 \text{ ml g}_{TSS}^{-1}$ in one SRT	Finger-like flocs made of tape-like films.	Binary: new smooth granules and older granules with finger-like outgrowth.	Partial recovery of SPUR. Sufficient for full P-removal.

### 2.3.3. Biological phosphorus removal during the stepwise increase of the aerobic acetate load

#### Stage II ( $\leq 20\%$ aerobic acetate load)

The stepwise increase of the aerobically dosed acetate to 20% of the total acetate did not affect sludge settleability, and the overall removal performances of nitrogen (data not shown) and phosphorus were also not affected. Acetate concentrations were below the detection limit ( $<1 \text{ mg}_{COD} \text{ L}^{-1}$ ) during the aerobic acetate feeding phase under all experimental conditions  $\leq 20\%$  aerobic acetate load, sampled in the first cycle after the aerobic acetate load had been increased. The addition of acetate under aerobic conditions did have a clear negative impact on the SPUR. The development of the SPUR over time is shown in figure 2.4a. Rates were calculated based on measured concentrations from samples taken during a cycle within an experimental phase (sample interval similar to depicted in figure 2.1). The SPUR decreased sharply after increasing the aerobic acetate load to 5%. The uptake rate increased again during the stepwise transition from 5% to 20% aerobic acetate load, as well as the anaerobic P/COD-ratio (figure 2.4b).

#### Stage III ( $> 20\%$ aerobic acetate load)

The transition from 20% to 25% aerobic acetate load resulted in a further decrease of the SPUR. The phosphate uptake was completely lost over the course the next 25 days (first part of stage III).

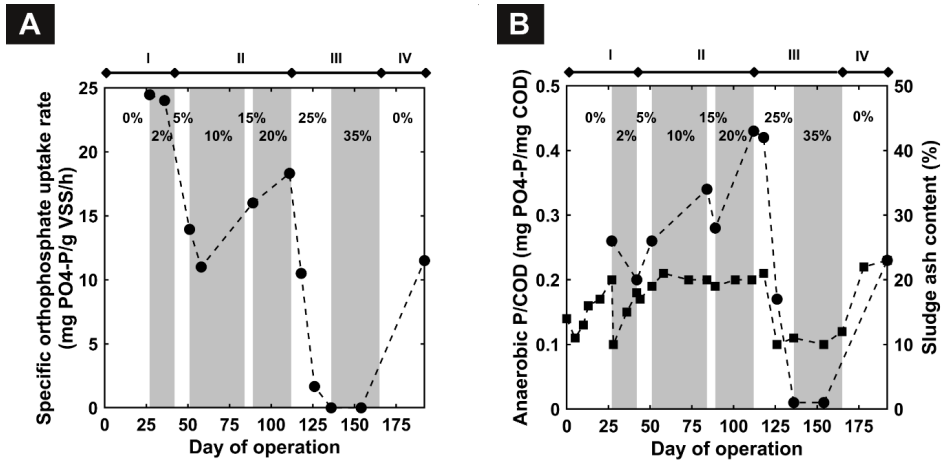


Figure 2.4: (a) SPUR during operation of the reactor. (b) Ratio of  $\text{PO}_4^{3-}\text{-P}$  released per amount of acetate fed in the anaerobic phase (circles, dashed line) and ash content as indicator for loss of polyphosphate storage polymer content (squares, dashed line). Alternating shading represent a change in aerobic acetate load. Percentage values in graphs indicate the aerobically dosed acetate as fraction of the total acetate load. Roman numerals indicate stage in morphological transition mentioned in the text.

Upon closer inspection, a series of events occurred after the aerobic acetate load was increased from 20% to 25% that resulted in the twofold increase in  $\text{SVI}_{10}$  during stage III. The transition from 20% to 25% aerobic acetate load had to be accompanied by a twofold increase in aerobic acetate dosage rate (i.e., to  $116 \text{ mg}_{\text{COD}} \text{ h}^{-1}$ ), since the aerobic acetate load of 25% could not be achieved at the initial aerobic dosage rate of (i.e.,  $58 \text{ mg}_{\text{COD}} \text{ h}^{-1}$ ) while maintaining the same total organic loading within the fixed total cycle time. Although this dosage rate still forced a transport-limited acetate uptake rate, the increase in the aerobic acetate dosage rate had a negative effect on the SPUR. This was initially observed during stage II as well.

Additionally, the concentration profiles of phosphate during the final cycle before the transition (figure 2.5a) and a cycle on the fourth day after the transition (figure 2.5b) showed that the initial SPUR rapidly decreased as the aeration phase progressed. It increased again after the dosage of acetate had finished, but the remaining aeration time was insufficient for complete removal of phosphate. Biological phosphorus removal became kinetically limited due to increased aerobic acetate dosage rate.

The phosphorus removal during the remaining cycles was less than the combined phosphate load from the influent and the anaerobic phosphate release, resulting in a net decrease of the intracellular polyphosphate storage pool. In between day four (figure 2.5b) and day twelve (figure 2.5c) after the increase to 25% aerobic acetate load and increased feeding rate (see table 2.1), two changes were observed in the reactor operation.

- First, the anaerobic ratio of phosphate release over the anaerobic acetate load decreased. The decreasing intracellular polyphosphate pool likely resulted in insufficient anaerobic uptake capacity for acetate, as it coincided with a 10 percent point decrease in the inorganic sludge fraction depicted in figure 2.4b. The increase in oxygen uptake rate (OUR, first seen on day 6) at the start of aeration indicated the presence of a residual acetate concentration, as was deduced from the sudden change in dissolved-oxygen concentration measured in the bulk liquid. This increase came on top of the acetate load dosed as part of the experimental set-up (figure 2.5c).
- Second, the anaerobic uptake of acetate was further decreased by a shorter anaerobic contact time due to short circuit flows. This was most likely caused by increased granular surface roughness due to outgrowth. The short circuit flows increased dispersion in the flow through and above the sludge bed, which was indicated by a non-zero DO concentration at the end of anaerobic feeding (figure 2.5c). The short circuit flows first occurred on an irregular basis (first seen on day 10 after increasing the aerobic acetate load to 25%), but increased in frequency as the experiment progressed. The aerobic acetate load was thereby increased higher than intended.

Both of these mechanisms shifted more of the anaerobic acetate load to the aeration phase besides the already imposed aerobic acetate load. The absence of anaerobic release of phosphate and negligible effective anaerobic contact time resulted in mainly aerobic conversion of the complete acetate load. Biological phosphorus removal remained negligible throughout this period.

#### **Stage IV (recovery with complete anaerobic acetate dosage)**

The recovery of granular morphology was studied after letting it deteriorate at an aerobic acetate load of 35% prior to switching to complete anaerobic feeding (stage IV). Both the ash fraction and the ratio of anaerobic phosphate release over acetate uptake returned to baseline levels after one SRT (figure 2.4b) and complete biological phosphorus removal was restored. Short circuit flow channels still occurred on an irregular basis during anaerobic feeding after the switch, until sludge morphology had significantly improved. The remaining effective anaerobic contact time was sufficient to restore the intracellular polyphosphate pool (restored ash-fraction, figure 2.4b), thus recovering biological phosphorus removal. The combined observations of settleability, morphology and nutrient removal for all stages are summarized in table 2.2.

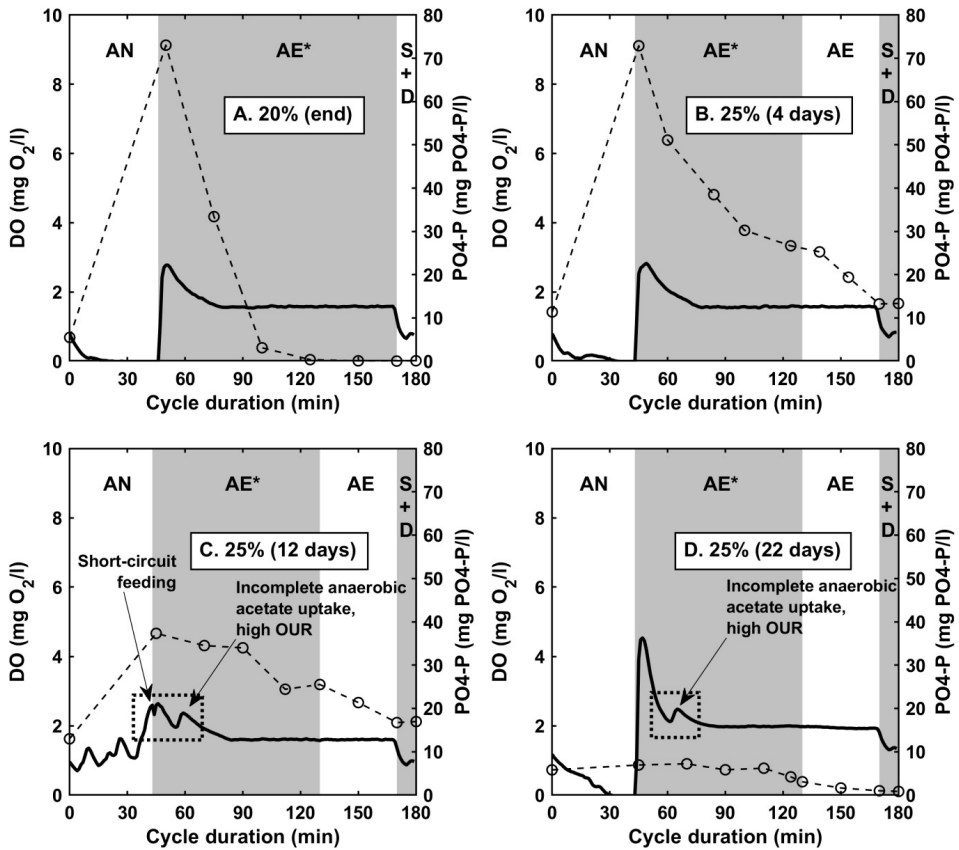


Figure 2.5: Concentration profiles during a cycle for  $\text{PO}_4^{3-}\text{-P}$  (circles, dashed line) and dissolved oxygen (solid line) for respective cycles on (a) the last day operating at 20% aerobic acetate load, (b) after 4 days of 25% aerobic acetate load, (c) after 12 days and (d) after 22 days. Alternating shading denote phase changes within the cycle (AN = anaerobic phase,  $\text{AE}^*$  = aerobic phase with acetate dosage, AE = aerobic phase without acetate dosage, S+D = settling and discharge).

## 2.4. Discussion

In this study, we investigated the effect of an increasing fraction of the total acetate load on the morphology of AGS enriched for anaerobic PHA formation through EBPR (stage I). Acetate was dosed aerobically at a rate that forced transport-limited uptake. This simulated rbCOD leaking through an anaerobic phase as well as the release of rbCOD from slowly biodegradable COD during aeration. These conditions are known to result in the proliferation of filamentous bacteria and poor-settling AS [23]. Smooth granular sludge morphology and good settleability ( $SVI_{10} = 3\text{-}40 \text{ ml g}_{\text{TSS}}^{-1}$ ) up to and including 20% aerobic acetate load (stage II) were maintained. PAOs were able to aerobically compete with aerobic OHOs for acetate uptake and oxygen. This ability of PAOs has been previously described for flocculent sludge [77, 117] and shown to aid in controlling the SVI in flocculent sludge [94]. Although a flocculent sludge fraction with filamentous bacteria formed when acetate was partially fed aerobically, the fraction in the reactor remained negligible due to selective wasting based on settling speed. Additionally, bottom-feeding favoured PAOs growing in well-settling granules and contributed maximally to the ability to aerobically compete for acetate. This work underlines that the selection principles that result in AGS at the same time contribute to mitigation of the adverse effects of an aerobic rbCOD load on sludge morphology.

### 2.4.1. Theoretical aspects of sludge morphology

Selection for anaerobic rbCOD conversion to storage polymers results in well-settling flocculent sludge [94]. These slow-growing organisms generally form dense biofilms [43, 159] and transport-limitation of the electron acceptor in a subsequent stage does not affect the growth morphology. It was hypothesized that the ability of these slow-growing organisms to aerobically convert rbCOD also reduces the fraction consumed for growth of filamentous bacteria when part of the rbCOD load was available under aerobic conditions [94]. Similarly, the majority of the growth of filamentous bacteria was found in suspension in this study (stage II, figure 2.3b), while filamentous outgrowth on granules remained limited (stage II, figure 2.3a). At least up to 20% aerobic acetate load could be sustained without adverse effect on settleability of flocculent sludge enriched for EBPR [94], but the upper limit was not reported. At least the same extent of stability was observed for AGS in this study. Mainly anaerobic acetate uptake capacity thus ensures the aerobic competition for substrate uptake with OHOs.

The morphological fate of aerobically consumed acetate by OHOs, observed in this study, was in line with [93, 95], who formulated the hypothesis that transport-limited aerobic uptake of substrates drives the formation of poor-settling sludge. Transport-limited uptake rates of either rbCOD or oxygen due to low bulk concentrations favours one-dimensional growth in the direction of the concentration gradient. The specific morphology that causes the poor settleability depends on the type aerobic presence of rbCOD, which can be divided into two categories:

- negligible bulk rbCOD concentrations during a large part of the aerated phase (e.g., from hydrolysis of slowly biodegradable COD or continuous supply of rbCOD to the aeration zone in continuous-flow reactors from complete anaerobic uptake), or
- high bulk rbCOD concentrations during a short pulse in the first part of the aerated phase (e.g. from incomplete anaerobic uptake in SBRs)

For the first category, mainly suspended filamentous bacteria were found in this study, aerobically growing on the low concentration of acetate from active feeding during the majority of the aerated time (stage II, figure 2.3b). This is similar as previously observed for acetate fed CSTRs, where the low concentration of acetate also resulted in growth of mainly filamentous bacteria [163].

The second category was observed when the significant decrease in the anaerobic acetate uptake after loss of EBPR (section 2.4.3) caused a pulse of acetate at the start of aeration. During this initial pulse of acetate, the transport-limitation switched to oxygen. This led to overgrowth of the filamentous bacteria in suspension and attached to granular surfaces. The finger-like flocs that formed in this study resembled observations from work on flocculation by [29] and selects for aerobic storage of acetate rather than direct growth. The similarly shaped flocs and finger-like films that formed on granular surfaces closely resembled those from work performed on granular sludge with completely aerobic pulse feeding. There, the relatively low DO (all between 2-4 mg<sub>O<sub>2</sub></sub> L<sup>-1</sup>) led to transport-limitation and high shear stress was required to erode this outgrowth and achieve well-settling granular sludge [16, 102, 104].

These observations emphasize that aerobic transport-limitation in substrate uptake drives irregular growth in AS as well as granular systems, as was shown in a recent modeling study by [191] as well. Combined with the level of shear and mixing, the bulk concentration and duration of aerobic presence of rbCOD thus determine the extent of the transport-limitation and overall effect of sludge morphology.

#### 2.4.2. Reactor operation and the morphological effect of rbCOD

Minor filamentous outgrowth on granular surfaces was observed at 20% aerobic acetate load, supporting a good resilience towards acetate presence (stage II, figure 2.3a). Consequently, the majority of the aerobic growth on acetate formed suspended filamentous bacteria (stage II, figure 2.3b). The large difference in settling speed of both fractions allowed for efficient wasting of most filamentous bacteria and prevented an increase in SVI. Furthermore, anaerobic bottom-feeding favours PHA storage in the granular sludge fraction, in this study leading to a significant PAO-fraction in the granules [78]. The PAO-fraction therefore competed substantially for aerobically available acetate with filamentous bacteria. The selection for anaerobic PHA formation and selective wasting contribute to maintaining a smooth granular morphology and good settleability. The effect of aerobic conversion of rbCOD on granular sludge morphology previously enriched for anaerobic storage has been generalized in figure 2.6a.

In stage III, the loss of significant anaerobic storage leads to mainly aerobic conversion of rbCOD. As was observed in this study, the aerobic competition for rbCOD will be more in favour of flocculent growth or filamentous bacteria (figure 2.6b). Since this becomes the main growth morphology, selective wasting is insufficient to maintain stable granulation and eventually results in loss of granulation.

When granular sludge morphology has deteriorated or is not well established, it can strongly hinder the start-up or recovery of granular sludge morphology. In line with this reasoning, the  $SVI_{10}$  did not improve in this study until after the active aerobic feeding was stopped and complete anaerobic acetate feeding was applied. In stage IV, the  $SVI_{10}$  recovered substantially within one SRT with the formation of new granules and increase in MLVSS. The recovery of the sludge volume took approximately 2-3 SRTs. In lab-scale reactors the waste sludge withdrawal is less optimized for selection compared to full-scale plants, which could result in different time scales for recovery. On the other hand, the less favorable substrate composition of sewage (i.e., not only rbCOD) might result in slower recovery of the sludge volume.

### 2.4.3. Limits of morphological stabilization by anaerobic storage

The experimental results showed that phosphate uptake was negatively influenced each time by an increase in the aerobic feeding rate of acetate. Likely, the decreased SPUR was the result of the PAOs modulating their metabolism towards storage in the presence of an electron acceptor [77]. The simultaneous aerobic acetate uptake seems to limit the SPUR [62, 117]. The incomplete aerobic phosphate uptake initiated the cascaded collapse of biological phosphorus removal (figure 2.5) through the gradual decrease in polyphosphate storage pool (figure 2.4b). As reported also by [118], the latter resulted in complete loss of P-removal. Good granular morphology due to anaerobic storage of rbCOD can thus be maintained if the combination of the aerobic rbCOD uptake rate and the aerobic load allows for sufficient phosphate uptake and glycogen synthesis. In principle, granular stability is not dependent on PAOs or EBPR [43], and stable granular systems with GAOs have been regularly reported [100, 120]. The short circuit flows observed during anaerobic feeding shortly after loss of P-removal, likely minimized the effective anaerobic contact time and prevented continued selection for anaerobic conversion of acetate to PHA by GAOs. Future studies should focus on the impact of rbCOD availability on the phosphate removal process and the risk of GAOs outcompeting PAOs to ensure good phosphate removal.

### Considerations for full-scale AGS processes

Aerobic presence of rbCOD has potential consequences for process stability in full-scale AGS reactors. The rate at which rbCOD becomes available in the bulk and the duration of availability compared to the total aerated time are the critical parameters to maintain stable granulation (section 2.4.3). In practice, these are determined by the reactor design (i.e., a SBR or a continuous-flow reactor) and the source of rbCOD (i.e., incomplete



2

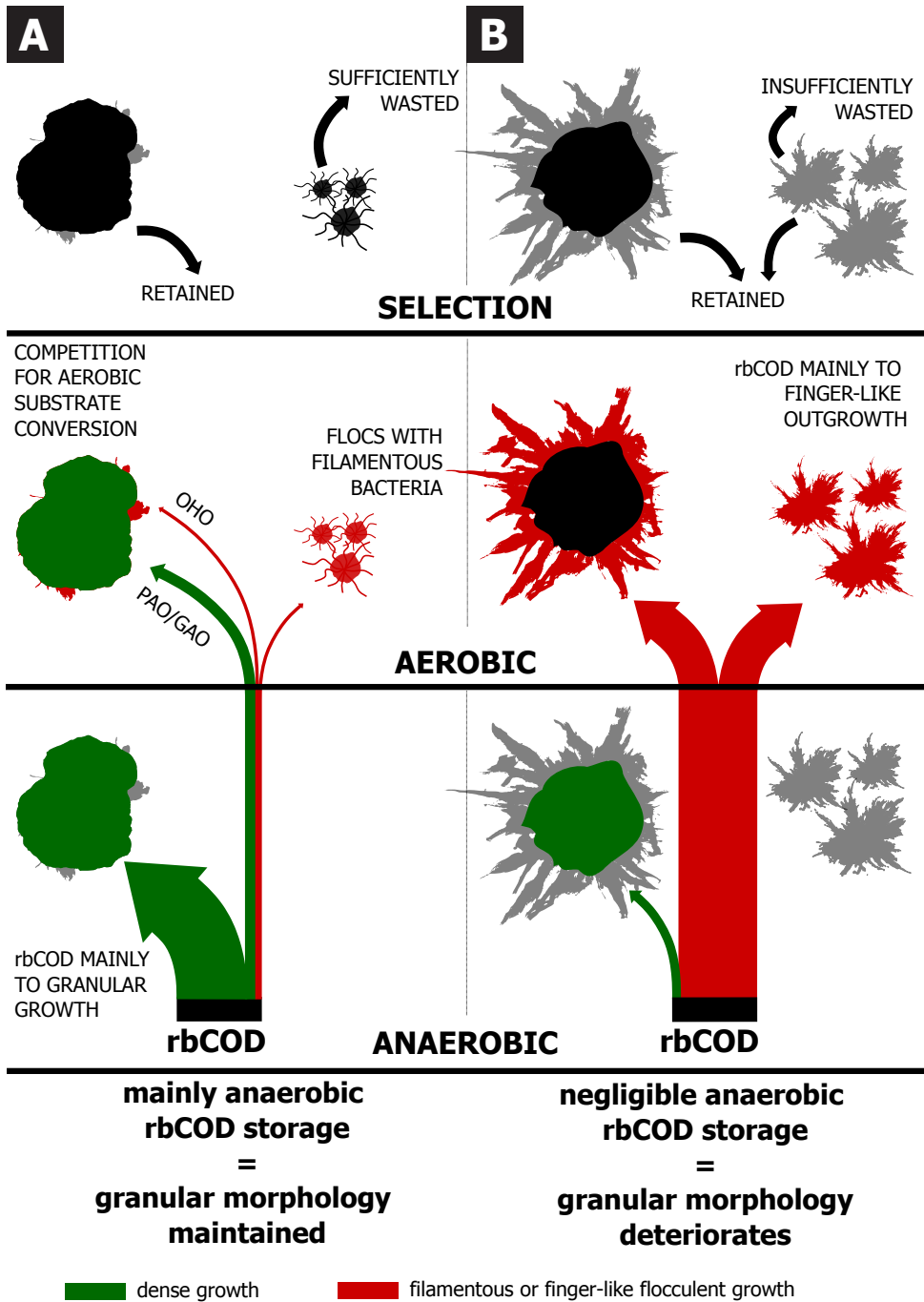


Figure 2.6: Schematic representation of the morphological stabilization by anaerobic PHA storage in case of (a) an additional aerobic rbCOD load and (b) after loss of anaerobic storage capacity. Colors of arrows corresponds morphological destination of rbCOD. The size of arrows indicate the relative amount of rbCOD of the load per cycle.

anaerobic uptake of rbCOD or aerobic hydrolysis of slowly biodegradable COD, see section 2.4.1).

In case of incomplete anaerobic rbCOD uptake, it will result in a very dilute availability of rbCOD during the complete residence time of the mixed aeration zone in continuous-flow reactors. As this study showed, dilute availability of acetate during most of the aerated time was detrimental to the anaerobic acetate uptake capacity and sludge morphology due to insufficient aerobic phosphate uptake (stage III). On the other hand, SBRs will have a higher residual rbCOD concentration at the start of the aeration phase for a relatively short time. Once active aerobic dosage of acetate was stopped in stage IV, acetate was only present during aeration for a short time (10-15 minutes of 110 minutes) since short circuit flows through the sludge bed still occurred during anaerobic feeding. Despite this aerobic acetate load, phosphate uptake and sludge morphology recovered (figure 2.3a, stage IV). Our results therefore indicate that SBRs will be less prone to deterioration of granular morphology compared to continuous-flow reactors. Thus, it is of vital importance for granular stability in continuous-flow reactors to limit the rbCOD presence in the aeration zones.

Besides incomplete anaerobic uptake, aerobic availability of rbCOD will also arise from aerobic hydrolysis of slowly biodegradable COD that is not converted anaerobically [40, 78, 121]. Particulate COD will either be consumed by protozoa or incorporated in the flocculent sludge fraction before being hydrolyzed [96]. The hydrolysis products will then be converted into more flocculent sludge. A good selective removal of the flocculent sludge fraction is therefore required for keeping a stable granular sludge bed. Note that a certain level of flocculent sludge is always present in AGS plants treating sewage and has been shown to aid in achieving good suspended solids effluent quality [158]. The release rate of both sources of rbCOD are relatively slow and will always result in negligible residual concentrations and transport-limited uptake rates, but continuous-flow reactors will still be more affected due to the intrinsic dilution in the mixed aeration zone compared to SBRs.

When granular sludge is well-established, the presence of a large PHA storing fraction (PAOs and GAOs) in the microbial community will stabilize the granular morphology by competing with more flocculent growth for rbCOD during aeration. A recent study by [2] showed a three-fold higher level of enrichment of PAOs in the largest granular size fraction (>1 mm, 60% of biomass) than in the smaller granules and flocculent sludge (<1 mm, 40% of biomass) fraction in a full-scale Nereda<sup>®</sup>. The extra selection for PAO (and thus PHA storage) increases the capacity for aerobic rbCOD uptake in the largest granular sludge fraction. This limits the negative impact of aerobic presence of rbCOD on the granular morphology.

## 2.5. Conclusions

- Selection for anaerobic storage of rbCOD in AGS through EBPR limited the adverse effect of a partial aerobic rbCOD load on sludge morphology through aerobic competition for substrate uptake with OHOs ( $\leq 20\%$  aerobic acetate load at a SAADR of  $4 \text{ mg}_{\text{COD}} \text{ g}_{\text{VSS}} \text{ h}^{-1}$ ). Sufficient aerobic competition could be maintained while the combined negative effect of the aerobic rbCOD uptake rate and the aerobic rbCOD load on phosphate uptake (PAOs) still allowed for full P-removal.
- The reactor configuration with anaerobic bottom-feeding and selective wasting of formed slow-settling flocculent sludge further limited the negative effect of aerobic presence of rbCOD on the sludge morphology of AGS.
- Loss of anaerobic rbCOD uptake and aerobic competition deteriorated the granular sludge morphology due to increased aerobic growth of finger-like structures on the granules and as flocs in suspension ( $>20\%$  aerobic acetate load at a SAADR of  $8 \text{ mg}_{\text{COD}} \text{ g}_{\text{VSS}} \text{ h}^{-1}$ ).
- Finger-like structures on the granular surfaces provoked non-uniform flow through the sludge bed during anaerobic feeding, resulting in extra acetate availability in the aerated phase and further deterioration of the granular sludge morphology.
- Recovery of the sludge morphology through the formation of new, smooth granules occurred only after active aerobic feeding of acetate was stopped. It is therefore important to ensure maximum anaerobic rbCOD removal and prevent transport-limited substrate uptake rates in the aeration phase during recovery or start-up.

In general, the sludge morphology of AGS systems with good anaerobic storage of rbCOD can be considered resilient to low concentrations of rbCOD under aerobic conditions. The selection principles that result in AGS formation also contribute to mitigation of the adverse effects of low aerobic rbCOD concentrations on settleability.

## Acknowledgements

The authors would like to thank Roel van de Wijngaart for the sample preparation and microscopy performed for the FISH-images.

## Appendix

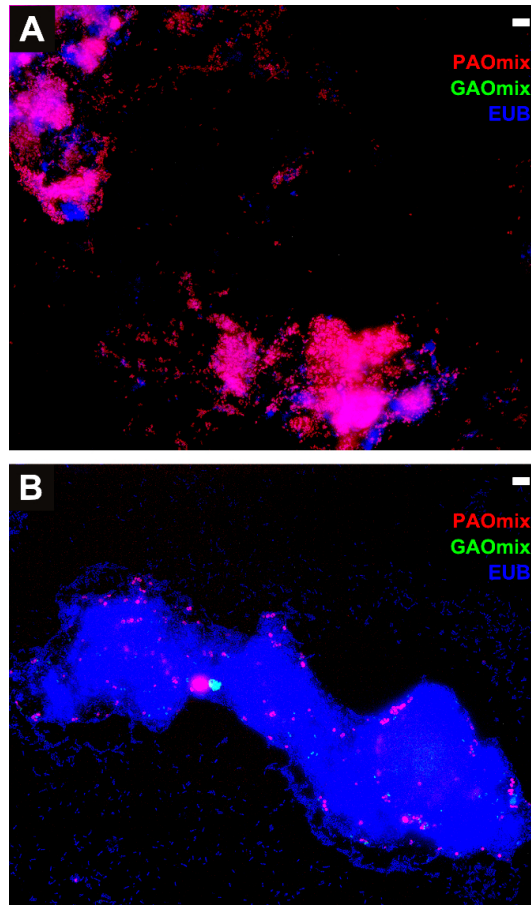


Figure 2.7: Images of potted samples prepared for FISH-microscopy from (a) the reference period with complete anaerobic acetate uptake (day 27) prior to the start of active acetate dosage in the aerobic phase and (b) at the end of the period with 35% aerobic acetate load dosed at  $8 \text{ mg}_{\text{COD}} \text{ g}_{\text{VSS}} \text{ h}^{-1}$  (day 162). A mixture of PAO462, PAO651, and PAO846 probes (PAOmixon) was used for visualizing PAOs [30]. A mixture of GAOQ431 and GAOQ989 probes (GAOmixon) was used for visualizing GAOs [31]. A mixture of EUB338, EUB338-II and EUB338-III probes was used for staining all bacteria (EUB) [3, 35]. Length represented by white scale bars is  $10 \mu\text{m}$ .



# 3

## **Distribution of rbCOD via the anaerobic feeding mode**

### 3.1. Introduction

AGS is a novel technology for compact treatment of wastewater, applied mainly in SBRs at full-scale [122]. There is a growing interest to implement AGS in existing CAS systems, mostly with a continuous-flow configuration [74, 188]. The increased settleability of AGS compared to conventional AS would allow for a higher mixed-liquor suspended solids (MLSS) for the same volumetric loading rate, yielding an increase in biological treatment capacity. Simultaneous nutrient removal processes within the biofilms also could be utilized to a larger extent [147].

For a similar successful implementation of AGS in conventional AS systems, the required selective pressures for the formation and retention of AGS must be translated from the SBRs to continuous-flow systems. The anaerobic storage of rbCOD as PHA (PHA) ensures dense growth of OHOs during subsequent aeration by preventing transport-limited growth [43]. At full-scale, the fraction of rbCOD in municipal wastewater is often limited and the more slowly biodegradable, especially the particulate COD fraction, has been hypothesized to result in flocculent growth under aerobic conditions [78, 121]. Ensuring that anaerobic storage of the limited rbCOD is performed by the sludge fraction with the highest settling velocity speeds up the formation of granular sludge when starting from a flocculent morphology, and results in a larger mean granule size [156]. The selection criterion for AGS is therefore not only to ensure anaerobic uptake of rbCOD and storage as PHA, but to concentrate the available rbCOD in the best settling sludge fraction as well (i.e. selective feeding). In bottom-fed SBRs, both criteria are automatically achieved since the best-settling granules have a higher probability to accumulate at the bottom of the sludge bed. In other reactor configurations, particularly in continuous-flow reactors, this might be more difficult to achieve.

The method of anaerobic contact of raw sewage with the sludge is an important aspect in the adaptation of CFAS systems to accommodate AGS. CFAS systems designed for EBPR generally employ a plug-flow anaerobic selector zone in which part of the recycled sludge is contacted with the influent while in suspension [94]. The applied loading rate (mass of rbCOD/mass of sludge/amount time) aims to minimize diffusion gradients of rbCOD inside the sludge flocs and the sludge loading (mass of rbCOD/mass of sludge) sets the amount of flocs over which the incoming rbCOD is distributed. These parameters respectively determine the initial penetration depth of rbCOD and the total amount of stored COD per sludge particle/floc, resulting in relatively dense and well-settling flocs [177]. Since the sludge is kept in suspension, sludge particles with a larger surface area to volume ratio can achieve a higher volumetric rbCOD uptake rate if the penetration depth is limited. This favours a flocculent morphology over a granular morphology. A higher initial concentration gradient of rbCOD (i.e. an increased loading rate) can partially counteract the lower surface to volume ratio of granules compared to flocs due to full penetration of even the largest granules. Whether this can be achieved to such an extent that granules can be formed that are substantially larger than flocs, likely depends on the fraction of rbCOD compared to the total COD in the wastewater [156].

Some full-scale studies have investigated the relation between the design of an anaerobic selector and the sludge morphology with a focus on aerobic granulation. [129] investigated the effect of the sludge settleability of a WWTP which had the flow pattern of the anaerobic selector converted from a tanks-in-series configuration to a step-feed. The characteristics of the sludge settleability were very similar to that of AGS in the tanks-in-series configuration, with a SVI<sub>5</sub>/SVI<sub>30</sub>-ratio close to unity. The ratio gradually increased after the transition to a more flocculent morphology in the step-feed configuration. These findings demonstrated the adverse effect of a decrease in initial rbCOD loading and initial rbCOD loading rate on the granular sludge morphology. [180] investigated the process conditions of several full-scale conventional AS facilities in the USA with varying levels of spontaneous granulation. No correlation was found between the COD loading rate of the anaerobic selector and the level of granulation observed (the rbCOD loading rates were not reported). The level of granulation did correlate strongly with the fraction of PAOs found in the granular sludge fraction compared to the flocculent fraction, indicative of an increased enrichment for anaerobic uptake of rbCOD in the granular fraction. It remains unclear how the distribution of substrate over the sludge by a conventional anaerobic selector compares to the distribution via bottom-feeding applied in SBRs, and how it impacts the granulation process. The implementation of stable AGS into existing continuous-flow WWTPs thus requires further study on the impact of the anaerobic feeding mode of sewage with sludge.

To investigate the effect of the anaerobic feeding mode on the substrate (and storage) distribution, the granulation potential, the size distribution, and related conversions, we operated two lab-scale SBRs; one with the traditional bottom-feeding through a settled sludge bed similar to full-scale AGS systems, and one where the synthetic wastewater was fed as a pulse at the start of the anaerobic phase while the reactor was mixed by sparging of nitrogen gas. The latter generates exposure of the sludge to a high substrate concentration at the start of the anaerobic period, which gradually decreases to zero. From a biological process view this can be considered a scaled down version of a plug-flow anaerobic selector as employed in conventional AS systems. Starting from flocculent sludge, the formation of AGS was followed. The effect of the contact method on the distribution of the substrate over the sludge particle population was quantified via PHA analysis, combined with the granule size distribution. The interactions between the anaerobic feeding mode and aerobic conversion processes were investigated. Implications for application in continuous systems and the nutrient removal process are discussed.

## 3.2. Methodology

### 3.2.1. Reactor set-up and operation

Two cylindrical lab-scale reactors (i.e. one pulse-fed, one bottom-fed), each with a working volume of 3 L during aeration and an aspect ratio of 20, were operated as a sequential batch reactor with a volume exchange ratio of 0.47. The reactors were operated continuously



in 205 min cycles during 144 days. After settling and discharge of effluent, the working volume of the reactor was 1.6 L. A cycle started with an anaerobic phase in which synthetic wastewater was fed. A different anaerobic feeding mode was used in each reactor. The pulse-fed reactor was first sparged with dinitrogen gas (5 min) with  $5 \text{ L min}^{-1}$  (superficial gas velocity of  $3.5 \text{ cm s}^{-1}$ ) to deplete the bulk-liquid of dissolved oxygen. The batch of synthetic wastewater was then fed while sparging and mixing continued (2 min). The pulse-fed reactor was subsequently mixed with dinitrogen gas for the remainder of the anaerobic phase (53 min). For the bottom-fed reactor, synthetic wastewater was fed through the bottom of the settled sludge bed with a superficial liquid velocity of  $0.46 \text{ m h}^{-1}$  (60 min). The remainder of the cycles were identical for both reactors: an aeration phase (maximum duration of 137 min), a settling period (minimum duration of 3 min), and finally the discharge of effluent (1 min) and a waiting phase to allow packing of the sludge bed (4 min). All sludge unable to meet the settleability criterion, was discharged with the effluent. During start-up, the settling period started at 30 min at the expense of the aeration phase and was gradually decreased to 5 min, while maintaining a constant total cycle duration. The temperature was controlled at  $20 \pm 1 \text{ }^\circ\text{C}$  through the double-jacketed reactor wall using a water bath with thermostat. The pH was controlled during aeration (and during the mixed anaerobic phase of the pulse-fed reactor) at  $7.0 \pm 0.1$  by dosage of either a 1 M solution of hydrochloric acid or a 1 M sodium hydroxide solution. A conductivity sensor was used to monitor the anaerobic release and aerobic removal of ortho-phosphate [181]. During aeration, a recirculation gas flow was maintained at  $6 \text{ L min}^{-1}$  (superficial gas velocity of  $4.2 \text{ cm s}^{-1}$ ). A DO concentration of  $2 \text{ mg O}_2 \text{ L}^{-1}$  was maintained during the aeration phase via addition of compressed air or dinitrogen gas using mass flow controllers. The total organic loading rate ( $1.12 \text{ g COD L}^{-1} \text{ d}^{-1}$ ) was kept constant over the course of the study. Granular sludge previously enriched under the same conditions as applied in the bottom-fed reactor, and with the same synthetic influent, was used as inoculum. The inoculum was crushed using an ULTRA-TURRAX homogenizer T-18 (IKA, Staufen im Breisgau, Germany), after which the sieve fraction between  $63 \text{ }\mu\text{m}$  and  $100 \text{ }\mu\text{m}$  added to both reactors to yield an initial MLSS concentration of  $0.5 \text{ g TSS L}^{-1}$ .

### 3.2.2. Composition of synthetic wastewater

A synthetic wastewater of 1.4 L per cycle was used as anaerobic feed and consisted of 1.2 L of deionized water together with 100 mL carbon source (medium A) and 100 mL nitrogen and phosphorous source (medium B). Medium A contained 65.6 mM  $\text{NaCH}_3\text{COO}\cdot 3\text{H}_2\text{O}$ , 4.1 mM  $\text{MgSO}_4\cdot 7\text{H}_2\text{O}$ , and 5.4 mM KCl. Medium B contained 15 mM  $\text{NH}_4\text{Cl}$ , 1.3 mM  $\text{K}_2\text{HPO}_4$ , 2.1 mM  $\text{KH}_2\text{PO}_4$ , and  $16.6 \text{ mL}^{-1}$  trace elements solution (Vishniac and Santer, 1957), but using  $2.2 \text{ mg L}^{-1}$   $\text{ZnSO}_4\cdot 7\text{H}_2\text{O}$  instead of  $22 \text{ mg L}^{-1}$  [123, 121]. The combination of medium A, medium B, and tap water led to a synthetic wastewater composition of  $300 \text{ mg COD L}^{-1}$ ,  $15 \text{ mg NH}_4^+\text{-N L}^{-1}$ , and  $7.5 \text{ mg PO}_4^{3-}\text{-P L}^{-1}$ . Allylthiourea (ATU,  $5 \text{ mg L}^{-1}$  of synthetic wastewater) was dosed to suppress nitrification. This enabled the calculation of biomass yield directly from the consumption of ammonium and ensured anaerobic conditions at the start of the feeding phase due to the absence of nitrate from the previous

cycle. All media were dosed using peristaltic pumps.

### 3.2.3. Anaerobic kinetics and storage capacity for uptake of acetate

Anaerobic batch tests were performed on the granule size fractions obtained by sieving once a dynamic equilibrium had been reached in the granule size distribution in both reactors (after 140 days). A mixed sludge sample was obtained at the end of the aeration phase and fractionated over a stack of sieves with varying mesh size (fractions 400-800  $\mu\text{m}$ , 800-1000  $\mu\text{m}$ , 1000-1400  $\mu\text{m}$  and >1400  $\mu\text{m}$ ). Each fraction was added to a separate container with filtered reactor effluent (63  $\mu\text{m}$ ) to obtain a total volume of 200 mL, containing 0.1 M HEPES acting as a buffer to ensure a constant pH throughout the experiment, equivalent to normal reactor operation. The pH was set to  $7 \pm 0.5$  using a 4 M solution of sodium hydroxide. Temperature was constant throughout the experiment at 20 °C. Each container was sparged with dinitrogen gas ( $1 \text{ L min}^{-1}$ ) for 5 min to strip DO from the liquid, after which a sample was taken for the initial ortho-phosphate concentration. Sparging continued throughout the remainder of the experiment to maintain anaerobic conditions. The experiment was initiated by addition of a concentrated solution of sodium acetate to obtain an initial concentration of  $500 \text{ mg}_{\text{Ac}^-} \text{ L}^{-1}$  to prevent incomplete penetration of the largest granule size (full penetration up to largest granule size of 1.5 mm and  $t_{90}$  penetration time of 5.3 min according to [146] using  $D = 0.87 \times 10^{-9} \text{ m}^2 \text{ s}^{-1}$  [167] and  $q_{\text{Ac}^-, \text{max}} = 0.15 \text{ g}_{\text{Ac}^-} \text{ g}_{\text{VSS}}^{-1} \text{ h}^{-1}$  (this work)). After addition of the sodium acetate, a sample (approximately 2.5 mL) was taken every 5 min (up to 30 min) and immediately filtered through a 0.45  $\mu\text{m}$  syringe filter (CA membrane, Millipore) and put on ice for later determination of ortho-phosphate and acetate concentration profiles. A final sample was taken after 100 min to determine total release of ortho-phosphate and uptake of acetate. Negligible biomass was removed during sampling. The decrease in liquid volume due to sampling was determined after the experiment had finished, which was used in the calculation of the specific activity of the biomass. The biomass in each container was sampled for determination of the MLVSS concentration after the experiment had finished.

### 3.2.4. Analytical procedures

#### Determination of ML(VSS), solute concentrations and sludge volume (index)

$\text{NH}_4^+$ -N and  $\text{PO}_4^{3-}$ -P concentrations were measured by using a Thermo Fisher Gallery Discrete analyzer (Thermo Fisher Scientific, Waltham, USA). The concentration of acetate was determined by HPLC with an Aminex HPX-87H column from Biorad, coupled to an UV detector, using 0.01 M phosphoric acid as eluent. MLSS and MLVSS concentrations in the reactor were determined according to the standard methods [5]. The sludge volume after 5 min of settling ( $\text{SV}_5$ ) was determined in-situ in between cycles.

#### Biomass density within granules

The biomass density of the granules was measured using a Dextran Blue-method [19, 165]. A dilution series of Dextran Blue 2000 was prepared in the filtered effluent (0.45  $\mu\text{m}$  CA membrane, Millipore) up to  $2 \text{ g L}^{-1}$  and the absorption of light at a wavelength 620 nm

measured with a spectrophotometer (DR3900, HACH) as a calibration line. The whole sludge volume from a reactor was transferred to a measuring cylinder and effluent was added to a total volume of 1 L. Effluent collected from the previous cycle was decanted and filtered through a 0.45  $\mu\text{m}$  filter. 1 g of Dextran Blue 2000 was added to the measuring cylinder and subsequently the whole cylinder was mixed. The total volume and settled sludge volume were measured after five min of settling. Samples were taken from the supernatant in triplicate and filtered through a 0.45  $\mu\text{m}$ . After determination of the concentration of Dextran Blue 2000 by spectrophotometry, the volume occupied by the biomass was calculated and combined with the VSS previously determined to yield the biomass density.

### 3

#### **Level of PHA in granule sieve fractions before and after anaerobic feeding**

Mixed biomass samples were taken after the anaerobic reaction phase and at the end of the aeration phase of both reactors to determine the average acetate stored as PHA per granule sieve fraction. The bottom-fed reactor was modified to accommodate anaerobic sampling after the feeding. During the feeding, the liquid above the sludge bed was stripped with nitrogen gas to remove residual oxygen without disturbing the influent flow through the bed. After anaerobic feeding, the bottom-fed reactor was mixed by sparging dinitrogen gas and a mixed biomass sample was taken. The biomass was inactivated with formaldehyde and subsequently sieved (fractions <400  $\mu\text{m}$ , 400-800  $\mu\text{m}$ , 800-1000  $\mu\text{m}$ , 1000-1400  $\mu\text{m}$  and >1400  $\mu\text{m}$ ) to prepare for determination of the PHB and poly- $\beta$ -hydroxyvalerate (PHV) content of each size fraction according to the method of [72].

#### **Stereo microscopy for counting individual granules**

Sludge was collected from the reactor at the end of the aeration phase and from the effluent directly after discharge while kept in suspension. A mixed sample from either source was transferred to a glass petri dish and examined according to [60] by the means of an Olympus reverse microscope coupled with a Leica Digital Camera, together with its software QWin Pro (version 3.1.). The granule size distribution was determined by counting individual granules with a minimum of 1000 hits. The equivalent diameter of each granule was calculated based on the projected area of a granule, which was used to calculate the volume assuming the shape of a sphere. False hits were identified by manual inspection of a subset of the images obtained in one measurement. These false hits were consistently caused by aberrations in the glass dish containing the sample and were smaller than 100  $\mu\text{m}$ . Therefore, hits with an equivalent diameter smaller than 100  $\mu\text{m}$  were discarded.

#### **Fluorescent in-situ hybridization (FISH)**

The handling, fixation and staining of FISH samples was performed as described by [12]. A mixture of PAO462, PAO651, and PAO846 probes (PAOm<sub>ix</sub>) was used for visualizing PAOs [30]. A mixture of GAOQ431 and GAOQ989 probes (GAOm<sub>ix</sub>) was used for visualizing GAOs [31]. A mixture of EUB338, EUB338-II and EUB338-III probes was

used for staining all bacteria [3, 35]. Images were taken with a Zeiss Axioplan 2 epifluorescence microscope equipped with filter set 26 (bp 575e625/FT645/bp 660e710), 20 (bp 546/12/FT560/bp 575e640) and 17 (bp 485/20/FT 510/bp 5515e565) for Cy5, Cy3 and fluos respectively.

### 3.2.5. Calculation procedures

#### Granule size distribution

Hits from counting individual granules through stereo microscopy were binned in size fractions <400  $\mu\text{m}$ , 400-800  $\mu\text{m}$ , 800-1000  $\mu\text{m}$ , 1000-1400  $\mu\text{m}$  and >1400  $\mu\text{m}$  based on the equivalent diameter. A volume was calculated for each granule in every bin by assuming sphericity. Finally, the mass distribution over each bin was calculated by multiplying the volume fraction of a bin of the total volume of all counted granules, assuming a constant biomass density not dependent on granule size.

#### Conversion of PHA mass fractions to acetate equivalents

A ratio of 0.75 C-mol acetate/C-mol PHB was used to calculate the anaerobically consumed acetate equivalents for the measured PHB for both polyphosphate-accumulating metabolism (PAM) [144] and glycogen-accumulating metabolism (GAM) [196]. Besides PHB, the accumulation of PHV in acetate fed communities dominated by PAO occurs in the case of low phosphate availability [140, 182]. The energy required for the sequestration of acetate is then derived partly from glycolysis besides the hydrolysis of polyphosphate. The surplus reduction equivalents from glycolysis are used to reduce either part of the acetyl-CoA (glyoxylate shunt) or of the glycolysis products (reductive branch of the tri carboxylic acid (TCA) cycle). Both yield propionyl-CoA, which is subsequently converted with PHB to PHV (and to small amounts of poly- $\beta$ -hydroxy-2-methylvalerate (PH2MV), disregarded in this analysis). Based on the conditions applied, it was assumed that all PHV originated from pure GAM, yielding a ratio of acetate carbon incorporated in PHV of 0.26 C-mol/C-mol [196].

#### Calculation of anaerobic acetate distribution

The anaerobic acetate distribution over the sludge population was calculated by combining the mass fraction ( $f_{j,X}$ ) of a granule size class ( $j$ ), the total reactor volume ( $V_L$ ), the total MLVSS concentration ( $c_{MLVSS}$ ) and the acetate equivalents calculated from the difference of PHA levels at the end of the aerated phase and the end of the anaerobic phase ( $\Delta\text{Ac}_j^-$ ). The calculation of the amount of acetate accumulated in a size class relative to the total amount of acetate fed ( $f_{j,\text{Ac}^-}$ ) is shown in equation (3.1):

$$f_{j,\text{Ac}^-} = \frac{V_L c_{MLVSS} f_{j,X} \Delta\text{Ac}_j^-}{\text{Ac}_{\text{fed}}^-} \quad (3.1)$$

### Determination of SRT of granule size fractions

The SRT for the granule size fractions at steady-state were calculated based on the cumulative excess sludge removed during one day (~7 cycles) via selective wasting and the granule size distribution in the reactor. The collected excess sludge was fractioned via a stack of sieves with mesh sizes 1400 $\mu\text{m}$ , 1000 $\mu\text{m}$ , 800 $\mu\text{m}$  and 400 $\mu\text{m}$  and the amounts of total suspended solids (TSS) were subsequently determined for all fractions ( $WS_j$ ,  $\text{kg}_{\text{TSS}} \text{d}^{-1}$ ). The fraction smaller than 400 $\mu\text{m}$  was negligible at steady state and was therefore discarded. The total mass of sludge of each fraction was calculated from the granule size distribution and the total MLSS in the reactor ( $V_L c_{\text{MLSS}} f_{j,X}$ ). The SRT of a size fraction ( $SRT_j$ ) was calculated from through equation (3.2):

$$SRT_j = \frac{WS_j}{V_L c_{\text{MLSS}} f_{j,X}} \quad (3.2)$$

## 3.3. Results

### 3.3.1. Start-up

The pulse-fed and bottom-fed reactors were both inoculated with approximately  $0.5 \text{ g}_{\text{TSS}} \text{ L}^{-1}$  of crushed AGS previously enriched in a laboratory reactor operated under similar conditions [63]. The crushed seed sludge was sieved over a cascade of a 100  $\mu\text{m}$  and a 63  $\mu\text{m}$  sieve, after which the fraction retained at the 63  $\mu\text{m}$  sieve was used as inoculum (figure 3.1). Both the reactors were immediately operated under the same volumetric substrate (acetate) loading rate of  $1.12 \text{ g}_{\text{COD}} \text{ L}^{-1} \text{ d}$ . The initial settling rate selection criterion was set at  $1 \text{ m h}^{-1}$  and was gradually increased to  $10 \text{ m/h}$  over the course of 19 days for both reactors.

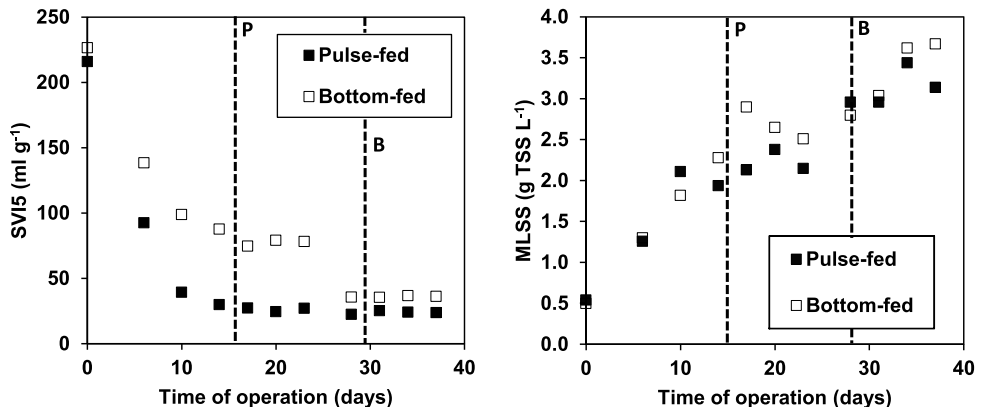


Figure 3.1: (left) Development of SVI5 and (right) MLSS over time for the pulse-fed (solid squares) and bottom-fed (open squares) reactors. Vertical dashed lines denote transition to only granular growth as observed using stereo microscopy for both the pulse-fed (P) and bottom-fed (B) reactors.

### Settleability and morphology

Development of the granular sludge in terms of  $SVI_5$  and MLSS in the reactors is depicted in figure 3.1. Both reactors developed well settling granular sludge ( $SVI_5$  between 30-40 ml  $g_{TSS}^{-1}$ ), but the granulation occurred faster in the bottom-fed reactor ( $26 \mu m d^{-1}$  for the pulse-fed reactor, versus  $40 \mu m d^{-1}$  for the bottom-fed reactor). The amount of dry mass increased at a similar rate, regardless of the anaerobic feeding regime. The initial growth morphology of both systems was characterized by flocculent as well as granular growth (figures 3.2a and 3.2b). Flocs were identified as translucent clusters using stereo zoom microscopy, while small granules (100-200 $\mu m$ ) appeared as opaque and dense aggregates. Flocculent growth could not be detected in the pulse-fed reactor after 15 days (figure 3.2c), while flocs were observed in the bottom-fed reactor up to 28 days of operation (figure 3.2f). These observations coincided with the development of the  $SVI_5$  (figure 3.1). The further development of the granular morphology was similar for both anaerobic feeding regimes.

### Anaerobic acetate uptake efficiency

The anaerobic acetate uptake was monitored on-line by conductivity measurements (see figure 3.8 for the estimated completeness of acetate uptake as function of time). The pulse-fed system developed complete anaerobic acetate uptake within two weeks after start-up. The bottom-fed reactor took four weeks for obtaining full anaerobic acetate uptake. This was due to short-cut flow of the influent through the sludge bed during the first month after start-up, decreasing the effective anaerobic contact time with the sludge. Therefore, part of the fed acetate was then not taken up anaerobically. This can be considered a scale-effect due to the limited sludge bed height and less optimized influent distribution manifold compared to full-scale reactors. This prolonged the aerobic availability of acetate compared to the pulse-fed reactor and caused the extended presence of flocs in the bottom-fed reactor. The disappearance of flocculent growth coincided in both reactors with the moment of full anaerobic acetate uptake in the pulse-fed and bottom-fed reactors at days 15 and 28, respectively.

#### 3.3.2. Steady-state operation

The pulse-fed and bottom-fed reactors were operated for a duration of 5 months until a stable granule size distribution had been achieved. Both systems were characterized and typical process parameters for both reactors are listed in table 3.1. The reactors have been operated at a similar average MLVSS concentration, substrate loading rate and SRT. Considering the fluctuations in MLVSS concentration (sampled over the course of five weeks, centred around 144<sup>th</sup> day of operation), the biomass characteristics had developed to a similar level in both reactors. The bottom-fed reactor showed a slightly higher  $SVI_5$ , which had been observed since the start of the experiment. Other than that, the difference in anaerobic feeding regime did not result in differences in biomass characteristics. FISH microscopy indicated an enrichment of *Ca. Accumulibacter phosphatis* clade I at similar high levels in both reactors (figure 3.11). The mass distribution over the granules size fractions showed a higher unevenness for the bottom-fed reactor compared to the

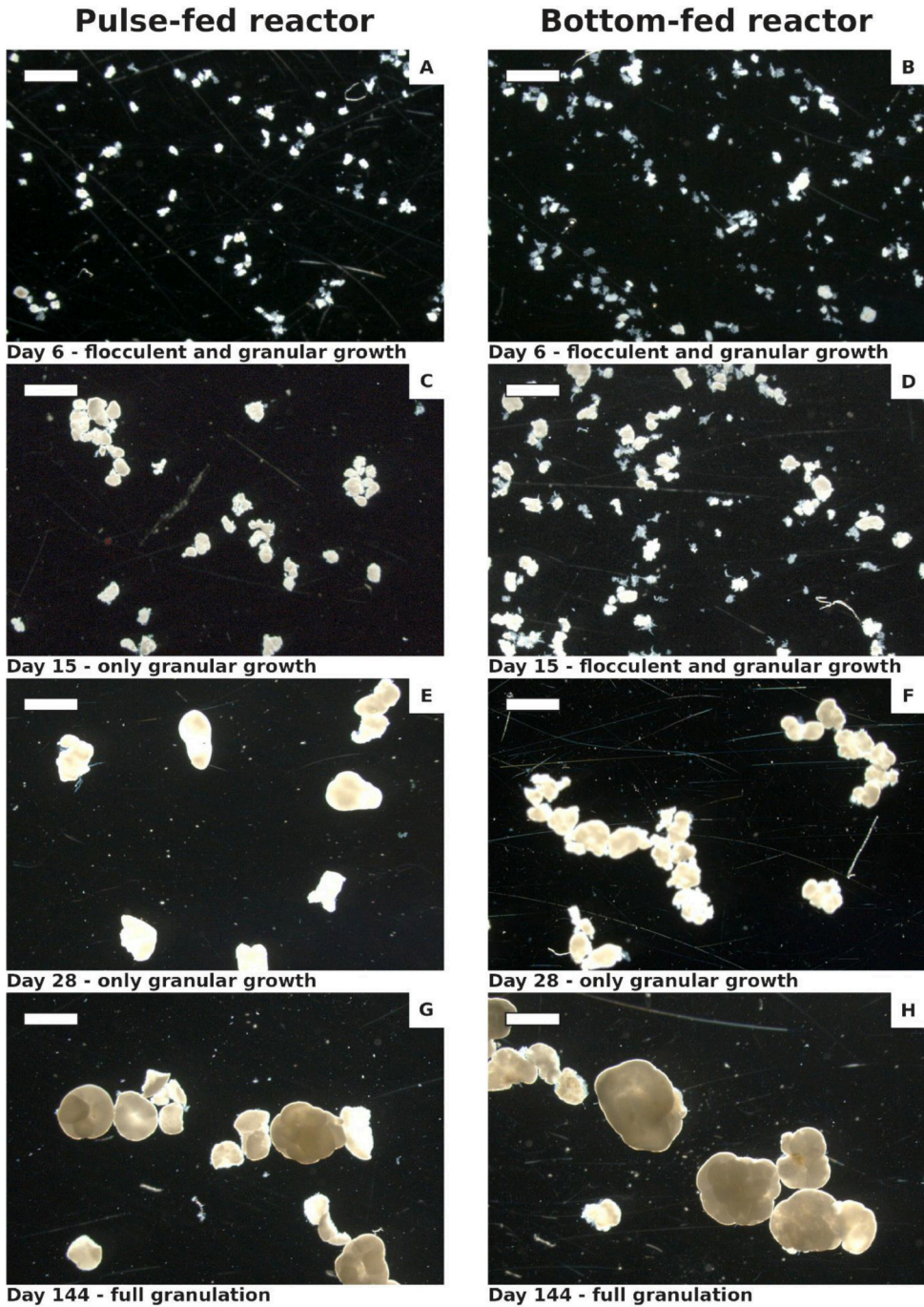


Figure 3.2: Development of sludge morphology as observed by stereo zoom microscopy. Four stages in the development are depicted for both the pulse-fed and bottom-fed reactors: 6 days after start-up (a + b), 15 days after start-up (c + d, complete granular growth in pulse-fed reactor), 28 days after start-up (e + f, complete granular growth in bottom-fed reactor) and 144 days after start-up (g + h). Scale bar represents 1000  $\mu\text{m}$ .

pulse-fed reactor; 81% of the mass was present in granules larger than 1 mm in the bottom-fed reactor, compared to 66% in the pulse-fed reactor (figure 3.3). The main difference in BNR was the substantially higher anaerobic P/COD-ratio and higher SPUR of the pulse-fed reactor. Other reactor characteristics relevant for further analysis of the effect of the anaerobic feeding regime on aerobic granulation are reported below.

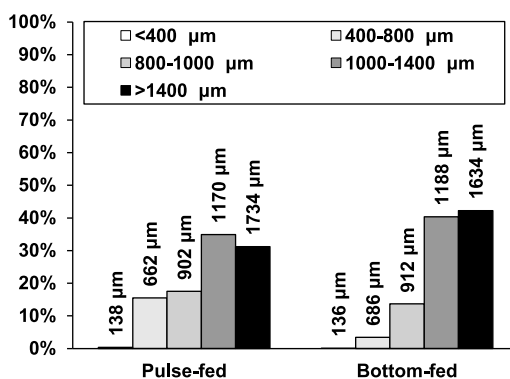


Figure 3.3: Mass distribution (VSS) over granule size fractions in both the pulse-fed and bottom-fed reactors based on stereo zoom microscopy and bed porosity measurements. Labels represent the mean particle size per fraction as determined via analysis of images obtained using stereo microscopy. Sludge samples were taken at steady state conditions on the 144<sup>th</sup> day of operation.

### PHA storage polymer distribution over granule size fractions

The impact of the anaerobic feeding regime on the distribution of acetate over the granule size fractions was assessed once the granule population had stabilized in both the pulse-fed and bottom-fed reactors. Samples were taken from the mixed granular sludge suspension before and after the anaerobic feeding stage within the same cycle. The mass fractions of PHB and PHV in the sludge samples were quantified after fractionation by sieving. The majority of the PHA storage pool was PHB, but considerable amounts of PHV were detected in both the pulse-fed and bottom-fed systems (table 3.2). The levels of PHB and PHV in the biomass were converted to the equivalent amount of acetate consumed before and after the anaerobic phase per amount of VSS (figure 3.4). A decreasing trend was observed for the relative amount of acetate consumed in the pulse-fed system for increasing granule size fraction. On the other hand, the anaerobic bottom-feeding favoured substrate uptake by the largest granule size fraction. A considerable amount of PHA remained in the bottom-fed reactor at the end of aeration, and this amount increased with granule size. The pulse-fed system showed a complete depletion of the PHA storage pool. Negligible differences were observed between anaerobic acetate uptake rates and maximal storage capacities between both reactors and per sieve fraction in batch tests (table 3.1). Therefore, the observed differences can be attributed to the difference in anaerobic feeding mode applied in each reactor.



Table 3.1: Overview of biomass characteristics (based on data from five consecutive weeks) and parameters regarding biological conversions.

Property (unit)	Pulse-fed	Bottom-fed
MLVSS ( $\text{g}_{\text{VSS}} \text{L}_{\text{reactor}}^{-1}$ )	3.7 ± 0.7	3.5 ± 0.6
Organics content ( $\text{g}_{\text{VSS}} \text{g}_{\text{TSS}}^{-1}$ )	0.79 ± 0.03	0.82 ± 0.03
Sludge volume ( $\text{mL}_{\text{bed}} \text{L}_{\text{reactor}}^{-1}$ )	149 ± 19	184 ± 34
Biomass density ( $\text{g}_{\text{VSS}} \text{L}_{\text{biomass}}^{-1}$ ) <sup>a</sup>	31	27
Estimated biomass yield ( $\text{g}_{\text{VSS}} \text{g}_{\text{COD}}^{-1}$ ) <sup>d</sup>	0.19	0.19
Average SRT based on yield (d) <sup>d</sup>	18	18
Anaerobic conversions		
P/COD ratio ( $\text{g g}^{-1}$ ) <sup>b</sup>	0.57	0.32
Maximum specific $\text{Ac}^-$ uptake rate ( $\text{mg}_{\text{COD}} \text{g}_{\text{VSS}}^{-1} \text{h}^{-1}$ ) <sup>c</sup>	156	149
Maximum specific $\text{Ac}^-$ uptake capacity ( $\text{mg}_{\text{COD}} \text{g}_{\text{VSS}}^{-1}$ ) <sup>c</sup>	155	145
Aerobic conversions		
Specific $\text{PO}_4^{3-}$ -P uptake rate ( $\text{mg}_{\text{P}} \text{g}_{\text{VSS}}^{-1} \text{h}^{-1}$ ) <sup>c</sup>	34	18
Initial specific $\text{PO}_4^{3-}$ -P uptake rate ( $\text{mg}_{\text{N}} \text{g}_{\text{VSS}}^{-1} \text{h}^{-1}$ ) <sup>c</sup>	0.67	0.44
$\text{NH}_4^+$ -N/VSS ( $\text{g g}^{-1}$ )	0.11	0.11

<sup>a</sup> Determined using Dextran Blue-method.

<sup>b</sup> Calculated based on cycle measurement(s) (see figure 3.9).

<sup>c</sup> Maximum acetate uptake rates and storage capacity under anaerobic conditions were determined in batch tests with a surplus of substrate for each reactor and for each sieve fraction. Negligible differences were observed between sieve fractions, therefore average values were reported per reactor.

<sup>d</sup> The synthetic wastewater was supplemented with allylthiourea to inhibit nitrification. The reported ratios of aerobically consumed  $\text{NH}_4^+$ -N/fed COD were therefore directly related to biomass formation.

### Anaerobic acetate load distribution and solids residence time

To show the acetate load difference between the anaerobic feeding regimes, the amounts of acetate converted to PHA were combined with the measured VSS distributions over the granule size fractions in each reactor (figure 3.5). Using this approach, 94% and 81% of the acetate loads per cycle were recovered for the pulse-fed and bottom-fed reactors, respectively. In the bottom-fed reactor a negligible expansion of the settled sludge bed was observed during the anaerobic phase and no acetate could be detected in the bulk-liquid above the sludge bed throughout the anaerobic phase. The acetate concentration in the bulk-liquid therefore decreased from the initial level in the synthetic wastewater at the inlet to depletion before exiting at the top of the sludge bed. Although both reactors had fully granulated with similar size distributions, the net acetate distribution differed substantially. The pulse-fed system showed minor differences in acetate load distribution over the granule size fractions, while most of the acetate load was anaerobically consumed by the largest granule size fractions (>1 mm) present in the bottom-fed reactor.

The acetate load distribution data were subsequently used to calculate the sludge loading rate per size fraction in both reactors. The mass distribution over the granule size fractions in the reactor, sludge wasted selectively with the effluent and sludge wasted manually were then used to calculate the SRT of the individual granule size fractions. The granule size distribution of all sludge removed from the reactor was averaged over a period

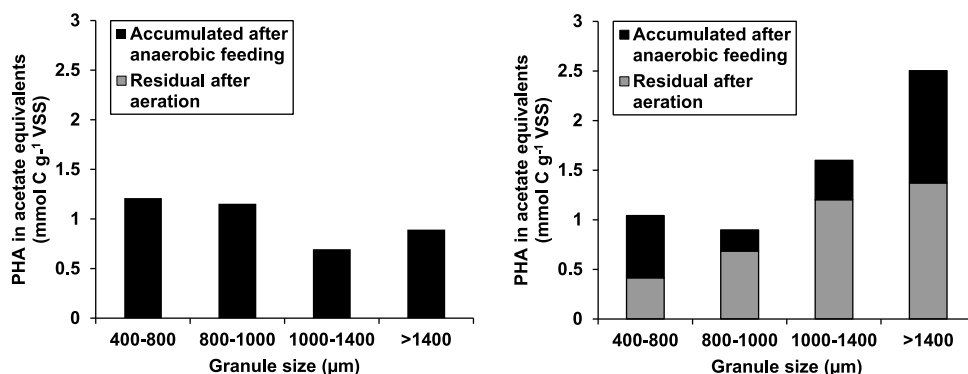


Figure 3.4: PHA storage polymer contents per granule size fractions expressed as acetate equivalents consumed during the anaerobic feeding phase (cumulative PHB and PHV) for (left) the pulse-fed reactor and (right) the bottom-fed reactor. Sludge samples were taken on the 144<sup>th</sup> day of operation.

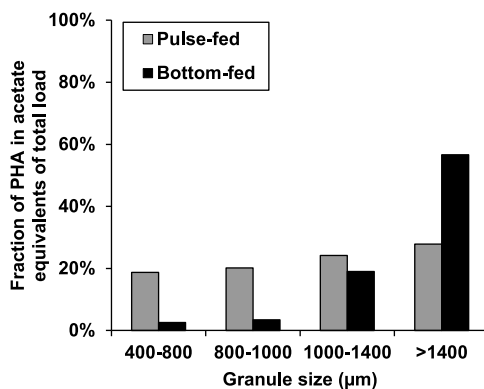


Figure 3.5: Anaerobic acetate load distribution over the granule size fractions for the pulse-fed and bottom-fed reactors. Distribution was calculated based on consumed acetate equivalents of difference in PHA content before and after anaerobic feeding. Samples were taken on the 144<sup>th</sup> day of operation.

of five days in the same week as the samples for measurement of the PHA content had been taken. Both the sludge loading rate and SRT per granule size fraction are depicted in figure 3.6. Both systems showed an increase in SRT for an increasing granule size, regardless of the anaerobic feeding strategy. The SRT of the fraction >1400μm was shorter in the pulse-fed reactor than in the bottom-fed reactor due to unintended accumulation of large granules in the effluent discharge port during aeration. This had only a minor effect on the obtained size distribution compared to the bottom-fed reactor. In the pulse-fed reactor the loading rate decreased as the granule size increased. For the bottom-fed reactor, the sludge loading rate increased with increasing granule size.

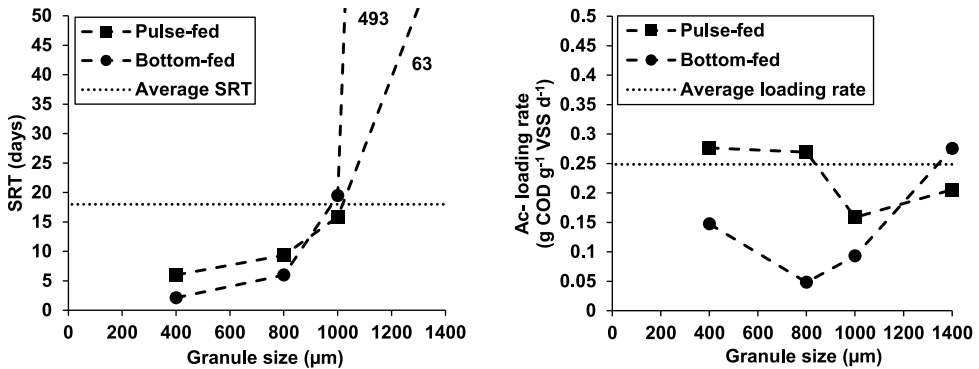


Figure 3.6: Comparison between SRT (left) and acetate sludge loading rate (right) of granule size fractions between the pulse-fed (dashed line, closed squares) and bottom-fed (dashed line, closed circles) reactors. Reactor averages were the same in both systems for acetate loading rate and SRT, denoted by dashed horizontal lines.

## 3.4. Discussion

Two sequencing batch AGS reactors were operated to investigate the effect of the anaerobic feeding mode on acetate distribution over granular size fractions and its effect on sludge granulation and dynamics of EBPR organisms. Synthetic wastewater was anaerobically pulse-fed in one reactor, while bottom-feeding was applied in the other. Both reactors were inoculated with the same crushed AGS and were operated in the same way except for the aforementioned anaerobic phase. The observed differences in the steady-state characterization will be discussed next in more detail in relation to the applied anaerobic feeding mode.

### 3.4.1. Acetate distribution over granule size fractions

The biomass specific anaerobic acetate uptake ( $\text{mmol}_C \text{Ac}^- \text{equivalents g}_{VSS}^{-1}$ ) and storage as PHA was nearly independent of granule size for the pulse-fed reactor, while for the bottom-fed reactor there was a clear increasing acetate uptake with increasing granule size (figure 3.6). Experimental estimation of the maximum acetate storage capacity ( $150 \text{ mg}_{\text{Ac}^-} \text{g}_{VSS}^{-1}$ ), specific anaerobic acetate uptake rate ( $150 \text{ mg}_{\text{Ac}^-} \text{g}_{VSS}^{-1} \text{h}^{-1}$ ) and biomass concentration were similar for both reactors (table 3.1). Also, the dominant PAO clade, determined by FISH, was the same in both reactors (clade I). This indicates that the potential of the microbial EBPR population was highly similar between both operating regimes, and in both systems the maximum acetate uptake capacity was not limiting the observed acetate uptake (granules close to the influent distributor in the bottom-fed reactor could only just be saturated at the end of the 60-minute feeding period). This indicates that the differences in COD loading can be explained by the differences in liquid-biofilm mass transfer to the granules for the two anaerobic feeding modes. The driving force from the concentration of acetate in the bulk liquid over time and place experienced by granules, and mass transfer rate are the main differentiating variables.

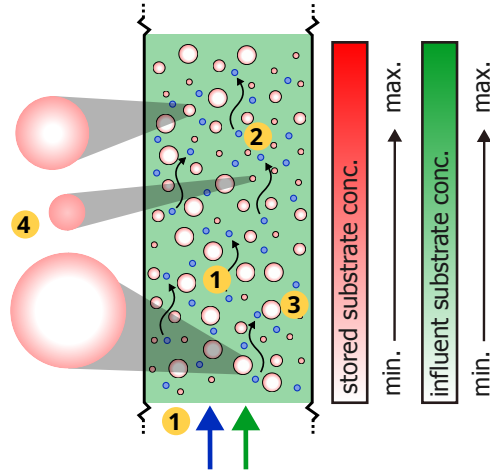
For the pulse-fed reactor, both the acetate concentration and effective contact time were the same for all granules due to the mixed anaerobic reaction phase. Therefore, the liquid-biofilm mass transfer was the determining mechanism. The mass transfer coefficient through a liquid-biofilm interface depends on liquid velocity local around the biofilm and the surface area. Since the surface to volume ratio decreases with increasing granule size, the overall mass transfer coefficient decreases for increasing granule size [108, 32]. Effectively, the efficiency of the granular volume usage decreases with increasing granule size [86]. The extent of the actual difference in loading between, depends on the initial penetrated volume. The near equal acetate loading with a slightly decreasing trend with increasing granule size observed in the pulse-fed reactor is consistent with substrate uptake limited by surface-to-volume ratio. The effect is limited due to the high initial acetate concentration, acetate loading rate and selective retention of larger granules. If an anaerobic zone with mixed tanks-in-series would get continuous feeding with real wastewater, as in a continuous-flow system with both lower concentrations of rbCOD and rbCOD loading rate, the advantage for smaller granules would be more pronounced.

The same analysis yields a different result for the bottom-fed reactor. The observed increase in anaerobic acetate loading with increasing granule size is due to a decreasing acetate concentration together with a (potentially) decreasing average granule size over the height of the sludge bed. The mass transfer limitation for granules of increasing size, due to the decreasing surface to volume ratio, is thus counteracted and reversed by the higher probability for larger granules to experience a higher bulk-liquid substrate concentration. The importance of this selective feeding of the largest granule size fraction has recently been underlined as one of the main mechanisms for stable aerobic granulation in bottom-fed AGS reactors in practice [156]. Bottom-feeding through a sludge bed thus favours increased anaerobic substrate uptake by the larger granule size fractions. The difference in the distribution of stored substrate forced by the anaerobic feeding mode is illustrated in figure 3.7.

## ANAEROBIC SUBSTRATE DISTRIBUTION

### pulse-feeding

- 1 pulse-feeding  
N<sub>2</sub>-gas mixing
- 2 homogenous bulk-liquid  
substrate concentration
- 3 granules of equal size  
accumulate the same  
amount of substrate
- 4 substrate distribution  
favoured towards  
smaller granules (i.e. higher  
area-to-volume ratio)



### bottom-feeding

- 5 bottom-feeding  
through a settled bed
- 6 decreasing substrate  
gradient through  
the settled bed
- 7 granules of equal size  
accumulate different  
amounts of substrate  
each cycle
- 8 substrate distribution  
favoured towards  
larger granules (i.e. larger  
volume and often  
closer to the bottom)

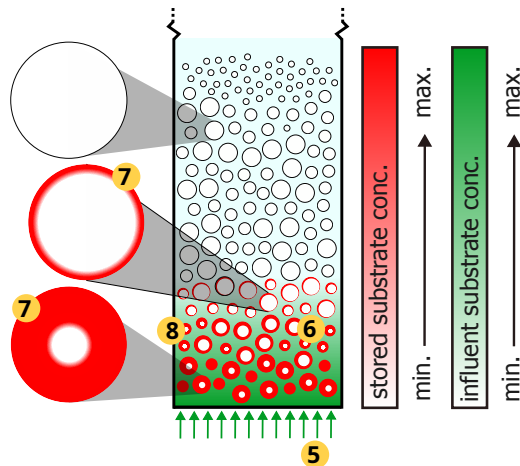


Figure 3.7: Schematic representation of the difference in the anaerobic distribution of stored substrate forced by the anaerobic feeding mode (either (left) pulse-feeding or (right) bottom-feeding). A random part of the pulse-fed bubble column is depicted, while the settled sludge bed is shown for the bottom-fed reactor. The shading of the bulk-liquid depicts the maximum substrate concentration during the anaerobic feeding of influent (pulse-feeding: 2 min, bottom-feeding: 60 min) as a fraction of the substrate concentration in the influent. The maximum bulk-liquid concentration of substrate in turn determines the maximum penetration depth achieved during the total anaerobic reaction time 60 min for both reactors. The radial color gradient in the granules of represents the local concentration of stored substrate inside a granule after feeding. Influent concentration of substrate (acetate):  $0.3 \text{ g}_{\text{COD}} \text{ L}^{-1}$ . Maximum concentration of stored substrate inside a granule (acetate-equivalents):  $4.5 \text{ g L}^{-1}$ . Blue circles and black arrows depict the mixing through sparging of dinitrogen gas during and after pulse-feeding. Legend of numbers: (1, 5): anaerobic feeding mode, (2,6): resulting bulk-liquid substrate concentration pattern, (3, 6): difference in substrate accumulation for equally sized granules per cycle, (4, 8): trend of overall substrate distribution due to anaerobic feeding mode.

### 3.4.2. COD loading rate versus SRT

Both the pulse-fed and bottom-fed reactors showed an increasing SRT for increasing granule size fractions (figure 3.6). Such a trend was expected based on the preferential wasting of slower settling sludge fraction as means of granular sludge selection. For the COD loading rate on the other hand (figure 3.6), the pulse-fed system showed a slight decrease with granule size, while in the bottom-fed reactor the acetate loading rate increased substantially with granule size. In continuous-flow CAS-systems, the sludge loading rate decreases on average with increasing SRT for all sludge particles [99]. This relation does also apply to AGS systems on average. In CAS-systems, however, the probability distributions around the average of both substrate and sludge discharge follow the hydraulic residence time distribution, without any impact of the properties of sludge particles (e.g. size or difference in settling rate). In this study, the average sludge yield was the same for both reactors, however the difference between granules sizes indicates that the internal redistribution of biomass growth between size fractions was different in the pulse-fed reactor compared to the bottom-fed reactor. The redistribution of biomass from larger to smaller aggregates is a common property of biofilm systems, which balances growth and biomass removal [112]. This yields an increase of SRT deeper into a biofilm [151], and is specifically of interest for AGS systems performing EBPR [189, 103]. While the SRT distribution of biofilm aggregates of different sizes can be influenced via selective wasting and process conditions affecting detachment, adjusting the distribution of substrate (i.e. the distribution of biomass growth) over size fractions is more difficult. The kinetics of substrate uptake and mass transfer determine the distribution of growth in biofilm systems with completely mixed reactors, as was previously discussed for the pulse-fed reactor. The comparison with a bottom-fed reactor in the current study shows that the uncoupling of COD uptake in the anaerobic phase from growth in the aerobic phase in AGS systems provides a means of control over the distribution of biomass growth.

This has two main implications. First, the granule size distribution can be influenced by directing the available COD towards smaller or larger granules. Second, the anaerobic penetration depth of COD can be influenced, which in turn influences the location of microbial conversions within granules. The anaerobic feeding mode thus provides an additional tool that can be used to optimize the granule size distribution and BNR in AGS processes for wastewater treatment.

### 3.4.3. Residual levels of PHA after aeration

A remarkable difference in residual PHA levels at the end of aeration was observed between the pulse-fed and bottom-fed reactors. The bottom-fed reactor showed substantial levels of residual PHA after aeration for all granule size fractions, while the fractions were depleted of PHA in the pulse-fed reactor (figure 3.4). Cultures enriched for EBPR have been shown to exhibit flexibility in the residual PHA content depending on the operational parameters, including SRT [143], influent P/COD-ratio [182], polyphosphate storage levels [1], pH [52], and cycle length [77]. The operational conditions during the

aerobic phase were the same for both reactors (i.e.  $kLa$ , DO concentration and duration) and thus did not cause the difference in remaining PHA. The remaining PHA was observed in all granule size classes of the bottom fed reactor, indicating the residual levels of PHA were not affected by the differences between the granule size distributions of the reactors. Therefore, the anaerobic feeding mode likely caused this difference, specifically the ratio of anaerobic loading of acetate of a granule size fraction to aerobic time.

## 3

In completely mixed enrichment cultures and in the pulse-fed granular system presented here, most organisms in the active layer of all granular size fractions experience the same conditions each cycle, i.e. same amount of acetate taken-up, same penetration depth and same aerobic time to convert it. This gives the organisms the opportunity to fully optimize their resource allocation to maximal growth [141]. In the bottom-fed reactor, all granules are distributed over the settled bed prior to the anaerobic feeding. The largest granules will be more distributed towards the bottom of the sludge bed while the smallest granules would be more towards the top. It was estimated that the acetate front reached up to 36% of the sludge bed from the bottom of the reactor, based on the measured specific acetate uptake rate, bed porosity and superficial liquid velocity during feeding (figure 3.10). The partial anaerobic contact of the sludge bed with acetate led to a highly variable acetate uptake for a granule per cycle, depending on its position in the sludge bed after settling. Although larger granules have a higher probability of settling more towards the bottom of the sludge bed, the applied superficial liquid velocity during feeding (i.e. 0.46 m/h) is well below the minimum fluidizing velocity. Therefore, negligible bed expansion and no further stratification were observed during feeding. Granules of all size fractions thus had a substantial probability of residing in the bottom part of the sludge bed and thus be in contact with acetate during feeding. This might force the organisms' storage metabolism into a more resilient state so it can deal with variations in substrate availability. This would underline the flexibility of *Ca. Accumulibacter phosphatis* to modulate the metabolism for optimal carbon utilization to the prevailing conditions [140].

Another possible explanation is that the fixed length of the aerobic phase was too short to fully convert all PHA for that part of the granules that received a peak anaerobic loading during a specific cycle. Granules at the bottom of the bottom-fed reactor will have been exposed to acetate during the full 60 min of feeding and these granules will have therefore a higher PHA content than average. The aerobic time is equal for all granules, and potentially too short when a granules has been near the inlet at the bottom during feeding. This would, on average, lead to a residual level of PHA. This hypothesis could not be investigated any further based on the available data and could the topic of future study.

Some work has been done studying the effect of fluctuating operational conditions on the performance of EBPR [137], mainly due to the residence time distribution in continuous-flow reactors. However, the width of the anaerobic load distribution as observed in the bottom-fed reactor used here was substantially larger and cannot be directly compared. Furthermore, full-scale AGS systems will be even more variable than

the lab scale systems. This effect has not been considered well in the literature, but is essential to further optimize EBPR systems, especially when employing AGS.

#### 3.4.4. Impact of the feeding mode on anaerobic storage metabolism

The anaerobic conversion stoichiometry of acetate to PHA was, surprisingly, different for the pulse-fed and bottom-fed reactors as well as for different granule size fractions within each reactor; the ratio of PHV/PHB accumulated during the anaerobic phase was on average twofold higher in bottom-fed reactor compared to the pulse-fed reactor with the largest granule size fraction having the highest ratio (table 3.2). Both reactors were dominated by *Ca. Accumulibacter phosphatis* (figure 3.8). The observed amount of ortho-phosphate released anaerobically was lower in the bottom-fed reactor compared to the pulse-fed reactor. These two observations are congruent. The trend continued further during the aerobic phase, where a nearly two-fold lower SPUR was observed in the bottom-fed reactor compared to the pulse-fed reactor (table 3.1). It has been indicated before that *Ca. Accumulibacter phosphatis* has a flexible metabolism and can operate between a full PAM [182] and a full GAM [140, 183, 109]. It seems that the pulse-fed system operated at full PAM, while the bottom fed system exhibited a mixed PAM/GAM phenotype. FISH has confirmed a full absence of known GAOs in the microbial population, while *Ca. Accumulibacter phosphatis* clade I was dominant (figure 3.11).

These observations underline again the ability of *Ca. Accumulibacter phosphatis* to modulate its metabolism depending on the environmental conditions [140], although the driver for the differences in metabolism were not determined. A decrease of the P/COD-ratio in the influent has been found to increase the ratio of GAM/PAM in suspended growth systems [182]. In this study, this was likely not a factor since the influent composition was the same. Sufficient polyphosphate was present in both reactors at the applied average SRT for full PAM to take place. If the differences are examined at the aggregate level (i.e. assuming similar microbial activity throughout each granule with negligible spatial gradients), the difference in PAM/GAM could be related to the aforementioned difference in PHA remaining at the end of the aeration phase. In that case, the PAM could be the most optimal metabolism for systems with stable substrate loading, while GAM contributes to resilience to more dynamic substrate loading per granule.

Another hypothesis is that differences in spatial gradients within granules contributed to the observed difference in PAM/GAM ratios between both reactors. The anaerobic penetration depth of acetate in the granules in the bottom-fed reactor is larger compared to granules in the pulse-fed reactor (figure 3.7). The aerobic penetration depth of oxygen was estimated to be similar for both reactors due to the same operational conditions (i.e. the same transfer resistances for gas-liquid and liquid-biofilms) during uptake of phosphate, and always more shallow than acetate. Oxygen only penetrates further into the granules once the phosphate in the bulk-liquid has been depleted, thereby limiting the interior of the



granules to perform GAM. The outer regions initially penetrated with oxygen are able to perform full PAM. The spatial separation between metabolisms would be most pronounced for the granules in the bottom-fed reactor, which could in turn contribute the observed difference in PAM/GAM ratio between anaerobic pulse-feeding and bottom-feeding at the reactor level.

These observations warrant further investigation into the effect on the metabolism of *Ca. Accumulibacter phosphatis* of both the dynamic anaerobic loading, as well as the effect of differences in penetration depth of acetate and oxygen on potential spatial separation of PAM and GAM within individual granules, which could not be separated in this study. If the impact of dynamic operational conditions is also reflected in the PAM/GAM ratio for *Ca. Accumulibacter phosphatis* it might form a proxy for the study of the occurring variability on the cellular level.

## 3

### 3.4.5. Practical implications

The influent with acetate as sole carbon source combined with an anaerobic contact phase selects completely for granular growth morphology and low SVIs [94], regardless of the anaerobic feeding mode applied. Municipal sewage contains lower concentrations of volatile fatty acid (VFA)s [68] than the synthetic wastewater used in this study. In full scale EBPR systems easy hydrolyzable and fermentable COD, after biological conversion into VFA, also contribute to the growth of EBPR organisms [22, 49, 154]. These extra microbial conversions will have to be considered when translating the observations here to full scale systems, however general principles can be deduced of the present work.

Design of the anaerobic feeding is an important aspect for obtaining stable AGS. The current implemented full-scale AGS process (Nereda<sup>®</sup>) applies bottom feeding and excess sludge extraction from the top of the bed. This removes the weakest settling part of the sludge and provides most substrate to the best settling (large granules) fraction of the sludge [156], thereby enhancing stability of the granular sludge bed. There are ongoing developments for alternative implementations of the AGS technology, in SBR as well as continuous systems. A completely mixed anaerobic feeding SBR has been proposed and tested at pilot scale [133]. However, there it was shown that this only resulted in stable operation if the wastewater has already high acetate concentrations in the influent. With a large rbCOD fraction in the influent, like in this study, selective wasting based on sludge settleability becomes the main driver for stable granulation. This can be deduced from the similarity in the granule size distribution of both reactors with different anaerobic feeding modes. This underlines the observations in this study that granulation can be obtained independent of anaerobic feeding mode, but that bottom feeding more readily results in stable operation if the influent composition is less favorable.

With the aim to further develop AGS technology for the application in CFRs [74], the attention for the design of the anaerobic contact tank is likely even more critical. As has been reported in existing plants with strong plug-flow conditions granule formation

is already induced [129, 180], indicating the advantage of having a strong concentration gradient as in the pulse-fed system in this study. In a completely mixed anaerobic tank acetate concentrations remain very low, and diffusion limitation will likely prevent *Ca. Accumulibacter phosphatis* microcolonies to grow out into larger granules. Especially for real wastewater, where only a limited amount of rbCOD is available for anaerobic conversion and storage, it is important to preferentially feed the largest granules. The challenge for stable granulation will be to design a system where, also under continuous feeding conditions, the rbCOD is directed preferentially to the largest granule fraction.

Interestingly we observed quite a difference in EBPR metabolism between the two feeding modes with respect to ratio of PAM/GAM and PHA remaining at the end of the aerated period. This is not well recognized yet in the literature and would need further attention. Our initial data seem to indicate that the bio-P removal capacity is not directly influenced, but the overall stability and response to disturbances (e.g. Monday effect) might be related to these differences [21, 130]. [53] indeed indicated that stabilizing the feed to an EBPR process minimized disturbances, however the effect of different PAM/GAM was not yet well recognized and evaluated at the time. It might be relevant for the batch scheduling of the existing AGS facilities, for example.

### 3.5. Conclusions

An experimental study was performed at lab-scale to investigate the anaerobic feeding mode of AGS with substrate on the distribution of substrate storage over the granule size fractions and the effects on sludge characteristics. Two reactors were operated identically, except for the anaerobic feeding phases. One reactor was fed from the bottom through the sludge bed, while the other was fed in a short pulse and subsequently mixed anaerobically. The following conclusions were derived from the observations.

- Bottom feeding primarily directs substrate towards the large granular size classes (i.e. large volume and closer to the bottom), while completely mixed pulse-feeding gives a more equal distribution of substrate over all granule sizes (i.e. surface area dependent).
- Both feeding methods resulted in stable granulation with large granules. However, in the completely mixed pulse-fed system the smaller granules are preferentially supplied with substrate due to their relatively higher surface-to-volume ratio. The preferential feeding of the larger granules in bottom-feeding will enhance and stabilize the granulation in such systems, certainly under less advantageous wastewater compositions than the acetate feed used in this study.
- The anaerobic feeding mode directly impacts the substrate distribution over the different granule sizes, irrespective of the SRT of a granule as a unit.
- The systems showed very similar microbial populations with mainly *Ca. Accumulibacter phosphatis* present in the biomass. They differed strongly in their phenotype with respect to PAM/GAM, SPUR, and residual PHA at the end of the

eration phase. These phenomena need attention in future EBPR studies since they are likely relevant for the full-scale stability of EBPR processes.

## Acknowledgements

The authors would like to thank Roel van de Wijngaart for the sample preparation and microscopy performed in obtaining FISH-images and Jeffrey Croonenberg for the PHA analyses.

# 3

## Appendix

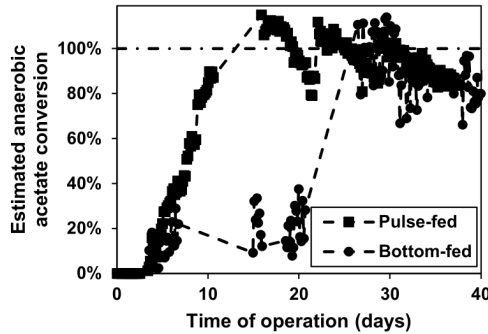


Figure 3.8: Estimated efficiency of anaerobic acetate uptake for the pulse-fed and bottom-fed reactors during start-up, based on conductivity measurements and steady-state anaerobic phosphate release. Horizontal line (dash-dot) indicates complete anaerobic acetate uptake efficiency. The decreasing trend observed on short time-scales (days) was attributed to fouling of the conductivity sensor. The anaerobic feeding regime furthermore affected the manner in which biological phosphorus removal developed. Aerobic phosphate uptake was kinetically limited in the pulse-fed reactor due to the low MLSS concentrations during start-up. The anaerobic acetate uptake efficiency and the resulting amount of phosphate released, developed faster than in the bottom-fed reactor as MLSS increased. The SPUR and aeration time in the pulse-fed reactor were, however, insufficient for complete phosphate removal until 21 days after start-up. Since the anaerobic acetate uptake efficiency increased at a lower rate in the bottom-fed reactor, the lower phosphate release coupled to this resulted in complete phosphorus removal after 7 days of operation.

Table 3.2: Ratios of PHV to PHB at the end of aeration and after anaerobic feeding in the subsequent cycle. Samples were taken on the 144<sup>th</sup> day of operation.

Size class ( $\mu\text{m}$ )	PHV/PHB ( $\text{mol}_C \text{mol}_C^{-1}$ )			
	Pulse-fed		Bottom-fed	
	AE	AN	AE	AN
400-800	-	0.08	0.19	0.24
800-1000	-	0.18	0.16	0.22
1000-1400	-	0.07	0.22	0.25
>1400	-	0.11	0.26	0.22

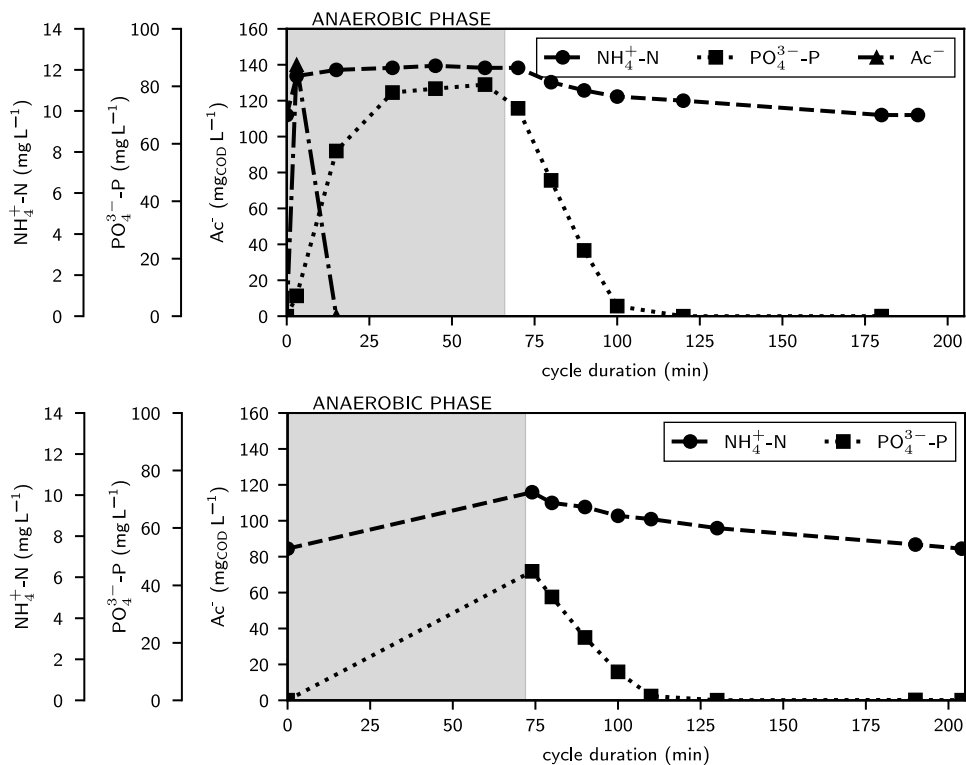


Figure 3.9: Cycle measurement on the 144<sup>th</sup> day of operation for (a, top) the pulse-fed reactor and (b, bottom) the bottom-fed reactor. The grey area denotes the duration of the anaerobic phase.

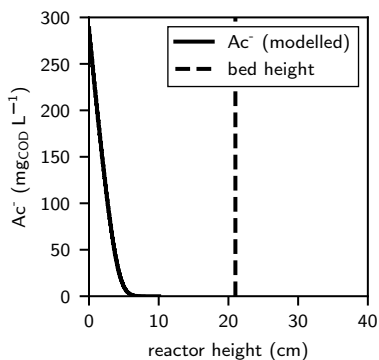


Figure 3.10: Bulk-liquid concentration profile (solid) of acetate in the bottom-fed reactor at the end of the anaerobic phase. The concentration profile was computed based on the bulk-liquid phase and biofilm phase mass balances as described in chapter 4, but using the granule size distribution in the bottom-fed reactor at the 144<sup>th</sup> day of operation. Model implementation in COMSOL 5.6 (COMSOL, Inc. Burlington, MA). The height of the sludge bed (21 cm) is depicted as a vertical line (dashed). All biological input parameters were obtained in this study. The model predicts that the concentration front of acetate reached up to 36% of the bed height in steady-state conditions at the 144<sup>th</sup> day of operation.

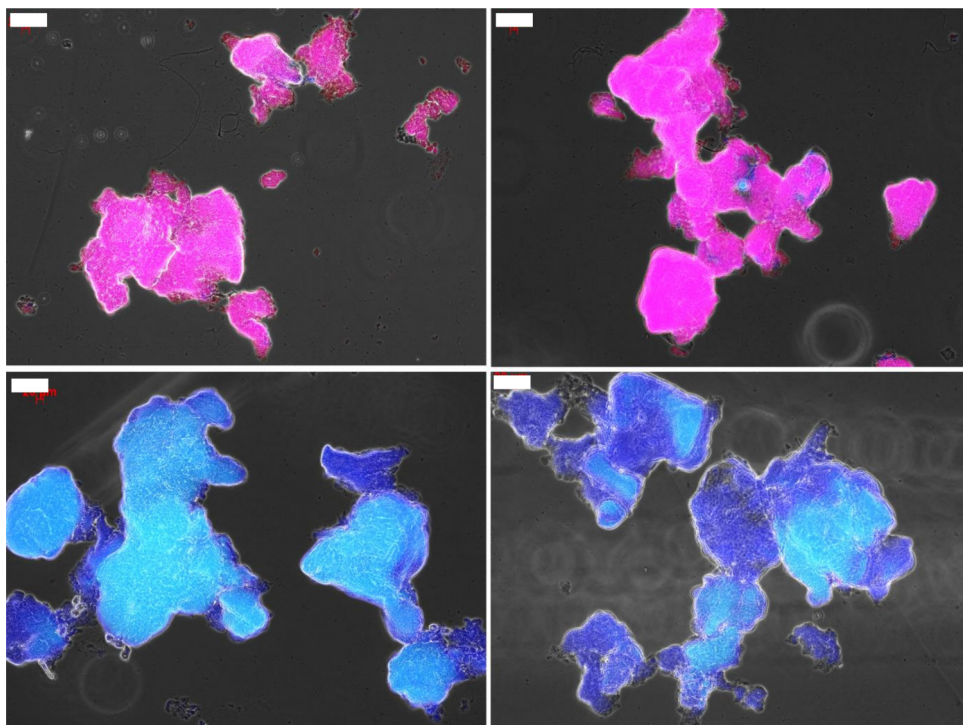


Figure 3.11: Granules stained with FISH probes from the pulse-fed reactor (*left column*) and the bottom-fed reactor (*right column*). Images in the top row are stained for PAO, Eubacteria, GAO (r, b, g), the images in the bottom row for ACC2, Eubacteria, ACC1 (r, b, g). The with scale bar represents a length of 100  $\mu\text{m}$ . Sludge samples were taken on the 144<sup>th</sup> day of operation.

# 4

## **On the mechanisms for aerobic granulation - model based evaluation**

**Edward van Dijk and Viktor Haaksman**

## 4.1. Introduction

AGS is a technology for biological treatment of domestic and industrial wastewater. Microbial aggregates of AGS are large compared to CAS, allowing for a more efficient treatment process. Although the technology was invented more than 20 years ago [102, 66] and the first full-scale applications treating sewage started to appear from 2005 under the trade name Nereda<sup>®</sup> [57], there is no consensus in literature on the underlying mechanisms for aerobic granulation and the process is influenced by many factors [190]. Factors often described are hydrodynamic shear [87, 149, 191], physical selection on settling velocity [98, 157], the flow regime during contact of the sludge with influent [132, 89, 64], DO concentration [104], feast/famine ratio [19, 43, 26], influent substrate composition [121, 78], organic loading rate [70], quorum sensing [176] and aggregation through EPS [83]. It is unclear which factors matter most and how their interplay is affected by the process conditions applied. A framework for biofilm morphology has been proposed [116], but this framework only explains granule stability on the micro-scale, but it cannot explain granulation dynamics on a reactor scale. For anaerobic granular sludge, such a framework has been developed [13], but this framework is not as such applicable for AGS.

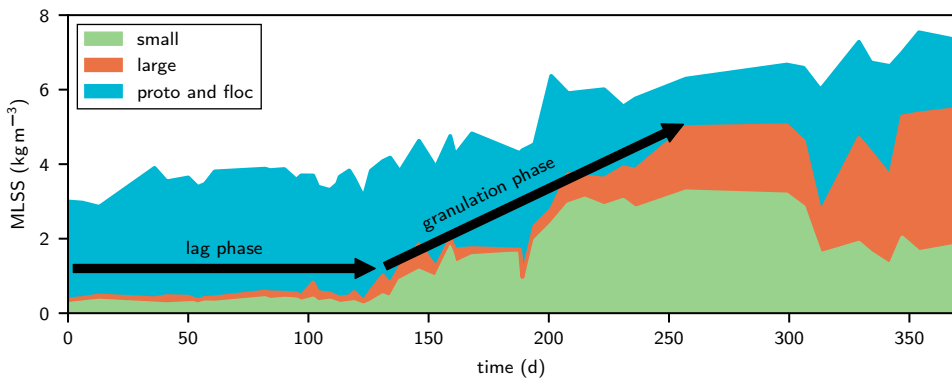


Figure 4.1: Typical startup of an AGS reactor from flocs, showing an initial lag phase with slow improvement of the sludge morphology, followed by the granulation phase, where granules appear in the reactor. The colors indicate the size of the biomass aggregates, showing proto-granules and flocs (<200  $\mu\text{m}$ ), small granules (>200  $\mu\text{m}$ ) and large granules (>1000  $\mu\text{m}$ ). Data derived from the Nereda<sup>®</sup> reactor in Utrecht, the Netherlands.

When a AGS reactor is seeded with AS, under the right circumstances, granular sludge will develop from flocculent sludge. In practice this granulation process shows dynamics that are not easily explained. The granulation process commonly has a lag phase, in which not much change in the granulation grade (biomass fraction of the granules) seems to happen. Secondly, there is the granulation phase, in which granules start to appear in the reactor and the granulation grade increases (figure 4.1). The reason behind the lag phase and the trigger for the sudden start of granulation is unclear. We hypothesize that there are six main mechanisms that are of most importance for successful granulation (figure 4.2).

*Microbial selection* is important for the formation of granules. It has been shown that a stable dense biofilm can be best achieved, when the uptake rate of substrates is lower than the transport rate of the substrates into the granules [160]. Therefore, the process is optimized towards organisms that anaerobically sequester readily biodegradable substrate by converting it into storage polymers and subsequently utilizing these polymers for aerobic growth [107, 145, 43]. This effectively separates the substrate uptake and the growth into two processes (called feast and famine). Phosphate accumulating organisms (PAO) and GAOs are examples of species that can make this split and these organisms are commonly observed in full-scale AGS processes [2]. Not all substrates can be sequestered anaerobically into storage polymers for aerobic growth of bacteria in the granules. We call these substrates *non-GFS*. Substrates that can lead to growth of aerobic granules (e.g. VFAs, but also readily biodegradable substrates that can be converted anaerobically) we call *GFS* (GFS).

*Physical selection* is also an important driver for growing AGS [102, 19, 43, 126]. AGS has advantageous settling properties compared to AS flocs [102, 66]. In AGS reactors flocs will always be present to some extent [122] as not all carbon sources present in sewage can be converted to storage polymers during anaerobic feeding [79]. Therefore, it is needed to preferentially remove the flocculent sludge fraction with the excess sludge to give granules a competitive advantage. This is achieved by using the differential settling velocity between flocculent and granular sludge [84, 157]. This is called the physical selection pressure.

Another well-known driver is *maximizing transport of substrate* into the biofilm. Higher substrate concentrations in the bulk liquid result in a deeper penetration of the substrate in the biofilm [9]. This helps to grow and support a thicker biofilm. In AGS reactors a higher substrate concentration is achieved by either pulse feeding at the start [19] or more practical relevant by plug-flow feeding from the bottom of the reactor [43, 122]. This gives a competitive advantage for larger granules. Larger granules settle faster than smaller granules and flocs, and therefore accumulate at the bottom of the settled sludge bed [157]. Feeding from the bottom therefore results a longer contact time with the influent and contact with higher substrate concentrations for the larger granules. As a result, they will have more opportunity for growth than smaller fraction. Hence the term *selective feeding*.

Aerobic granules go through a typical life cycle that has a strong influence on the granulation process and reactor performance. When an AGS reactor is seeded with AS flocs, these flocs will first form proto-granules. Flocs and proto-granules share similar bulk settling properties. An important difference is that the proto-granules already have the granular morphology but are smaller than 200  $\mu\text{m}$ , which is considered to be the minimum size for an aggregate to be called an aerobic granule [41]. Proto-granules already have been observed in CAS processes, especially in systems with high anaerobic food to mass ratios, unmixed in-line fermentation, and a high influent soluble COD fraction [180].



Proto-granules are embedded in the floc matrix and settle together with the flocculent material.

Biological conversions in proto-granules are comparable to conversions in flocs, because the small radius of the proto-granules allows for full penetration with oxygen. SND thus will be limited to very low DO conditions. When proto-granules grow out into small granules ( $>200\ \mu\text{m}$ ), these small granules will settle significant faster and independent of the flocculent mass. The result is that small granules can experience the benefits regarding sludge selection, remain longer in the reactor with selective wasting and receive more influent with bottom feeding. When the granules continue to grow, the biofilm kinetics become more pronounced and full penetration of oxygen is less likely and SND will increase. Large granules ( $>1000\ \mu\text{m}$ ) are more susceptible to breakage [37]. When a granule breaks into smaller pieces some will be spilled and others will become a seed for new granules, restarting the granule life cycle. Thus we hypothesized that *breakage of granules* is an integral part of the granulation process, similar as proposed for anaerobic sludge [13].

The aforementioned factors for aerobic granulation are not absolute. For example, only part of the substrate of domestic wastewater can be taken up anaerobically by the AGS directly or after fermentation. Still, it is possible to grow AGS on the complex composition of domestic wastewater [122, 78]. The selection pressure applied in full-scale reactors will be less effective than in lab-reactors, because of less favorable H/D ratios and other scaling factors. Apparently, the favorable mechanisms can be allowed to be implemented suboptimal to a certain extent without harming the granulation process. It is however unclear, how the different mechanisms influence one another positively or negatively if the process conditions become less favorable.

Analysis of the quantitative interplay between the aforementioned mechanisms in combination with varying process conditions requires a mathematical modeling approach. A mature granular bed in practice exists of a collection of granules with sizes up to 5 mm [157]. For the purpose of this study, a framework was required in which the lifecycle of granules could be tracked. Simulated granules should be allowed to have different time-variable spatial positions in the reactor and should be exposed to different bulk-liquid conditions, within a cycle and from one cycle to the next. This approach is required to capture the stochastic properties of an AGS system. Several models are available describing the AGS process with different emphases [11]. Models that describe granulation as the development of a characteristic mean granule size [195, 106] or assume a single granule size to study, for example, microbial speciation in granules and nutrient removal [42, 192] are not suitable for the purpose of this study. The same holds for models that assume successful granulation using a fixed granule size distribution to investigate reactor performance [79, 48]. Models with a dynamic granule size distribution [82, 13] often use a population balance model (PBM) to describe the number of granules in a certain size class and the processes that influence these amounts (i.e. growth and

detachment) via transitions from or to another size class. However, the available PBMs are only suited for completely mixed reactors, not for typical AGS reactors with combined spatial and temporal differences between the conditions experienced by aggregates. We hypothesized that the process for aerobic granulation can be described by six mechanisms (figure 4.2) with a minimal required description of the biological conversions, tracking the development of individual granule clusters in the reactor over time.

In this study, we aimed to understand the underlying principles for aerobic granulation. A mathematical model was constructed that describes the full life cycle of aerobic granules. We performed a sensitivity analysis on the six mechanisms proposed and we evaluated their individual contribution to the granulation process.

## 4.2. Methodology

A model was developed integrating several sub-models describing all the proposed mechanisms responsible for the granulation process. The main process steps in current full-scale AGS reactors according to the Nereda<sup>®</sup> concept are the feeding phase, in which fresh influent is fed to the reactor from the bottom, the reaction phase, where the wastewater is cleaned by different aeration strategies and finally the settling and decanting phase, in which the selective wasting takes place. In full-scale applications feeding and effluent decanting happens simultaneously [122, 57].

### 4.2.1. Theoretical background

#### **Biomass morphology**

The morphology of biofilms is dependent on a combination of convection, diffusion, reaction, growth and detachment [114]. All biomass clusters are assumed to have constant smooth and spherical morphology with a constant density. This specific biofilm morphology occurs when substrate uptake is limited by the maximum biomass specific uptake rate and not by transport [115]. Since substrate uptake (anaerobic) is uncoupled from growth (aerobic) in full-scale AGS, a smooth, spherical biofilm morphology was assumed for all simulations. Wherever the distinction is made between flocs and granules, this is solely based on the sludge particle diameter. The smallest particles of 100  $\mu\text{m}$  are referred to as flocs, while all larger particles are considered (proto-) granules.

#### **Microbial ecology**

The microbial population differs over the radius of the biofilm due to concentration gradients of substrates [116]. Different organisms present in the biofilm are responsible for processes like nitrification, denitrification and phosphate removal [38, 187]. However, since the aim of this study was to investigate the impact of the different mechanisms on the growth of aerobic granules, the biomass clusters are assumed to have constant ecology. Furthermore, biomass formation in WWTP is mostly related to COD conversions. No nitrogen and phosphorus conversions are considered in the model as they contribute marginally to biomass formation. All modelled biomass can store COD anaerobically as

4

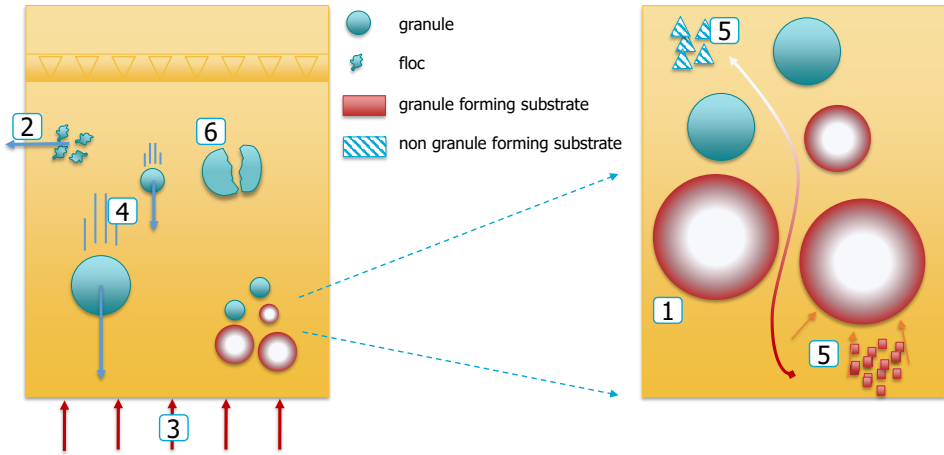


Figure 4.2: A graphical representation of the six mechanisms for granulation: (1) microbial selection, (2) selective wasting, (3) maximizing transport of substrate into the biofilm, (4) selective feeding, (5) (non-)GFS, (6) breakage of granules.

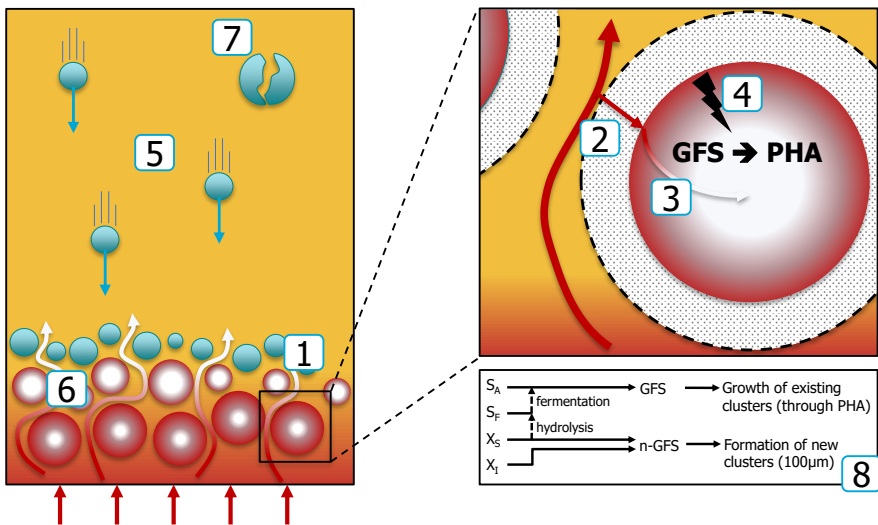


Figure 4.3: Model overview, with (1) convection and dispersion in the bulk liquid, (2) mass transfer through the boundary layer, (3) 1D radial diffusion, (4) conversion of GFS to PHA, (5) settling of granules in the reactor, (6) individual based population model, (7) breakage. Schematic representation of the translation from organic substrates in ASM2d [68] into the granulation model (8).

storage polymers. Therefore, only the conversions of COD into storage polymers, and storage polymers into biomass, were simulated to describe granular growth.

### Biological fate of COD-types in wastewater

The COD present in domestic wastewater can be divided in multiple fractions [69]. These fractions can be divided based on the availability for biological conversions [78]. The soluble and suspended inert COD and inorganic solids are not available for any biological conversion and are thus disregarded in this model. Both the soluble rbCOD and the colloid fast hydrolyzable COD are available for anaerobic conversion into storage polymers and are thus categorized as GFS. The suspended slowly hydrolyzable COD is available for biological conversions, but not for anaerobic storage and are categorized as non-GFS. A schematic representation is shown in figure 4.3.

#### 4.2.2. Model overview

Four mathematical models were combined to perform a sensitivity analysis on the hypothesized main mechanisms for aerobic granulation (see also figure 4.3). The four model components are described below.

1. *Cluster-based biomass population model*: An AGS reactor typically contains a dynamic distribution of granule sizes, all of different age, shape and ecology. To capture the probability of granules of similar size to be at the different locations in the reactor at the same time, a cluster-based approach was used. The sludge population was discretized into clusters of aggregates with the same diameter, where each simulated cluster represented the same amount of physical biomass in the reactor. The amount of biomass represented by a cluster scaled linearly with the surface area of the simulated reactor, since the spatial gradients in an AGS reactor are mainly 1D (i.e. over the height). A convergence analysis showed that a discretization of  $1.75 \times 10^{-2}$  simulated mass per real mass per reactor area ( $\text{kg kg}^{-1} \text{m}^{-2}$ ) yielded a discretization-independent solution. This resulted in  $\sim 10\,000$  clusters at start-up in the reference case with only flocs of  $100\ \mu\text{m}$ , and the population cloud increase to  $\sim 100\,000$  upon successful granulation. New clusters were formed from non-GFS as clusters with a diameter of  $100\ \mu\text{m}$ . The clusters could be subjected to the following mechanisms:
  - Growth: in the reaction phase, the diameter of each cluster of particles grew according to the amount of PHA formed obtained during the anaerobic feeding phase. This resulted in a different increase in volume for each cluster of granules. The increase was based on an apparent yield coefficient (including decay) and a constant biomass concentration in the granule, resulting in a constant VSS/TSS ratio. All PHA was assumed to be consumed and converted to new biomass, without any time dependence in the reaction phase (section 4.2.3).
  - Breakage: the larger aerobic granules become, the more likely they will break up into smaller pieces [37]. In the model, granule clusters larger than  $3\ \text{mm}$  have an increasing chance of breaking (increasing to 99% for granules larger than

5 mm). Breakage leads to two clusters with random diameter between 100  $\mu\text{m}$  and the original diameter, with a combined biomass equal to the original cluster (section 4.2.3).

- **Redistribution:** if a cluster of granules exceeded the maximum amount of represented real biomass, it was split into two clusters of granules with same diameter. Each cluster would represent half of the original biomass.
- **Wasting:** Biomass discharge from the reactor was performed by the removal of number of complete clusters. Clusters were selected, depending on the wasting method used (a mixed sample for MLSS control or based on settling velocity for selective wasting).

## 4

2. *Bulk-liquid solute mass balance:* the anaerobic feeding in an AGS sequencing-batch reactor (SBR) is mainly a 1D process, since reactors are fed from the bottom and the process is designed to get an optimal plug-flow. Some axial mixing does occur [158]. Therefore, the concentration profile of GFS during feeding was described by an 1D convection-dispersion model [44, 158]. It was solved with one-way coupling to the settling model, since during the feeding phase granules will still be settling and partially fluidize. The calculated effective voidage is thus dynamic and will hence influence the local fluid velocity.
3. *Biofilm solute mass balance:* The flux of GFS into a granule depends on the local concentration in the bulk-liquid surrounding the granule and the rate of mass transfer, which varies over the height of the reactor. It is in turn affected by the rate of diffusion in the granules and rate of reaction of GFS to PHA. Furthermore, anaerobic storage capacity of PHA is limited by a maximum PHA content, used as a simplification for depletion of glycogen [42]. The dynamic mass balances of GFS and PHA were modelled using a 1D radial reaction-diffusion model for each cluster of particles, solved fully coupled to the bulk-liquid mass balance. The combined processes in the bulk-liquid phase, biofilm phase and the settling model determined the total amount of storage polymer per cluster of granule after the feeding phase.
4. *Settling model:* the settling velocity of a granule depends on the physical properties of the granule (i.e. size and density) and the biomass concentration in the near vicinity of the granule. As a result, every granule will have a unique settling velocity, eventually determining the position in the reactor during feeding. To describe this settling behavior, we used the settling model by [157] and adapted it to describe the settling and fluidization of clusters of granules. The model was also adapted to better describe the settling of flocs and proto-granules. The latter involved a change in the calculation of the expansion index, which is now calculated based on the Archimedes number.

### Cycle build-up

A typical Nereda<sup>®</sup> cycle was simulated in the model. This typical cycle has a duration of 6 hours, and consists of 60 min of anaerobic feeding and decanting, 270 min of reaction

time, and 30 min for settling and wasting of biomass. These typical values could vary in the scenarios. Table 4.1 shows the different processes being modelled in the different phases of the cycle.

Table 4.1: Typical batch scheduling for the AGS process and the various active processes in the model.

Time (min)	15	30	45	60	75 .. 330	345	360
Base case							
Fill/draw							
Reaction/aeration							
Settling							
Sludge selection							•
Processes modelled							
Convective transport of substrate							
Dispersion of substrates							
Settling of granule clusters							
GFS uptake to PHA							
Growth of particles on PHA					•		
Formation of flocs from n-GFS					•		
Breakage of large granules					•		
Redistribution of clusters					•		
Selective biomass wasting							•
Mixed biomass wasting					•		

Cycle phase  
 Time dependent process  
 Instantaneous process

### Biological and physical constants

The model parameters are listed in table 4.2. Parameters for the settling model not listed here, can be found in [157].

Table 4.2: Biological and physical constants used for the sensitivity analyses.

Constant	Symbol	Value	Unit	Reference
Péclet number	Pe	$2.5 \times 10^2$	-	[158]
Reactor height	H	6	m	this study
Feeding velocity	$v_{in}$	4	$m h^{-1}$	this study
Bulk-liquid density	$\rho_L$	$1 \times 10^3$	$kg m^{-3}$	[157]
Granule density	$\rho_B$	$1.035 \times 10^3$	$kg m^{-3}$	[157]
Temperature	T	293	K	this study
Biomass concentration granule	$c_X$	$5 \times 10^1$	$kg m^{-3}$	[157]
Diffusion coefficient GFS in bulk (298 K)	$D_{GFS,L}$	$1.21 \times 10^{-9}$	$m^2 s^{-1}$	[32]
Diffusion coefficient GFS in biofilm (298 K)	$D_{GFS,B}$	$2.4 \times 10^{-10}$	$m^2 s^{-1}$	[167]
Monod constant for GFS	$K_{GFS}$	$1 \times 10^{-3}$	$kg m^{-3}$	this study
Monod constant for PHA	$K_{PHA}$	$1 \times 10^{-3}$	$kg m^{-3}$	this study
Maximum biomass specific substrate uptake rate	$q_{AN,max}$	$2.78 \times 10^{-5}$	$kg kg^{-1} s^{-1}$	this study
Maximum storage capacity of GFS	$c_{PHA,max}$	7.5	$kg m^{-3}$	this study
Yield of biomass on storage polymers	$Y_{X,PHA}$	0.32	$kg kg^{-1}$	this study
Yield of biomass on non-GFS	$Y_{X,n-GFS}$	0.32	$kg kg^{-1}$	this study

### 4.2.3. Mathematical model description

The model is build-up out of several components to simulate the change in time and in space of the dependent variables listed in table table 4.3, which are described below.

Table 4.3: Dependent variables and interdependence in submodels. An 'X' denotes that the variable is used in a submodel. A shaded 'O' indicates that the variable is dynamically computed in that submodel. Arrows indicate the extent of coupling between submodels (either one-way coupled ( $\leftarrow$  or  $\rightarrow$ ) or fully coupled ( $\leftrightarrow$ )). Subscript  $j$  denotes the index of the cluster of sludge particles.

	Bulk-liquid solute mass balance	Biofilm solute mass balance	Settling model	Granule population model
$c_{\text{GFS,L}}(x, t)$	O $\rightarrow$	$\leftarrow$ X		X
$c_{\text{GFS,B},j}(r, t)$	X $\rightarrow$	$\leftarrow$ O $\rightarrow$		X
$c_{\text{PHA,B},j}(r, t)$		O $\rightarrow$		X
$x_j(t)$	X	X	$\leftarrow$ O	
$d_j(t)$	X	X	X	$\leftarrow$ O

#### Bulk-liquid solute mass balance (1D convection-dispersion-transfer)

The mass balance of GFS during anaerobic feeding was formulated as follows, describing axial dispersion, convective transport and mass transfer between the bulk and the biofilm (from/to all granules in the set of clusters  $N_i$  at a certain height):

$$\frac{\partial c_{\text{GFS,L}}}{\partial t} = -D_{\text{ax}} \frac{\partial^2 c_{\text{GFS,L}}}{\partial x^2} + \frac{v_{\text{in}}}{\varepsilon_{\text{L}}(x)} \frac{\partial c_{\text{GFS,L}}}{\partial x} + \sum_{j=1}^{N_i} k_{\text{LB,GFS}} \frac{a_j}{\varepsilon_{\text{L}}(x)} (c_{\text{GFS,B},j}|_{r=d_j/2} - c_{\text{GFS,L}}) \quad (4.1)$$

The boundary conditions were defined as follows:

- Bottom inlet (Danckwerts):

$$\left( \frac{v_{\text{in}}}{\varepsilon_{\text{L}}(x)} c_{\text{GFS,L}} - D_{\text{ax}} \frac{\partial c_{\text{GFS,L}}}{\partial x} \right) \Big|_{x=0} = v_{\text{in}} c_{\text{GFS,in}}, t > 0 \quad (4.2)$$

- Top outlet (zero-dispersion):

$$-D_{\text{ax}} \frac{\partial c_{\text{GFS,L}}}{\partial x} \Big|_{x=H} = 0, t > 0 \quad (4.3)$$

#### Biofilm phase solute mass balance (1D radial diffusion-reaction)

The mass balance of GFS and storage polymers PHA) over the biofilm phase was modelled according to the following equation:

$$\frac{\partial c_{\text{GFS},\text{B},j}}{\partial t} = -D_{\text{GFS},\text{B}} \left( \frac{\partial^2 c_{\text{GFS},\text{B},j}}{\partial r^2} + \frac{2}{r} \frac{\partial c_{\text{GFS},\text{B},j}}{\partial r} \right) + R_{\text{GFS}}(c_{\text{GFS},\text{B},j}(r), c_{\text{PHA},\text{B},j}(r)) \quad (4.4)$$

$$\frac{\partial c_{\text{PHA},\text{B},j}}{\partial t} = R_{\text{PHA}}(c_{\text{GFS},\text{B},j}(r), c_{\text{PHA},\text{B},j}(r)) \quad (4.5)$$

Here the volumetric reaction rate  $R$  is based on Monod kinetics [42]. Both Monod constants are an order of magnitude smaller than the actual concentrations, therefore practically serve as switching terms:

$$R_{\text{GFS}} = q_{\text{AN},\text{max}} X \frac{c_{\text{GFS},\text{B},j}}{K_{\text{GFS}} + c_{\text{GFS},\text{B},j}} \frac{c_{\text{PHA},\text{max}} - c_{\text{PHA},\text{B},j}}{K_{\text{PHA}} + c_{\text{PHA},\text{max}} - c_{\text{PHA},\text{B},j}}, R_{\text{PHA}} = -R_{\text{GFS}} \quad (4.6)$$

Boundary conditions were defined as follows:

- Biofilm surface (flux-continuity with transfer from/to bulk-liquid):

$$-D_{\text{GFS},\text{B}} \frac{\partial c_{\text{GFS},\text{B},j}}{\partial r} \Big|_{r=d_j/2} = k_{\text{LB},\text{GFS}} (c_{\text{GFS},\text{B},j}|_{r=d_j/2} - c_{\text{GFS},\text{L}}|_{x=x_j}), t > 0 \quad (4.7)$$

- Biofilm center (symmetry boundary condition):

$$-D_{\text{GFS},\text{B}} \frac{\partial c_{\text{GFS},\text{B},j}}{\partial r} \Big|_{r=0} = 0, t > 0 \quad (4.8)$$

### Mass transfer between bulk-liquid and biofilm

The mass transfer coefficient was calculated based on Sherwood relations for forced convection around a free sphere [32] (top relation) or semi-fluidized beds [50] (bottom relation). The choice depended on the local voidage of the sludge bed during feeding since no relation covered the complete voidage range (from settled granular bed (0.5) to nearly void of biomass):

$$k_{\text{LB},\text{GFS}}(\varepsilon_{\text{L}}, d_j) = \max \left\{ \begin{array}{l} \left( 2.0 + 0.6 \left( \frac{d_j v_{\text{in}}}{v \varepsilon_{\text{L}}} \right)^{\frac{1}{2}} \left( \frac{v}{D_{\text{GFS},\text{L}}} \right)^{\frac{1}{3}} \right) \frac{D_{\text{GFS},\text{L}}}{d_j}, \\ \left( 2.0 + 1.51 \left( (1 - \varepsilon_{\text{L}}) \frac{d_j v_{\text{in}}}{v} \right)^{\frac{1}{2}} \left( \frac{v}{D_{\text{GFS},\text{L}}} \right)^{\frac{1}{3}} \right) \frac{D_{\text{GFS},\text{L}}}{d_j} \end{array} \right\} \quad (4.9)$$

### Settling model

The settling model for AGS developed by [157] was used to describe the settling of the individual groups of granules. In this model the settling velocity of different size classed



of granules is described. Since this model only describes the settling behavior of classes of granules, it was adapted to describe the settling behavior of individual clusters of granules of the same size ( $j$ ):

$$v_j = k v_{f,j} \varepsilon_{e,j}^{n_j-2} \frac{\rho_{B,j} - \rho_{bed,i}}{\rho_{B,j} - \rho_L} \quad (4.10)$$

, where  $k$  is a correction factor wall effects. Furthermore, every cluster of granules (instead of classes) experienced an apparent voidage fraction of the surrounding liquid  $\varepsilon_{e,j}$ . The calculation of this apparent voidage fraction for individual granules is identical to the calculation for granule classes, only in this case is the diameter represents the individual granule instead of the granule class.

4

$$\varepsilon_{e,j} = 1 - \left[ 1 + \left( \frac{\bar{d}_i}{d_j} \right) \left[ (1 - \varepsilon_L)^{-\frac{1}{3}} - 1 \right] \right]^{-3} \quad (4.11)$$

Similarly, the average granule diameter can be calculated based on groups of similarly sized granules at the same height in the reactor:

$$\bar{d}_i = \frac{\sum_{j=1}^{N_i} c_j d_j}{1 - \varepsilon_L} \quad (4.12)$$

Although this approach works well for classes of granules, the model outcome is unrealistic when a large granule is surrounded by lots of small granules or flocs.  $\bar{d}_i$  will approach the size of the flocs in this case, leading to a very low value of  $\varepsilon_{e,j}$  for the large granule. The resulting low value of  $\frac{\bar{d}_i}{d_j}$  makes the large granules stop settling all together. To cope with these rare cases, the value of  $\varepsilon_{e,j}$  is set to  $\varepsilon_L$  when  $\varepsilon_{e,j} - \varepsilon_L < 0.1$ .

In the original model the ratio between the fluidizing velocity and the terminal velocity was found to be 0.5, after calibration with a single fraction between 1.0 and 2.0 mm. In this study we found that a value of 0.8 would give a better estimate for the smallest size fraction 100 and 200  $\mu\text{m}$ , and still agree with the original data. A similar correction was made for the calculation of the expansion index. In the current model this was calculated based on the Archimedes number [4]:

$$n_j = \frac{1}{9.143 \times 10^{-6} \text{Ar}^{0.7728} + 0.2} \quad (4.13)$$

The position of a cluster of granules during feeding or settling (i.e.  $v_{in} = 0$ ) was modelled as follows:

$$\frac{dx_j}{dt} = v_j + v_{in} \quad (4.14)$$

### Growth of granules within a cluster

During each reaction phase, the volume (and thus the diameter) of a granule cluster was increased according to the amount of GFS accumulated as storage polymers during the anaerobic feeding phase, and a constant density and apparent yield throughout the granule. The new diameter of a granule cluster ( $j$ ) was calculated using the following equation, assuming a spherical geometry:

$$d_j = 2 \left( \frac{V_{j,old} + \frac{Y_{X,PHA}}{c_X} \int_0^{d_{j,old}/2} c_{PHA,j} A dr}{\frac{4}{3} \rho_i} \right)^{\frac{1}{3}} \quad (4.15)$$

### Breakage of biofilm clusters

The probability of breakage is calculated with a logistic function:

$$Z = \frac{1}{e^{-5000 \cdot (d-0.004)} + 1} \quad (4.16)$$

### Aerobic reaction phase

Processes taking place during the reaction phase were not modelled with time dependence, nor with a spatial dependence, but as a sequence of events. First, the residual GFS that was not stored anaerobically was distributed over all existing clusters based on specific biofilm surface area. Next, the diameter of all clusters was increased due to growth, based on an apparent yield (i.e. including loss from decay). All non-GFS fed during the anaerobic phase was subsequently converted into new flocs. The final step was breakage of particles. This is different from the time dependent approach often used in single biofilm modeling [178], but the simplification was justified due to the requirement of a discrete, cluster-based approach. Mixed wasting of sludge was applied for MLSS control at the end of the aeration phase.

### Model solution

Model equations for the sludge movement were computed using an explicit forward Euler approach (anaerobic feeding phase and settling phase). Solute mass balances in the bulk-liquid and biofilm phases were discretized using finite differencing with an implicit Crank-Nicholson scheme (central difference in space, average in time). The source term representing biological conversion in the biofilm mass balance was discretized using an

explicit forward Euler approach. The mass balances in both liquid and biofilm phases were solved (anaerobic feeding phase) fully coupled using LU-decomposition followed by forward- and back substitution as outlined by [75]. Operations on the sludge cluster population were performed during the reaction phase the end of each phase.

#### 4.2.4. Metrics for the inequality of substrate distribution

A well-known method of analyzing the inequality is the Gini coefficient [58]. This Gini coefficient quantifies the inequality using the Lorenz curve, which plots the cumulative fraction of the total income (y-axis) earned by a population fraction sorted (x-axis) [91]. The Gini coefficient is determined by the ratio of the area between the equality line and the Lorenz curve, and the area between the Lorenz curve. To utilize the Gini coefficient for the quantitative analysis of the distribution of GFS in the feeding phase, the amount of GFS accumulated as storage polymers by each cluster was calculated weighted by the number of granules ( $G$ ) represented by a simulated cluster ( $j$ ). Before calculation, the clusters were sorted based on the amount of accumulated GFS from low to high. The y-axis of the Lorenz curve was defined as:

$$y_j = \frac{\sum_{m=1}^j G_m \int_0^{d_m/2} c_{\text{PHA},m} A dr}{\sum_{m=1}^N G_m \int_0^{d_m/2} c_{\text{PHA},m} A dr} \quad (4.17)$$

The x-axis was calculated via:

$$x_j = \frac{\sum_{m=1}^j G_m}{\sum_{m=1}^N G_m} \quad (4.18)$$

#### 4.2.5. Size distribution

The granule size distribution of the sludge in the Nereda<sup>®</sup> reactor used as reference in figure 4.1 were measured over time. To determine the granule size distribution 1 L of sample was poured over a series of sieves with different mesh sizes (212, 425, 630, 1000, 1400 and 2000  $\mu\text{m}$ ). A mixed sample of 100 mL was filtered for the determination of the total dry weight. The obtained granular biomass of the different sieve fractions and the mixed sample were dried at 105  $^{\circ}\text{C}$  until no change in weight was detected anymore. Then the sieve fractions are grouped together: small granules are the sum of 212, 425 and 630  $\mu\text{m}$ , large granules are the sum of 1000, 1400 and 2000  $\mu\text{m}$  and the concentration of proto-granules and flocs is obtained by subtracting the sum of all granule fractions from the concentration of the mixed sample.

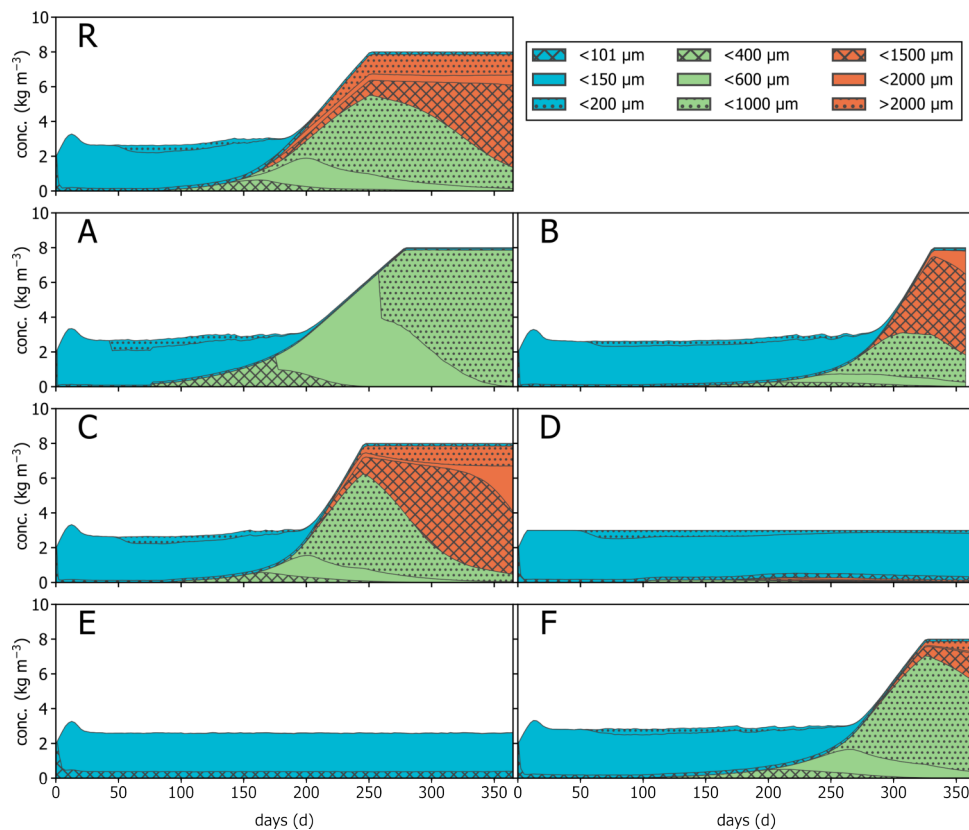


Figure 4.4: Concentration and evolution of granule fractions in the scenarios: blue area shows flocs and proto-granules, green area shows small granules, orange area shows large granules. R: reference case, A: mixed feeding, B: 15 min feeding, C: 30 min feeding, D: no selective wasting, E: 100 mg L<sup>-1</sup> GFS, F: no selective feeding.

### 4.3. Results and discussion

A sensitivity analysis was done to compare the influence of the major mechanisms on the granulation process. The main results for all scenarios are summarized in table 4.4 and figure 4.4.

#### 4.3.1. Reference case

A reference case was defined and the different scenarios in the sensitivity analysis were compared to this reference case. The reference case was a full-scale reactor with a water depth of 6 m, that was seeded with  $2 \text{ g L}^{-1}$  of flocs of  $100 \mu\text{m}$ . The selection pressure at the start was  $3 \text{ m h}^{-1}$  and it was slowly increased whenever the sludge concentration reached  $3.0 \text{ g L}^{-1}$ . The reactor was fed from the bottom of the reactor, with a Péclet number of 250. The exchange ratio was 25 % and there were no rain weather conditions, or other variation to the influent flow or composition. The reactor was fed four batches per day, containing  $500 \text{ mg L}^{-1}$  of COD, which was composed of  $200 \text{ mg L}^{-1}$  GFS and  $300 \text{ mg L}^{-1}$  non-GFS. The feeding time was 60 min. Feeding and decanting was done simultaneously, as is normal for full-scale AGS installations.

For analyses the particles in the reactor are classified in three main types: the *proto-granules*, which are particles in the range of  $100\text{-}200 \mu\text{m}$ . These particles have the granular morphology, but settling behavior is floc-like, so they are not able to separate from the sludge matrix. *Flocs* are mathematically treated similar to the proto-granules, because they both have the same floc-like behavior. In the model a floc is represented by particles of  $100 \mu\text{m}$  and smaller. *Small granules* are particles in the range of  $200\text{-}1000 \mu\text{m}$ . These particles (larger than  $200 \mu\text{m}$ ) are aerobic granules according to the definition of AGS [41]. These granules settle better than the proto-granule fraction and are small enough to be fully penetrated with substrate (acetate and oxygen). Particles larger than  $1000 \mu\text{m}$  are called *large granules*. These granules settle very quickly and accumulate near the bottom of the reactor during the feeding phase. Large granules are large enough to only be partially penetrated with substrates.

The granulation process in the reference case is shown in figure 4.4. Since the reactor is seeded with particles of  $100 \mu\text{m}$ , it takes time before the first small granules appear in the reactor. All proto-granules have the same bulk-like settling behavior, so selective wasting has no effect yet. This means every particle has the same chance of being wasted. Until this point the growth of the granules is based on chance. The proto-granules will not receive substrate every cycle. The substrate load depends on the position in the sludge bed, the volumetric exchange ratio and the amount of sequestered substrate by the particles beneath it. Over the course of multiple cycles, the combination of these factors will determine whether a proto-granule will receive enough substrate to grow into a small granule before it is spilled.

After 90 d the first small granules appear and these granules settle faster than the proto-granules. This gives these granules a competitive advantage: the granules will be

fed more frequently, because they settle towards the bottom of the reactor. This can be seen as a race towards the substrate. The fastest settling granule will always win the race and can take up a maximum amount of substrate. On top of this, the fastest settling granule will also be spilled less likely in the selective wasting from the top of the settled sludge bed. Larger granules therefore have a double benefit: they receive more substrate and they are less likely to be spilled. This process is also visible in figure 4.4: small granules dominate the population in the reactor a few weeks after the first small granules appeared.

In the simulation the first large granules appear after 165 d. These granules have better settling properties than the small granules, the largest ones having settling velocities well over  $100 \text{ m h}^{-1}$ . This means the large granules will reach the bottom of the reactor in several minutes and they will be fed every cycle. The chance of being spilled through selective wasting is close to zero, because the settling velocity of large granules is much larger than the maximum applied selection pressure of  $6 \text{ m h}^{-1}$ . This is a matter of the winner takes it all. The large granules will accumulate most of the GFS (figure 4.5), essentially leading to the extinction of the proto-granules.

The end of the lag phase is defined as the moment the biomass concentration increases more than 10 % above the target concentration of  $3 \text{ g L}^{-1}$ . This means the maximum selection pressure of  $6 \text{ m h}^{-1}$  is reached and due to the increasing amount of granules, the biomass concentrations keeps increasing. The reference case has a lag phase of 193 d. The end of the lag phase marks the start of the granulation phase, which ends when the target biomass concentration of  $8 \text{ g L}^{-1}$  is reached. Hereafter the biomass concentration is kept on  $8 \text{ g L}^{-1}$  through mixed wasting in the aeration phase. The duration of the granulation phase was 58 d (see table 4.4).

The granulation process in the reference case is very similar to what is observed in practice (figure 4.1). It shows a similar apparent steady state in the lag phase after which large granules appear in the granulation phase. Granulation in practice shows a bit more variation due to processes that are not taken into account in the model, such as rain weather events, load variations and temperature variations, but the overall process compares well.

Table 4.4: Results of the sensitivity analysis.

	first small granule (d)	first large granule (d)	lag phase (d)	granulation phase (d)	average granule size ( $\mu\text{m}$ )	maximum granule size ( $\mu\text{m}$ )
reference case	90	165	193	58	1371	3742
no plug flow	78	-	205	73	695	742
15 minutes feeding	125	278	290	42	1206	2399
30 minutes feeding	95	203	205	42	1575	3716
no selective wasting	98	193	-	-	189	3518
$100 \text{ mg L}^{-1}$ GFS	-	-	-	-	110	736
no selective feeding	115	278	275	52	1126	3886

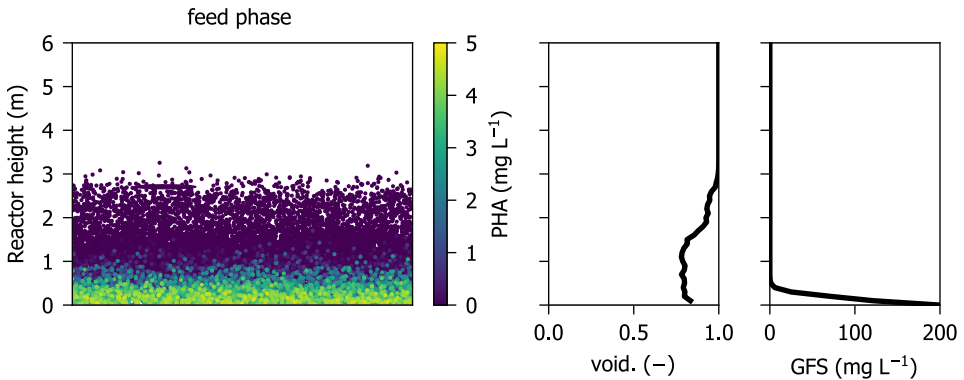


Figure 4.5: Granules in the reactor after the feeding phase at day 75. All graphs show the depth of the reactor on the y-axis. Left: individual groups of granules, color based on PHA concentration ( $\text{g L}^{-1}$ ) in the granule, x location is randomly chosen for visualization. Middle: the voidage fraction in the bed. Right: GFS in the bulk liquid.

#### 4.3.2. Microbial selection

The effect of changing feast/famine conditions was shown by shortening the anaerobic feeding time, thus limiting the anaerobic uptake of GFS. Since the batch size (and thus the loading rate) was kept constant, shortening the feeding time resulted in a higher feed flow velocity. In the reference case the anaerobic feeding time was 60 min, which was reduced to 30 min and 15 min. The shorter feeding time has a clear effect on the duration of the lag phase, which was 193 d in the reference case and was increased to 290 d in the case with a 15 minute feeding phase (table 4.4). The granulation phase was a bit faster, when the feeding phase was shortened, reducing from 58-42 d. The final granule size distribution after 365 d was quite similar.

The difference in the lag phase is a consequence of the higher up-flow velocity and the shorter contact time in the scenarios. A consequence of the higher up-flow velocity is a larger sludge bed expansion, leading to less proto-granules in contact with the influent. The shorter contact time also leads to less uptake of substrate by the particles. As a result, less proto-granules grow towards small granules due to the more even distribution of the residual GFS left over after the feeding phase.

In the granulation phase the bed expansion is not an issue anymore, because small granules can settle faster than flocs and proto-granules. So, the substrate-rich influent is more effectively in contact with the largest granule size fraction. The higher up-flow velocity causes a distribution of the GFS to be more skewed towards the small granules. As a result small granules are converted into larger granules more quickly, slightly reducing length of the granulation phase.

Overall, the duration of the feast period is especially important in the lag phase, which is shortened by a longer feast period at equal daily volumetric loading rates. In the

granulation period, the duration of the feast period is of less importance and might even provide a means to control the granule size distribution.

### 4.3.3. Selective wasting

The contribution of selective wasting to the aerobic granulation process was shown by switching from selective wasting to mixed wasting. In selective wasting the slowest settling biomass is removed from the top of the sludge bed, while faster settling particles remain in the reactor. In mixed wasting, the biomass concentration is kept constant by wasting both fast and slow settling biomass, all particles having the same chance to get wasted. The mixed wasting is representative for the situation in a CAS process. The biomass was wasted to maintain a concentration of  $3 \text{ g L}^{-1}$ . This mixed wasting did not lead to a significant granular fraction, although after 98 d the first small granules appeared in the reactor. Some large granules were present at the end of the simulation, although their contribution was small ( $0.3 \text{ g L}^{-1}$ ) and with insufficient effect on the settleability to allow for an increase in MLSS.

This scenario clearly shows the importance of selective wasting, because without it significant granulation does not happen. It also shows the drive towards granulation from the other mechanisms in the reactor. Although the granules are not preferentially maintained in the reactor as they are randomly wasted, new granules are constantly formed, due to spread in anaerobic distribution of GFS. This might explain, why (small) granules are observed in many CAS systems [180]. Even without selective wasting, some growth of granules can happen, when the other drivers for granulation are sufficiently present in the reactor. However, selective wasting is essential to drive the sludge towards full granulation.

### 4.3.4. Concentration gradients

To show the positive effect of upwards plug-flow feeding on the granule formation, in the simulation the plug-flow feeding was removed. The reactor was changed into an ideally mixed reactor during the feeding period. In full-scale AGS reactor feeding and decanting is done simultaneously, which is possible because of the plug-flow [158]. When the reactor would be ideally mixed during feeding, biomass would wash-out, resulting in poor effluent quality. For a good comparison between the scenarios, in the simulation biomass was not allowed to leave the reactor with the effluent. The results show a strong shift towards smaller granules. Compared to the reference case the duration of the lag phase was only slightly longer (205 d compared to 193 d). Also, the duration of granulation phase was very similar. The real difference is visible in the granule size distribution at the end of the simulation. Without the plug flow feeding, no large granules appeared in the reactor and the average granule size was  $703 \mu\text{m}$  (compared to  $1371 \mu\text{m}$  in the reference case).

This shift towards smaller granules is caused by several different processes. Lower substrate concentrations in the bulk liquid limit the diffusion depth of substrate into the



granules. This results in slower granule growth. Also, all substrate is distributed evenly over all particles, where in the reference case the best settling fraction receives most of the substrate. Pilot-scale work with anaerobic pulse-feeding of municipal wastewater showed a smaller mean granule size compared to the plug-flow of full-scale bottom-fed reactors [133]. Because the other mechanisms for granulation are still present (microbial selection, selective wasting and GFS), the system can still achieve a high granulation grade, but only with small granules.

#### 4.3.5. Selective feeding

The effect of the selective feeding was shown by removing the differences in settling velocity between the different particle sizes during the feeding phase. As a result, all particles have the same chance to be exposed to substrate, regardless of their settling properties, while the concentration gradient resulting from the plug-flow was kept intact. The effect is most noticeable in the duration of the lag phase, which takes 275 d compared to 193 d in the reference case. The duration of granulation phase is comparable with the reference case, but the granulation phase starts without any large granules present. In the end the average granule size is slightly smaller than in the reference case. This outcome indicates that whether a system transitions from the lag phase to the granulation phase is not only determined by the formation of some small granules that settle faster than proto-granules and flocs. The ability to exploit the faster settling properties of small granules for the uptake of GFS is key in accelerating the transition from the lag-phase to the granulation-phase and of the granulation phase itself.

The selective feeding can thus be seen as a race to the substrate: the best settling granules will have the longest exposure to the substrate and will see the highest concentration gradients. Because the settling properties of granules get better as they get larger, selective feeding allows for an increase substrate utilization with an increasing granule size. Removing selective feeding from the simulation shows, as expected, a shift towards smaller granules. Although in the end large granules still appear in the reactor, selective feeding is an important driver for granulation, which has not been recognized before in literature.

#### 4.3.6. Granule forming substrate

In the model non-GFS will always lead to the formation of flocs and GFS can lead to the formation of granules, if it is converted into storage polymers. Especially in the lag phase the ratio between GFS and non-GFS will influence the chance of proto-granules to grow into small granules. When too many flocs are formed compared to the growth of the proto-granules, the proto-granules will get spilled before they grow into small granules and can preferentially be retained in the reactor. This is clearly shown in the scenario where the GFS was reduced from  $200 \text{ mg L}^{-1}$  to  $100 \text{ mg L}^{-1}$  (i.e. decreased from 40 % to 20 % of the influent COD). Under these conditions the lag phase does not finish in the 365 d of simulation. Although some small granules appear in the reactor (the maximum

granule size is 736  $\mu\text{m}$ ), the average granule size is only 110  $\mu\text{m}$  and the simulation clearly shows a shift towards flocs in the lag phase.

In the model transport and conversion characteristics of GFS were modelled as acetate, which is the most abundant GFS in municipal wastewater treatment. GFS is derived from the fatty acids in the influent supplemented with the fatty acids formed by fermentation and hydrolysis of more complex influent COD [78, 152]. The amount of GFS is in this context partly depending on the process conditions. Fermentation and hydrolysis were not included in the presented modeling framework, since for this sensitivity analysis the origin of the GFS is not important. The amount of GFS will determine if the wastewater is suitable for AGS. For future modeling and better design of AGS processes these fermentation and hydrolysis processes will need better characterization in order to include them in a reliable manner in AGS simulation platforms.

#### 4.3.7. Breakage

Granules will eventually break into smaller pieces. In the model the chance of breaking is coupled to the granule size: larger granules have higher chance of breaking. The resulting pieces can become a seed for new granules. In the simulations the origin of granules (floc or breakage) was monitored. At the start, all granules originate from flocs. When large granules appear in the reactor, an increasing fraction of the biomass originates from broken-up granules. At the end of the simulation (after 365 d) almost 20 % originates from broken up large granules. This process can be seen as a bypass of the lag phase. Some pieces will be larger than proto-granules and can develop into new granules without going through the stochastic growth process of the proto-granules. In this work, the probability of breakage was increased with increasing granule size based on a decreasing granule strength, as was reported by [37]. The granule size beyond which a granule would have a definite probability to break-up was based on the maximum granule size observed in full scale Nereda<sup>®</sup> [157]. Granules can break-up in two parts of random volume, adding up to the volume of the original granule. In practice, breakage into multiple parts as well as attrition will occur [13]. Reality is clearly more complicated than the implementation used for the sensitivity analysis in this study. However, all implementations would have the same qualitative effect as was observed in this study, determining the maximum granule size and generate nuclei of varying size for granulation to continue. For a part the breakage of large granules will be a driver for the acceleration of the granulation process in the granulation phase. Breakage of granules has a similar effect as adding an external seed of granules to a reactor [119]. Both act as a source of new granules, bypassing the slow stochastic process of growing small granules out of flocs and proto-granules. So during start-up of AGS systems in practice a granular seed could speed up start-up times significantly.

### 4.3.8. Model validity

Various mathematical models have been developed to describe biofilm growth [178] and biochemical conversions in (partially) aerobic reactors for wastewater treatment [68]. For the sensitivity analysis presented here, we opted to implement only conversions required to capture the basic dynamics a mechanism has on distribution of biomass over the size classes of granules. The model was intended for systems with an anaerobic feast phase and an aerobic famine phase. Only heterotrophic growth was assumed, with a constant VSS/TSS ratio, using two substrates (non-GFS and GFS) and an apparent yield for growth (modeling decay and growth combined). Consequently, the active biomass density was constant, homogeneous over the radius of a granule and independent of the historical substrate loading rate of a cluster. This history could also not impact the storage capacity of PHA. Regardless of these simplifications, the model was able to describe the principle behavior of the granulation process, consisting of a lag phase and a granulation phase, without focus on mimicking actual reactor performance. In the future the model could be extended to incorporate BNR to investigate the effects of the mechanisms on reactor performance.

4

### 4.3.9. Further analysis

The sensitivity analysis performed in this study shows how delicate the start-up is of a AGS reactor from flocs. The lag phase that is seen in practice can be explained by the slow stochastic process of turning flocs into proto-granules and proto-granules into small granules. Selective wasting is an important mechanism for granulation, but in the lag phase, because of the entrapment of proto-granules in the sludge flocs, it has limited effect. Granules are only selectively retained in the reactor, when they settle faster than the flocculent sludge fraction. So the selective wasting only starts to be effective when small granules appear in the reactor. The lag phase seems to be mainly driven by the presence of GFS and the ratio between proto-granule growth and production of new flocs. The latter is important for the retention time distribution of the proto-granules. Both flocs and proto-granules will have a different age. The distribution of age needs to allow for small granules to be formed, so the maximum retention time in distribution determines if and how fast small granules are formed.

In the granulation phase the other mechanisms become more important for the granulation process. Large granules will not be spilled through the selective wasting and will only disappear from the reactor through breakage. The largest granules receive the highest amount of substrate, because of the selective feeding. Their substrate uptake capacity combined with their abundance is large enough to take up all the substrate. As a consequence only a limited amount of GFS is available for the flocs and proto-granules in a mature granular bed. The large granules will filter out all substrate from the influent at the bottom of the reactor. It is a matter of "the winner takes it all", as can be seen in figure 4.6, where we used a Lorenz curve to visualize this process. In economics the Lorenz curve [91] is used to visualize the inequality of the wealth distribution. We used it

to visualize the inequality in the substrate sequestered by the granules. The accompanying Gini coefficients [58] are also shown. In the plot the cumulative amount of substrate taken up by the granules was plotted versus the cumulative amount of granules. The diagonal line would represent a completely even distribution of the substrate over all granules. The Lorenz curve at 3 different days is plotted. At the start of the simulation there is some inequality, but this is caused by the batch size that is smaller than the bed height. At the end of the lag phase there is already a large inequality with a Gini coefficient dropping from 0.351 to 0.941, indicating a large change in substrate distribution. So at the end of the lag phase, already a large part of the substrate is sequestered by a small part of the granules. At the end of the granulation phase the inequality is even larger, with a Gini coefficient of 0.998, indicating that only a small fraction of granules sequester almost all the substrate, clearly showing the effect of the selective feeding.

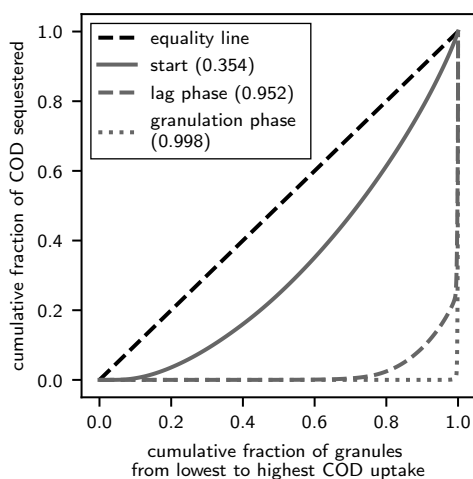


Figure 4.6: Lorenz curve showing the inequality in substrate distribution over the granules in the reference case. The curves are given at the start of the simulation, at the end of the lag phase and the end of the granulation phase, indicating an increasing inequality in substrate distribution. The numbers in the legend indicate the Gini coefficient (0 for equal distribution, 1 of complete unequal distribution).

#### 4.3.10. Practical implications

Growing granules from AS flocs in a full-scale reactor can be a lengthy process, as shown in figure 4.1. The model shows that a lag phase is a natural part of the granulation process. In practice reactors are often seeded with AGS from other plants to shorten the lag phase. Seeding is a method to break out of the stochastic processes that dominate the length of the lag-phase. Besides providing insights on the granulation process, the model can help to optimize the start-up process and find an optimum between cost for seeding and length of the start-up process. The model can also be used to optimize the start-up strategy regarding selective wasting, applied batch size and cycle times. When in the future the model is extended with a more elaborate biological model, it can also be used to investigate

the effect of granule size distribution on conversion rates and effluent quality.

#### 4.4. Conclusions

A model was developed to provide a theoretical framework to analyze the different relevant mechanisms for AGS formation and can form the basis for a comprehensive model that includes detailed nutrient removal aspects. The insights from this study can be used to further improve the granule formation in AGS reactors.

- The model describes the dynamics of a lag and a granulation phase, found in practice.
- Selective feeding and breakage of large granules were identified as important mechanisms, not reported in literature.
- Granulation is a combined result of six mechanisms, allowing a sub-optimal mechanism to be compensated by the other mechanisms.
- The GFS/non-GFS ratio and feast/famine ratio are the most important mechanisms in determining whether a system *can* transition from the lag phase to the granulation phase.
- Selective wasting and selective feeding mainly determine whether the transition from lag to the granulation phase *will* occur and at which rate.
- Breaking of granules can have a positive effect on granulation, similar to seeding of reactors with granules.

#### Acknowledgements

The authors wish to thank Lindsey Carver and Pieter Brorens for their invaluable contribution to this project.

# 5

## Implementation of selective pressures in a continuous-flow reactor

Viktor Haaksman and Edward van Dijk

## 5.1. Introduction

The development of continuous flow reactors (CFRs) employing AGS for the retrofit of existing WWTP with a CFAS system has received increasing interest following the world-wide adoption of the AGS technology in SBRs, commercialized as Nereda<sup>®</sup> [57, 122]. The better settleability of AGS compared to AS allows for process intensification of existing treatment facilities without the difficult conversion of often relatively shallow CFRs to deeper SBRs [188].

To fulfill the promise of AGS in CFRs, the process conditions necessary for sufficient granular growth must be adapted from full-scale AGS-SBRs. CFAS systems designed for EBPR, which have been developed to yield well settling flocculent sludge and prevent filamentous bulking [97], share process characteristics with AGS-SBRs with respect to the anaerobic stage [34]. A plug-flow anaerobic selector with a high initial rbCOD loading rate provides penetration depth into the flocs and ensures complete conversion of the rbCOD to storage polymers, prior to the aeration stage, to prevent transport-limited substrate uptake [92]. A strong rbCOD concentration gradient in the expanded bed during bottom-feeding is the equivalent in AGS-SBRs [158]. Considering this similarity, spontaneous aerobic granulation events in CFAS systems have been reported [129]. In all cases an  $SVI_{30}$  similar to AGS from full-scale SBRs was found [122, 157], although the mean granule sizes were smaller (i.e. <1 mm) [180]. No significant quantitative correlations between operational parameters and the fraction of granular sludge (i.e. >200  $\mu\text{m}$ ) could be determined. The degree of granulation was positively correlated with the increased enrichment of PAOs and GAOs in the granular sludge relative to flocculent sludge fraction in the study by [180]. This underlines once again the importance of the selection for slow-growing OHOs as a driver of aerobic granulation [43].

Full-scale endeavors to enhance settling characteristics has mainly focused on the selective retention of better settling sludge [33]. An external selector to keep better settling fraction in the sludge can be readily implemented on existing WWTPs [54]. Selective wasting based on differences in density or particle size using hydrocyclones have yielded better settling (densified) AS with diluted sludge volume indices ( $dSVI_{30}$ ) [131, 54, 56, 10]. This is akin to the undiluted  $SVI_{30}$  of AGS from full-scale SBRs [122], although the degree of granulation varied and the mean granule sizes were <1 mm [33]. Apart from stabilization of the sludge settleability, an increase in hydraulic or biological treatment capacity of an existing CFAS system using external selectors alone has not yet been reported.

In contrast, the hallmark of AGS in SBRs is the combination of increased settleability and higher volumetric nutrient removal rates. This combination allows for both higher surface loading rates of final clarifiers and greater biological treatment capacity. These factors are crucial for a retrofit concept for CFAS systems based on AGS. Increased nutrient removal rates are achieved through higher MLSS concentrations and strong nutrient concentrations during the aerated phase of an SBR. These conditions result in sufficient penetration depth to effectively utilize the full potential of granular biomass [122].

Full-scale AGS-SBRs achieve higher MLSS concentrations of granular sludge, while controlling the concentration of flocculent sludge, which limits the overall sludge volume [157]. The diluted  $SVI_{30}$  of dAS can be similar to the undiluted  $SVI_{30}$  of full-scale AGS [131]. However, the relatively higher coherence of dAS compared to AGS [131] means that the settling occurs more in the compression regime at higher MLSS concentrations, and this decreases overall settleability. This also limits sludge loading to a final clarifier, and thereby limits the potential for increase of the total sludge concentration in the aeration stage.

To upgrade CFAS systems designed with BNR with additional capacity through AGS, the selective pressures from full-scale AGS-SBRs must thus be implemented in the CFAS system. Several designs have been reported that do employ selective wasting to retain granular sludge [74, 33], but do not maximize granular growth to the same extent as in bottom-fed SBRs. Selection for anaerobic storage of rbCOD and a macro-gradient of substrate in the mixed liquor to maximize penetration depth are used, but they are not coupled to selective feeding of the largest granular size class [156]. Bioaugmentation with sludge from a side stream AGS-SBR has also been proposed as a strategy to increase the nitrogen removal performance of CFAS systems with a relatively low SRT [51, 101]. No study thus far has investigated a direct translation of all relevant conditions from SBRs to CFAS systems in a mainstream application.

In addition, the quantitative comparison between the effectiveness of design considerations for aerobic granulation in CFRs has been hampered by the absence of a framework describing how process conditions affect growth of AGS in SBRs. The distribution of substrate has been shown to drive the development of the sludge particle size distribution in granular sludge reactors in general [13]. For AGS specifically, the sensitivity analysis by [156] showed that the mode of operation in the anaerobic phase of a SBR can have a large impact on granulation through the distribution of GFS. Heterotrophic microorganisms utilize GFS as a carbon source, storing it as intracellular polymers. Non-GFS are organic compounds that cannot diffuse into granules or are hardly converted to storage polymers, and therefore lead to flocculent growth that hinders granule formation [78]. Three mechanisms impact the anaerobic distribution of GFS: microbial selection for anaerobic storage of GFS, maximizing diffusive substrate transport into granules, and selective feeding of large granules. Both selective and non-selective anaerobic substrate distribution could drive granulation on synthetic wastewater with only GFS [64]. Using selective feeding to maximize granular growth is more critical for real wastewater when a substantial part of the COD consists of non-GFS [78, 132], and requires further investigation.

In this study, a pilot-scale CFR was developed to best mimic the implementation of the granulation mechanisms of full-scale AGS-SBRs proposed by [156]. Selective feeding and selective wasting drive granulation through the targeted growth and retention of granular sludge, respectively. The reactor was fed with pre-settled municipal wastewater



from the Harnaspolder WWTP (The Netherlands). We established metrics to assess the degree to which the proposed mechanisms were implemented in the pilot-scale CFR and compared them to data from AGS-SBRs. To further study the impact of anaerobic substrate distribution on the growth of AGS, the pilot-scale CFR was also operated with a completely mixed anaerobic stage typical for CFAS systems employing EBPR.

## 5.2. Methodology

### 5.2.1. Description of the Harnaspolder WWTP

The pilot-scale research was conducted at the DBI research facility [45] at the Harnaspolder WWTP in The Netherlands (52°0'59.724'' N, 4°19'4.4076'' E). The WWTP was designed for a capacity 1.26 million population equivalents (1 p.e. = 150 mg<sub>COD</sub> d<sup>-1</sup>) and a DDWF of 215 000 m<sup>3</sup> d<sup>-1</sup>. Pre-settled influent is treated by the BNR-stage for removal of phosphorus, nitrogen and COD according to the PhoSim-process [164].

## 5

### 5.2.2. Description of the pilot-scale CFR

The design of the pilot-scale reactor was set-up as a translation from an AGS-SBR to an equivalent CFR. The aim was to translate the operational conditions that drive the growth of AGS as well as the possibility to obtain the same granular sludge morphology. Each research period was started by seeding AGS from a full-scale SBR. This approach was chosen to directly study the effect of the design and operation of the pilot-scale CFR on all mechanisms affecting the sludge morphology [156]. The reactor was sized to operate at the same average SRT as the CAS system of the Harnaspolder WWTP (20 d), while maintaining an MLSS concentration of 8 g<sub>TSS</sub> l<sup>-1</sup> of granular sludge. The volumetric loading rate of the pilot-scale CFR at DDWF was therefore increased twofold compared to the Harnaspolder WWTP designed for a MLSS concentration of 4 g<sub>TSS</sub> l<sup>-1</sup> of AS (i.e. from 1.04 to 2.08 m<sup>3</sup><sub>influent</sub> m<sup>-3</sup><sub>reactor</sub> d<sup>-1</sup>).

An overview of the pilot-scale CFR is depicted in figure 5.1. Influent was continuously supplied to the reactor at a constant flow rate of 0.5 m<sup>3</sup> h<sup>-1</sup>. The flow rate was set to the average DDWF volumetric loading rate of the Harnaspolder WWTP. The reactor therefore received a lower loading during rain weather flow (RWF) due to dilution of the wastewater. The WWTP receives a peak RWF flow rate of 35 800 m<sup>3</sup> h<sup>-1</sup>. An electrical conductivity sensor in the influent supply was used to monitor the decrease in strength of the wastewater during RWF, based on which the sludge production was estimated, and the interval of excess sludge removal adjusted accordingly. The influent was directed to the anaerobic stage (section 5.2.3). The mixed liquor then flowed to the subsequent stage of six tanks in series. Each tank had a working volume of 1 m<sup>3</sup> that could be mechanically mixed, mixed through fine bubble aeration, or both. The airflow to each tank was controlled from 0.42-1.04 mm s<sup>-1</sup> via a valve. The last of the tanks in series was equipped with a manifold used for batchwise selective wasting, submerged at a depth of 35 cm. The flow to the last tank (C6) and the mechanical mixing were intermittently stopped to allow for the sludge

to settle for a preset period of time, after which the mixed liquor above the manifold was discharged to an excess sludge buffer. During normal operation between waste sludge discharge events, the mixed liquor flowed from the last tank to the final clarifier (cone shaped) with a surface loading rate of  $1.39 \text{ m h}^{-1}$ . Thickened sludge was returned to the anaerobic stage via a peristaltic pump. Another pump of the same model was used to pump  $\text{NO}_x$ -rich mixed liquor from last aerated (C5) tank to the first anoxic tank acting as a pre-DN zone (C1). The reactor performance was monitored and controlled via on-line sensors.

### 5.2.3. Anaerobic stage configurations

#### Two alternating anaerobic upflow selectors (period I)

The anaerobic stage was designed based on an analysis of AGS-SBRs with respect to aerobic granulation [156]. For the same wastewater, the anaerobic distribution of substrate over the granule size classes could be kept the same if the same superficial liquid velocity would be applied to expand a sludge bed. This would ensure a similar amount of bed expansion, degree of stratification over the height and degree of axial dispersion, which in turn would yield the same anaerobic substrate distribution. Second, the anaerobic residence time of the sludge in the CFR should be the same as the duration of the anaerobic feeding phase in the SBR.

A continuous anaerobic stage with two upflow selectors (figure 5.1) was designed to achieve this. Each selector was operated as an anaerobic SBR in an alternating fashion. While either one of the upflow selectors was receiving the influent, the return sludge flow was directed to the other selector. A working height of 2.5 m was chosen to allow for the accumulation of the same settled bed height as in the reference SBR [122]. Each upflow selector had a conical bottom with a slope of  $60^\circ$  that was used to displace saturated sludge to the first anoxic tank after the feeding phase. Influent was fed via a pipe directed at the bottom of the cone. Return sludge was added at a height of 1.5 m. Mixed liquor could overflow through an outlet at the top of the selector to first anoxic tank. A cycle of an anaerobic upflow selector consisted of the following phases (see figure 5.1):

1. *Displacement phase*: return sludge was added to selector A at 1.5 m and was allowed to settle on to the top of the remaining sludge bed after anaerobic feeding. The sludge saturated with storage polymers at the bottom of the bed was simultaneously displaced through the bottom outlet to first anoxic tank.
2. *Accumulation phase*: after the complete volume of the sludge bed in upflow selector A had been displaced by granular sludge from the return sludge, the withdrawal of sludge at the bottom was stopped. The supply of return sludge was continued for the accumulation of granular sludge on top of the bed, if the sludge could settle faster than the applied superficial upflow velocity. Sludge size classes with a too low settleability overflowed at the top of the selector towards the anoxic tank and effectively bypassed the anaerobic stage.

3. *Feeding phase*: once the feeding phase in selector B had finished, the flow of influent was directed to selector A. The flow of return sludge was simultaneously switched to upflow selector B. The sludge bed in selector A would then expand due to applied superficial liquid velocity. Sludge size classes with insufficient settleability would wash out of the expanded bed and overflow at the selector. Furthermore, the sludge size classes that remained in the expanded bed would stratify from top to bottom with increasing settleability. Once the feeding phase in selector A had finished, the cycle was restarted.

### **Mixed anaerobic selector and anaerobic tank (control, period II)**

To investigate the contribution of the upflow selectors to the growth of AGS, the anaerobic stage was altered during the control period to resemble that of the full-scale CAS system at the Harnaspolder WWTP. It consisted of a completely mixed anaerobic selector compartment with a mixed liquor residence time of 16 min, followed by a completely mixed anaerobic compartment with a residence time of 1 h. The return sludge was directed partly to the anaerobic selector (45 %) and partly to the second anaerobic tank (55 %). The complete flow of influent was directed to the anaerobic selector. The residence time distribution was the same for all sludge size classes due to mechanical mixing, regardless of differences in settleability. The anaerobic distribution of GFS was determined only by the kinetics of mass transfer and biological conversions. This removed the selective advantage for the best-settling granular sludge size classes over flocculent sludge in the anaerobic distribution of GFS [64], reducing this selective pressure for aerobic granulation compared to the anaerobic upflow selectors. The average sludge loading of GFS in the anaerobic stage was similar to period I. To investigate the contribution of the upflow selectors to the growth of AGS, the anaerobic stage was altered during the control period to resemble that of the full-scale CFAS system at the Harnaspolder WWTP figure 5.1. It consisted of a completely mixed anaerobic selector compartment with a mixed liquor residence time of 16 min, followed by a completely mixed anaerobic compartment (C1) with a residence time of 1 h. The return sludge was directed partly to the anaerobic selector (45 %) and partly to the second anaerobic tank (55 %). The complete flow of influent was directed to the anaerobic selector. The residence time distribution was the same for all sludge size classes due to mechanical mixing, regardless of differences in settleability. The anaerobic distribution of GFS was determined only by the kinetics of mass transfer and biological conversions. This removed the selective advantage for the best-settling granular sludge size classes over flocculent sludge in the anaerobic distribution of GFS [64], reducing this selective pressure for aerobic granulation compared to the anaerobic upflow selectors. The average sludge loading of GFS in the anaerobic stage was similar to period I.

### **Control of nutrient removal**

Compartments C2 till C5 of the tanks in series served as an aerobic zone. Compartments C2 and C3 were continuously aerated and the airflow was regulated to maintain a setpoint for the DO concentration between 1-2 mg l<sup>-1</sup>. The airflows to compartments 4 and 5 were controlled to limit the concentration of nitrate in the effluent (and return sludge) to a

maximum of  $10 \text{ mg NO}_3^- \text{-N l}^{-1}$ . If the ammonium concentration in the effluent came below  $1 \text{ mg NH}_4\text{-N l}^{-1}$ , the airflows to compartments C4 and C5 were lowered to achieve maximum SND.

$\text{NO}_x$ -rich mixed liquor was recycled from the last aerated compartment (C5) to the first anoxic tank (C1) for pre-DN (figure 5.1). The ratio of the recycle flow rate compared to the flow of influent was between 1 and  $2 \text{ m}_{\text{ML}}^3 \text{ m}_{\text{influent}}^{-3}$ .

#### **Discharge of excess sludge (selective wasting)**

Excess sludge was discharged through a submerged manifold in the last compartment of the tanks in series (C6), prior to the final clarifier (figure 5.1). A batchwise procedure was used to perform selective wasting of sludge based on a settling speed criterion of  $3.6 \text{ m h}^{-1}$ , within the range of superficial upflow velocities used in Nereda<sup>®</sup> reactors [158]. The flow to the last compartment was stopped and the mechanical mixer was turned off, after which the sludge was allowed to settle. After a preset time the outlet valve was opened, and the excess sludge was discharged. Operation would continue as normal until the next discharge cycle. The interval between discharge cycles was set to maintain a sludge volume after five minutes of settling ( $\text{SV}_5$ ) of  $400\text{-}500 \text{ ml mL}^{-1}$ .

#### **5.2.4. Analytical procedures**

Concentrations of compounds in mixed liquor samples were determined via analysis kits from the LCK-system and a DR3900 spectrophotometer from HACH (Loveland (CO), USA). Samples were prepared using  $0.45 \mu\text{m}$  Puradisc AQUA syringe filter from Whatman (Marlborough (MA), USA). The concentration of acetate was determined by HPLC with an Aminex HPX-87H column from Bio-rad (Hercules (CA), USA), coupled to an UV detector, using  $0.01 \text{ M}$  phosphoric acid as the eluent. Samples for HPLC were filtered through a  $0.2 \mu\text{m}$  PVDF-membrane from Whatman (Marlborough (MA), USA). MLSS concentrations, MLVSS concentrations and sludge volume indices after 5 min and 30 min were determined according to [22]. The size class distribution of a sludge sample was determined by first pouring the sample over a stack of sieves with decreasing mesh size and rinsing each sieve with tap water. Samples for characterization of the sludge morphology were transferred to a glass petri dish and examined with an Olympus reverse microscope (Shinjuku (Tokyo), Japan) with a Leica digital camera (Wetzlar, Germany).

#### **5.2.5. Specific activities of sludge size classes**

##### **Anaerobic uptake rate and storage capacity of GFS**

The maximum anaerobic conversion rate of GFS and the storage capacity of PHA were determined via batch tests using acetate. A mixed liquor sample was taken from the return sludge, prior the anaerobic stage. If the sludge was fractionated using sieves, each fraction was recombined with filtered effluent ( $7 \mu\text{m}$ ). In either case, the initial volume was  $840 \text{ ml}$  with an approximate MLSS concentration of  $2 \text{ g}_{\text{TSS}} \text{ L}^{-1}$ , containing a  $10 \mu\text{mol L}^{-1}$  HEPES-buffer to ensure a stable pH of 7. The temperature was kept constant at  $20 \text{ }^\circ\text{C}$ .

Oxygen was first stripped from the liquid by sparging dinitrogen gas at a rate of  $1 \text{ L min}^{-1}$ , which continued throughout the experiment. The experiment was started via the addition of 10 ml of a solution of  $42.5 \text{ g}_{\text{Ac}} \cdot \text{L}^{-1}$  to reach an initial concentration of  $500 \text{ mg}_{\text{Ac}} \cdot \text{L}^{-1}$ . This set-up was developed to achieve complete penetration of acetate of in the largest granule size class within 5 min and to allow sampling in the zero-order kinetics range during the first 60 min of the experiment [64]. The loading was sufficient to achieve saturation of the storage capacity of PHA. Samples of 10 ml were taken every 10 min during to 60 min and immediately filtered through a  $0.45 \mu\text{m}$  Puradisc AQUA filter from Whatman (Marlborough (MA), USA) and stored at  $4^\circ\text{C}$  for analysis. A final sample was taken after 150 min to determine total storage capacity of PHA through the remaining concentration of acetate. All biomass in each container was subjected to the determination of the MLSS and MLVSS at the end of the experiment. The maximum anaerobic conversion rate of GFS and the capacity for storage as intracellular polymers were determined via batch tests using acetate. A mixed liquor sample was taken from the return sludge, prior the anaerobic stage. If the sludge was fractionated using sieves, each fraction was recombined with filtered effluent ( $7 \mu\text{m}$ ). In either case, the initial volume was 840 mm with an approximate MLSS concentration of  $2 \text{ g}_{\text{TSS}} \cdot \text{L}^{-1}$ , containing a  $10 \mu\text{mol L}^{-1}$  HEPES-buffer to ensure a stable pH of 7. The temperature was kept constant at  $20^\circ\text{C}$ . Oxygen was first stripped from the liquid by sparging dinitrogen gas at a rate of  $1 \text{ L min}^{-1}$ , which continued throughout the experiment. The experiment was started via the addition of 10 ml of a solution of  $42.5 \text{ g}_{\text{Ac}} \cdot \text{L}^{-1}$  to reach an initial concentration of  $500 \text{ mg}_{\text{Ac}} \cdot \text{L}^{-1}$ . This set-up was developed to achieve complete penetration of acetate of in the largest granule size class within 5 min and to allow sampling in the zero-order kinetics range during the first 60 min of the experiment [64]. The loading was sufficient to achieve saturation of the storage capacity. Samples of 10 ml were taken every 10 min during to 60 min and immediately filtered through a  $0.45 \mu\text{m}$  Puradisc AQUA filter from Whatman (Marlborough (MA), USA) and stored at  $4^\circ\text{C}$  for analysis. A final sample was taken after 150 min to determine total storage capacity through the remaining concentration of acetate. All biomass in each container was subjected to the determination of the MLSS and MLVSS at the end of the experiment.

## 5

**Fraction of GFS in the influent**

The maximum fraction of  $\text{COD}_{<0.45 \mu\text{m}}$  in the pre-settled municipal wastewater available for anaerobic storage was estimated from batch tests with the influent combined with return sludge. The size of  $0.45 \mu\text{m}$  has been reported to be close to the cut-off point for particles to be diffusible into granules [166], and was therefore used as proxy for GFS. The ratio of influent to return sludge in the test was set to obtain a COD loading ( $\text{mg g}_{\text{TSS}}^{-1}$ ) such that the anaerobic storage capacity of the sludge was not exceeded. The batch tests were conducted in the same way as described in section 5.2.5.

**Aerobic conversion rates**

The maximum specific aerobic conversion rates for simultaneous removal of ammonium (SNUR) and phosphate (SPUR) were determined via batch tests. A mixed liquor sample

was taken from the end of the anaerobic stage. The sludge was either thickened through settling and decanting, or the sludge was fractionated into size classes using sieves. In both cases, the sludge was recombined with filtered mixed liquor (7  $\mu\text{m}$ ) from the end of the anaerobic stage. The initial volume was 840 mm with an approximate MLSS concentration of 3  $\text{g}_{\text{TSS}} \text{L}^{-1}$ , containing a 10  $\mu\text{molL}^{-1}$  HEPES-buffer to ensure a stable pH of 7. The temperature was kept constant at 20 °C. The experiment was initiated by starting the supply of oxygen via sparging of air at a rate of 1  $\text{L min}^{-1}$  and ensured saturation of the liquid with dissolved oxygen. This set-up was developed to allow sampling in the zero-order kinetics range during the first 60 min of the experiment. Samples of 10 ml were taken every 10 min during to 60 min. The sample processing and the remainder of the experiment were performed according to 5.2.5.

### 5.2.6. Calculation procedures

#### Retention efficiency of anaerobic upflow selectors

The upflow selectors used as anaerobic stage imposed distribution in anaerobic retention time for sludge size classes depending on their settleability. Size classes unable to meet the selection criterion would overflow at the top during either the sludge accumulation phase or the feeding phase. The probability to be retained ( $Z_{j,\text{AN}}$ ) for each size class ( $j$ ) was calculated based on sieve tests on sludge samples from both the return sludge and the expanded sludge bed at the end of the anaerobic feeding phase via equation (5.1). The expanded bed volume ( $V_{\text{bed}}$ ) was determined via measurement of the bed height using a sludge blanket detector (SoliTechw<sup>2</sup> IR 0-10 000  $\text{mg L}^{-1}$ , Partech. St. Austell, UK).

$$Z_{j,\text{AN}} = \frac{V_{\text{bed}} c_{j,\text{bed}}}{c_{j,\text{MLSS}} \frac{1+\text{RSR}}{\text{RSR}} F_{\text{influent}} t_{\text{AN},s}} \quad (5.1)$$

The anaerobic retention probability per size class was used to calculate the anaerobic residence time ( $\text{RT}_{j,\text{AN}}$ ) of a size class in an upflow selectors and the remaining residence time in the aerobic/anoxic volume of the pilot-scale CFR (equation (5.2)). The distribution of each size class was compared to the hypothetical distribution based on the relative volume fractions of the anaerobic stage and the aerobic/anoxic stage, as if the sludge was completely mixed in all compartments.

$$\text{RT}_{j,\text{AN}} = \frac{2 \times V_{\text{bed}} c_{j,\text{bed}}}{2 \times V_{\text{bed}} c_{j,\text{bed}} + c_{j,\text{MLSS}} V_{\text{AE/AO}}} \quad (5.2)$$

#### Retention efficiency of selective sludge wasting

The efficiency of the selective sludge wasting based on settleability for each size class was calculated based on mixed samples taken from the compartment prior to the discharge of excess sludge, and from samples taken from the collected excess sludge. The probability to be retained ( $Z_{j,\text{WS}}$ ) was expressed as the fraction of the load of a size class ( $j$ ) wasted

using selective wasting, relative to the hypothetical load of a size class wasted without allowing the sludge to settle prior to the discharge (see equation (5.3)).

$$Z_{j,WS} = 1 - \frac{c_{j,WS} V_{WS}}{c_{j,MLSS} V_{\text{manifold}}} \quad (5.3)$$

The SRT per size class (equation (5.4)) was calculated based on the measured selective sludge discharge load ( $M_{j,WS}$ ), the number of discharge events per day ( $n_d$ ), the amount of the sludge mass in the entire system of each size class ( $M_{j,MLSS}$ ) and was related to the mean SRT ( $\overline{\text{SRT}}$ ) for the total volume of the pilot-scale reactor (equation (5.5)).

$$\text{SRT}_i = \frac{M_{j,MLSS}}{n_d M_{j,WS}} \quad (5.4)$$

$$\overline{\text{SRT}} = \frac{\sum_j^N M_{j,MLSS}}{n_d \sum_j^N M_{j,WS}} \quad (5.5)$$

5

### Hydraulic residence time distribution (RTD)

The mixing characteristics of the anaerobic stages used in both research periods were analyzed via determination of the residence time distribution. The concentration of ammonium in the influent of the pilot-scale CFR was used as a step-tracer ( $c_{\text{NH}_4^+-\text{N},\text{inf}}$ ). First, the liquid in the compartment under study was completely displaced with effluent. The anaerobic compartment was then fed with influent as during normal operation for the same duration ( $t_{\text{RTD}}$ ) and the concentration of ammonium in the outflow ( $c_{\text{NH}_4^+-\text{N},\text{out}}$ ) was determined via grab samples at regular intervals. The cumulative RTD ( $F$ ) and RTD ( $E$ ) were computed based on the normalized tracer concentration via equation (5.6):

$$F(t) = \frac{c_{\text{NH}_4^+-\text{N},\text{out}}(t) - c_{\text{NH}_4^+-\text{N},\text{eff}}}{c_{\text{NH}_4^+-\text{N},\text{inf}}}, \quad E(t) = \frac{dF(t)}{dt} \quad (5.6)$$

The mean residence time (first moment) and the normalized variance (second moment) were calculated via equation (5.7):

$$t_m = \int_0^{t_{\text{RTD}}} tE(t)dt, \quad \sigma^2 = \int_0^{t_{\text{RTD}}} (t - t_m)^2 E(t)dt \quad (5.7)$$

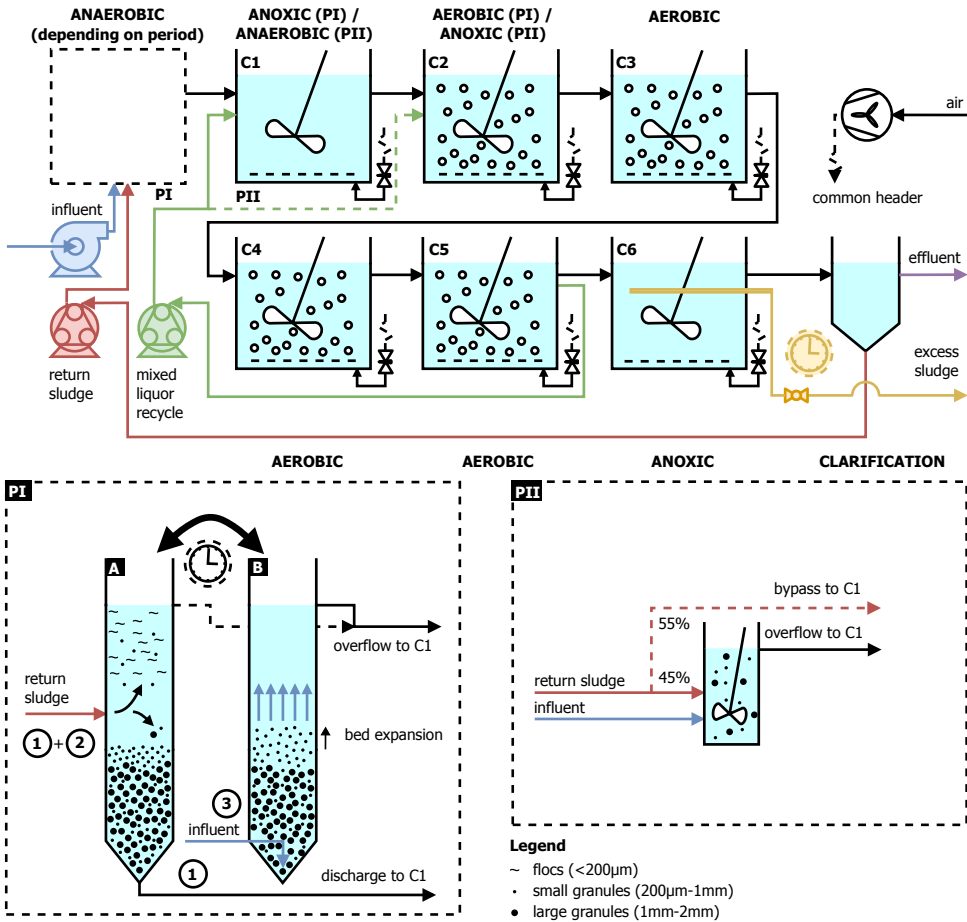


Figure 5.1: (top) Schematic overview of the pilot-scale continuous flow reactor. The differences between the configuration during trial period 1 and trial period 2 are indicated via PI en PII, respectively. (bottom) Detailed description of the anaerobic stages of the pilot-scale CFR during the two operational periods. (bottom left) Period I (PI): two alternating upflow selectors based on the anaerobic phase of a SBR employing AGS. The numbers in the image refer to the numbering of the phases of an anaerobic feeding cycle described in section 5.2.3. (bottom right) Period II (PII): an anaerobic selector followed by a larger anaerobic tank (both completely mixed) that resembled after the anaerobic stage of the Harnaschpolder WWTP.



### 5.3. Results

The pilot-scale CFR was fed with pre-settled municipal wastewater of the Harnaspolder WWTP as influent. The characteristics of the pre-settled wastewater are listed in table 5.1. Each of the two research period was started by seeding AGS from a full-scale SBR. The initial MLSS concentration was between 6-8 g<sub>TSS</sub> l<sup>-1</sup>. If conditions for granular growth were inadequate, the granular sludge fraction would decrease rapidly after seeding. If the AGS grew and maintained its morphology after seeding, it indicated favorable conditions for granular sludge formation.

Table 5.1: Characteristics of the pre-settled municipal wastewater of the Harnaspolder WWTP over a time period of one year.

Component (unit)	Influent concentration
NK <sub>j</sub> (mg <sub>N</sub> L <sup>-1</sup> )	57.4 ± 7.8
P <sub>total</sub> (mg <sub>P</sub> L <sup>-1</sup> )	9.3 ± 1.4
PO <sub>4</sub> <sup>3-</sup> (mg <sub>P</sub> L <sup>-1</sup> )	6.8 ± 0.9
COD (mg <sub>COD</sub> L <sup>-1</sup> )	503 ± 84
COD <sub>&lt;0.45 μm</sub> (mg <sub>COD</sub> L <sup>-1</sup> )	257 ± 38
COD <sub>VFA</sub> (mg <sub>COD</sub> L <sup>-1</sup> )	109 ± 32
inert COD <sub>&lt;0.45 μm</sub> (mg <sub>COD</sub> L <sup>-1</sup> ) <sup>a</sup>	29
COD <sub>&lt;0.45 μm</sub> converted anaerobically (%) <sup>b</sup>	40-60

<sup>a</sup> equal to the average concentration of COD<sub><0.45 μm</sub> in the effluent of the CFR.

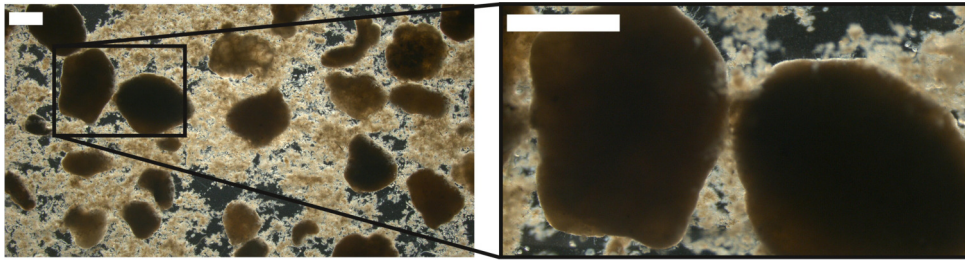
<sup>b</sup> estimated according to section 5.2.5.

#### 5.3.1. Seed sludge characteristics

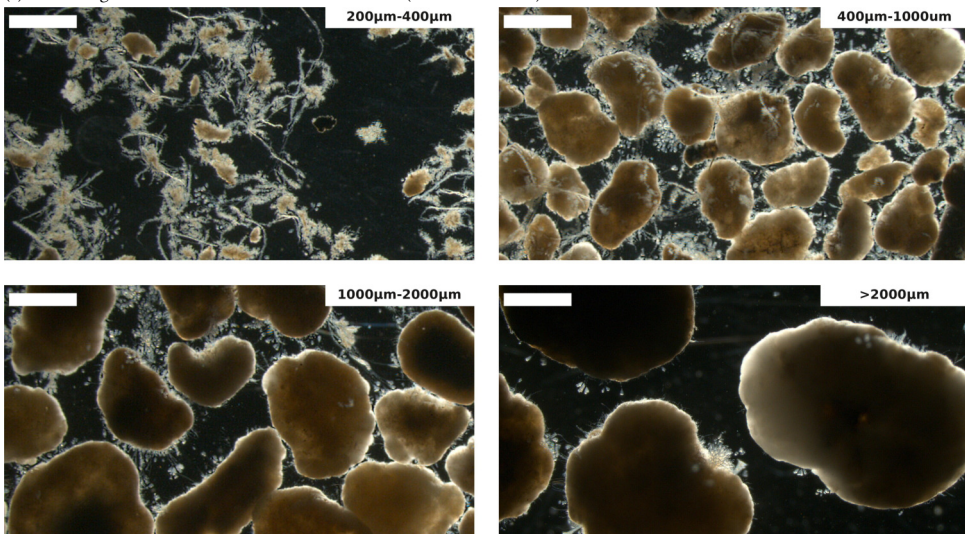
The seed sludge originated from an AGS-SBR at Utrecht WWTP (The Netherlands) designed for biological removal of nitrogen, phosphorus and COD, similar to the reactor described by [122]. The granule size distribution of the seed sludge is listed in table 5.2. The morphology of seed sludge is depicted in figure 5.2a. The size class <200 μm consisted of compact flocs, while the class from 200-400 μm contained cellulose and granular nuclei. Small (400-1000 μm), medium (1000-2000 μm) and large granules (>2000 μm) shared a similar smooth morphology with limited surface outgrowth. The shape of the granules did show a decrease in sphericity with increasing size. The average ratio of VSS/TSS was 80 %.

Table 5.2: Size distribution of the seed sludge from an AGS-SBR at Utrecht WWTP (The Netherlands) used for the pilot-scale CFR.

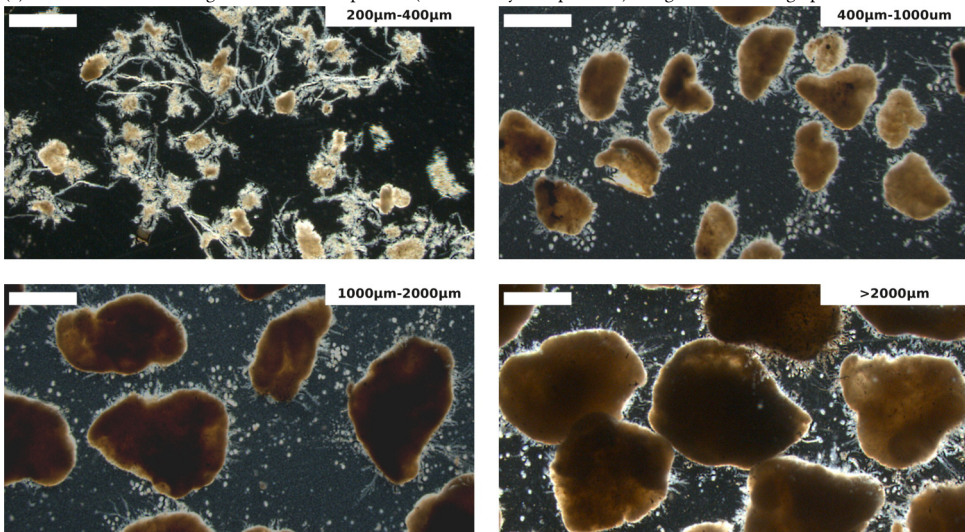
Size class	MLSS (g <sub>TSS</sub> L <sup>-1</sup> )	Relative contribution
<200 μm	1.85	22 %
200-400 μm	0.28	3 %
400-1000 μm	0.89	11 %
1000-2000 μm	2.47	29 %
>2000 μm	2.96	35 %



(a) Seed sludge from an AGS-SBR at Utrecht WWTP (The Netherlands).



(b) Sieved fractions of sludge from the end of period I (after 166 days of operation) using two alternating upflow selectors.



(c) Sieved fractions of sludge from the end of period II (after 129 days of operation) using a completely mixed anaerobic selector and subsequent anaerobic tank.

Figure 5.2: Morphology of AGS size classes, fractionated using sieves and imaged via stereoscopic microscopy. The scale bar represents a length of 1 mm.

### 5.3.2. Period I: two alternating anaerobic upflow selectors

The anaerobic upflow selectors had to be operated such that the three mechanisms for the anaerobic distribution of GFS were implemented similarly to an AGS-SBR: microbial selection for anaerobic storage of GFS, maximizing transport of substrate into the granules and selective feeding of largest granules. Based on the modeling procedure from [156], a superficial feeding velocity of  $3.6 \text{ m h}^{-1}$  with an anaerobic feeding time of 1.5 h (average time to saturation of the anaerobic storage capacity, see section 5.2.5) was expected to yield an anaerobic distribution of GFS similar to a full-scale AGS-SBR [122, 157]. Using the maximum anaerobic conversion rate of GFS from the AS from Harnaschpolder WWTP, it was estimated that an expanded bed height of 1.2 m of granules  $>1 \text{ mm}$  was required for complete anaerobic removal of GFS from the pre-settled influent.

After a trial period of 44 d during which the process control of the anaerobic upflow selectors (figure 5.1) was tested with a small amount of AGS, the CFR was seeded to approximately  $8 \text{ g}_{\text{TSS}} \text{ l}^{-1}$ . The initial granular sludge mass fraction ( $>200 \mu\text{m}$ ) was 78 %, with 64 %  $>1 \text{ mm}$  and 35 %  $>2 \text{ mm}$  (see figure 5.3a). The MLSS concentration decreased slightly during the first two days, mainly due to the loss of the granules in the size class  $>2 \text{ mm}$ . This was likely caused by disintegration due to the exposure to increased shear stress from the mechanical mixing and recycle pumps in the CFR, compared to only fine bubble aeration in the full-scale SBRs to which the seed sludge had been accustomed [157].

5

#### Sludge characteristics

The mass distribution and sludge properties stabilized after the initial seeding and were maintained during 166 days, after which the experiment was terminated. The average MLSS concentration was  $6.4 \pm 0.7 \text{ g}_{\text{TSS}} \text{ l}^{-1}$  with a VSS/TSS ratio of 79 %. The average size of granules ( $>200 \mu\text{m}$ ) was 1.34 mm and the mass fraction of all granular sludge size classes was 66 % (see figure 5.3a). The variation of the MLSS distribution over time observed in the pilot-scale CFR is common for AGS reactors treating sewage [169]. The sludge settleability was stable throughout period I with an average  $\text{SVI}_{30}$  of  $51 \pm 6 \text{ mL g}_{\text{TSS}}^{-1}$  and a  $\text{SVI}_5/\text{SVI}_{30}$  ratio of  $1.65 \pm 0.1$ , which were comparable to values reported for full-scale AGS-SBRs (1.56, [122]). The  $\text{dSVI}_{30}$  of the AS from the full-scale CFAS system at Harnaschpolder WWTP averaged  $100 \text{ ml g}_{\text{TSS}}^{-1}$  during the same period. Visual inspection showed that the morphology of the granular sludge remained smooth throughout period I, based on the absence of filamentous or finger-type outgrowth [121]. Parts of the granular surfaces were occupied by stalked ciliates (see figure 5.2b).

#### Anaerobic loading distribution

The extent to which the selective pressures for aerobic granulation were implemented were analyzed based on the framework proposed by [156]. The quantitative metrics for the mechanisms are listed in 5.2.6.

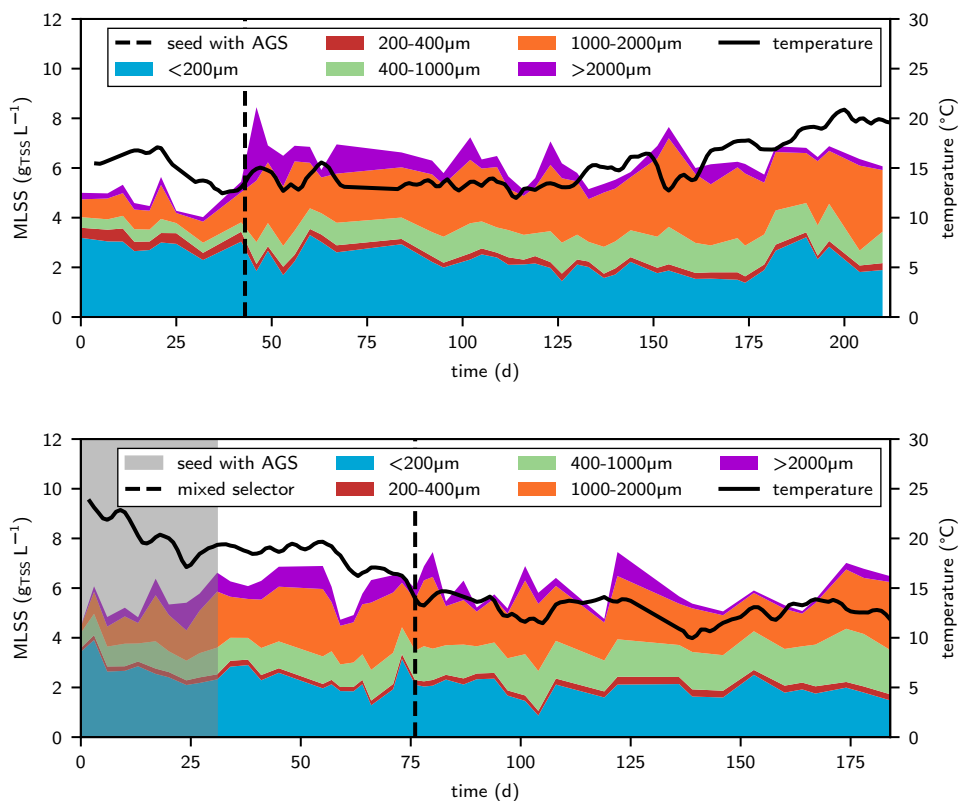


Figure 5.3: Total MLSS and mass distribution over sludge particle size classes, and the temperature profile during the operational periods with (a, top) two alternating anaerobic upflow selectors (period I) and (b, bottom) a mixed anaerobic selector and anaerobic tank (period II). The vertical line (black, dashed) indicates the transition to the mixed anaerobic stage. The shaded area (gray) denotes the period during which AGS was seeded (period II).

All COD available for anaerobic conversion (GFS) was removed in the selector, ensuring microbial selection for anaerobic storage. This was determined from the removal of  $\text{COD}_{<0.45\mu\text{m}}$  in the overflow during DWF, shown in table 5.3. The anaerobically removable  $\text{COD}_{<0.45\mu\text{m}}$  fraction in the influent ranged from 40-60 %, which was considered to be the fraction of GFS (table 5.1). The anaerobically removable  $\text{COD}_{<0.45\mu\text{m}}$  consisted of VFAs and a fermentable fraction of COD. The removal efficiency of  $\text{COD}_{<0.45\mu\text{m}}$  in the anaerobic upflow selector was 49 %. Therefore, the amount of GFS in the influent was completely removed in the selector. The uptake of  $\text{COD}_{<0.45\mu\text{m}}$  was coupled to the release of phosphate with an average P/COD-ratio of 0.39

The degree of plug-flow was investigated by measuring the RTD (see figure 5.4). A cumulative RTD was determined by first expanding and stratifying the accumulated sludge in the upflow selector with effluent, followed by a normal feeding phase with influent. The concentration of ammonium in the overflow was used as a step-tracer. This concentration

Table 5.3: Characteristics for the anaerobic conversions for one of the alternating upflow selectors at the end of the anaerobic feeding phase (period I).

Component (unit)	Influent	Outflow of anaerobic upflow selector (removal)
COD ( $\text{mg}_{\text{COD}} \text{L}^{-1}$ )	579	- <sup>a</sup>
$\text{COD}_{<0.45\mu\text{m}}$ <sup>b</sup> ( $\text{mg}_{\text{COD}} \text{L}^{-1}$ )	273	138 (49%)
$\text{COD}_{\text{VFA}}$ <sup>c</sup> ( $\text{mg}_{\text{COD}} \text{L}^{-1}$ )	115	<5 (>96%)
$\text{NH}_4^+$ ( $\text{mg}_{\text{N}} \text{L}^{-1}$ )	48.6	47.8
$\text{PO}_4^{3-}$ ( $\text{mg}_{\text{P}} \text{L}^{-1}$ )	6.5	58.8

<sup>a</sup> Could not be determined since the overflow of the upflow selector contained substantial amounts of sludge.

<sup>b</sup> Corrected for the inert fraction of  $\text{COD}_{<0.45\mu\text{m}}$ , based on the amount in the effluent of the CFR (see table 5.1).

<sup>c</sup> Combined value for all VFAs detected (i.e. acetate and propionate).

was normalized using the concentration of ammonium in the influent and the effluent, and fitted to an 1D axial dispersion model (5.2.6) which yielded an axial dispersion coefficient  $D_{\text{ax}}$  of  $0.8 \times 10^{-4} \text{ m}^2 \text{ s}^{-1}$ . Therefore, the Péclet-number for the expanded bed in the upflow selector ( $Pe_B$ ) was 13. An axial dispersion coefficient in the same order of magnitude has been reported for full-scale AGS-SBRs (i.e.  $1 \times 10^{-4} \text{ m}^2 \text{ s}^{-1}$ , [158]) and the flow was characterized by a similar Péclet-number of 14. The upflow selector of the pilot-scale CFR thus exhibited a degree of plug-flow similar to a full-scale AGS-SBR.

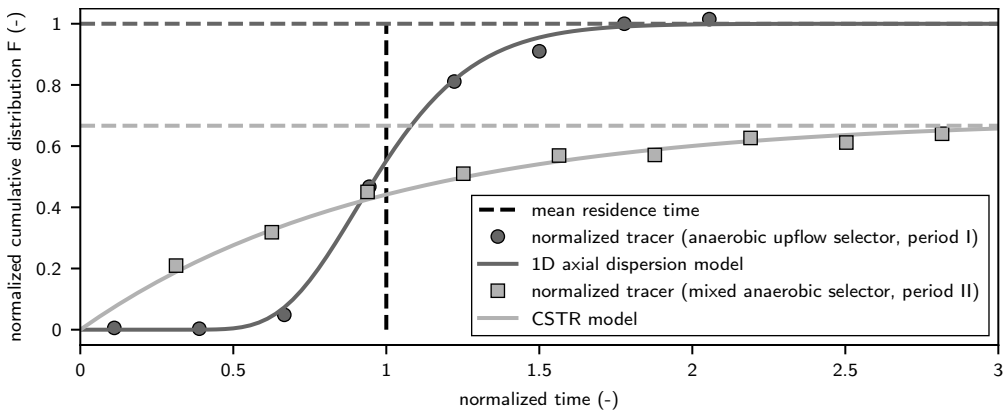


Figure 5.4: Normalized cumulative RTD for the feeding phase of an anaerobic upflow selector used in the CFR during period I (solid spheres) and the anaerobic selector used in period II (solid squares). The normalized variances ( $\sigma^2$ ) were 0.07 and 0.81, respectively. The normalized concentrations were fitted to a transient 1D axial dispersion model with an axial dispersion coefficient ( $D_{\text{ax}}$ ) of  $0.8 \times 10^{-4} \text{ m}^2 \text{ s}^{-1}$  for period I (solid line), and to a single CSTR-model for period II (solid line). The horizontal lines (dashed) depicts the reduced maximum concentration in the completely mixed anaerobic selector relative to the influent due to the dilution by the return sludge flow in period II, while this was not the case for the anaerobic upflow selector in period I.

To analyze the extent of selective feeding, the accumulation of granular size classes in the expanded bed during the feeding phase were compared to their mass fractions in the return sludge (5.2.6). This comparison served as a metric for the likelihood of these particles being retained in the anaerobic upflow selector (see figure 5.5). The average

concentrations of sludge particles from a size class in the expanded bed were compared to the hypothetical maximum accumulated mass. While for the size class  $<400\ \mu\text{m}$  only  $<10\%$  had been retained at the end of the feeding phase, the retention probability increased with increasing particle size up to  $90\%$  for granules  $>2\ \text{mm}$ . Most of the biomass ( $85\%$ ) fell in the size class  $>1\ \text{mm}$  and the total MLSS concentration was  $40\ \text{g}_{\text{TSS}}\ \text{L}^{-1}$  (figure 5.5), and the average expanded bed height at the end of the feeding phase was  $105 \pm 13\ \text{cm}$ , both as intended.

The upflow selectors imposed a non-uniform distribution of the anaerobic retention time due to wash-out of smaller size classes through the overflow (figure 5.5). While all sludge in a completely mixed anaerobic stage has the same residence time, a below average anaerobic retention time was imposed on the flocculent sludge ( $<200\ \mu\text{m}$ ) and the smallest granule size class ( $200\text{--}400\ \mu\text{m}$ ). Granules in the size classes  $>1000\ \mu\text{m}$  experienced an above average residence time. A reversed trend was observed for the residence time in the aerobic/anoxic stages.

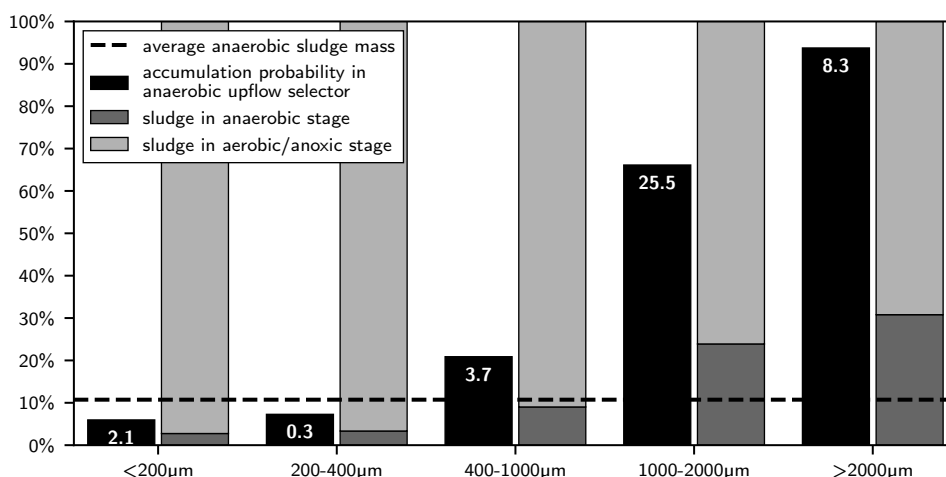


Figure 5.5: The selective anaerobic retention probability of sludge is depicted, as a function of granule size class in an anaerobic upflow selector. The numbers (white) above the bars denote the average MLSS concentration ( $\text{g}_{\text{TSS}}\ \text{L}^{-1}$ ) of a size class in the expanded bed. The residence time distribution of sludge over either the anaerobic upflow selectors or the combined aerobic/anoxic volume is shown as function of the size class. The theoretical average anaerobic residence time (dashed line) was calculated based on the working volume of the anaerobic stage relative to the aerobic/anoxic stage.

### Selective discharge of excess sludge

The effect of selective wasting was assessed by comparing the mass fractions of different size classes in the discharged sludge with those in the MLSS (see figure 5.6a). While the sludge  $<400\ \mu\text{m}$  had a retention probability of  $55\%$ , all granular size classes  $>400\ \mu\text{m}$  were almost completely retained with probabilities  $>90\%$ .

The observed retention probabilities were used to calculate the overall SRT of each size class for comparison with the average overall SRT of  $18 \pm 4$  d. Sludge in size classes  $< 400 \mu\text{m}$  had a below average SRT shorter than 10 d, while the granular size classes  $> 1 \text{ mm}$  exhibited SRTs more than one order of magnitude larger than the average SRT. The same increasing trend was observed in the SRT distribution of size classes as in the selective wasting of excess sludge.

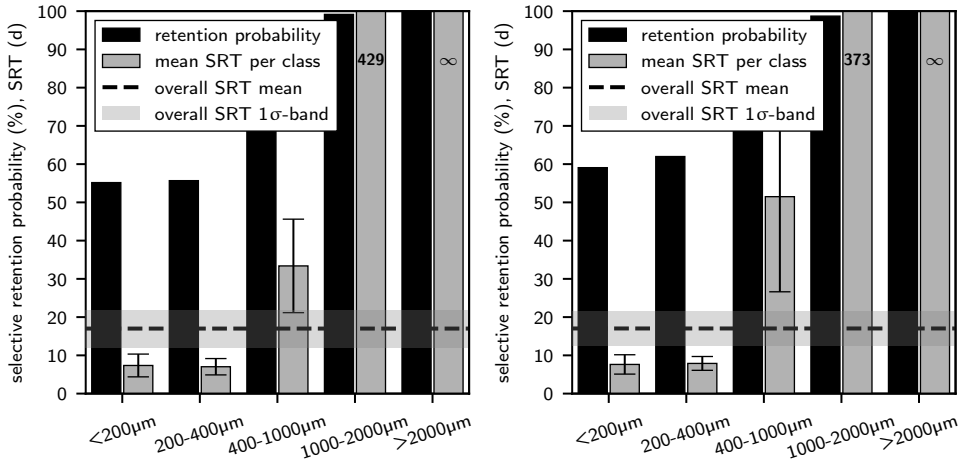


Figure 5.6: Selective retention probabilities of the different size classes of sludge particles (bars), SRT of individual size classes (bars) and the weighted average SRT for the MLSS as a whole (dashed line). All error bars and error bands represent a distance  $1\sigma$  from the respective means as an indication of the variability observed during the research period. (a, left) Two alternating anaerobic upflow selectors (period I). (b, right) Mixed anaerobic selector and anaerobic tank (period II).

### 5.3.3. Period II: mixed anaerobic selector and anaerobic tank

The configuration of the CFR was altered during period II to resemble the completely mixed anaerobic stage of the CFAS system of Harnaspolder WWTP (figure 5.1). The CFR was again seeded with sludge from the Utrecht WWTP to start the experiment with a similar granular sludge distribution as in period I (figure 5.3b). The seeding took place over the course of one month due to a more dilute shipment of AGS used for seeding, which complicated the transfer to the CFR. The reactor was operated with the upflow selectors as anaerobic stage to allow the sludge to adjust for approximately four average SRTs (day 76), after which the configuration of the anaerobic stage was transitioned to the mixed compartments. The average loading of the sludge in the anaerobic stage with  $\text{COD}_{<0.45 \mu\text{m}}$  was  $10 \text{ mgO}_2 \text{ g}_{\text{TSS}}^{-1}$ , similar to period I.

#### Sludge characteristics

Stable sludge properties were maintained after transitioning to the mixed anaerobic stage over the course of 108 days (figure 5.3b). The average MLSS concentration was

$6.0 \pm 0.8 \text{ g}_{\text{TSS}} \text{ l}^{-1}$  with a VSS/TSS ratio of 81 %, and the average granular mass fraction ( $>200 \mu\text{m}$ ) was 68 %. Compared to period I, the mass distribution had shifted down from the 1000-2000  $\mu\text{m}$  size class to the 400-1000  $\mu\text{m}$  size class. This decreased the average granule diameter slightly to 1.28 mm. The sludge settleability was stable throughout the whole operational period with an average  $\text{SVI}_{30}$  of  $53 \pm 7 \text{ mL g}_{\text{TSS}}^{-1}$  and a  $\text{SVI}_5/\text{SVI}_{30}$  ratio of  $1.76 \pm 0.1$ , which were both slightly higher than during period I. The  $\text{dSVI}_{30}$  of the AS from Harnaspolder WWTP remained on average  $100 \text{ ml g}_{\text{TSS}}^{-1}$ . The smoothness of the granular surfaces did not show major differences compared to period I.

### Anaerobic loading distribution

Complete removal of the  $\text{COD}_{\text{VFA}}$  was achieved in the combined anaerobic selector and subsequent anaerobic tank table 5.4, part of the total fraction of 59 % of  $\text{COD}_{<0.45 \mu\text{m}}$  that was removed. This was similar to the anaerobic upflow selector used in period I and within range of the fraction of  $\text{COD}_{<0.45 \mu\text{m}}$  from the influent that was anaerobically removable and considered the fraction of GFS (table 5.1). The COD removed in the anaerobic selector was mainly  $\text{COD}_{\text{VFA}}$  and was coupled to a higher P/COD-ratio than in the subsequent anaerobic tank, although the average P/COD-ratio for both anaerobic tanks was 0.34, similar to period I.

Table 5.4: Characteristics anaerobic conversions for the mixed anaerobic selector and the subsequent anaerobic tank (period II). All values were scaled to account for dilution of the influent by the return sludge flow (45 % to the anaerobic selector, 55 % to the subsequent anaerobic tank) to allow for mutual comparison.

Component (unit)	Influent	Anaerobic selector (removal)	Anaerobic tank (removal)
COD ( $\text{mg}_{\text{COD}} \text{ L}^{-1}$ )	497	- <sup>a</sup>	- <sup>a</sup>
$\text{COD}_{<0.45 \mu\text{m}}$ <sup>b</sup> ( $\text{mg}_{\text{COD}} \text{ L}^{-1}$ )	250	189 (24 %)	102 (59 %)
$\text{COD}_{\text{VFA}}$ <sup>c</sup> ( $\text{mg}_{\text{COD}} \text{ L}^{-1}$ )	112	51 (54 %)	<5 (>96 %)
$\text{NH}_4^+$ ( $\text{mg}_{\text{N}} \text{ L}^{-1}$ )	51	50.8	52.4
$\text{PO}_4^{3-}$ ( $\text{mg}_{\text{P}} \text{ L}^{-1}$ )	6.7	39.2	51.7

<sup>a</sup> Could not be determined since particulate COD was mixed with MLSS.

<sup>b</sup> Corrected for the inert fraction of  $\text{COD}_{<0.45 \mu\text{m}}$ , based on the amount in the effluent of the CFR (see table 5.1).

<sup>c</sup> Combined value for all VFAs detected (i.e. acetate and propionate).

The cumulative RTDs of the anaerobic selector and subsequent anaerobic tank in series were determined using the same method as used for the anaerobic upflow selectors. The residual concentration of GFS in the completely mixed anaerobic selector was lower than the influent concentration due to the mixing of influent and (part of) the return sludge. This lowered the maximum substrate penetration depth compared to the anaerobic upflow selectors (figure 5.4).

The RTD of the anaerobic selector was measured to compare the extent of selective feeding. All sludge was kept in suspension via the mechanical mixing, and therefore the RTD of all sludge size classes were the same. The residence time for the largest granules in the expanded bed in an upflow selector during period I was 1.5 h (i.e. equal to the duration



of the feeding phase) and continuously in contact with fresh influent. On the other hand, the average residence time of all the sludge in the anaerobic selector was 16 min. The mean residence time of the subsequent anaerobic tank was longer (i.e. 66 min). The total mean anaerobic residence time was thus similar to period I, but the residual concentration of  $\text{COD}_{\text{VFA}}$  was close to zero in this second anaerobic compartment (table 5.4). For equal contact time, the lower concentrations favor the uptake of substrate by biomass in smaller sludge particles with more specific area.

### Selective discharge of excess sludge

The selective discharge of excess sludge was operated the same as during period I. The selective retention probabilities (figure 5.6b) were nearly identical to those observed for all size classes in period I. The SRT distribution was almost identical as well, except for the increase in average SRT for the size class (400-1000  $\mu\text{m}$ ) from 33 d to 51 d due to the increase in MLSS of this fraction (figure 5.3b). The SRT of the size class of 1000-2000  $\mu\text{m}$  decreased from 429 d to 373 d. The differences in SRT distribution between periods I and II were relatively small compared to the shift in anaerobic distribution of GFS towards the flocculent sludge fraction (section 5.3.3).

5

## 5.3.4. Biological treatment performance

### Removal efficiencies and effluent quality

The nutrient removal performance of the CFR was analyzed for the last 30 days of period I for comparison with the full-scale CFAS system. The concentration of organic pollutants in the secondary effluent was  $<30 \text{ COD}_{<0.45\mu\text{m}}$  for both the full-scale CFAS system and the pilot-scale CFR. The removal efficiencies for phosphorus and nitrogen in the CFR were 97 % and 84 %, respectively. The overall volumetric removal rates were  $15 \text{ g}_\text{P} \text{ m}_{\text{reactor}}^{-3} \text{ d}^{-1}$  and  $98 \text{ g}_\text{N} \text{ m}_{\text{reactor}}^{-3} \text{ d}^{-1}$ , which yielded average effluent concentrations of  $0.3 \text{ mg}_{\text{PO}_4\text{-P}} \text{ L}^{-1}$  and  $9.9 \text{ mg}_{\text{TN}} \text{ L}^{-1}$ . The BNR stage of Harnaschpolder WWTP, treating the same pre-settled wastewater, achieved similar removal efficiencies (i.e. 92 % for phosphorus and 92 % for nitrogen). The CFAS system reached a better effluent quality with respect to the total nitrogen concentration (i.e.  $0.7 \text{ mg}_{\text{PO}_4\text{-P}} \text{ L}^{-1}$  and  $5.4 \text{ mg}_{\text{TN}} \text{ L}^{-1}$ ). The overall volumetric removal rates of the full-scale CFAS system were  $7 \text{ g}_\text{P} \text{ m}_{\text{reactor}}^{-3} \text{ d}^{-1}$  and  $48 \text{ g}_\text{N} \text{ m}_{\text{reactor}}^{-3} \text{ d}^{-1}$ . A more than twofold increase in both the volumetric phosphorus and nitrogen removal rates were achieved (at similar reactor temperatures of  $17.5 \pm 0.5^\circ\text{C}$ ) with the AGS in the CFR compared to the full-scale CFAS system.

### Biomass specific conversion rates per size class

To determine the specific conversion rates for both ammonium (SNUR, nitrification and growth) and phosphate (SPUR, EBPR and growth), aerobic batch tests were conducted on sieved sludge fractions at the end of both research periods (figure 5.7). The obtained rates were used to examine how the differences in the anaerobic stage between periods I and II impacted the distribution of microbial activity over the size classes, and how they compared to the AS of Harnaschpolder WWTP. Initial concentrations for ammonium

and phosphate were the same as in the CFR and the liquid phase was saturated with oxygen to minimize mass transfer limitations. The obtained specific conversion rates were interpreted as the maximum that could be obtained under reactor conditions.

The SNUR for period I showed a decreasing trend with an increasing average diameter of the sludge size class (figure 5.7a). On the other hand, the SNURs of sludge  $<400\ \mu\text{m}$  in the CFR were similar to that of the CFAS system. The rates showed a sharp decrease from the size class  $<1000\ \mu\text{m}$  to  $>1\ \text{mm}$ . The same experiment performed at the end of period II showed a similar, but more gradual decreasing trend for the SNUR with increasing particle size. Furthermore, the bandwidth between the highest rates (i.e. flocculent sludge fraction) and the lowest rates (i.e. largest granule size class) was smaller (figure 5.7b).

The SPUR for period I showed a different trend compared to the ammonium removal (figure 5.7a). For the size classes  $>400\ \mu\text{m}$  the maximum specific rates were comparable, but they were substantially larger than the rate of the flocculent sludge fraction from the CFR. The maximum SPUR of the AS was 1.8-fold larger than the maximum rate observed in the pilot-scale CFR, while for ammonium removal the difference was negligible. The distribution in the SPUR between size classes showed a parallel with the retention probability of each class in the anaerobic upflow selectors (see figure 5.5). The flocculent sludge fraction ( $<200\ \mu\text{m}$ ) had a retention probability lower than the average retention without selective feeding and showed the lowest SPUR. On the other hand, the transition to an above average retention probability in the upflow selector for granules  $>400\ \mu\text{m}$  coincided with the transition to a substantially larger SPUR compared to the flocculent fraction. The trend for the SPUR at the end of period II differed substantially from period I, showing an inverse trend with increasing particle size (figure 5.7b). The SPUR of the flocculent sludge in period II was 2.7-fold larger than those of the granular size classes (i.e.  $>400\ \mu\text{m}$ ).

### Contributions to volumetric removal rates

Based on the specific nutrient removal rates per size class, the contribution of each class to the overall nutrient removal was estimated (see figure 5.8). The contribution of the flocculent fraction ( $<200\ \mu\text{m}$ ) to volumetric removal rate of ammonium was similar for both research periods and amounted to at least 50 %. The remaining contributions from the granular sludge fractions showed similar trends for both periods as well. The contributions to the total volumetric phosphate removal rate did differ substantially between both periods. The granular sludge fractions  $>400\ \mu\text{m}$  contributed 78 % to the total volumetric rate during period I, while this was 30 % in period II. The changes in anaerobic process conditions therefore caused relatively small changes in the MLSS-distribution over size classes between (figure 5.3), but induced relatively large shifts in the distribution of EBPR activity over the size classes.

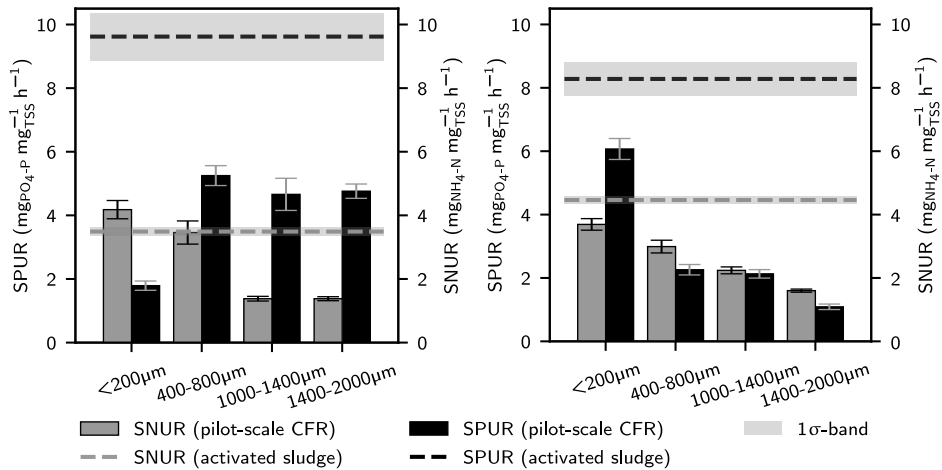


Figure 5.7: Maximum specific aerobic ammonium (SNUR) and phosphate uptake (SPUR) rates for different sludge size fractions from the pilot-scale CFR and the end of each operational period (bars) compared to the maximum specific rates determined for AS from Harnaschpolder WWTP (dashed lines). (a, left) Two alternating anaerobic upflow selectors (period I). (b, right) Mixed anaerobic selector and anaerobic tank (period II).

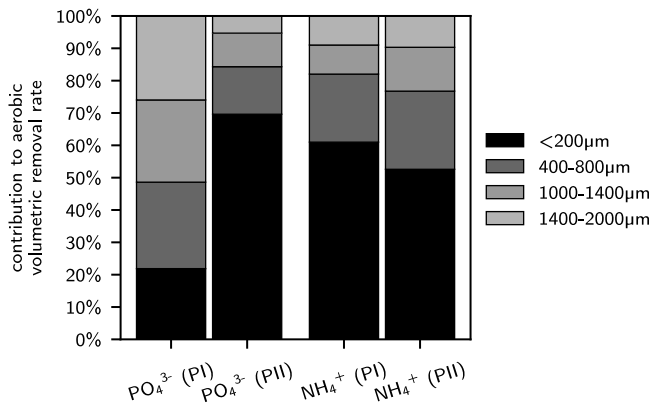


Figure 5.8: Calculated contributions of each sludge size fraction to the total volumetric removal rates for ammonium and phosphate. The estimated maximum volumetric conversion rates for ammonium and phosphate for all size classes combined amounted to  $-18.8 \text{ mg}_{\text{PO}_4\text{-P}} \text{ L}^{-1} \text{ h}^{-1}$  and  $-15.7 \text{ mg}_{\text{NH}_4\text{-N}} \text{ L}^{-1} \text{ h}^{-1}$  for period I with the anaerobic upflow selectors, respectively, and to  $-18.9 \text{ mg}_{\text{PO}_4\text{-P}} \text{ L}^{-1} \text{ h}^{-1}$  and  $-15.2 \text{ mg}_{\text{NH}_4\text{-N}} \text{ L}^{-1} \text{ h}^{-1}$  for period II with the mixed anaerobic selector, respectively.

## 5.4. Discussion

This study investigated the potential growth of AGS in a CFAS system. The selective pressures responsible for aerobic granulation in a SBR, as proposed by [156], were used to design a pilot-scale CFR. Metrics were defined for the extent to which mechanisms were implemented. The impact of the anaerobic distribution of GFS on granular growth were explicitly investigated. An anaerobic stage with bottom-feeding through an expanded sludge bed similar to a SBRs (period I) was compared to a configuration with a mixed anaerobic selector used in the CFAS system of the Harnaschpolder WWTP (period II).

### 5.4.1. From mechanisms for growth of AGS in a SBR to a CFR

The first hypothesis was that sufficient growth of AGS could be achieved in a CFR treating pre-settled municipal wastewater, if the mechanisms for granulation proposed by [156] were implemented to a similar extent as in a SBR. The biomass obtained using two alternating anaerobic upflow selectors showed similar properties to the seed sludge after 166 days of operation. The smoothness of the granular surfaces (figure 5.2) and the settleability were close to those reported for SBRs [122, 157]. The MLSS concentration of the flocculent fraction (i.e.  $2 \text{ g}_{\text{TSS}} \text{ L}^{-1}$ ) was also similar. The maximum total MLSS concentration (i.e.  $6.4 \text{ g}_{\text{TSS}} \text{ L}^{-1}$ ) was lower than has been achieved in full-scale AGS-SBRs, where the large granule fraction  $>2 \text{ mm}$  can yield total MLSS concentrations  $>10 \text{ g}_{\text{TSS}} \text{ L}^{-1}$  while maintaining the increased settleability compared to AS [169, 122]. Nevertheless, the selective enrichment of the granular sludge for EBPR activity using the anaerobic upflow selectors indicated that the AGS was obtained using the same selection principles as in full-scale AGS-SBRs.

#### Anaerobic distribution of granule forming substrate

Three aspects were studied determining the substrate distribution: microbial selection for anaerobic storage of GFS, maximizing transport of substrate into the granules and selective feeding. Complete conversion of the anaerobically storable fraction of  $\text{COD}_{<0.45 \mu\text{m}}$  was achieved (table 5.3) and the degree of plug-flow in the expanded bed during the feeding phase (figure 5.4) was similar to full-scale SBRs [158]. The extent of selective feeding of the largest granule size class was quantified by the retention probability in the expanded bed and the resulting average MLSS concentration in the bed of each size class (figure 5.5). There are no reports on this stratification in expanded beds of full-scale SBRs during feeding. However, the increasing retention probability for granules of increasing size was expected based on the ability of a Richardson-Zaki model to describe the settling of AGS [157], and the similar superficial velocity applied during feeding. The lower water depth of the upflow selector (2.5 m) did hamper the separation of flocs and granules due to limited volume above the granular bed, causing substantial parts of the granules  $>1000 \mu\text{m}$  and the  $400\text{-}1000 \mu\text{m}$  to exit through the overflow (figure 5.5). Therefore, the height of the granular part of the expanded bed at the end of the feeding phase (1.05 m) was lower than in a full-scale AGS-SBR (1.4 m, [157]) with similar average MLSS and feeding velocity as used in this study [157]. While the bed height was adequate for the complete removal

of GFS, the stratification did not fully mimic that of full-scale AGS-SBRs, resulting in less selective feeding of the largest granules. The water depth of the anaerobic upflow selector is thus a critical design parameter for steering the GFS towards the largest granules.

Although all three mechanisms were implemented like in SBRs, these data are not sufficient to quantify that the anaerobic distribution of GFS was similar. A numerical modelling approach could be used in future work to integrate the information of all mechanisms to estimate the distribution of GFS, including the specific GFS conversion rates for individual size classes. Subsequently, the distribution could be compared to the distribution of GFS determined experimentally. The levels of intracellular storage polymers (i.e. PHA and glycogen) would have to be determined for sludge from the expanded bed to construct a mass balance for GFS over the feeding phase [64]. The distribution of granular growth could then be estimated for different anaerobic stage configurations in CFRs or SBRs [74, 47, 129], and to further test the assumptions of the framework by [156].

## 5

### Ratio of GFS to non-GFS

For the classification of GFS and non-GFS in the primary effluent of Harnaschpolder WWTP, a mapping was made from the characterization of different COD fractions as either GFS or non-GFS (table 5.1). The fraction of  $\text{COD}_{<0.45\mu\text{m}}$  was first equated to the available GFS because it was reported to closely match the maximum able to diffuse into full-scale AGS [166]. Batch tests using AS from Harnaschpolder WWTP were used to determine which part of the  $\text{COD}_{<0.45\mu\text{m}}$  was anaerobically removed. Hydrolysis of particulate organic substrate and fermentation to soluble COD [78, 156] to GFS were neglected using this method, and therefore the fraction of GFS might have been underestimated. Full-scale SBRs with AGS typically use raw wastewater as influent [122, 153, 157], but implementation of AGS in CFAS systems will often rely on pre-settled wastewater [180]. The impact of pre-settling on both process types should be studied further. Development of the methodology to determine the fraction of GFS is therefore needed. This is emphasized by the finding that initial specific  $\text{BOD}_5$  loading rate of mixed anaerobic selectors did not correlate with the observed degree of granulation [180]. A standardized method has to be developed to determine the fraction of GFS in wastewater.

### Redistribution of growth through erosion and breakage

Erosion and break-up of granules in the CFR was larger than in the AGS-SBRs at Utrecht WWTP (The Netherlands), since granule size class  $>2\text{ mm}$  was diminished several days after the initial seeding (see figure 5.3a). Erosion and breakage of the largest granular size class were sufficient to balance the growth in the pilot-scale CFR, while this balance is commonly reached at a larger maximum granule size in the referenced full-scale SBRs. The rate of detachment has been shown to increase per surface area increases for granular biofilms with increasing size due to the higher probability for particle collisions and the higher momentum of larger sludge particles [61]. Our findings are also consistent with work by [37] showing that the rate of erosion for the same shear rate increases with

granule size. Implementing AGS in CFRs requires transportation of biomass between compartments, potentially yielding a larger energy input per volume than for SBRs. The typically lower water depth in aerated compartments of CFAS systems also requires a larger superficial gas velocity to achieve as similar volumetric oxygen transfer rates as in SBRs. Anoxic tanks in CFAS systems need mechanical mixing, contributing further to higher erosion rates of the granular sludge. The pilot-scale CFR required a specific energy input of  $20 \text{ W m}^{-3}$  for sludge suspension, which was higher than customary for full-scale CFAS systems ( $6 \text{ W m}^{-3}$ , [15]) and AGS-SBRs ( $3\text{-}12 \text{ W m}^{-3}$ , [158]). The rate of detachment therefore decreases during scale-up to full-scale and will likely yield a larger maximum granule size.

### **Selective wasting of surplus sludge**

Selective wasting was implemented in the CFR in a similar fashion as in SBRs [156] and yielded the expected increase in retention probability with increasing granule size (figure 5.6a). The probability for a sludge particle to be subjected to the selective wasting was different than in full-scale SBRs due to the intermittent discharge every 2.5 h. A sludge particle needed to be above the discharge manifold at the start of a discharge cycle like in full-scale AGS-SBRs, but also in a specific compartment. Still, a similar  $\text{SVI}_5/\text{SVI}_{30}$  ratio was obtained as has been reported for full-scale SBRs with the same MLSS concentration [122] and was stable over time. This indicated that selective wasting was imposed to a similar extent. Selective wasting was done via removal of the top of a sludge bed after a settling phase. Sludge particles were therefore not separated based on the difference in terminal settling velocity, but rather on the ability to settle sufficiently fast given the properties of the sludge matrix. Selective sludge wasting based on settleability thus ensures increased retainment of better settling individual sludge particles, while at the same time providing control over the settleability of the sludge as a whole [157]. This is different from other methods used to, for example, select for better settling dAS using hydrocyclones [10, 54, 131, 56]. These methods selectively waste and retain sludge based on properties affecting the settleability, but not the settleability itself.

## **5.4.2. Differences between selective pressures in SBRs and CFRs**

### **Distribution of the ratio of anaerobic to aerobic/anoxic time**

A similar degree of selective feeding was achieved with shallow anaerobic upflow selectors with a water depth of 2.5 m compared to full-scale AGS-SBRs of 7-7.5 m deep [122, 158]. This design did cause part of the sludge to be washed out of the upflow selectors during the sludge accumulation phase and subsequent feeding phase. All size classes had a chance to be washed out, but the probability decreased with increasing granule size (figure 5.5). Flocculent sludge had a relatively longer residence time in the anoxic and aerobic stages, while granules  $>1 \text{ mm}$  experienced the opposite. This might have contributed further to the enrichment of the flocs and small granules for more nitrification, while the EBPR activity was more present in the larger granules (figure 5.7a).

### Residence time distribution of mixed anoxic and aerobic stages

The CFR design focused on translating the mechanisms for aerobic granulation from a SBR. Implicitly, it was assumed that the series of mixed anoxic and aerobic compartments behaved similar to the mixed phases in an SBR separated in time. The mixed tanks connected in series and the recycle flow from the aerobic stage to the anoxic stage of the CFR, however, exhibited the hydraulic RTD of an axial dispersion reactor with a large variance around the mean residence time. In AGS-SBRs all sludge is subjected to the selective pressures in synchronicity. The efficiencies of diverting substrate to the largest granules and selective discharge of excess sludge must be higher in a CFR than in a SBR to achieve the same stable granular sludge formation. This possibly contributed to the lower granular growth that was achieved. Existing CFAS systems often employ larger recycles than used in the pilot-scale CFR [164], increasing the adverse effects.

#### 5.4.3. Distribution of microbial growth and activity

The most apparent outcome was the stability of the granule size distribution in the CFR in both research periods, with and without selective feeding. The anaerobic upflow selectors used in period I were able to direct the available GFS towards the granular sludge fraction, which was reflected by the enrichment of all size classes  $>400\ \mu\text{m}$  for a higher SPUR compared to the flocculent fraction (figure 5.7a). Therefore, the contribution of the granular size classes to the volumetric phosphate removal rate was 78 %. As for the completely mixed anaerobic selector, all sludge fractions get equal access to substrate and the distribution is determined by the specific area of a size class. The specific area increases as the size of a sludge particle decreases, and therefore flocculent sludge and small granules are favored over larger granular size classes. In an anaerobic upflow selector, the larger granules can preferentially use the substrate due to the increased retention in the expanded bed. The disadvantage in specific area turns into an advantage in particle volume. We hypothesized that reducing the size advantage for granules using a completely mixed anaerobic compartment (period II) would lead to a decrease in the granular sludge fraction and the average granule size [156]. Most notably, the change in anaerobic substrate distribution was manifested in the shift of the SPUR distribution from larger to smaller granules and flocs (figure 5.7b). The shift occurred within a several SRTs, indicating substantially less GFS was steered towards the granular size classes. Only a small decrease was observed in the mass distribution of the granules from the size class  $1000\text{-}2000\ \mu\text{m}$  to  $400\text{-}1000\ \mu\text{m}$  from period I to period II (figure 5.3). A lab-scale study using two anaerobic feeding methods yielded similar results [64] and it was hypothesized that the anaerobic distribution of GFS would be more critical when treating real sewage due to a lower rbCOD fraction in real wastewater [132, 78]. However in this study, the stability of the granular sludge morphology proved to be relatively large despite the limited growth. The selective retention of the granular sludge fraction was likely a strong contributor to maintaining the degree of granulation and exemplifies the compounding effect of multiple mechanisms [156]. Although the completely mixed anaerobic feeding was sufficient to maintain good morphology and settleability, it is the authors' opinion that differences in

EBPR activity indicated a higher stability of the AGS when anaerobic selective feeding via bottom-feeding was applied.

The distribution of the aerobic ammonium removal activity was also affected by the change in the anaerobic distribution of GFS, but to a smaller extent. The trend in the SNUR for period I decreased with increasing granule size, with a relatively large step from the size class 400-800  $\mu\text{m}$  to 1000-1400  $\mu\text{m}$  (figure 5.7a). The trend found in period II decreased more gradually with increasing granule size, and is congruent with the results from [105] using a SBR with a mixed pulse-fed anaerobic phase. This configuration resembles the completely mixed anaerobic stage used in period II. The results from the current study support their hypothesis that the anaerobic bottom-feeding in full-scale AGS-SBRs would alter the distribution of nutrient removal activity compared to completely mixed pulse-feeding. However, we do believe that the current study has shown that bottom-feeding can also be employed in a CFR and that the anaerobic stage configuration is not restricted solely to completely mixed compartments. The anaerobic stage provides a way to control the distribution of the nutrient removal through the anaerobic distribution of GFS. Numerical models aiming to describe nutrient removal using AGS could be improved to capture these dynamics [80, 147].

#### 5.4.4. Treatment capacity in a AGS-CFR versus a CFAS system

##### Biological treatment capacity

More than twofold higher volumetric removal rates were achieved for both phosphorus and nitrogen with the AGS in the pilot-scale CFR compared to the full-scale CFAS system of Harnaschpolder WWTP, treating the same pre-settled wastewater. This shows great potential for upgrading existing CFAS systems for higher loading rates and increased effluent quality. Multiple factors contributed to the larger biological treatment capacity. The degree of plug-flow of the anoxic and aerobic compartments of the pilot-scale CFR was substantially larger than the full-scale CFAS system due to the smaller recirculation factor of mixed liquor in the pilot-scale CFR (i.e. 2) compared to the full-scale CFAS system (i.e. 27, see supplementary materials). This means that for the CFAS system, there is a small concentration gradient in the mixed liquor from the beginning to the end of the combined aerobic and anoxic zones and concentrations are close to the final effluent concentrations. These concentrations are rate limiting and therefore volumetric removal rates are lower than in more compartmentalized reactors [68, 147]. For this reason the volumetric rates achieved in the full-scale reactor were lower than for the pilot-scale CFR, even though the SNURs and SPURs were larger for the AS compared to the AGS from the pilot-scale CFR (figure 5.7a). The higher MLSS concentration in the pilot-scale CFR further contributed to the larger volumetric treatment capacity. The full-scale CFAS system had a superior nitrogen removal due to limited optimization of the pilot-scale CFR for denitrification (section 5.3.4), but the primary focus of this study was on the growth of AGS in a CFR and not on nutrient removal.



### Hydraulic treatment capacity

The larger biological treatment capacity of the CFR with AGS was accompanied by a twofold increase in the sludge settleability compared to the CFAS system (i.e.  $50 \text{ mL g}_{\text{TSS}}^{-1}$  versus  $100 \text{ mL g}_{\text{TSS}}^{-1}$ , respectively). A typical sludge volume loading rate for circular secondary clarifiers is  $400 \text{ L m}^{-2} \text{ h}^{-1}$  [76]. In comparison, full-scale AGS-SBRs are operated at an equivalent sludge volume loading rate in excess of  $1000 \text{ L m}^{-2} \text{ h}^{-1}$  during simultaneous feeding and effluent discharge [122]. Secondary clarifiers can therefore likely be operated at higher surface loading rates when using AGS, although the behavior of a mixture of flocculent and granular sludge requires further investigation in combination with the more complex hydrodynamics. The results of this study indicate that further optimization of the CFR concept can deliver a retrofit technology to increase capacity of CFAS systems.

## 5.5. Conclusions

Selective pressures responsible for aerobic granulation in full-scale AGS-SBRs were implemented in a pilot-scale CFR, fed with pre-settled municipal wastewater. The research focused on the role of the anaerobic distribution of GFS. The pilot-scale CFR can be developed further for process intensification in existing CFAS systems using AGS. Key findings of the study include:

- The selective pressures for growth of AGS applied in full-scale SBRs can be successfully translated to a CFR, fed with pre-settled influent from a municipal WWTP.
- Microbial selection for anaerobic removal of substrate and similar degrees of both of plug-flow and selective feeding of granular sludge can be combined in two continuously fed, alternating anaerobic upflow selectors, like AGS-SBRs.
- A more than twofold increase in the volumetric biological removal capacities for both phosphorus and nitrogen can be achieved compared to the full-scale CFAS system.
- Switching to a completely mixed anaerobic selector shifted the EBPR activity from the granular sludge fractions to the flocculent sludge, while nitrification was mainly unaffected. This indicates a shift in anaerobic substrate distribution favoring the larger specific surface area of flocculent sludge, which is less favorable for the long-term stability of AGS, particularly with less acidified wastewater.

## Acknowledgements

The authors would like to express their gratitude to Rogier van Kempen for his aid in shaping the research plan, discussing outcomes and his dedication throughout the research. The hospitality of the staff at the Harnaschpolder WWTP were instrumental to the project. We would like to thank Roel van de Wijngaart for his effort during the start-up of the pilot-scale CFR. The contributions of Dion Boekelaar, Xiaoyan Lin, Daan van der Vorm and Wladimir Rios are also much appreciated.

# 6

## Outlook

This thesis set out to investigate the feasibility of an AGS process for the treatment of wastewater in CFRs. The aim was to investigate both the required process conditions for stable aerobic granulation in existing CFAS systems of WWTP (WWTPs). The findings highlight the intimate relation between the stability of the morphology of aerobic granular sludge, selection for anaerobic storage of rbCOD, and the way in which rbCOD is distributed in the anaerobic stage. The research described in this thesis has led to a proof-of-principle for growing AGS in a CFR with properties similar to the sludge from full-scale SBRs with AGS. Each chapter also generated outcomes that warrant further investigation to improve the understanding of how process conditions affect the formation and optimal use of AGS in general. Potential directions of research to address these and other topics will be discussed next.

## 6.1. Anaerobic distribution of substrate

The main outcome of this thesis is the increased understanding of the various functions of the anaerobic stage, not only in achieving a smooth granular morphology, but also in managing the granule size distribution. The anaerobic distribution of substrate over the sludge particles was shown to be directly controlled by the anaerobic feeding mode (**Chapter 3**), impacting the granulation rate during start-up (**Chapter 4**), and controls the distribution of EBPR activity (**Chapter 5**). For further improvement of AGS processes in general, and development of CFR concepts with AGS in particular, it would be beneficial to be able to accurately model the anaerobic distribution of substrate across a granule size distribution for a specific wastewater. This is particularly relevant for domestic wastewater in which only a minority of the COD can be anaerobically converted to storage polymers that can lead to granular growth [78]. This is essential to limit the flocculent sludge fraction and have the sludge consist majorly of granular sludge. Thus, modeling the anaerobic distribution of substrate is crucial for predicting the development of the granule size distribution, when combined with the other mechanisms governing the dynamics of the granule size distribution.

A constructive next step would involve integrating quantitative modeling of the anaerobic distribution of substrate (**Chapter 4**) with experimental measurement of the actual distribution (**Chapter 3**) in a reactor where the granule size distribution is in a dynamic equilibrium, and attempt to close the mass balance over the anaerobic stage. The subsequent sections list suggested improvements on the methodology used in this thesis.

### 6.1.1. Experimental measurement

Starting with the case of a (synthetic) wastewater with only anaerobically storable substrate (e.g. acetate), measurement of the storage polymer levels (i.e. PHA and glycogen) before and after the anaerobic stage should be performed, not only on sieved size classes (**Chapter 3**), but also on representative mixed sludge samples. The sum of the COD in the storage polymer pools of the size classes should be equal to the total amounts determined for the mixed samples. In addition, these measurements should be expanded

to measurement of the spatial distribution of storage polymers over the radius of granules within a size class. These could subsequently be compared to the modelled anaerobic penetration depth of substrate.

Ultimately, this approach should be used to determine the anaerobic distribution of substrate in AGS reactors treating real domestic wastewater. First, this requires a metric to characterize the total amount of substrate that can be potentially converted to granular biomass through anaerobic storage. Categorizing different COD fractions into either anaerobically storable substrate (GFS) and substrates that cannot be converted to storage polymers due to insufficient anaerobic time and aerobically lead to flocculent growth (non-GFS) [78] proved sufficient to capture the dynamics of granulation starting from flocculent sludge (**Chapter 4**). A preliminary attempt was made to develop an experimental metric for the amount of anaerobically storable COD in **Chapter 5**, based on the amount of  $\text{COD}_{<0.45\mu\text{m}}$  that could be anaerobically converted by a sludge sample enriched for anaerobic storage on the same wastewater. Although the molecular weight of all  $\text{COD}_{<0.45\mu\text{m}}$  is sufficiently small to diffuse into AGS [166], only 40-60 % of the  $\text{COD}_{<0.45\mu\text{m}}$  (already excluding inert  $\text{COD}_{<0.45\mu\text{m}}$ ) was found to be anaerobically removed using this method for pre-settled wastewater from Harnaschpolder WWTP. It also does not include products from hydrolysis that could occur in expanded granular bed [152, 175, 78], and the contribution to sludge growth of either flocs or granules must be further investigated [153]. Measuring the increase in storage polymer levels with a surplus of sludge enriched for anaerobic storage should therefore be the preferred method.

### 6.1.2. Mathematical modeling

Experiments can be performed to improve the model employed in **Chapter 4** to better incorporate (1) the spatial macro-gradients over the height of an expanded bed during bottom-feeding and (2) the heterogeneity within and between granules, depending on size. As for the macro-gradients over the reactor depth, this entails:

- investigation of the degree of anisotropic axial dispersion over the height of full-scale reactors, since most of the uptake of substrate was modeled to occur within one meter from the influent distributor and thus has a large impact on the calculated distribution of substrate,
- experimental validation of the stratification of the granule size distribution in the expanded bed during bottom-feeding as predicted by the model of [157], and
- further study of the hindered settling of a mixture of flocculent sludge and granular sludge during settling and expansion through bottom-feeding.

As for the mass balance over the granules, the current model assumes homogeneous physical properties for all granules (i.e. surface area to volume ratio, biomass concentration and porosity) as well as a homogeneous distribution of the average specific substrate uptake rate and storage capacity over the granule radius that had been

experimentally determined. Considering the decreasing fraction of volume penetrated with oxygen for granules of increasing size, the activity is likely located more in the outer shells of granules. The spatial distribution of activity further depends on the historical loading of the sludge in the reactor under study. Analysis of this spatial heterogeneity should therefore be part of the characterization of the sludge prior to measurement of the anaerobic distribution of substrate.

Furthermore, a spherical geometry was assumed for the relation between the surface area of a granule for mass transfer, and the volume through which substrate diffuses and where microbial activity is located. Due to the irregular shape of granules, this increasingly underestimates the surface area for mass transfer for smaller granules. More importantly, flocs are treated as spherical sludge particles, which likely yielded an even larger underestimation given the more open structure compared to granules. Future research should investigate how to treat these different growth morphologies within a model with respect to mass transfer.

## 6.2. Biomass redistribution within the sludge

The set of mechanisms presented in **Chapter 4** as the most important factors affecting aerobic granulation could describe the transition of the lag phase with a flocculent sludge with a relatively uniform sludge particle size distribution to a mostly granular sludge population. The importance of selective wasting and the mechanisms determining the anaerobic distribution of GFS (i.e. microbial selection, penetration depth of substrate and selective feeding of larger granules) are most strongly supported by work presented in this thesis (**Chapters 3 and 5**). Future work should aim to further develop the framework to be able to describe the dynamic equilibrium of a granule size distribution after prolonged operation, given a certain wastewater composition. This would enable a coupling to the modeling of nutrient removal for further optimization of process control and granule size distribution.

When viewed in the context of the general size distribution model by [13] (figure 6.1), an improved understanding of the processes that affect the internal redistribution of biomass growth between granular size classes (growth,  $gr$ , and fragmentation,  $fr$ ) is required to balance selective feeding ( $co$ ) and SRT distribution applied by the (selective) wasting strategy ( $wo$ ). Fragmentation processes on the one hand limits the maximum granule size combined with the average SRT that is applied through mixed discharge of excess sludge, but the way in which biomass is redistributed to smaller size classes also impacts how substrate is distributed in the anaerobic stage. Although the rate of erosion for a constant hydrodynamic shear rate was shown to increase with increasing granule size [37], the contributions of erosion, sloughing and/or breakage of granules at conditions representative for full-scale AGS-SBRs (or CFAS systems) are not well known. Erosion can for example be described by a surface detachment rate, but sloughing and breakage are governed by a probability distribution for biofilm systems in which

stochastic properties can be captured using cluster-based models (**Chapter 4**) instead of population-based models. Attempts to find generalized relations between process conditions, particle size and the rate of detachment processes have been hampered by the multitude of interactions [59]. Future work should therefore focus on measurement of the rate of internal biomass distribution within an AGS reactor, for example by following the distribution of intermittently fed labeled substrates or the incorporation of fluorescent particles in the granules [151]. This is also of direct relevance to better modeling the distribution of polyphosphate over granule size classes and the stability of EBPR [103]. Furthermore, it would allow experimental investigation of the observation from **Chapter 4** that smaller numbers of granules made the transition to larger size classes as granulation progressed, very similar to the work from [13].

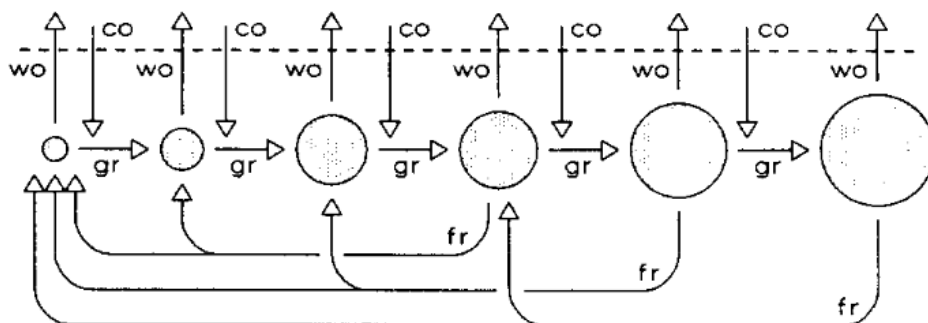


Figure 6.1: Schematic representation of processes governing the distribution of aggregates: consumption of GFS (co), growth on storage polymers (gr), wash-out due to (selective) wasting (wo), fragmentation due to erosion, sloughing and/or breakage (fr). The system boundary is denoted by the dashed line. Adapted from [13].

### 6.3. Stability of the granular matrix

The variety in granule size distributions for the same process conditions as a function of the initially seeded sludge has also been observed in the other direction: a similar granule size distribution, despite a different anaerobic distribution of substrate (**Chapters 3 and 5**). The common denominator here is that the mechanisms, aside from those influencing the anaerobic distribution of substrate (i.e. selective feeding and the degree of plug-flow, see **Chapter 4**), remained constant. These include the COD fractionation of the influent, the selective pressure on settleability in the discharge of excess sludge, and the rate of biomass detachment through hydrodynamic shear or particle collisions. It seems that the similar granule size distributions and morphological properties are reflected by similar distributions in SRT for differently sized granules. This suggests that, once established, the physical traits of the biopolymer matrix depend to a limited extent on the amount of biomass growth within that matrix. Granules can thus remain in the system if selectively retained based on their settleability. This contrasts with models that assume a rapid decline in granular stability due to insufficient penetration depth of substrate, once a certain

critical size is surpassed [171].

First, this stability warrants future experiments to investigate whether smooth granules can be grown while selecting for anaerobic storage of rbCOD under transport-limited substrate uptake rates and negligible penetration depth. If so, the stability of the biopolymers could be part of the ecology of microorganisms performing of anaerobic storage of a substrate without the need for an external electron acceptor, and less the result of a lower aerobic growth rate on the storage polymers [159]. Maintaining a sufficiently high surface loading rate by selecting for a minimum number of granules through selective wasting would then be sufficient to grow AGS, although only for the case of wastewater containing mostly anaerobically storable COD.

Second, shifting the anaerobic substrate distribution from favoring larger granules to smaller granules and flocs did cause a shift in the distribution of aerobic EBPR activity over the granule size classes in the same direction **Chapter 5**. Combined with the observed stability of the granule size distribution, an existing granular matrix could be used as a scaffold that can be recolonized by microorganisms. Future studies should investigate whether this concept can be employed to steer and optimize BNR using AGS.

## 6

### 6.4. Development of continuous-flow AGS processes

Now that a working reactor set-up using real wastewater has been achieved, it does provide a valuable tool for further process development and has narrowed the gap towards a successful application at full-scale. Further research is underway with the aim to simplify the anaerobic stage with two alternating upflow selectors to a fully continuous configuration combined with selective wasting, which would ease the retrofit of existing anaerobic selectors. Plans are being made for a follow-up project to demonstrate the aerobic granulation in the CFAS system of a full-scale WWTP. Further investigation is required to develop a useful retrofit technology for intensification of both the biological and hydraulic treatment capacities of continuous-flow processes. The following subjects are of main interest.

- The effect of the difference in settleability between the flocculent sludge fraction and the granular sludge fraction on the performance of secondary clarifiers. The flocculent sludge fraction within a mixture of flocculent and granular sludge ensures the entrapment poor-settling fines during clarification [158], which is the same as for CAS. The large difference in settling speed between flocs and granules [157] might hamper this entrapment, requiring modifications to the designs of existing sedimentation tanks designed for CAS. Furthermore, generally lower sludge blanket levels are to be expected due the increased settleability of the flocculent sludge fraction, based on studies that obtained better settling dAS using hydrocyclones [56, 131]. Proper down-scaling of large secondary clarifiers is troublesome [7], therefore investigations at full-scale are recommended;

- The suspension of AGS in anoxic and aerobic zones, and the (re)circulation of the mixed liquor between stages. The energy input through mechanical mixers or propellers of CFAS systems is sized to ensure suspension of flocculent sludge. In case process configurations with a circulating loop between anoxic and aerobic zones, the rate of circulation is an integral part of the design to obtain both the desired nutrient removal performance and maintain suspension of flocculent sludge. The settleability of AGS requires a larger energy input for suspension, exemplified by the difficulty to take a representative mixed liquor sample after seeding a CFAS system with a lignocellulosic carrier with a density similar to AGS [165, 179]. The amount of additional energy input as a function of the granule size distribution should be further investigated and acknowledged when discussing the potential benefits of a retrofit;
- The configuration of anaerobic, anoxic and aerobic redox zones and the aeration strategy to optimize the additional biomass from AGS for nutrient removal, in combination with the granule size distribution. The benefits of the additional biomass from AGS for biological treatment capacity rely on the ability (1) to increase the overall nitrification capacity using this additional granular biomass and (2) to make use of available biofilm thickness to maximize SND.
  1. The relatively high concentration of nutrients in the mixed liquor and the start of the aeration phase in AGS-SBRs allow for high volumetric conversion rates due to deeper penetration of these nutrients into granules, compared to the more diluted concentrations close to the effluent concentrations in CFAS systems with large nitrate recycles [147]. The longer SRT of larger granule size classes (>1 mm) has been linked to the higher relative abundance of ammonium oxidizing bacteria (AOB) and nitrite oxidizing bacteria (NOB) compared to small granules (<1 mm) and the flocculent sludge fraction (<0.2 mm) in AGS-SBRs using 16S rRNA gene sequencing [2, 78]. In contrast, work by [127, 105] showed that the specific ammonium removal rates were directly proportional to the area to volume ratio of a granule size class, as well as amoA gene copy numbers. They attributed this to the mixed anaerobic feeding that was applied, instead of bottom-feeding used in full-scale AGS-SBRs. However, the same decreasing relation between the specific ammonium conversion rates for increasing granule size was found to be independent from the use of either bottom-feeding or pulse-feeding in **Chapter 5**. However, it is probable that the aerobic penetration of nutrients and oxygen, respectively resulting from the concentration profile and the aeration strategy, determine the contribution of a size class to the overall volumetric ammonium removal rate, since these are directly related to the specific surface area of a granule. In that case, the relative abundance of nitrifying bacteria in a granule size class based on 16s rRNA gene sequencing is not a good predictor for the contribution to nitrification. Data on specific ammonium oxidation rates as a function of granule size from full-scale AGS-SBRs using bottom-feeding are not available for comparison, and should be determined in future work to test this hypothesis. Increasing the degree of plug-flow of the aeration



stage of CFAS systems will at least be a prerequisite for further optimization of the contribution of the larger granule size classes to the volumetric ammonium removal rate.

2. Adjusting the mixing pattern of anoxic and aerobic stages of CFAS systems also aids in maximizing the use of SND. A carefully controlled DO profile applied through alternating aeration has been shown to be crucial for using the limited amount of anaerobically stored COD from real domestic wastewater to denitrification instead of aerobic oxidation in SBRs [80, 170]. This is difficult to achieve in CFAS configurations with high internal recirculation factors and limited macro-concentration gradients in the mixed liquor, and thus a higher degree of plug-flow should be realized to better mimic the reaction phase of AGS-SBRs.

All in all, future work should focus on combining the granule size distribution and the distribution of microbial conversions in mathematical modeling tools to aid the design of an optimal mixing pattern and aeration strategy for AGS in CFRs.

## 6.5. Application niche of AGS in CFRs

A MLSS concentration, granule size distribution and sludge morphology similar to AGS from full-scale Nereda<sup>®</sup>-SBRs were obtained while treating pre-settled domestic wastewater in the pilot-scale CFR (Chapter 5). Therefore, a continuous-flow process using both selective wasting and selective feeding (like in full-scale SBRs [156]) is suited to achieve a substantial increase in both the biological and hydraulic treatment capacities of existing CFAS systems. dAS would be a more economical option to ensure year-round stable settling properties in case of periodic episodes of filamentous bulking that would otherwise require the dosage of chemicals, or when the settleability of the AS is in general limiting during peak hydraulic loading rates. Future work should investigate whether increased MLSS concentrations of dAS can be achieved while maintaining the same degree of granulation and limited compression settling compared to AGS, which would also enable a substantial increase of biological treatment capacity.

Making full use of the benefits of AGS, with size distributions similar to those achieved in full-scale SBRs [157], in a CFAS system will require substantial changes to the existing configuration. These are likely only economical if the lifespan of the existing infrastructure is increased with several decades. Most of the changes are needed to make the hydrodynamic characteristics of the existing CFAS system more like those of an SBR, but in space instead of time. It is justified to emphasize the potential of AGS for CFAS systems while the investigations are still focused on how to obtain AGS (or dAS) morphology in CFRs. However, the requirements to actually achieve increased biological [147] and hydraulic treatment capacity should receive more attention in the near future, since utilities require a full picture of benefits and requirements of the technology to be compared to other concepts for process intensification of existing CFAS systems.

## 6.6. Thoughts on research at pilot-scale

The extended duration of the project pays testimony of the practical and theoretical hurdles that were encountered while developing a CFR at pilot-scale. Using real pre-settled wastewater as the influent quickly showed the difficulty of growing AGS compared to using synthetic wastewater with only rbCOD often used at lab-scale, and further focused the research on the various roles of the anaerobic stage in an AGS process (**Chapters 2 to 4**). On the other hand, the technical difficulties encountered while working at pilot-scale (e.g. downtime due to broken equipment, lead time of physical modifications to the setup, variable wastewater strength due to rain weather events, etc.) did hamper the progress as well and can be a distraction from the research being conducted. Although the use of the pre-settled wastewater was the main reason to work at the DBI pilot facility, the availability of a larger water depth turned out to be a key prerequisite (superficial upflow velocity scales with increasing reactor size, but the settling properties of granules do not), and could not have been applied with the same ease at lab-scale. On the other hand, research questions resulting from the complexity of the COD fractionation in real wastewater can be investigated in lab-scale reactors as well. The approach taken in the HARKOS project paid dividends, but it is good to recognize in an early stage whether the problem lies in the transition from lab-scale to full-scale, in the transition from synthetic wastewater to real wastewater, or both.



# References

- [1] B. Acevedo, A. Oehmen, G. Carvalho, A. Seco, L. Borrás, and R. Barat. Metabolic shift of polyphosphate-accumulating organisms with different levels of polyphosphate storage. *Water Research*, 46(6):1889–1900, April 15, 2012. ISSN: 0043-1354. DOI: 10.1016/j.watres.2012.01.003.
- [2] M. Ali, Z. Wang, K. W. Salam, A. R. Hari, M. Pronk, M. C. M. van Loosdrecht, and P. E. Saikaly. Importance of species sorting and immigration on the bacterial assembly of different-sized aggregates in a full-scale aerobic granular sludge plant. *Environmental Science & Technology*, 53(14):8291–8301, July 16, 2019. ISSN: 0013-936X. DOI: 10.1021/acs.est.8b07303.
- [3] R. Amann, B. Binder, R. Olson, S. Chisholm, R. Devereux, and D. Stahl. Combination of 16s rRNA-targeted oligonucleotide probes with flow cytometry for analyzing mixed microbial populations. *Applied and Environmental Microbiology*, 56(6):1919–1925, 1990. ISSN: 00992240. DOI: 10.1128/aem.56.6.1919-1925.1990.
- [4] M. Andalib, J. Zhu, and G. Nakhla. A new definition of bed expansion index and voidage for fluidized biofilm-coated particles. *Chem. Eng. J.*, 189-190:244–249, May 2012. ISSN: 1385-8947. DOI: 10.1016/J.CEJ.2012.02.065.
- [5] APHA. *Standard methods for the examination of water and wastewater*. American Public Health Association (APHA), Washington DC, USA, 2005.
- [6] E. Arden and W. T. Lockett. Experiments on the oxidation of sewage without the aid of filters. *Journal of the Society of Chemical Industry*, 33(10):523–539, 1914. ISSN: 1934-9971. DOI: 10.1002/jctb.5000331005.
- [7] M. Armbruster. *Modelling of Circular Secondary Sedimentation Tanks - Physical SST Model*. STOWA, Stichting Toegepast Onderzoek Waterbeheer ; Hageman Fulfilment [distr., Utrecht; Zwijndrecht, 2002. ISBN: 978-90-5773-176-1.
- [8] B. Arrojo, A. Mosquera-Corral, J. M. Garrido, and R. Méndez. Aerobic granulation with industrial wastewater in sequencing batch reactors. *Water Research*, 38(14):3389–3399, August 2004. ISSN: 0043-1354. DOI: 10.1016/j.watres.2004.05.002.
- [9] E. Arvin and P. Harremoës. Concepts and models for biofilm reactor performance. *Water Science and Technology*, 22(1):171–192, January 1, 1990. ISSN: 0273-1223. DOI: 10.2166/wst.1990.0145.
- [10] I. Avila, D. Freedman, J. Johnston, B. Wisdom, and J. McQuarrie. Inducing granulation within a full-scale activated sludge system to improve settling. *Water Science and Technology*, 84(2):302–313, January 2, 2021. ISSN: 0273-1223. DOI: 10.2166/wst.2021.006.
- [11] J. E. Baeten, D. J. Batstone, O. J. Schraa, M. C. M. van Loosdrecht, and E. I. P. Volcke. Modelling anaerobic, aerobic and partial nitrification-anammox granular sludge reactors - a review. *Water Research*, 149:322–341, February 1, 2019. ISSN: 0043-1354. DOI: 10.1016/j.watres.2018.11.026.
- [12] J. P. Bassin, M. Pronk, G. Muyzer, R. Kleerebezem, M. Dezotti, and M. C. M. van Loosdrecht. Effect of elevated salt concentrations on the aerobic granular sludge process: linking microbial activity with microbial community structure. *Applied and Environmental Microbiology*, 77(22):7942–7953, 2011. DOI: 10.1128/AEM.05016-11.
- [13] H. H. Beefink and J. C. van den Heuvel. Bacterial aggregates of various and varying size and density: a structured model for biomass retention. *The Chemical Engineering Journal*, 44(1):B1–B13, June 1, 1990. ISSN: 0300-9467. DOI: 10.1016/0300-9467(90)80055-H.
- [14] S. Bengtsson, M. d. Blois, B.-M. Wilén, and D. Gustavsson. Treatment of municipal wastewater with aerobic granular sludge. *Critical Reviews in Environmental Science and Technology*, 48(2):119–166, January 17, 2018. ISSN: 1064-3389. DOI: 10.1080/10643389.2018.1439653.

- [15] S. Bengtsson, M. de Blois, B.-M. Wilén, and D. Gustavsson. A comparison of aerobic granular sludge with conventional and compact biological treatment technologies. *Environmental Technology*, 40(21):2769–2778, September 19, 2019. ISSN: 0959-3330. DOI: 10.1080/09593330.2018.1452985.
- [16] J. J. Beun, A. Hendriks, M. C. M. van Loosdrecht, E. Morgenroth, P. A. Wilderer, and J. J. Heijnen. Aerobic granulation in a sequencing batch reactor. *Water Research*, 33(10):2283–2290, July 1, 1999. ISSN: 0043-1354. DOI: 10.1016/S0043-1354(98)00463-1.
- [17] J. J. Beun, J. J. Heijnen, and M. C. M. van Loosdrecht. N-removal in a granular sludge sequencing batch airlift reactor. *Biotechnology and Bioengineering*, 75(1):82–92, 2001. ISSN: 1097-0290. DOI: 10.1002/bit.1167.
- [18] J. J. Beun, M. C. M. van Loosdrecht, and J. J. Heijnen. Aerobic granulation. *Water Science and Technology*, 41(4):41–48, February 1, 2000. ISSN: 0273-1223. DOI: 10.2166/wst.2000.0423.
- [19] J. J. Beun, M. C. M. van Loosdrecht, and J. J. Heijnen. Aerobic granulation in a sequencing batch airlift reactor. *Water Research*, 36(3):702–712, February 1, 2002. ISSN: 0043-1354. DOI: 10.1016/S0043-1354(01)00250-0.
- [20] J. P. Boltz and G. T. Daigger. A mobile-organic biofilm process for wastewater treatment. *Water Environment Research*, 94(9):e10792, 2022. ISSN: 1554-7531. DOI: 10.1002/wer.10792.
- [21] D. Brdjanovic, A. Slamet, M. C. M. van Loosdrecht, C. M. Hooijmans, G. J. Alaerts, and J. J. Heijnen. Impact of excessive aeration on biological phosphorus removal from wastewater. *Water Research*, 32(1):200–208, January 1, 1998. ISSN: 0043-1354. DOI: 10.1016/S0043-1354(97)00183-8.
- [22] D. Brdjanovic, P. Halkjaer Nielsen, C. M. Lopez-Vazquez, and M. C. M. van Loosdrecht, editors. *Experimental Methods in Wastewater Treatment*. IWA Publishing, 2016. ISBN: 978-1-78040-475-2 978-1-78040-474-5. DOI: 10.2166/9781780404752.
- [23] J. Chudoba. Control of activated sludge filamentous bulking-VI. formulation of basic principles. *Water Research*, 19(8):1017–1022, 1985. ISSN: 00431354. DOI: 10.1016/0043-1354(85)90370-7.
- [24] J. Chudoba, J. Čech, J. Farkač, and P. Grau. Control of activated sludge filamentous bulking. experimental verification of a kinetic selection theory. *Water Research*, 19(2):191–196, 1985. DOI: 10.1016/0043-1354(85)90198-8.
- [25] J. Chudoba, P. Grau, and V. Ottová. Control of activated-sludge filamentous bulking—II. selection of microorganisms by means of a selector. *Water Research*, 7(10):1389–1406, October 1, 1973. ISSN: 0043-1354. DOI: 10.1016/0043-1354(73)90113-9.
- [26] C. Cofré, J. L. Campos, D. Valenzuela-Heredia, J. P. Pavissich, N. Camus, M. Belmonte, A. Pedrouso, P. Carrera, A. Mosquera-Corral, and A. Val del Río. Novel system configuration with activated sludge like-geometry to develop aerobic granular biomass under continuous flow. *Bioresource Technology*, July 31, 2018. ISSN: 0960-8524. DOI: 10.1016/j.biortech.2018.07.146.
- [27] S. F. Corsino, A. di Biase, T. R. Devlin, G. Munz, M. Torregrossa, and J. A. Oleszkiewicz. Effect of extended famine conditions on aerobic granular sludge stability in the treatment of brewery wastewater. *Bioresource Technology*, 226:150–157, February 1, 2017. ISSN: 0960-8524. DOI: 10.1016/j.biortech.2016.12.026.
- [28] Council directive 91/271/EEC of 21 may 1991 concerning urban waste-water treatment, May 21, 1991.
- [29] K. Crabtree, W. Boyle, E. McCoy, and G. A. Rohlich. A mechanism of floc formation by zoogloea ramigera. *Journal of Water Pollution Control Federation*, 38(12):1968–1980, 1966. ISSN: 0043-1303. DOI: 10.2307/25035694.
- [30] G. Crocetti, P. Hugenholtz, P. Bond, A. Schuler, J. Keller, D. Jenkins, and L. Blackall. Identification of polyphosphate-accumulating organisms and design of 16s rRNA-directed probes for their detection and quantitation. *Applied and Environmental Microbiology*, 66(3):1175–1182, 2000. DOI: 10.1128/AEM.66.3.1175-1182.2000.
- [31] G. R. Crocetti, J. F. Banfield, J. Keller, P. L. Bond, and L. L. Blackall. Glycogen-accumulating organisms in laboratory-scale and full-scale wastewater treatment processes. *Microbiology*, 148(11):3353–3364, 2002. ISSN: 1350-0872, DOI: 10.1099/00221287-148-11-3353.

- [32] E. L. Cussler. *Diffusion: Mass Transfer in Fluid Systems*. Cambridge Series in Chemical Engineering. Cambridge University Press, Cambridge, 3rd edition, 2009. ISBN: 978-0-521-87121-1. DOI: 10.1017/CB09780511805134.
- [33] G. T. Daigger, J. Kuo, N. Derlon, D. Houweling, J. A. Jimenez, B. R. Johnson, J. P. McQuarrie, S. Murthy, P. Regmi, C. Roche, B. Sturm, B. Wett, M. Winkler, and J. P. Boltz. Biological and physical selectors for mobile biofilms, aerobic granules, and densified-biological flocs in continuously flowing wastewater treatment processes: a state-of-the-art review. *Water Research*, 242:120245, August 15, 2023. ISSN: 0043-1354. DOI: 10.1016/j.watres.2023.120245.
- [34] G. T. Daigger, E. Redmond, and L. Downing. Enhanced settling in activated sludge: design and operation considerations. *Water Science and Technology*, 78(2):247–258, August 13, 2018. ISSN: 0273-1223. DOI: 10.2166/wst.2018.287.
- [35] H. Daims, A. Brühl, R. Amann, K.-H. Schleifer, and M. Wagner. The domain-specific probe EUB338 is insufficient for the detection of all bacteria: development and evaluation of a more comprehensive probe set. *Systematic and Applied Microbiology*, 22(3):434–444, 1999. DOI: 10.1016/S0723-2020(99)80053-8.
- [36] B. de Bruin, M. de Kreuk, C. Uijterlinde, and C. Marcelis. Aeroob korrelslib klaar voor de praktijk. *H2O: tijdschrift voor watervoorziening en waterbeheer*, 39(3):31–34, 2006. ISSN: 0166-8439.
- [37] D. R. de Graaff, E. J. H. v. Dijk, M. C. M. van Loosdrecht, and M. Pronk. Strength characterization of full-scale aerobic granular sludge. *Environmental Technology*, 41(13):1637–1647, June 6, 2020. ISSN: 0959-3330. DOI: 10.1080/09593330.2018.1543357.
- [38] M. K. de Kreuk, M. Pronk, and M. C. M. van Loosdrecht. Formation of aerobic granules and conversion processes in an aerobic granular sludge reactor at moderate and low temperatures. *Water Res.*, 39(18):4476–4484, 2005. DOI: 10.1016/j.watres.2005.08.031.
- [39] M. K. De Kreuk, J. J. Heijnen, and M. C. M. van Loosdrecht. Simultaneous cod, nitrogen, and phosphate removal by aerobic granular sludge. *Biotechnology and Bioengineering*, 90(6):761–769, June 20, 2005. ISSN: 1097-0290. DOI: 10.1002/bit.20470.
- [40] M. K. De Kreuk, N. Kishida, S. Tsuneda, and M. C. M. van Loosdrecht. Behavior of polymeric substrates in an aerobic granular sludge system. *Water Research*, 44(20):5929–5938, December 2010. ISSN: 0043-1354. DOI: 10.1016/j.watres.2010.07.033.
- [41] M. K. De Kreuk, N. Kishida, and M. C. M. van Loosdrecht. Aerobic granular sludge – state of the art. *Water Science and Technology*, 55(8):75–81, April 1, 2007. ISSN: 0273-1223, 1996-9732. DOI: 10.2166/wst.2007.244.
- [42] M. K. De Kreuk, C. Picioreanu, M. Hosseini, J. B. Xavier, and M. C. M. van Loosdrecht. Kinetic model of a granular sludge SBR: influences on nutrient removal. *Biotechnology and Bioengineering*, 97(4):801–815, July 1, 2007. ISSN: 0006-3592. DOI: 10.1002/bit.21196.
- [43] M. K. De Kreuk and M. C. M. van Loosdrecht. Selection of slow growing organisms as a means for improving aerobic granular sludge stability. *Water Science and Technology*, 49(11):9–17, June 1, 2004. ISSN: 0273-1223, 1996-9732. DOI: 10.2166/wst.2004.0792.
- [44] S. Degaleesan and M. P. Dudukovic. Liquid backmixing in bubble columns and the axial dispersion coefficient. *AIChE J.*, 44(11):2369–2378, 1998. DOI: 10.1002/aic.690441105.
- [45] Delfluent Services, Evides Industrierwater and the Delfland Water Authority. Delft blue innovations research facility. Delft Blue Innovations research facility. November 28, 2022. URL: <https://www.delftblueinnovations.nl/> (visited on 07/06/2023).
- [46] N. Derlon, J. Wagner, R. H. R. da Costa, and E. Morgenroth. Formation of aerobic granules for the treatment of real and low-strength municipal wastewater using a sequencing batch reactor operated at constant volume. *Water Research*, 105:341–350, November 15, 2016. ISSN: 0043-1354. DOI: 10.1016/j.watres.2016.09.007.
- [47] T. R. Devlin and J. A. Oleszkiewicz. Cultivation of aerobic granular sludge in continuous flow under various selective pressure. *Bioresource Technology*, January 11, 2018. ISSN: 0960-8524. DOI: 10.1016/j.biortech.2018.01.056.

- [48] P. Dold, B. Alexander, G. Burger, M. Fairlamb, D. Conidi, C. Bye, and W. Du. Modeling full-scale granular sludge sequencing tank performance. *91st Annu. Water Environ. Fed. Tech. Exhib. Conf. WEFTEC 2018*:3813–3826, 2019. ISSN: 1938-6478. DOI: 10.2175/193864718825135937.
- [49] J. Drewnowski and J. Makinia. The role of colloidal and particulate organic compounds in denitrification and EBPR occurring in a full-scale activated sludge system. *Water Science and Technology*, 63(2):318–324, January 1, 2011. ISSN: 0273-1223, 1996-9732. DOI: 10.2166/wst.2011.056.
- [50] L.-T. Fan, Y.-C. Yang, and C.-Y. Wen. Mass transfer in semifluidized beds for solid-liquid system. *AIChE Journal*, 6(3):482–487, 1960. ISSN: 1547-5905. DOI: 10.1002/aic.690060327.
- [51] B. A. Figdore, H. David Stensel, and M.-K. H. Winkler. Bioaugmentation of sidestream nitrifying-denitrifying phosphorus-accumulating granules in a low-SRT activated sludge system at low temperature. *Water Research*, 135:241–250, May 15, 2018. ISSN: 0043-1354. DOI: 10.1016/j.watres.2018.02.035.
- [52] C. D. M. Filipe, G. T. Daigger, and C. P. L. Grady Jr. Stoichiometry and kinetics of acetate uptake under anaerobic conditions by an enriched culture of phosphorus-accumulating organisms at different pHs. *Biotechnology and Bioengineering*, 76(1):32–43, 2001. ISSN: 1097-0290. DOI: 10.1002/bit.1023.
- [53] C. D. M. Filipe, J. Meinhold, S.-B. Jørgensen, G. T. Daigger, and C. P. L. Grady. Evaluation of the potential effects of equalization on the performance of biological phosphorus removal systems. *Water Environment Research*, 73(3):276–285, May 1, 2001. ISSN: 1554-7531. DOI: 10.2175/106143001X139281.
- [54] A. Ford, B. Rutherford, B. Wett, and C. Bott. Implementing hydrocyclones in mainstream process for enhancing biological phosphorus removal and increasing settleability through aerobic granulation. *Proceedings of the Water Environment Federation*, 2016(9):2798–2811, 2016.
- [55] R. D. G. Franca, H. M. Pinheiro, M. C. M. van Loosdrecht, and N. D. Lourenço. Stability of aerobic granules during long-term bioreactor operation. *Biotechnology Advances*, 36(1):228–246, January 1, 2018. ISSN: 0734-9750. DOI: 10.1016/j.biotechadv.2017.11.005.
- [56] N. Gemza, K. Janiak, B. Zięba, J. Przyszlak, and M. Kuśnierz. Long-term effects of hydrocyclone operation on activated sludge morphology and full-scale secondary settling tank wet-weather operation in long sludge age WWTP. *Science of The Total Environment*, 845:157224, November 1, 2022. ISSN: 0048-9697. DOI: 10.1016/j.scitotenv.2022.157224.
- [57] A. Giesen, L. M. M. De Bruin, R. P. Niermans, and H. F. Van Der Roest. Advancements in the application of aerobic granular biomass technology for sustainable treatment of wastewater. *Water Practice and Technology*, 8(1):47–54, March 1, 2013. ISSN: 1751-231X. DOI: 10.2166/wpt.2013.007.
- [58] C. Gini. *Variabilita e mutabilita contributo allo studio delle distribuzioni e delle relazioni statistiche*. Tipogr. di P. Cuppini, Bologna, 1912.
- [59] A. Gjaltema. *Biofilm development: Growth versus detachment*. PhD thesis, Delft University of Technology, 1996.
- [60] A. Gjaltema, L. Tjihuis, M. C. M. van Loosdrecht, and J. J. Heijnen. Detachment of biomass from suspended nongrowing spherical biofilms in airlift reactors. *Biotechnology and Bioengineering*, 46(3):258–269, 1995. ISSN: 1097-0290. DOI: 10.1002/bit.260460309.
- [61] A. Gjaltema, J. L. Vinke, M. C. M. van Loosdrecht, and J. J. Heijnen. Abrasion of suspended biofilm pellets in airlift reactors: importance of shape, structure, and particle concentrations. *Biotechnology and Bioengineering*, 53(1):88–99, 1997. ISSN: 1097-0290. DOI: [https://doi.org/10.1002/\(SICI\)1097-0290\(19970105\)53:1<88::AID-BIT12>3.0.CO;2-5](https://doi.org/10.1002/(SICI)1097-0290(19970105)53:1<88::AID-BIT12>3.0.CO;2-5).
- [62] A. Guisasola, M. Pijuan, J. A. Baeza, J. Carrera, C. Casas, and J. Lafuente. Aerobic phosphorus release linked to acetate uptake in bio-p sludge: process modeling using oxygen uptake rate. *Biotechnology and Bioengineering*, 85(7):722–733, 2004. ISSN: 1097-0290. DOI: 10.1002/bit.10868.
- [63] V. A. Haaksman, M. Mirghorayshi, M. C. M. van Loosdrecht, and M. Pronk. Impact of aerobic availability of readily biodegradable COD on morphological stability of aerobic granular sludge. *Water Research*, 187:116402, December 15, 2020. ISSN: 0043-1354. DOI: 10.1016/j.watres.2020.116402.
- [64] V. A. Haaksman, M. Schouteren, M. C. M. van Loosdrecht, and M. Pronk. Impact of the anaerobic feeding mode on substrate distribution in aerobic granular sludge. *Water Research*, 233:119803, 2023. ISSN: 0043-1354. DOI: 10.1016/j.watres.2023.119803.

- [65] B. A. Heide and A. Pasveer. Oxidation ditch: prevention and control of filamentous sludge. *H2O*, 7(18):373–7, 1974.
- [66] J. J. Heijnen and M. C. M. van Loosdrecht. Method for acquiring grain-shaped growth of a microorganism in a reactor. Patent (WO9837027 (A1)). August 27, 1998.
- [67] L. J. Hem, B. Rusten, and H. Ødegaard. Nitrification in a moving bed biofilm reactor. *Water Research*, 28(6):1425–1433, June 1, 1994. ISSN: 0043-1354. DOI: 10.1016/0043-1354(94)90310-7.
- [68] M. Henze, editor. Activated sludge models ASM1, ASM2, ASM2d and ASM3. reprinted edition. (9) in Scientific and technical report / IWA. IWA Publ, London, reprinted edition, 2007. 121 pages. ISBN: 978-1-900222-24-2.
- [69] M. Henze. Characterization of wastewater for modelling of activated sludge processes. *Water Science and Technology*, 25(6):1–15, 1992. DOI: 10.2166/wst.1992.0110.
- [70] O. T. Iorhemen and Y. Liu. Effect of feeding strategy and organic loading rate on the formation and stability of aerobic granular sludge. *Journal of Water Process Engineering*:101709, October 8, 2020. ISSN: 2214-7144. DOI: 10.1016/j.jwpe.2020.101709.
- [71] D. Jenkins. *Activated Sludge – 100 Years and Counting*, volume 13. April 2014.
- [72] K. Johnson, Y. Jiang, R. Kleerebezem, G. Muyzer, and M. C. M. van Loosdrecht. Enrichment of a mixed bacterial culture with a high polyhydroxyalkanoate storage capacity. *Biomacromolecules*, 10(4):670–676, April 13, 2009. ISSN: 1525-7797. DOI: 10.1021/bm8013796.
- [73] P. Kehrein, M. van Loosdrecht, P. Osseweijer, and J. Posada. Exploring resource recovery potentials for the aerobic granular sludge process by mass and energy balances – energy, biopolymer and phosphorus recovery from municipal wastewater. *Environmental Science: Water Research & Technology*, 6(8):2164–2179, July 31, 2020. ISSN: 2053-1419. DOI: 10.1039/D0EW00310G.
- [74] T. R. Kent, C. B. Bott, and Z.-W. Wang. State of the art of aerobic granulation in continuous flow bioreactors. *Biotechnology Advances*, 36(4):1139–1166, July 1, 2018. ISSN: 0734-9750. DOI: 10.1016/j.biotechadv.2018.03.015.
- [75] D. Koester, S. Ranka, and G. Fox. Parallel block-diagonal-bordered sparse linear solvers for electrical power system applications. In *Proceedings of Scalable Parallel Libraries Conference*. Proceedings of Scalable Parallel Libraries Conference, pages 195–203, October 1993. DOI: 10.1109/SPLC.1993.365566.
- [76] J. Krijgsman. *Optimalisatie van ronde nabezinktanks: Ontwerprichtlijnen en toepassing van het nabezinktankmodel : ontwerpen tussen STORA-1981 en solids flux theorie*. STOWA;2002 23. STOWA, Stichting Toegepast Onderzoek Waterbeheer, Utrecht, 2002. ISBN: 90-5773-179-7.
- [77] T. Kuba, A. Wachtmeister, M. C. M. van Loosdrecht, and J. J. Heijnen. Effect of nitrate on phosphorus release in biological phosphorus removal systems. *Water Science and Technology*, 30(6):263–269, 1994. ISSN: 02731223. DOI: 10.2166/wst.1994.0277.
- [78] M. Layer, A. Adler, E. Reynaert, A. Hernandez, M. Pagni, E. Morgenroth, C. Holliger, and N. Derlon. Organic substrate diffusibility governs microbial community composition, nutrient removal performance and kinetics of granulation of aerobic granular sludge. *Water Research X*, 4:100033, August 1, 2019. ISSN: 2589-9147. DOI: 10.1016/j.wroa.2019.100033.
- [79] M. Layer, K. Bock, F. Ranzinger, H. Horn, E. Morgenroth, and N. Derlon. Particulate substrate retention in plug-flow and fully-mixed conditions during operation of aerobic granular sludge systems. *Water Res. X*, 9:100075, December 2020. ISSN: 2589-9147. DOI: 10.1016/J.WROA.2020.100075.
- [80] M. Layer, M. G. Villodres, A. Hernandez, E. Reynaert, E. Morgenroth, and N. Derlon. Limited simultaneous nitrification-denitrification (SND) in aerobic granular sludge systems treating municipal wastewater: mechanisms and practical implications. *Water Research X*, 7:100048, May 1, 2020. ISSN: 2589-9147. DOI: 10.1016/j.wroa.2020.100048.
- [81] G. Lettinga, R. Roersma, and P. Grin. Anaerobic treatment of raw domestic sewage at ambient temperatures using a granular bed UASB reactor. *Biotechnology and Bioengineering*, 25(7):1701–1723, 1983. ISSN: 1097-0290. DOI: 10.1002/bit.260250703.
- [82] A.-J. Li and X.-Y. Li. Selective sludge discharge as the determining factor in SBR aerobic granulation: numerical modelling and experimental verification. *Water Research*, 43(14):3387–3396, August 1, 2009. ISSN: 0043-1354. DOI: 10.1016/j.watres.2009.05.004.



- [83] X.-M. Liu, G.-P. Sheng, H.-W. Luo, F. Zhang, S.-J. Yuan, J. Xu, R. J. Zeng, J.-G. Wu, and H.-Q. Yu. Contribution of extracellular polymeric substances (EPS) to the sludge aggregation. *Environmental Science & Technology*, 44(11):4355–4360, June 1, 2010. ISSN: 0013-936X. DOI: 10.1021/es9016766.
- [84] Y. Liu, Z.-W. Wang, Y.-Q. Liu, L. Qin, and J.-H. Tay. A generalized model for settling velocity of aerobic granular sludge. *Biotechnology Progress*, 21(2):621–626, 2005. DOI: 10.1021/bp049674u.
- [85] Y. Liu and Q.-S. Liu. Causes and control of filamentous growth in aerobic granular sludge sequencing batch reactors. *Biotechnology Advances*, 24(1):115–127, January 2006. ISSN: 07349750. DOI: 10.1016/j.biotechadv.2005.08.001.
- [86] Y. Liu, Y.-Q. Liu, Z.-W. Wang, S.-F. Yang, and J.-H. Tay. Influence of substrate surface loading on the kinetic behaviour of aerobic granules. *Applied Microbiology and Biotechnology*, 67(4):484–488, June 1, 2005. ISSN: 1432-0614. DOI: 10.1007/s00253-004-1785-1.
- [87] Y. Liu and J.-H. Tay. The essential role of hydrodynamic shear force in the formation of biofilm and granular sludge. *Water Research*, 36(7):1653–1665, April 2002. ISSN: 0043-1354. DOI: 10.1016/S0043-1354(01)00379-7.
- [88] Y. Liu, Z.-W. Wang, L. Qin, Y.-Q. Liu, and J.-H. Tay. Selection pressure-driven aerobic granulation in a sequencing batch reactor. *Applied Microbiology and Biotechnology*, 67(1):26–32, April 1, 2005. ISSN: 0175-7598, 1432-0614. DOI: 10.1007/s00253-004-1820-2.
- [89] S. Lochmatter and C. Holliger. Optimization of operation conditions for the startup of aerobic granular sludge reactors biologically removing carbon, nitrogen, and phosphorous. *Water Res.*, 59:58–70, 2014. ISSN: 18792448. DOI: 10.1016/j.watres.2014.04.011.
- [90] K. v. Lohuizen. *Afvalwaterzuivering in Nederland: van beerput tot oxidatiesloot*. RWS-RIZA, Lelystad, 2006. ISBN: 978-90-369-5727-4.
- [91] M. O. Lorenz. Methods of measuring the concentration of wealth. *Publ. Am. Stat. Assoc.*, 9(70):209–219, June 1905. ISSN: 1522-5437. DOI: 10.1080/15225437.1905.10503443.
- [92] A. M. P. Martins. *Bulking sludge control. Kinetics, substrate storage, and process design aspects*. PhD thesis, Delft University of Technology, 2004.
- [93] A. M. P. Martins, J. J. Heijnen, and M. C. M. van Loosdrecht. Effect of dissolved oxygen concentration on sludge settleability. *Applied Microbiology and Biotechnology*, 62(5):586–593, October 1, 2003. ISSN: 0175-7598, 1432-0614. DOI: 10.1007/s00253-003-1384-6.
- [94] A. M. P. Martins, J. J. Heijnen, and M. C. M. van Loosdrecht. Bulking sludge in biological nutrient removal systems. *Biotechnology and Bioengineering*, 86(2):125–135, April 20, 2004. ISSN: 1097-0290. DOI: 10.1002/bit.20029.
- [95] A. M. P. Martins, J. J. Heijnen, and M. C. M. van Loosdrecht. Effect of feeding pattern and storage on the sludge settleability under aerobic conditions. *Water Research*, 37(11):2555–2570, June 2003. ISSN: 0043-1354. DOI: 10.1016/S0043-1354(03)00070-8.
- [96] A. M. P. Martins, Ö. Karahan, and M. C. M. van Loosdrecht. Effect of polymeric substrate on sludge settleability. *Water Research*, 45(1):263–273, January 1, 2011. ISSN: 0043-1354. DOI: 10.1016/j.watres.2010.07.055.
- [97] A. M. P. Martins, K. Pagilla, J. J. Heijnen, and M. C. M. van Loosdrecht. Filamentous bulking sludge—a critical review. *Water Research*, 38(4):793–817, February 2004. ISSN: 0043-1354. DOI: 10.1016/j.watres.2003.11.005.
- [98] B. McSwain, R. Irvine, and P. Wilderer. The influence of settling time on the formation of aerobic granules. *Water Science and Technology*, 50(10):195–202, 2004. DOI: 10.2166/wst.2004.0643.
- [99] Metcalf and Eddy. *Wastewater Engineering: Treatment and Reuse*. McGraw-Hill Education, August 30, 2013. 2049 pages. ISBN: 978-0-07-744121-0.
- [100] R. L. Meyer, A. M. Saunders, R. J. Zeng, J. Keller, and L. L. Blackall. Microscale structure and function of anaerobic–aerobic granules containing glycogen accumulating organisms. *FEMS Microbiology Ecology*, 45(3):253–261, August 1, 2003. ISSN: 0168-6496. DOI: 10.1016/S0168-6496(03)00159-4.

- [101] M. Miyake, Y. Hasebe, K. Furusawa, H. Shiomi, D. Inoue, and M. Ike. Enhancement of nutrient removal in an activated sludge process using aerobic granular sludge augmentation strategy with ammonium-based aeration control. *Chemosphere*, 340:139826, November 2023. ISSN: 00456535. DOI: 10.1016/j.chemosphere.2023.139826.
- [102] E. Morgenroth, T. Sherden, M. C. M. van Loosdrecht, J. J. Heijnen, and P. A. Wilderer. Aerobic granular sludge in a sequencing batch reactor. *Water Research*, 31(12):3191–3194, December 1, 1997. ISSN: 0043-1354. DOI: 10.1016/S0043-1354(97)00216-9.
- [103] E. Morgenroth and P. Wilderer. Controlled biomass removal - the key parameter to achieve enhanced biological phosphorus removal in biofilm systems. *Water Science and Technology*, 39(7):33–40, 1999. ISSN: 02731223. DOI: 10.1016/S0273-1223(99)00147-X.
- [104] A. Mosquera-Corral, M. K. de Kreuk, J. J. Heijnen, and M. C. M. van Loosdrecht. Effects of oxygen concentration on n-removal in an aerobic granular sludge reactor. *Water Research*, 39(12):2676–2686, July 2005. ISSN: 0043-1354. DOI: 10.1016/j.watres.2005.04.065.
- [105] B. Nguyen Quoc, S. Wei, M. Armenta, R. Bucher, P. Sukapantharam, D. A. Stahl, H. D. Stensel, and M.-K. H. Winkler. Aerobic granular sludge: impact of size distribution on nitrification capacity. *Water Research*, 188:116445, January 1, 2021. ISSN: 0043-1354. DOI: 10.1016/j.watres.2020.116445.
- [106] B.-J. Ni, G.-P. Sheng, X.-Y. Li, and H.-Q. Yu. Quantitative simulation of the granulation process of activated sludge for wastewater treatment. *Industrial & Engineering Chemistry Research*, 49(6):2864–2873, March 17, 2010. ISSN: 0888-5885, 1520-5045. DOI: 10.1021/ie901252k.
- [107] H. A. Nicholls and D. W. Osborn. Bacterial stress: prerequisite for biological removal of phosphorus. *J. Water Pollut. Control Fed.*, 51(3):557–569, 1979. ISSN: 00431303. DOI: 10.2307/25039864.
- [108] C. Nicolella, M. C. M. van Loosdrecht, and J. J. Heijnen. Mass transfer and reaction in a biofilm airlift suspension reactor. *Chemical engineering science*, 53(15):2743–2753, 1998.
- [109] B. O. Oyserman, D. R. Noguera, T. G. del Rio, S. G. Tringe, and K. D. McMahon. Metatranscriptomic insights on gene expression and regulatory controls in *Candidatus* *accumulibacter phosphatis*. *The ISME Journal*, 10(4):810–822, April 2016. ISSN: 1751-7370. DOI: 10.1038/ismej.2015.155.
- [110] A. E. Ozinsky and G. A. Ekama. Secondary settling tank modelling and design. part 1: review of theoretical and practical developments. *Water S. A.*, 21(4):325–322, 1995.
- [111] A. Pasveer. The oxidation ditch : principle, results and applications. In Symposium on "Low cost waste treatment" held at CIPHERI, Nagpur. Instituut voor Gezondheidstechniek TNO, October 27, 1969.
- [112] J. H. F. Pereboom. Size distribution model for methanogenic granules from full scale UASB and IC reactors. *Water Science and Technology*, 30(12):211–221, December 1, 1994. ISSN: 0273-1223. DOI: 10.2166/wst.1994.0613.
- [113] C. Picioreanu. *Multidimensional Modeling of Biofilm Structure*. PhD thesis, Delft University of Technology, 1999.
- [114] C. Picioreanu, M. C. M. van Loosdrecht, and J. J. Heijnen. A theoretical study on the effect of surface roughness on mass transport and transformation in biofilms. *Biotechnol. Bioeng.*, 68(4):355–369, 2000. DOI: 10.1002/(SICI)1097-0290(20000520)68:4<355::AID-BIT1>3.0.CO;2-A.
- [115] C. Picioreanu, M. C. M. van Loosdrecht, and J. J. Heijnen. Effect of diffusive and convective substrate transport on biofilm structure formation: a two-dimensional modeling study. *Biotechnology and Bioengineering*, 69(5):504–515, September 5, 2000. ISSN: 1097-0290. DOI: 10.1002/1097-0290(20000905)69:5<504::AID-BIT5>3.0.CO;2-S.
- [116] C. Picioreanu, M. C. M. van Loosdrecht, and J. J. Heijnen. Mathematical modeling of biofilm structure with a hybrid differential-discrete cellular automaton approach. *Biotechnology and bioengineering*, 58(1):101–116, 1998. DOI: 10.1002/(SICI)1097-0290(19980405)58:1<101::AID-BIT1>3.0.CO;2-M.
- [117] M. Pijuan, A. Guisasaola, J. A. Baeza, J. Carrera, C. Casas, and J. Lafuente. Aerobic phosphorus release linked to acetate uptake: influence of PAO intracellular storage compounds. *Biochemical Engineering Journal*. Engineering Bioreaction Systems: A Spanish Perspective, 26(2):184–190, November 15, 2005. ISSN: 1369-703X. DOI: 10.1016/j.bej.2005.04.014.

- [118] M. Pijuan, A. Guisasaola, J. A. Baeza, J. Carrera, C. Casas, and J. Lafuente. Net p-removal deterioration in enriched PAO sludge subjected to permanent aerobic conditions. *Journal of Biotechnology*, 123(1):117–126, May 3, 2006. ISSN: 0168-1656. DOI: 10.1016/j.jbiotec.2005.10.018.
- [119] M. Pijuan, U. Werner, and Z. Yuan. Reducing the startup time of aerobic granular sludge reactors through seeding floccular sludge with crushed aerobic granules. *Water Research*, 45(16):5075–5083, October 15, 2011. ISSN: 0043-1354. DOI: 10.1016/j.watres.2011.07.009.
- [120] M. Pronk, B. Abbas, R. Kleerebezem, and M. C. M. van Loosdrecht. Effect of sludge age on methanogenic and glycogen accumulating organisms in an aerobic granular sludge process fed with methanol and acetate: effect of sludge age. *Microbial Biotechnology*, 8(5):853–864, September 2015. ISSN: 17517915. DOI: 10.1111/1751-7915.12292.
- [121] M. Pronk, B. Abbas, S. H. K. Al-zuhairy, R. Kraan, R. Kleerebezem, and M. C. M. van Loosdrecht. Effect and behaviour of different substrates in relation to the formation of aerobic granular sludge. *Applied Microbiology and Biotechnology*, 99(12):5257–5268, January 24, 2015. ISSN: 0175-7598, 1432-0614. DOI: 10.1007/s00253-014-6358-3.
- [122] M. Pronk, M. K. de Kreuk, B. de Bruin, P. Kamminga, R. Kleerebezem, and M. C. M. van Loosdrecht. Full scale performance of the aerobic granular sludge process for sewage treatment. *Water Research*, 84:207–217, November 1, 2015. ISSN: 0043-1354. DOI: 10.1016/j.watres.2015.07.011.
- [123] M. Pronk, T. R. Neu, M. C. M. van Loosdrecht, and Y. M. Lin. The acid soluble extracellular polymeric substance of aerobic granular sludge dominated by *defluviicoccus* sp. *Water Research*, 122:148–158, October 1, 2017. ISSN: 0043-1354. DOI: 10.1016/j.watres.2017.05.068.
- [124] M. Pronk, A. Giesen, A. Thompson, S. Robertson, and M. van Loosdrecht. Aerobic granular biomass technology: advancements in design, applications and further developments. *Water Practice and Technology*, 12(4):987–996, December 1, 2017. ISSN: 1751-231X. DOI: 10.2166/wpt.2017.101.
- [125] Proposal for a revised urban wastewater treatment directive, October 26, 2022.
- [126] L. Qin, J.-H. Tay, and Y. Liu. Selection pressure is a driving force of aerobic granulation in sequencing batch reactors. *Process Biochemistry*, 39(5):579–584, January 30, 2004. ISSN: 1359-5113. DOI: 10.1016/S0032-9592(03)00125-0.
- [127] B. N. Quoc, M. Armenta, J. A. Carter, R. Bucher, P. Sukapantharam, S. J. Bryson, D. A. Stahl, H. D. Stensel, and M.-K. H. Winkler. An investigation into the optimal granular sludge size for simultaneous nitrogen and phosphate removal. *Water Research*:117119, April 4, 2021. ISSN: 0043-1354. DOI: 10.1016/j.watres.2021.117119.
- [128] C. W. Randall and D. Sen. Full-scale evaluation of an integrated fixed-film activated sludge (IFAS) process for enhanced nitrogen removal. *Water Science and Technology*, 33(12):155–162, June 1, 1996. ISSN: 0273-1223. DOI: 10.2166/wst.1996.0325.
- [129] E. Redmond, M. Jalbert, M. Young, R. Faraj, B. Sturm, and L. Downing. Full-scale continuous flow selective pressures for sludge granulation. In *Proceedings. WEFTEC 2019 - 92nd Annual Water Environment Federation's Technical Exhibition and Conference*, pages 3490–3497. Water Environment Federation, 2019.
- [130] L. Rieger, G. Koch, M. Kühni, W. Gujer, and H. Siegrist. The eawag bio-p module for activated sludge model no. 3. *Water Research*, 35(16):3887–3903, November 1, 2001. ISSN: 0043-1354. DOI: 10.1016/S0043-1354(01)00110-5.
- [131] C. Roche, S. Donnaz, S. Murthy, and B. Wett. Biological process architecture in continuous-flow activated sludge by gravimetry: controlling densified biomass form and function in a hybrid granule-floc process at dijon WRRF, france. *Water Environment Research: A Research Publication of the Water Environment Federation*, 94(1):e1664, January 2022. ISSN: 1554-7531. DOI: 10.1002/wer.1664.
- [132] T. Rocktäschel, C. Klarmann, B. Helmreich, J. Ochoa, P. Boisson, K. H. Sørensen, and H. Horn. Comparison of two different anaerobic feeding strategies to establish a stable aerobic granulated sludge bed. *Water Research*, 47(17):6423–6431, November 1, 2013. ISSN: 0043-1354. DOI: 10.1016/j.watres.2013.08.014.

- [133] T. Rocktäschel, C. Klarmann, J. Ochoa, P. Boisson, K. Sørensen, and H. Horn. Influence of the granulation grade on the concentration of suspended solids in the effluent of a pilot scale sequencing batch reactor operated with aerobic granular sludge. *Separation and Purification Technology*, 142:234–241, March 4, 2015. ISSN: 1383-5866. DOI: 10.1016/j.seppur.2015.01.013.
- [134] J. Sandino, A. Willoughby, D. Houweling, L. Havsteen, P. Nielsen, and T. Constantine. Improved settleability in a BNR process from hydrocyclone-induced biomass granulation. In WEFTEC 2016. Water Environment Federation, September 24, 2016.
- [135] S. J. Sarma, J. H. Tay, and A. Chu. Finding knowledge gaps in aerobic granulation technology. *Trends in Biotechnology*, 35(1):66–78, January 2017. ISSN: 0167-7799. DOI: 10.1016/j.tibtech.2016.07.003.
- [136] C. N. Sawyer. Milestones in the development of the activated sludge process. *Journal (Water Pollution Control Federation)*, 37(2):151–162, 1965. ISSN: 0043-1303.
- [137] A. J. Schuler, N. Majed, V. Bucci, F. L. Hellweger, Y. Tu, and A. Z. Gu. Is the whole the sum of its parts? agent-based modelling of wastewater treatment systems. *Water Science and Technology*, 63(8):1590–1598, April 1, 2011. ISSN: 0273-1223. DOI: 10.2166/wst.2011.218.
- [138] A. J. Schuler and H. Jang. Causes of variable biomass density and its effects on settleability in full-scale biological wastewater treatment systems. *Environmental Science & Technology*, 41(5):1675–1681, March 1, 2007. ISSN: 0013-936X. DOI: 10.1021/es0616074.
- [139] N. Schwarzenbeck, R. Erley, and P. Wilderer. Aerobic granular sludge in an SBR-system treating wastewater rich in particulate matter. *Water Science and Technology*, 49(11):41–46, June 1, 2004. ISSN: 0273-1223, 1996-9732. DOI: 10.2166/wst.2004.0799.
- [140] L. G. d. Silva, K. O. Gamez, J. C. Gomes, K. Akkermans, L. Welles, B. Abbas, M. C. M. van Loosdrecht, and S. A. Wahl. Revealing the metabolic flexibility of *Candidatus Accumulibacter phosphatis* through redox cofactor analysis and metabolic network modeling. *Applied and Environmental Microbiology*, October 2, 2020. ISSN: 0099-2240, 1098-5336. DOI: 10.1128/AEM.00808-20.
- [141] L. G. d. Silva, S. Tomás-Martínez, M. C. M. van Loosdrecht, and S. A. Wahl. The environment selects: modeling energy allocation in microbial communities under dynamic environments. *bioRxiv*:689174, July 3, 2019. DOI: 10.1101/689174.
- [142] G. J. F. Smolders. *A metabolic model of the biological phosphorus removal. Stoichiometry, kinetics and dynamic behaviour*. PhD thesis, Delft University of Technology, 1995.
- [143] G. J. F. Smolders, J. M. Klop, M. C. M. van Loosdrecht, and J. J. Heijnen. A metabolic model of the biological phosphorus removal process: i. effect of the sludge retention time. *Biotechnology and Bioengineering*, 48(3):222–233, 1995. ISSN: 1097-0290. DOI: 10.1002/bit.260480309.
- [144] G. J. F. Smolders, J. v. d. Meij, M. C. M. van Loosdrecht, and J. J. Heijnen. A structured metabolic model for anaerobic and aerobic stoichiometry and kinetics of the biological phosphorus removal process. *Biotechnology and Bioengineering*, 47(3):277–287, 1995. ISSN: 1097-0290. DOI: 10.1002/bit.260470302.
- [145] G. J. F. Smolders, J. van der Meij, M. C. M. van Loosdrecht, and J. J. Heijnen. Model of the anaerobic metabolism of the biological phosphorus removal process: stoichiometry and pH influence. *Biotechnol. Bioeng.*, 43(6):461–470, March 1994. ISSN: 0006-3592. DOI: 10.1002/bit.260430605.
- [146] P. S. Stewart. Diffusion in biofilms. *Journal of Bacteriology*, 185(5):1485–1491, January 3, 2003. ISSN: 0021-9193, 1098-5530. DOI: 10.1128/JB.185.5.1485-1491.2003.
- [147] L. Strubbe, M. Pennewaerde, J. E. Baeten, and E. I. P. Volcke. Continuous aerobic granular sludge plants: better settling versus diffusion limitation. *Chemical Engineering Journal*, 428:131427, January 15, 2022. ISSN: 1385-8947. DOI: 10.1016/j.cej.2021.131427.
- [148] T. Tang, S. Wang, Z. Jiang, and J. Li. Progress in study of the function of quorum sensing and cell signaling in the formation of aerobic granular sludge. *Chinese Journal of Applied and Environmental Biology*, 22(4):718–724, 2016. ISSN: 1006687X. DOI: 10.3724/SP.J.1145.2015.12040.
- [149] J.-H. Tay, Q.-S. Liu, and Y. Liu. The effects of shear force on the formation, structure and metabolism of aerobic granules. *Applied Microbiology and Biotechnology*, 57(1):227–233, June 17, 2001. ISSN: 0175-7598, 1432-0614. DOI: 10.1007/s002530100766.
- [150] L. Tjihuis. *The biofilm airlift suspension reactor: Biofilm formation, detachment and heterogeneity*. PhD thesis, Delft University of Technology, 1994.

- [151] L. Tjihuis, W. A. J. v. Benthum, M. C. M. van Loosdrecht, and J. J. Heijnen. Solids retention time in spherical biofilms in a biofilm airlift suspension reactor. *Biotechnology and Bioengineering*, 44(8):867–879, 1994. ISSN: 1097-0290. DOI: <https://doi.org/10.1002/bit.260440802>.
- [152] S. Toja Ortega, M. Pronk, and M. K. de Kreuk. Anaerobic hydrolysis of complex substrates in full-scale aerobic granular sludge: enzymatic activity determined in different sludge fractions. *Applied Microbiology and Biotechnology*, 105(14):6073–6086, August 1, 2021. ISSN: 1432-0614. DOI: 10.1007/s00253-021-11443-3.
- [153] S. Toja Ortega, M. Pronk, and M. K. de Kreuk. Effect of an increased particulate COD load on the aerobic granular sludge process: a full scale study. *Processes*, 9(8):1472, August 2021. ISSN: 2227-9717. DOI: 10.3390/pr9081472.
- [154] E. Tykesson, H. Aspegren, M. Henze, P. Nielsen, and J. I. C. Jansen. Use of phosphorus release batch tests for modelling an EBPR pilot plant. *Water Science and Technology*, 45(6):99–106, March 1, 2002. ISSN: 0273-1223. DOI: 10.2166/wst.2002.0097.
- [155] H. van Delfland. Energie- en klimaatneutraal. Waterwerk. URL: <https://wbp6.hhdelfland.nl/themas/179> (visited on 12/05/2023).
- [156] E. J. H. van Dijk, V. A. Haaksman, M. C. M. van Loosdrecht, and M. Pronk. On the mechanisms for aerobic granulation - model based evaluation. *Water Research*, 216:118365, June 1, 2022. ISSN: 0043-1354. DOI: 10.1016/j.watres.2022.118365.
- [157] E. J. H. van Dijk, M. Pronk, and M. C. M. van Loosdrecht. A settling model for full-scale aerobic granular sludge. *Water Research*, 186:116135, November 2020. ISSN: 00431354. DOI: 10.1016/j.watres.2020.116135.
- [158] E. J. H. van Dijk, M. Pronk, and M. C. M. van Loosdrecht. Controlling effluent suspended solids in the aerobic granular sludge process. *Water Research*, 147:50–59, December 15, 2018. ISSN: 0043-1354. DOI: 10.1016/j.watres.2018.09.052.
- [159] M. C. M. van Loosdrecht, D. Eikelboom, A. Gjaltema, A. Mulder, L. Tjihuis, and J. J. Heijnen. Biofilm structures. *Water Science and Technology. Biofilm Structure, Growth and Dynamics*, 32(8):35–43, January 1, 1995. ISSN: 0273-1223. DOI: 10.1016/0273-1223(96)00005-4.
- [160] M. C. M. van Loosdrecht, J. J. Heijnen, H. Eberl, J. Kreft, and C. Picioreanu. Mathematical modelling of biofilm structures. *Antonie van Leeuwenhoek, Int. J. Gen. Mol. Microbiol.*, 81(1):245–256, 2002. ISSN: 00036072. DOI: 10.1023/A:1020527020464.
- [161] M. C. M. van Loosdrecht, C. Picioreanu, and J. J. Heijnen. A more unifying hypothesis for biofilm structures. *FEMS Microbiology Ecology*, 24(2):181–183, October 1, 1997. ISSN: 0168-6496. DOI: 10.1111/j.1574-6941.1997.tb00434.x.
- [162] M. C. M. van Loosdrecht, M. A. Pot, and J. J. Heijnen. Importance of bacterial storage polymers in bioprocesses. *Water Science and Technology. Sequencing Batch Reactor Technology: Batch Application of Periodic Unsteady-state Processes*, 35(1):41–47, January 1, 1997. ISSN: 0273-1223. DOI: 10.1016/S0273-1223(96)00877-3.
- [163] A. M. van Niekerk, D. Jenkins, and M. G. Richard. The competitive growth of zoogloea ramigera and type 021n in activated sludge and pure culture: a model for low f<sub>m</sub> bulking. *Journal (Water Pollution Control Federation)*, 59(5):262–273, 1987. ISSN: 0043-1303.
- [164] A. F. van Nieuwenhuijzen, A. G. N. van Bentem, A. Buunnen, B. A. Reitsma, and C. A. Uijterlinde. The limits and ultimate possibilities of technology of the activated sludge process. *Water Science and Technology*, 58(8):1671–1677, October 1, 2008. ISSN: 0273-1223. DOI: 10.2166/wst.2008.545.
- [165] L. van den Berg, M. Pronk, M. C. M. van Loosdrecht, and M. K. de Kreuk. Density measurements of aerobic granular sludge. *Environmental Technology*, 0(0):1–11, December 14, 2021. ISSN: 0959-3330. DOI: 10.1080/09593330.2021.2017492.
- [166] L. van den Berg, S. Toja Ortega, M. C. M. van Loosdrecht, and M. K. de Kreuk. Diffusion of soluble organic substrates in aerobic granular sludge: effect of molecular weight. *Water Research X*, 16:100148, August 1, 2022. ISSN: 2589-9147. DOI: 10.1016/j.wroa.2022.100148.

- [167] L. van den Berg, M. C. M. van Loosdrecht, and M. K. de Kreuk. How to measure diffusion coefficients in biofilms: a critical analysis. *Biotechnology and Bioengineering*, 118(3):1273–1285, 2021. ISSN: 1097-0290. DOI: 10.1002/bit.27650.
- [168] H. F. van der Roest, L. M. M. de Bruin, G. Gademan, and F. Coelho. Towards sustainable wastewater treatment with dutch nereda® technology. *Water Practice and Technology*, 6(3):wpt2011059, September 1, 2011. ISSN: 1751-231X. DOI: 10.2166/wpt.2011.059.
- [169] H. F. van der Roest, A. van Bentem, C. Uijterlinde, and A. de Man. Nereda technology shows a steep growth curve. *H2O/Water Matters*, 2, December 15, 2016.
- [170] E. J. H. Van Dijk, K. M. Van Schagen, and A. T. Oosterhoff. Controlled simultaneous nitrification and denitrification in wastewater treatment. Patent (WO2018215561A1). H. N. Bv. November 29, 2018.
- [171] M. Verawaty, S. Tait, M. Pijuan, Z. Yuan, and P. L. Bond. Breakage and growth towards a stable aerobic granule size during the treatment of wastewater. *Water Research*, 47(14):5338–5349, September 15, 2013. ISSN: 0043-1354. DOI: 10.1016/j.watres.2013.06.012.
- [172] P. A. Vesilind. Design of prototype thickeners from batch settling tests. *Water Sewage Works*, 115(7):302–307, 1968.
- [173] J. C. Villaseñor, M. C. M. van Loosdrecht, C. Picioreanu, and J. J. Heijnen. Influence of different substrates on the formation of biofilms in a biofilm airlift suspension reactor. *Water Science and Technology*, 41(4):323–330, February 1, 2000. ISSN: 0273-1223, 1996-9732. DOI: 10.2166/wst.2000.0462.
- [174] W. Vishniac and M. Santer. The thiobacilli. *Bacteriological Reviews*, 21(3):195–213, September 1957. ISSN: 0005-3678. DOI: 10.1128/mbr.21.3.195-213.1957.
- [175] J. Wagner, D. G. Weissbrodt, V. Manguin, R. H. Ribeiro da Costa, E. Morgenroth, and N. Derlon. Effect of particulate organic substrate on aerobic granulation and operating conditions of sequencing batch reactors. *Water Research*, 85:158–166, November 15, 2015. ISSN: 0043-1354. DOI: 10.1016/j.watres.2015.08.030.
- [176] S. Wang, W. Shi, T. Tang, Y. Wang, L. Zhi, J. Lv, and J. Li. Function of quorum sensing and cell signaling in the formation of aerobic granular sludge. *Reviews in Environmental Science and Bio/Technology*, 16(1):1–13, March 1, 2017. ISSN: 1569-1705, 1572-9826. DOI: 10.1007/s11157-017-9420-7.
- [177] J. Wanner, V. Ottova, and P. Grau. Effect of an anaerobic zone on settleability of activated sludge. *Advances in Water Pollution Control (IAWPRC), Biological Phosphorus Removal from Wastewaters*:155–164, January 1, 1987. DOI: 10.1016/B978-0-08-035592-4.50019-5.
- [178] O. Wanner and P. Reichert. Mathematical modeling of mixed-culture biofilms. en. *Biotechnology and Bioengineering*, 49(2):172–184, January 1996. ISSN: 1097-0290. DOI: 10.1002/(SICI)1097-0290(19960120)49:2<172::AID-BIT6>3.0.CO;2-N.
- [179] S. P. Wei, B. Nguyen Quoc, M. Shapiro, P. H. Chang, J. Calhoun, and M. K. H. Winkler. Application of aerobic kenaf granules for biological nutrient removal in a full-scale continuous flow activated sludge system. *Chemosphere*, 271:129522, May 1, 2021. ISSN: 0045-6535. DOI: 10.1016/j.chemosphere.2020.129522.
- [180] S. P. Wei, H. D. Stensel, B. N. Quoc, D. A. Stahl, X. Huang, P.-H. Lee, and M.-K. H. Winkler. Flocs in disguise? high granule abundance found in continuous-flow activated sludge treatment plants. *Water Research*:115865, April 29, 2020. ISSN: 0043-1354. DOI: 10.1016/j.watres.2020.115865.
- [181] D. G. Weissbrodt, J. Maillard, A. Brovelli, A. Chabreli, J. May, and C. Holliger. Multilevel correlations in the biological phosphorus removal process: from bacterial enrichment to conductivity-based metabolic batch tests and polyphosphatase assays. *Biotechnology and Bioengineering*, 111(12):2421–2435, December 1, 2014. ISSN: 1097-0290. DOI: 10.1002/bit.25320.
- [182] L. Welles, B. Abbas, D. Y. Sorokin, C. M. Lopez-Vazquez, C. M. Hooijmans, V. Loosdrecht, M. C. M., and D. Brdjanovic. Metabolic response of “candidatus accumulibacter phosphatis” clade II c to changes in influent p/c ratio. *Frontiers in Microbiology*, 7, 2017. ISSN: 1664-302X. DOI: 10.3389/fmicb.2016.02121.
- [183] C. M. Welling. *Improving settleability and achieving biological phosphorus removal through the application of sidestream gravimetric selectors*. Thesis, Virginia Tech, December 21, 2015.

- [184] B. Wett, S. Podmirseg, M. Gómez-Brandón, M. Hell, G. Nyhuis, C. Bott, and S. Murthy. Expanding DE-MON sidestream deammonification technology towards mainstream application. *Water Environment Research*, 87(12):2084–2089, 2015. ISSN: 1554-7531. DOI: 10.2175/106143015X14362865227319.
- [185] P. A. Wilderer, R. L. Irvine, and M. C. Goronszy. *Sequencing batch reactor technology*. IWA Publishing, April 2007. ISBN: 978-1-78040-224-6. DOI: 10.2166/9781780402246.
- [186] T. V. Winkel, S. E. Vlaeminck, A. Al-Omari, B. Bachmann, B. Sturm, B. Wett, I. Takács, C. Bott, S. N. Murthy, and H. D. Clippeleir. Screen versus cyclone for improved capacity and robustness for sidestream and mainstream deammonification. *Environmental Science: Water Research & Technology*, 5(10):1769–1781, 2019. DOI: 10.1039/C9EW00384C.
- [187] M. -. H. Winkler, R. Kleerebezem, L. M. M. De Bruin, P. J. T. Verheijen, B. Abbas, J. Habermacher, and M. C. M. van Loosdrecht. Microbial diversity differences within aerobic granular sludge and activated sludge flocs. *Appl. Microbiol. Biotechnol.*, 97(16):7447–7458, 2013. DOI: 10.1007/s00253-012-4472-7.
- [188] M.-K. H. Winkler and M. C. M. van Loosdrecht. Intensifying existing urban wastewater. *Science*, 375(6579):377–378, January 28, 2022. DOI: 10.1126/science.abm3900.
- [189] M. K. H. Winkler, R. Kleerebezem, W. O. Khunjar, B. de Bruin, and M. C. M. van Loosdrecht. Evaluating the solid retention time of bacteria in flocculent and granular sludge. *Water Research*, 46(16):4973–4980, October 15, 2012. ISSN: 0043-1354. DOI: 10.1016/j.watres.2012.06.027.
- [190] M.-K. H. Winkler, C. Meunier, O. Henriët, J. Mahillon, M. E. Suárez-Ojeda, G. Del Moro, M. De Sanctis, C. Di Iaconi, and D. G. Weissbrodt. An integrative review of granular sludge for the biological removal of nutrients and recalcitrant organic matter from wastewater. *Chemical Engineering Journal*, 336:489–502, March 2018. ISSN: 13858947. DOI: 10.1016/j.cej.2017.12.026.
- [191] J. Wu, F. L. de los Reyes, and J. J. Ducoste. Modeling cell aggregate morphology during aerobic granulation in activated sludge processes reveals the combined effect of substrate and shear. *Water Research*, 170:115384, March 1, 2020. ISSN: 0043-1354. DOI: 10.1016/j.watres.2019.115384.
- [192] J. B. Xavier, M. K. de Kreuk, C. Picioreanu, and M. C. M. van Loosdrecht. Multi-scale individual-based model of microbial and bioconversion dynamics in aerobic granular sludge. *Environmental Science & Technology*, 41(18):6410–6417, September 1, 2007. ISSN: 0013-936X. DOI: 10.1021/es070264m.
- [193] D. Xu, J. Li, J. Liu, and T. Ma. Rapid aerobic sludge granulation in an integrated oxidation ditch with two-zone clarifiers. *Water Research*, 175:115704, May 15, 2020. ISSN: 0043-1354. DOI: 10.1016/j.watres.2020.115704.
- [194] K. Yamamoto, M. Hiasa, T. Mahmood, and T. Matsuo. Direct solid-liquid separation using hollow fiber membrane in an activated sludge aeration tank. *Water Science and Technology*, 21(4):43–54, April 1989. ISSN: 0273-1223. DOI: 10.2166/wst.1989.0209.
- [195] S.-F. Yang, Q.-S. Liu, J.-H. Tay, and Y. Liu. Growth kinetics of aerobic granules developed in sequencing batch reactors. *Letters in Applied Microbiology*, 38(2):106–112, 2004. ISSN: 1472-765X. DOI: 10.1111/j.1472-765X.2003.01452.x.
- [196] R. J. Zeng, M. C. M. van Loosdrecht, Z. Yuan, and J. Keller. Metabolic model for glycogen-accumulating organisms in anaerobic/aerobic activated sludge systems. *Biotechnology and Bioengineering*, 81(1):92–105, 2003. ISSN: 1097-0290. DOI: <https://doi.org/10.1002/bit.10455>.

# Acronyms

BOD <sub>5</sub>	biochemical oxygen demand over 5 days
AE	aerobic
AGS	aerobic granular sludge
AN	anaerobic
AO	anoxic
AS	activated sludge
BNR	biological nutrient removal
CAS	conventional activated sludge
CFAS	continuous-flow activated sludge
CFR	continuous-flow reactor
COD	chemical oxygen demand
CSTR	continuous stirred-tank reactor
dAS	densified activated sludge
DBI	Delft Blue Innovations
DDWF	daily dry weather flow
DN	denitrification
DO	dissolved oxygen
dSVI	diluted sludge volume index
EBPR	enhanced biological phosphorus removal
GAM	glycogen-accumulating metabolism
GAO	glycogen-accumulating organism
GFS	granule forming substrates
HARKOS	HarnAschpolder KORrelSlib
HPLC	high-performance liquid chromatography
HRT	hydraulic residence time



---

IFAS	integrated fixed-film activated sludge
MBBR	moving bed biofilm reactor
MBR	membrane bioreactor
MLSS	mixed liquor suspended solids
MLVSS	mixed liquor volatile suspended solids
OHO	ordinary heterotrophic organism
P	phosphorus
PAM	polyphosphate-accumulating metabolism
PAO	polyphosphate-accumulating organism
PHA	polyhydroxyalkanoates
PHB	poly- $\beta$ -hydroxybutyrate
PHV	poly- $\beta$ -hydroxyvalerate
PPP	public-private partnership
PRWF	peak rain weather flow
RAS	return activated sludge
rbCOD	readily biodegradable chemical oxygen demand
RTD	residence time distribution
SAADR	specific aerobic acetate dosage rate
SBR	sequencing batch reactor
SND	simultaneous nitrification and denitrification
SNUR	specific ammonium uptake rate
SPUR	specific phosphate uptake rate
SRT	solids retention time
SV	sludge volume after settling
SVI	sludge volume index after settling
TSS	total suspended solids
VFA	volatile fatty acid
VSS	volatile suspended solids
WAS	waste activated sludge
WWTP	wastewater treatment plant

# Nomenclature

## Definitions

A	Area ( $\text{m}^2$ )
a	Cumulative area of granules in a cluster per volume of empty reactor ( $\text{m}^{-1}$ )
$\text{Ac}_{\text{fed}}^-$	Amount of acetate fed anaerobically during a cycle ( $\text{mmol}_C$ )
$\Delta\text{Ac}^-$	Biomass specific amount of acetate stored during anaerobic feeding ( $\text{mmol}_C \text{g}_{\text{VSS}}^{-1}$ )
Ar	Archimedes number (-)
c	Concentration ( $\text{kg m}^{-3}$ )
D	Diffusion coefficient ( $\text{m}^2/\text{s}$ )
d	Diameter of granules in a cluster (m)
$D_{\text{ax}}$	Axial dispersion coefficient in bulk-liquid during feeding ( $\text{m}^2/\text{s}$ )
f	Relative fraction (-)
G	Number of granules in a cluster (-)
H	Height of the reactor (m)
K	Monod constant ( $\text{kg m}^{-3}$ )
$k_{\text{LB}}$	Mass transfer coefficient for the bulk-liquid/biofilm interface ( $\text{m s}^{-1}$ )
N	Number of clusters in a set a set (-)
n	Expansion index (-)
$q_{\text{AN,max}}$	Maximum biomass specific anaerobic substrate uptake rate ( $\text{kg kg}^{-1} \text{s}^{-1}$ )
R	Volumetric reaction rate ( $\text{kg m}^{-3} \text{s}^{-1}$ )
r	Radial position from the center of a spherical granule (m)
t	Time (s)
v	Velocity ( $\text{m s}^{-1}$ )
$v_f$	Fluidizing velocity of granules in a clusters ( $\text{m s}^{-1}$ )
WS	Amount of sludge wasted ( $\text{kg}_{\text{TSS}} \text{d}^{-1}$ )

---

x	Position of granules in a cluster from the bottom of the reactor (m)
Y	Yield coefficient ( $\text{kg kg}^{-1}$ )
Z	Probability (-)

**Greek symbols**

$\nu$	Kinematic viscosity of bulk-liquid ( $\text{m}^2 \text{s}^{-1}$ )
$\rho$	Density ( $\text{kg m}^{-3}$ )
$\rho_{\text{bed}}$	Density of the sludge bed (combined liquid and biomass in set of clusters at certain height) ( $\text{kg m}^{-3}$ )
$\epsilon$	Voidage (-)
$\epsilon_e$	Apparent voidage around a cluster of granules (-)

**Subscripts**

$\text{Ac}^-$	Acetate
B	Biofilm phase
C	Carbon
fed	Total amount fed during a cycle
GFS	Granule forming substrate
i	Positional index denoting the vertical location in a reactor
in	Influent wastewater during feeding
j	Index of a biomass cluster or a size class
L	Bulk-liquid phase
ML	Mixed liquor
N	Nitrogen
PHA	Storage polymers (polyhydroxyalkanoates)
P	Phosphorus
X	Biomass

# Dankwoord

Het is een voorrecht om je een periode in het leven te mogen storten op het uitzoeken van een onderwerp. Voor dit proefschrift heb ik vooral bestaande inzichten op het gebied van biofilmmorfologie kunnen gebruiken om de dynamiek van aeroob korrelslib in de praktijk beter te begrijpen. Zijn de fundamentele inzichten nu anders dan bij aanvang? Het mooiste aspect van het onderzoek vind ik dat je nooit kunt voorspellen wanneer iemand in de toekomst weer een stap verder komt. Het geeft een gelukkig gevoel om parallellen te zien tussen onderzoek van nu en dat van decennia geleden op een manier die je niet had verwacht. Over de ideale duur van een promotietraject valt te twisten, maar een periode van zeven jaar zit daar waarschijnlijk ruim boven. Het gaf mij in ieder geval wel voldoende tijd voor reflectie op het onderzoek, al was de uitdaging eerder om überhaupt tot de kern van de zaak te komen. Een groot voordeel is dat ik met veel mensen heb mogen samenwerken, vooral omdat het project zo nauw verband hield met de praktijk van afvalwaterzuivering. Zonder al die hulp was dit proefschrift er niet geweest, en de uitkomst van het pilotonderzoek niet positief. Hoewel onmogelijk, ga ik een poging wagen om hieronder niemand te kort te doen.

Allereerst enkele woorden gericht aan het kernteam van het onderzoek. *Mario*, aan jou ben ik de meeste dank verschuldigd. Ik had het met jou als copromotor niet beter kunnen treffen. Er is wat mij betreft geen betere leermeester als het aankomt op het experimenteel onderzoek naar aeroob korrelslib, meer hoeft ik daarover niet te zeggen. Het is vooral jouw manier van samenwerken waar ik het meest aan heb gehad en van heb geleerd. Je discussieert met iedereen als een gelijke, ongeacht hun kennisniveau, en geeft alles wat je hebt om een project als team tot een succes te maken. Je waardeert expertise van anderen en durft ideeën te opperen, ook al weet je niet zeker of ze uiteindelijk standhouden. Juist dat voorbeeld heeft mij enorm geholpen, omdat ik van nature geneigd ben om alles eerst tot in detail te overdenken. Ik word nog steeds verrast door het gemak waarmee jij je op nieuwe onderwerpen stort, maar de rode draad niet uit het oog verliest. Daarnaast heb jij jezelf op de achtergrond de afgelopen jaren ingezet om de druk te verlichten die ik op mijn schouders voelde om het onderzoek te laten slagen. Ik ben je voor dit alles ontzettend dankbaar.

*Edward*, bij onze eerste kennismaking was ik nogal van mijn stuk gebracht door jouw zelfverzekerde uitstraling, toch wel het tegenovergestelde van mijzelf. Wellicht komt dat vanzelf wanneer je al lang bij een ingenieursbureau werkt. Gelukkig vonden we elkaar in de onze voorliefde voor numerieke methoden en transportverschijnselen. Het gemak waarmee jij problemen analyseert en oplossingen schetst is jaloersmakend, en wat ben ik

blij dat ik je vaak om hulp en advies heb kunnen vragen de afgelopen jaren. Het zou bijna frustrerend zijn, als het niet zo plezierig en uitdagend was om met jou samen te werken. Jouw optimisme is aanstekelijk en het werk aan ons gezamenlijke artikel was één van de leukste perioden uit het promotietraject. Als collega's vraag ik je nu nog steeds dagelijks om advies, en ik had mezelf geen betere mentor kunnen wensen.

*Mark*, bedankt dat je als promotor mij de kans hebt geboden om promotieonderzoek te doen, en op een project dat zo dicht bij de praktijk staat. De context die jij in discussies over eerder biofilmonderzoek gaf (je was er immers vaak zelf nauw bij betrokken), was voor mij onmisbaar. Binnen de vakgroep voelde het na een tijdje als de normaalste zaak van de wereld om van gedachten te wisselen. Samen bij een projectoverleg of bij een congres werd mij echter keer op keer duidelijk dat dit niet zo is, en niet alleen als het om aeroob korrelslib gaat. Ik moet toegeven dat ik, zeker in het begin, te weinig van jouw kennis gebruik heb durven maken. Onnodige schroom, want je geeft mensen de ruimte om zelf te groeien in het onderwerp en geeft richting waar nodig. Het kon soms een worsteling zijn, maar wel één waar je als onderzoeker beter van wordt. Bedankt.

Vanaf de start van het project verkeerde ik continu in twee werelden. Aan de ene kant het relatief rustige onderzoek aan de TU Delft, en aan andere kant midden in praktijk van de zuivering van rioolwater. Allereerst de vakgroep milieubiotechnologie (EBT), te beginnen met mijn kamergenoten. *Jules, Jure en Morez*, I can't deny that all the discussions we've had over the years had a profound impact on my view of the world and life in many ways. I guess working within EBT tends to have this effect. That aside, we've also shared more laughs than I can remember. It made life at the TU Delft so much richer than the research alone. Thank you.

*Cristian*, although not directly involved in the research during the thesis, your enthusiasm and guidance in many roles were the main reason that I got the opportunity to join this project in the first place. First as a teacher, then as the supervisor of my MSc thesis, but above all as the mentor who showed me the beauty of what can be accomplished using numerical methods. Thank you for these teachings and our discussions over the past decade.

Zonder technische ondersteuning is onderzoek niet mogelijk. *Dirk, Udo en Zita*, bedankt voor jullie hulp met het reactorwerk. *Cor*, ik heb veel gehad jouw advies over het analyseren van de samenstelling rioolwater. *Ben*, van jouw expertise op het gebied van moleculaire biologie heb ik weinig gebruik gemaakt, maar onze leuke gesprekken heb ik erg gewaardeerd. *Stef*, dank voor alle hulp met microscopie en de gesprekken over van alles terwijl we achter de microscoop zaten. *Marcel*, alle onderdelen die je hebt gefabriceerd voor de proefinstallatie op awzi Harnaspolder doen nog steeds dienst. Bedankt.

Bij de start van het onderzoek had ik nog veel te leren over reactorwerk met mengcultures. *Danny*, bedankt dat je mij wegwijs hebt gemaakt in het werken met

korrelslibreactoren. *Mahsa*, thank you for all the work you did for the first chapter, and for your patience during the writing process. *Lenno*, ik heb erg veel plezier beleefd aan onze discussies over de mechanismen rond de vorming van aeroob korrelslib en jouw zeer scherpe kijk op zowel microbiologische als de fysische aspecten. Hopelijk kunnen we die de komende jaren als collega's voortzetten. Together with *Sara*, your more fundamental research gave me more confidence in my own. Thank you both. The four of us also shared some stressful moments during the organization of the Granular Sludge Conference, together with *Martha*, *Simon* and *Hongxiao*, but it was a great event. I've also had the pleasure to work together with students for their own theses. *Wladimir*, thank you for helping me get started with the research. *Madelon* en *Pieter*, bedankt voor al het werk dat jullie hebben verzet voor jullie masterscripties, de goede gesprekken, en voor jullie geduld met mij als begeleider. Veel succes met je eigen promotieonderzoek, Pieter! Pas in het laatste jaar ging ik af en toe mee lunchen in het sportcentrum, wat ik eerder had moeten doen. *Gerben*, *Jelmer* en *Robbert*, dank voor alle gesprekken over milieubiotechnologie, autoritaire regimes, en alles daartussenin. I won't attempt to mention all the other colleagues that I've met over the years, since I will forget at least one of you. Thank you all for the atmosphere within the research group.

Dan over naar het HARKOS-project. *Rogier*, van Mark's beschrijving van jou als een 'eigenwijze ingenieur die waarschijnlijk een kleine bioreactor in zijn schuur heeft staan' voorafgaand aan onze eerste ontmoeting was geen woord gelogen. Bij aanvang van het project had ik nog weinig kaas gegeten van rioolwaterzuivering in de praktijk, en het meeste heb ik van jou mogen leren bij DSBV. Over aeroob korrelslib leerden we samen, en ik kijk met veel plezier terug op de vele uren die we samen hebben gediscussieerd over de werking en het nut van de techniek. Het aantal weekenddagen dat we elkaar troffen op awzi Harnaschpolder om de pilothorror het hoofd te bieden valt niet op twee handen te tellen. Je bent de aanstichter van het project en was de stabiele factor in goede tijden, maar ook wanneer het er minder rooskleurig uitzag. Door jouw inzet hebben we na vier jaar niet de handdoek in de ring gegooid, en gelukkig maar. We staan hopelijk ooit samen op een HARKOS-installatie. Daarnaast wil ik de overige leden van de stuurgroep (*Andreas*, *Jan Willem*, *Jeffrey*, *Joyce* en *Mathilde*) als vertegenwoordigers van de deelnemende partijen bedanken voor de niet-aflatende steun voor het project, ook nadat het de eerste jaren niet wilde vlotten met het pilotonderzoek. De aanhouder wint en het maakt trots dat er nu wordt toegewerkt naar een eerste demonstratie van het HARKOS-proces op volle schaal. Daarnaast heb ik zeven jaar lang samen met de andere leden van de onderzoeksgroep het pilotonderzoek mogen opzetten en uitvoeren. De samenstelling is over de jaren heen wat gewijzigd, maar ik ben jullie (*Mirabella*, *Mariska*, *Marthe*, *Oscar*, *Sanne* en *Sigrid*) dankbaar voor alle tijd die jullie maandelijks hebben gestopt in het discussiëren over de voortgang van het pilotonderzoek.

Het ontwerp, de bouw en het bedrijf van de pilotinstallatie op awzi Harnaschpolder heeft veel voeten in de aarde gehad. Allereerst wil ik alle medewerkers (en de laatste drie jaar collega's) van DSBV bedanken voor hun hulp bij het onderzoek en de gezelligheid

op de werkvloer. Dikwijls werd er gekscherend gesproken over het ‘hobbywerk’ in de proefhal, maar desinteresse was dit allerminst. Als de nood aan de man was, stond men altijd klaar om te helpen om de pilotinstallatie weer zo snel mogelijk in bedrijf te krijgen. Zonder anderen te kort te willen, wil ik *Abdel, André, Liesbeth, Paul* en *Richard* in het bijzonder bedanken. Vanuit EIW is er ook veel tijd en energie gestopt in het opzetten van de pilotinstallatie. *Han*, jouw ervaring met onderzoek op pilotschaal heeft mij voor veel valkuilen behoedt, hoewel ik sommige ook met open ogen in ben gelopen (nooit water proberen te verdelen op kleine schaal). Je stond altijd klaar om mij uit de brand te helpen met een vervangend onderdeel uit de krochten van de opslag, de contactgegevens van een technicus of gewoon een cynische grap. *Pascal* en *Peter*, bedankt voor het opzetten van de procesautomatisering. Vanuit RHDHV hebben *Kim, Hugo* en *Niels* de eerste versie van het controleplatform opgezet, waarvoor dank. I’m also grateful for the collaboration with other staff members from RHDHV (*Jelle, Lindsey, PASCALLE* and *Valerie*), especially during field trips. Tot slot wil ik ook *Erik* (projectmanagement), *Simon, Marco* en *Wojtek* (elektrotechniek), *Frank* (tanks en leidingwerk), en *Jaap* en *Thijs* (kunststoftechniek) bedanken voor al het werk tijdens de bouw van de pilotinstallatie en de vele aanpassingen in de jaren daarna.

Het eerste jaar van het pilotonderzoek is er enorm veel werk verzet, wat niet was gelukt zonder de hulp van enkele studenten. *Daan, Dion* en *Xiaoyan*, bedankt voor jullie hulp. In de jaren daarna was het erg fijn dat er door EIW ook ander onderzoek werd uitgevoerd in proefhal, waardoor we elkaar af en toe konden helpen en delen in de smart die pilotonderzoek soms met zich meebrengt. *Carlos, Dimitra, Han, Ioanna, Paula* and *Vincent*, thank you for the lively atmosphere in the pilot facility. *Salah*, dank voor alle dagen die we samen in de proefhal hebben doorgebracht, dagen waarop we over meer hebben gepraat dan enkel het onderzoek. Na vier jaar van vallen en opstaan was het bij de herstart van de pilotinstallatie vrijwel meteen raak, mede dankzij jouw inzet. Geen experiment of meting was te veel gevraagd en jouw werkplezier is aanstekelijk. Dankzij jouw groene vingers kreeg de proefhal toch een wat huiselijke sfeer, afgezien van al het lawaai en het rioolwater. Nu we niet meer dagelijks samenwerken is het fijn om te weten dat de proefinstallatie bij jou in goede handen is.

Met een aantal mensen heb ik samen heen en weer gereisd tussen de universiteit en de praktijk van rioolwaterzuivering. *Roel*, na een half jaar tegelijkertijd onderzoek te hebben gedaan in het laboratorium en op awzi Harnaschpolder kwam jij gelukkig het team versterken. Het was een verademing om een paar enorm vaardige handen erbij te hebben voor het werk op het lab, in de proefhal en de begeleiding van studenten. Toch was het geen makkelijke tijd door alle tegenslag, ondanks de grote hoeveelheden energie en tijd we er samen in staken. Uiteindelijk hebben we hier wel de basis gelegd voor het latere succes, en ik ben erg blij dat we samen deze periode hebben gewerkt. Bedankt!

*Michel* en *Marissa*, bedankt voor gezelligheid en hulp als procestechnologen bij DSBV na onze tijd bij de TU Delft. In de vakgroep hadden we nog niet zoveel contact met elkaar,

maar bij DSBV hebben we dat ingehaald. De laatste doorontwikkeling van het continu aeroob korrelslibproces hebben we samen gedaan, Michel, en ik heb er veel aan gehad dat je mij zowat iedere dag vroeg hoe het er voor stond met het proefschrift. Ik betwijfel sterk of het zonder die aansporing op tijd af was geweest. Je bent ongelooflijk betrokken, ik leer veel van je en het geeft mij veel energie dat we samen met Mario en Edward verder werken aan aeroob korrelslib.

Wellicht is het belangrijkste van het doen van onderzoek dat je er af en toe afstand van kan nemen. Er is geen betere manier om je hoofd helemaal leeg te maken dan op het water, en dan het liefst zeilend in een RS500 met vrienden. Bedankt voor de welkome afleiding!

Ik ben heel dankbaar voor de onvoorwaardelijke steun mijn familie, niet in de laatste plaats tijdens het (veel grotere) deel van mijn leven voorafgaand aan het promotieonderzoek. Mijn ouders, *Dirk en Angela* en zus, *Evelien*, bedankt voor dat jullie altijd voor mij klaarstaan en stimuleren, welke keuzes ik tot nu toe ook maakte in het leven. Ook mijn schoonfamilie ben ik zeer dankbaar voor alle ondersteuning.

Tot slot het thuisfront. Lieve *Emma*, woorden schieten hier tekort. Ik heb heel veel geduld van je gevraagd de afgelopen jaren, maar je hebt me altijd gesteund en aangemoedigd om door te blijven gaan. Het is prachtig om het leven met jou te delen en ik kijk enorm uit naar de nieuwe periode die nu aanbreekt!



# Curriculum Vitæ

## Viktor Albert Haaksman

09-09-1992                      Date of birth in Leiden, The Netherlands

### Education

2016-2020                      PhD  
Delft University of Technology  
*Thesis:* Aerobic granular sludge in continuous-flow reactors  
*Promotor:* prof. dr. ir. M.C.M. van Loosdrecht

2010-2016                      Master LST (Biochemical Engineering, cum laude)  
Delft University of Technology  
Environmental Biotechnology research group

2010-2014                      Bachelor Life Science and Technology (LST)  
Delft University of Technology and Leiden University

2004-2010                      Gymnasium at Adelbert College (cum laude), Wassenaar  
1996-2004                      KOBIS de Vink, Voorschoten

### Employment

2024-present                      Royal HaskoningDHV  
Process engineer

2021-2023                      Delfluent Services  
Process engineer in the HARKOS research project

2016-2020                      Delft University of Technology  
PhD candidate


# List of publications

## Journal articles

6. **Haaksman, V.A.**, Van Dijk, E.J.H., Al-Zuhairy, S., Mulders, M., Van Loosdrecht, M.C.M., Pronk, M., 2024. *Utilizing anaerobic substrate distribution for growth of aerobic granular sludge in continuous-flow reactors*. *Water Research* 121531.
5. **Haaksman, V.A.**, Schouteren, M., Van Loosdrecht, M.C.M., Pronk, M., 2023. *Impact of the anaerobic feeding mode on substrate distribution in aerobic granular sludge*. *Water Research* 233, 119803.
4. Van Dijk, E.J.H., **Haaksman, V.A.**, Van Loosdrecht, M.C.M., Pronk, M., 2022. *On the mechanisms for aerobic granulation - model based evaluation*. *Water Research* 216, 118365.
3. **Haaksman, V.A.**, Mirghorayshi, M., Van Loosdrecht, M.C.M., Pronk, M., 2020. *Impact of aerobic availability of readily biodegradable COD on morphological stability of aerobic granular sludge*. *Water Research* 187, 116402.
2. Siddiqui, A., Lehmann, S., **Haaksman, V.A.**, Ogier, J., Schellenberg, C., Van Loosdrecht, M.C.M., Kruithof, J.C., Vrouwenvelder, J.S., 2017. *Porosity of spacer-filled channels in spiral-wound membrane systems: Quantification methods and impact on hydraulic characterization*. *Water Research* 119, 304–311.
1. **Haaksman, V.A.**, Siddiqui, A., Schellenberg, C., Kidwell, J., Vrouwenvelder, J.S., Piciooreanu, C., 2017. *Characterization of feed channel spacer performance using geometries obtained by X-ray computed tomography*. *Journal of Membrane Science* 522, 124–139.

## Patents

1. Van Dijk, E.J.H., Pronk, M., **Haaksman, V.A.**. *Aerobic biological wastewater treatment in a continuous-flow reactor*. WO2022124901A1. June 16, 2022.

 Included in this thesis.

